INTERACTIONS AMONG ESTROGEN RECEPTOR-ALPHA, PARATHYROID HORMONE, AND MECHANICAL LOADING IN SKELETAL HEALTH

A Dissertation

Presented to the Faculty of the Graduate School

of Cornell University

In Partial Fulfillment of the Requirements for the Degree of

Doctor of Philosophy

by

Amanda Michelle Rooney

December 2020

INTERACTIONS AMONG ESTROGEN RECEPTOR-ALPHA, PARATHYROID HORMONE, AND MECHANICAL LOADING IN SKELETAL HEALTH

Amanda Michelle Rooney, Ph. D.

Cornell University 2020

Osteoporosis is a disease characterized by decreased bone mass and increased risk of fracture. Methods of increasing bone mass include applied mechanical loading and pharmaceutical treatments such as parathyroid hormone (PTH). Decreased bioavailable estrogen is a major contributor to bone loss with age and may alter the responses to loading or PTH. Understanding how these factors influence each other is important for the prevention and treatment of osteoporosis.

In bone, estrogen signals primarily through estrogen receptor-alpha (ERα), which has also been implicated in bone's response to mechanical loading. However, ERα's role in specific bone cells is less clear, particularly with age. We developed osteoblast-specific ERα knockout (pOC-ERαKO) mice and applied cyclic tibial compression to adult 26-week-old female and male mice. Female pOC-ERαKO mice had reduced cancellous and cortical bone mass but males had normal bone mass. Adult female mice had greatly reduced responses to loading than young mice, even at higher load magnitudes, but males retained loading responses with age.

PTH and mechanical loading have been shown to have synergistic anabolic skeletal effects. We hypothesized that the effects would differ by applied loading

modality, tension or compression. We analyzed human femoral neck samples from PTH-treated patients receiving total hip replacements. Under normal activity, the femoral neck experiences bending, with the superior side under tension and the inferior side under compression. PTH was more effective at increasing bone formation parameters in older, low body mass, female patients on the tensile surface of the femoral neck. We also investigated the effect of loading modality on PTH in 10- and 16-week-old female pOC-ERαKO mice using tibial compression, which induces bending at the midshaft due to the curvature of the mouse tibia. PTH increased the anabolic response of the mid-diaphysis in regions of applied compression more than applied tension. Lack of ERα did not influence the relationship between PTH and loading. Additionally, pre-treatment with PTH prior to tibial loading in 16-week-old female C57Bl/6J mice increased the cortical and cancellous response to loading more than concurrent treatment alone.

BIOGRAPHICAL SKETCH

Amanda Michelle Rooney was born in Schaumburg, Illinois in 1991. She graduated from Schaumburg High School in 2009 and attended the University of Minnesota – Twin Cities. While at the U of M, she served as an officer in Tau Beta Pi for two years before earning a Bachelor of Biomedical Engineering summa cum laude with an emphasis in biomechanics in 2013. As an undergraduate she participated in multiple research experiences involving the mechanical properties of tissue engineered constructs. She entered the Biomedical Engineering PhD program at Cornell University in 2014 where she was awarded the first Donald E. and Lauren B. Morel Graduate Fellowship and the Fischell Graduate Scholarship in Bioengineering. She received her Master of Science degree in Biomedical Engineering in 2017, and her Doctor of Philosophy degree in Biomedical Engineering in 2020.

I dedicate this work to Adèle Faith and Audrey Rose.

ACKNOWLEDGMENTS

I am extremely grateful to all the people who helped me reach this point. I would like to thank my committee chair, Dr. Marjolein van der Meulen, for her tremendous support and guidance, and my committee members, Dr. Christopher Hernandez, Dr. John Schimenti, and Dr. Matthew Greenblatt for their feedback and assistance.

I want to thank Dr. Mathias Bostrom for supplying a clinical perspective and an introduction into clinical research during my Immersion term. Dr. F. Patrick Ross also provided valuable feedback and expertise throughout my time at Cornell. Kirk Gunsallus kept the microCT analysis station functioning and provided indispensable technical support. Lyuda Lukashova and Hayat Ben Larbi microCT scanned many of my samples. Rasesh Kapadia went above and beyond during the COVID-19 pandemic, microCT scanning some of my samples during the lock down. I am grateful for the administrative support that Judy Thoroughman, Belinda Floyd, and Marcia Sawyer provided.

This work would not have been possible without the assistance of many people. Drs. Natalie Kelly, Funmi Ayobami, Julia Chen, Derek Holyoak, and Sophia Ziemian assisted in animal experiments and taught me many technical skills over the years. Tyler McNeill helped with animal work and processing during later experiments. Haley Antoine, Amy DeGaetano, and Anna Ashford were always willing to do whatever needed doing. Carolyn Chlebek, Tibra Wheeler, Adrien Antoinette, and Emma Briggs were incredible scientific sounding boards.

I would not be where I am today without the support of my friends and family. Thank you to my parents for urging me to apply for graduate school and providing significant moral support throughout the journey. Thank you to my brother, sister, brother-in-law, nieces, and entire extended family for your encouragement and support. I am incredibly grateful for the long-distance friendships of Emily Naik, who has stuck with me since childhood, and Kathleen Olson. Thank you for always being there for me when I need it. Orlando, Jay, Ed, and Dan comprised my COVID crew and helped keep me sane during these strange times. I would not have made it through without them. Pre-COVID-19, Nicole, Chris, Jill, and Jacob helped make my time in Ithaca much more enjoyable.

This work was funded by the Fischell Graduate Scholarship, the Morel Fellowship, and the following grants from the National Institutes of Health: R01-AR059204, R21-AR071587, and R21-AR064034.

TABLE OF CONTENTS

LIST OF FIGURES

LIST OF TABLES

Chapter 1

INTRODUCTION

1.1 Osteoporosis

Osteoporosis is a disease characterized by decreased bone mass and strength, resulting in an increased fracture risk. In the United States, approximately 54 million people have osteoporosis and low bone mass [1]. One in three women and one in five men over the age of 50 will experience an osteoporosis-related fracture [2]. Suffering a fracture is associated with an 86% increased risk of another fracture occuring, regardless of the location [3]. Better therapies and prevention strategies are clearly needed for osteoporosis.

Bone loss associated with aging is caused by an imbalance in the amount of bone formed by osteoblasts and resorbed by osteoclasts. During growth, modeling is the primary cellular process governing bone mass and morphology. Modeling involves formation or resorption occuring independently on separate surfaces to grow and shape bones. Once peak bone mass is achieved, remodeling replaces modeling as the primary cellular process. Remodeling, or bone turnover, is characterized by the coordinated removal of old tissue followed by the formation of new bone in the same location. In patients with osteoporosis, overall levels of remodeling are increased but skewed towards resorption due to decreased osteoblastogenesis [4].

Bone is primarily categorized as one of two tissue types: cortical or cancellous. Cortical bone is the dense bone found in the midshafts of long bones and in flat bones such as the skull, and cancellous bone is the spongy bone found in the ends of long

bones. Although both tissue types decrease bone mass with aging, cancellous bone is more affected than cortical bone and many osteoporosis-related fractures occur at corticocancellous sites such as the proximal femur and spine [4,5].

Current treatment options for osteoporosis include anti-resorptive therapies, which inhibit futher bone loss, and anabolic therapies, which form new bone. Selective estrogen receptor modulators (SERMs) are an alternative to hormone replacement therapy that can act as estrogen agonists in tissues such as bone, heart, and brain while acting as antagonists in tissues such as breast and endometrium where long term estrogen treatment causes adverse effects [6,7]. Other anti-resorptive treatments include bisphosphonates and RANKL antibody denosumab [8,9]. Bisphosphonates act primarily through osteoclasts, inhibiting osteoclast activity and inducing osteoclast apoptosis, and denosumab binds to RANKL, preventing osteoclast formation and activation [10]. Current options for anabolic therapies are more limited. Parathyroid hormone (PTH) and parathyroid hormone-related protein (PTHrP), teriparatide and abaloparatide, respectively, increase bone mass by increasing osteoblast differentiation, proliferation, and activity [11,12]. Romosozumab, an anti-sclerostin antibody, is the most recently FDA-approved anabolic therapy [13]. Sclerostin is an inhibitor of the bone-forming Wnt pathway. Thus, preventing sclerostin from inhibiting this signaling pathway results in increased bone mass.

1.2 Estrogen signaling in bone

Estrogen is an important skeletal regulator in both men and women throughout life. Estrogen signaling during puberty regulates skeletal growth, limiting endocortical

resorption and periosteal expansion in females and contributing to radial expansion in males [14,15]. Later in life, decreasing levels of bioavailable estrogen with age cause reductions in bone mass that often lead to osteoporosis and increased risk of fracture [4,16–18]. Women are particularly affected at the onset of menopause, when the loss of estrogen leads to increased bone turnover, disproportionately increased levels of resorption, and deteriorated skeletal structure, changes that can be attenuated by estrogen supplementation [4].

Animal models of menopause and hormone depletion such as ovariectomy (OVX) are useful tools for studying the role of estrogen signaling in skeletal health. OVX decreases bone mass in mice, but the results vary by location and mouse strain [19]. Rats have reduced cancellous bone mass in the proximal tibia, femoral neck, and lumbar vertebrae 14, 30, and 60 days post-surgery, respectively [20–22]. Although OVX models are useful for studying estrogen-related bone loss and possible treatment or prevention methods, there are several limitations. OVX is a major surgery that produces inflammatory responses, extra stress on the animals, and confounding weight gains [23]. Additionally, OVX results in a systemic loss of all estrogen, making it difficult to isolate estrogen signaling effects on specific tissues.

Estrogen signals through two receptors, estrogen receptor-alpha (ERα) and -beta (ERβ). Activated ERs dimerize and initiate transcriptional changes by translocating to the nucleus and binding to estrogen response elements (EREs) or other transcription factors, or nongenotropically activating other proteins in the cytoplasm (Fig. 1.1) [15]. The anti-apoptotic effects of estrogen are driven by a Src/Shc/ERK signaling cascade initiated at least in part by nongenotropic activation of ERs [24],

although the distinct nongenotropic nature of this effect is unclear [25]. Although both ERα and ERβ are expressed in bone cells [26,27], ERα has been of particular interest following the identification of an inactivating point mutation in the ERα gene in a man with unfused growth plates and osteoporosis [28].

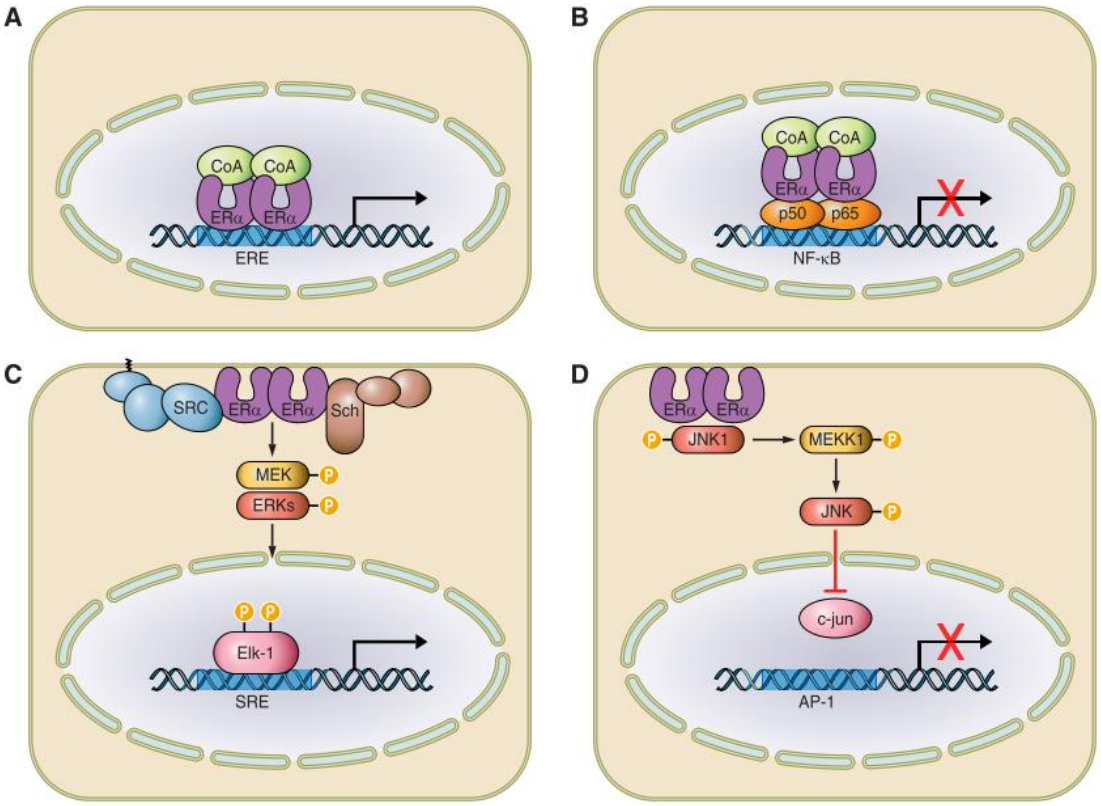

Figure 1.1 Mechanisms of estrogen receptor signaling. (A) Classical signaling in which dimerized ERα binds to estrogen response elements (EREs) or (B) other transcription factors to change transcription. (C,D) Dimerized ERα activates cytoplasmic kinases that phosphorylate proteins and transcription factors. Adapted from [15].

Global, germline ERα knockout mice (ERαKO) have been used to study the role of ERα in skeletal maintenance [29]. Female ERαKO mice display decreased bone turnover and increased cancellous and cortical bone mass [30,31], contradicting the known clinical effects of estrogen loss in postmenopausal women. Global ERα deletion resulted in compensatory increases in body weight and serum estrogen levels

and decreases in serum IGF-1 levels, all of which independently regulate bone mass [30–32]. Alterations to the balance of growth hormone and IGF-1 interfere with bone length, and decreased serum IGF-1 results in reduced bone mass by reducing periosteal expansion and BMD [33]. Increased body mass, however is associated with increased bone mass and density [34,35]. These confounding effects may explain the discrepancies between mouse models and postmenopausal women. Therefore, cell-specific ERαKO mice were developed to isolate the effects of ERα on bone (See *Chapter 2*).

1.3 Mechanical loading and bone

Bone tissue is mechanosensitive and adapts to its mechanical environment, increasing mass in response to dynamic loading and decreasing mass in response to disuse in adults [36,37]. In humans, mechanical loading through exercise increases bone mass [38–41]. Cortical thickness in the dominant playing arms of tennis players is greater than in their contralateral arms [36]. Exercise regimens have been shown to increase BMD in children [38] and pre- and postmenopausal women [41,42]. Disuse due to microgravity or immobilization, on the other hand, leads to bone loss [43,44]. This relationship is known as the mechanostat. Bone mass is maintained for an intermediate range of mechanical stimuli, below which bone mass is lost and above which bone mass is gained [45].

Several preclinical *in vivo* loading models have been developed in rodents to study the effects of mechanical loads on long bones (Fig. 1.2). These models were designed to apply controlled cyclic loading to a location of interest, and include four-

point tibial bending [46], cantilever tibial bending [47], ulnar compression [48,49], and tibial compression [50,51]. Although these loading models all provide useful information about mechanoadaptation, ulnar and tibial compression have the advantage of loading limbs in a physiologically-relevant direction and producing less woven bone. Additionally, tibial compression allows analysis of both cortical and cancellous bone, unlike ulnar loading. Loading regimens used in these models vary, but many are designed to induce a particular strain magnitude at the mid-diaphysis since physiological activity induces similar strain levels in many vertebrates regardless of bone size or load magnitude applied [52]. Therefore, *in vivo* strain gauging is commonly performed to determine the applied load that will induce the desired strain magnitude for a given mouse strain, age, and sex.

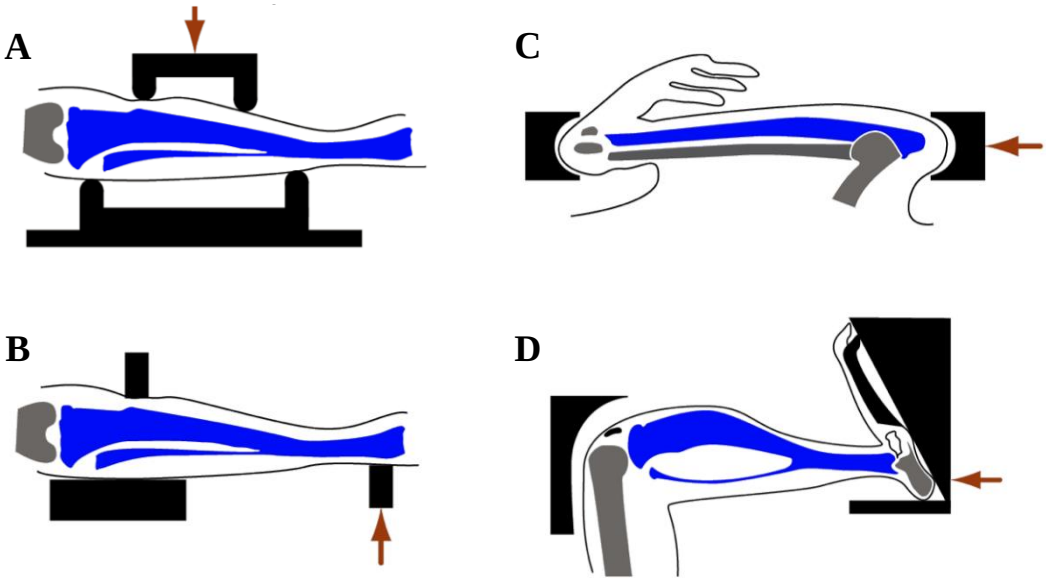

Figure 1.2 Preclinical models of in vivo mechanical loading. (A) Four-point tibial bending [40] (B) Cantilever tibial bending [41] (C) Ulnar compression [42] (D) Tibial compression [44].

Mechanical loading induces robust anabolic responses in younger populations, but adaptation decreases with age. Compared to premenopausal women, postmenopausal women have reduced responses to exercise regimens [53,54]. Cortical bone sites in adult animals are generally able to respond to mechanical loading, albeit to a lesser extent than in young animals, but cancellous sites are more impacted by the loss of mechanoadaptation [55–58]. Tibial compression in adult 26-week-old female mice was only anabolic when strain levels were nearly doubled compared to young mice, and the cancellous response was still greatly reduced compared to young 10-week-old mice [57]. The mechanisms behind these reductions in mechanoadaptation are not well understood. Contributing factors are thought to include reduced Wnt signaling, reductions in cell proliferation, and changes in bioenergetics in response to loading compared to young animals [59–61].

Although the relationship between mechanical loading and bone formation is well established, the precise mechanism driving the anabolic response is still unclear. Finite element (FE) analyses are often used to study local mechanical stimuli, which can then be correlated to regional functional adaptation and biological responses. However, which measurement of mechanical environment drives bone adaptation remains unknown. One common measure used is strain energy density (SED), which has the advantage of encapsulating the three-dimensional stress state in a positive scalar value [62,63]. However, SED values cannot distinguish between compressive and tensile strains. Loading modality can be investigated using maximum (tensile) and minimum (compressive) principal strains [64,65]. Additionally, axial strains are often

analyzed when loads are applied along the primary axis of a long bone, as in ulnar and tibial compression [66,67].

1.4 Parathyroid hormone

Parathyroid hormone (PTH) is an 84 amino acid peptide hormone that helps regulate calcium homeostasis. Circulating PTH alters serum calcium levels by influencing bone remodeling, releasing calcium from bone through increased bone resorption or removing calcium from circulation through increased bone formation [68]. Continuous, high levels of PTH lead to increased levels of resorption, but treatment with intermittent, low levels of PTH lead to increased formation.

PTH acts directly on osteoblasts and osteocytes through its receptor, PTH1R, and indirectly on osteoclasts via its effects on osteoblasts [69,70]. The lack of direct effects on osteoclasts is thought to contribute to the opposing effects of intermittent and continuous PTH. Because PTH has a short half-life of around 5 minutes [71], more prolonged doses are required for the indirect activation of osteoclasts via osteoblasts [69]. Additionally, intermittent PTH is limited by a timeframe known as the anabolic window [69]. When given at low doses intermittently, PTH causes a

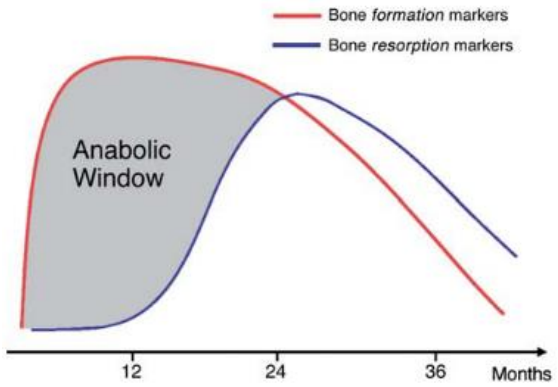

Figure 1.3 Anabolic window of PTH treatment [57].

drastic increase in bone formation, followed by a slower increase in bone resorption (Fig. 1.3). After a period of approximately 2 years, formation no longer exceeds resorption, ending the anabolic effects of PTH.

The physiological actions of PTH on bone represent a complex signaling network. PTH-bound PTH1R couples to heterotrimeric G proteins, particularly the G_S protein in bone, and initiates various signaling cascades [72,73]. PTH stimulates osteoblastic bone formation via cyclic adenosine monophosphate (cAMP) formation, one of the more prominent messengers of the G_S protein, increased intracellular calcium, and activation of Protein Kinase C (PKC) [74,75]. These pathways also lead to the production of receptor activator of nuclear factor-κB Ligand (RANKL) and macrophage colony stimulating factor (M-CSF), which induce osteoclast formation and resorption [69,76]. Sufficient PTH exposure is required to reach the levels necessary for osteoclastogenesis, allowing intermittent treatment to remain anabolic.

One mechanism through which PTH increases bone formation is by increasing the number of osteoblasts through recruitment, differentiation, proliferation, and prevention of apoptosis. PTH recruits osteoblasts from both quiescent bone lining cells [77] and mesenchymal stem cells (MSCs) from the bone marrow [78]. PTH also increases the expression levels of c-fos in osteoblasts via cAMP activation, which increases osteoblast proliferation and recruitment of stromal cells into mature osteoblasts [79]. Osteoblast survival is increased with PTH treatment through cAMP-mediated PKA signaling that inactivates pro-apoptotic protein Bad, increased transcription of survival gene Bcl-s, and the synthesis of growth factors and cytokines that promote osteoblast survival [80–82].

PTH also influences the activity of bone cells. Osteoblasts involved in a remodeling cycle increase their formation capacity in response to PTH, leading to overflow remodeling, when more bone is formed than resorbed in a single remodeling cycle [83–85]. PTH reduces the expression of sclerostin, a Wnt inhibitor [86]. Normally, Wnt proteins bind to frizzled and LRP5/6 co-receptors, leading to the translocation of β-catenin to the nucleus and transcription of Wnt target genes that increase bone formation [87]. Sclerostin is produced by osteocytes and binds to LRP5 and LRP6, preventing Wnt proteins from binding. By reducing the expression level of sclerostin, PTH increases Wnt signaling and bone formation.

Clinically, analogs of PTH [teriparatide, PTH(1-34)] and PTH-related protein [abaloparatide, PTHrP(1-34)] have been approved for treatment of osteoporosis [88–90]. Both agents increase hip and spine BMD in patients and reduce vertebral and nonvertebral fractures, although abaloparatide is slightly more effective [11,91]. Both teriparatide and abaloparatide act through PTHR1, but abaloparatide preferentially binds to the receptor conformation that favors formation more than teriparatide [92].

1.5 Mechanotransduction: Estrogen and PTH

Although mechanical loading is known to produce tissue-level changes in bone, the cellular mechanisms that drive this response are less well understood. One factor that has been shown to influence the response to loading is estrogen signaling. In rats, for instance, estrogen treatment reduced skeletal responsiveness to exercise and mechanical loading [93], and OVX-induced estrogen loss increased responsiveness [94,95].

Many *in vitro* studies have investigated the role of ERα in bone cell function and response to mechanical loading and shown that inhibiting ERα reduces the proliferative response to loading [96–101]. Conversely, when the amount of ERα per cell was increased the proliferative response to mechanical strain increased [102]. *In vivo*, female global knockout mice had a reduced response to loading, and male global knockout mice had an increased response to loading [32,103,104]. Bone-specific conditional knockout mice better model human effects of estrogen loss, but less is known about how cell-specific ERα deletion affects mechanical adaptation of bone (See *Chapter 2*).

PTH signaling has also been implicated in the anabolic response to loading. Thyroparathyroidectomized rats were unable to respond to mechanical loading unless supplemented with PTH [105]. When PTH signaling was blocked in osteoblast lineage cells via the conditional deletion of PTH/PTHrP type 1 receptor in mice, the skeletal benefits of exercise on tissue-level mechanical properties were reduced [106]. Similarly, conditional deletion of PTH receptor 1 was from osteocytes greatly reduced dynamic bone formation indices in response to ulnar loading [107].

In addition to physiological PTH signaling influencing mechanoadaptation, PTH treatment has been used to further increase the anabolic effects of mechanical loading. *In vitro*, fluid shear and PTH together increased COX-2 expression and intracellular calcium in osteoblast-like cells more than either treatment alone [108]. Synergistic anabolic effects of PTH and loading *in vivo* have primarily been shown in cortical bone. Rats with low bone mass following hindlimb immobilization increased cortical bone mass to a greater extent when remobilization was combined with PTH

[109]. New cortical bone formation following tibial four point bending in rats was further increased with PTH treatment [110,111]. In young, skeletally female mature mice, tibial compression had a synergistic anabolic effect in cortical bone, but the effects were only additive in cancellous bone [112]. However, cortical bone mass in aged, 19-month-old female mice increased additively, and PTH blunted the anabolic effects of tibial loading in cancellous bone [113]. Clinically, whole-body vibration further increased bone mineral density at the spine compared to PTH treatment alone [114].

The signaling pathways responsible for the synergistic effects of PTH and loading are not well understood, but calcium channels are thought to play an important role. Stretch loading of rat osteocytes via hypotonic swelling increased intracellular calcium and IGF-1 mRNA expression. These changes were synergistically increased with PTH treatment, and blocked with inhibitors of stretch-activated cation channels and voltage-operated L-type calcium channels [115]. Similarly, the anabolic effects of *in vivo* tibial loading in rats were synergistically increased with PTH, but the synergistic effect was eliminated with an L-type voltage-sensitive calcium channel blocker [116].

1.6 Aims

Osteoporosis is an increasingly prevalent disease that leads to increased fracture risk, decreased quality of life, and increased mortality. Changes in estrogen signaling contribute to bone loss, and mechanical loading and anabolic therapies increase bone mass. This thesis aims to better understand the relationships between

impaired estrogen signaling via ERα, mechanical loading, and PTH in skeletal health and how these relationships might change with age.

Aim 1

Estrogen signaling via ERα is an important regulator of bone mass, and its role in skeletal maintenance has been studied in a cell-specific manner. However, the role of bone cell-specific ERα in mechanotransduction is less clear, particularly in more clinically relevant adult populations. We bred mature osteoblast-specific ERα knockout (pOC-ERαKO) and littermate control (LC) mice. At 26 weeks of age, we performed strain gauge measurements at the tibial midshaft to calculate bone stiffness in males and females. Bone stiffness measurements were then used to determine the peak load magnitude values necessary to induce +1000με at the midshaft. We applied 2 weeks of cyclic tibial compression at these load magnitudes to the left limbs of 26-week-old male and female pOC-ERαKO and LC mice while the right limbs served as contralateral controls. Bone mass and morphology at the tibial metaphysis and mid-diaphysis were assessed using microCT. The data from 26-week-old mice was then compared to previous work in young, 10-week-old mice [117] to assess changes in bone phenotype and mechanoresponsiveness with age. We hypothesized that adult female pOC-ERαKO mice would have lower bone mass and greater adaptation to loading than adult female LC mice, and adult male pOC-ERαKO mice would have greater bone mass and similar adaptation to loading as adult male LC mice. We also hypothesized that adult mice would have reduced bone mass and adaptation to loading compared to young mice.

Aim 2

PTH has been shown to produce site-specific changes in BMD in both humans and animal models. Many of the anatomical sites that respond to PTH are load-bearing, but even amongst load-bearing locations there are differences in the effectiveness of PTH. We hypothesized that these differences may be partially due to differences in loading modality. Under normal physiological loading, the human femoral neck is under bending, with the superior surface under tension and the inferior surface under compression. We obtained femoral neck samples from patients undergoing elective total hip replacements that had been treated with teriparatide (TPTD), an analog of PTH, or placebo (PBO) and labeled for new bone formation. The femoral neck samples were sectioned and analyzed for static and dynamic bone formation indices in the tensile and compressive regions separately. Additionally, multiple regression models were conducted to identify relationships between intrinsic anatomical parameters (age, sex, BMI, body weight, femoral neck geometry, cortical bone morphology), loading modality, treatment, and bone formation indices. We hypothesized that bone formation indices would be greatest in the tensile region of patients that received TPTD, and that patient demographics and bone morphology would help predict the response to TPTD better than loading modality alone.

Aim 3

Although the data from Aim 2 were promising, the limitations present in that study (low sample number, wide range of demographics, short treatment duration)

made drawing strong conclusions difficult. Therefore, we investigated the role of loading modality in a better defined preclinical model. Due to the curvature of the mouse tibia, cyclic tibial compression produces bending at the midshaft, placing the anterior surface under tension and the posterior surface under compression. We wanted to evaluate the efficacy of PTH and mechanical loading in a more clinically relevant, low bone mass model and determine whether a PTH pre-treatment period would further increase the anabolic effects of treatment and loading by priming osteoblasts prior to loading. Therefore, we used female pOC-ERαKO mice as a model of low bone mass and LC mice as their normal bone mass controls. Bone stiffness and the peak load required to induce +1000με at the tibial midshaft were calculated using tibial strain gauging in 10- and 16-week-old female pOC-ERαKO and LC mice. The left limbs underwent cyclic tibial compression for 2 or 6 weeks, and mice were concurrently treated with either PTH or vehicle (VEH). The tibial midshafts were evaluated using microCT, and a custom MATLAB code analyzed the tensile, compressive, and neutral regions separately. Because we found no differences in the response to PTH in pOC-ERαKO compared to LC mice, we examined the effect of pre-treatment in female C57Bl/6J mice. Strain gauge analysis was performed on 16-week-old female C57Bl/6J mice that had been treated with VEH or PTH for 6 weeks. 10-week-old mice were pre-treated with either VEH or PTH for 6 weeks, and tibial compression commenced at 16 weeks of age for 2 or 6 weeks. One group of VEH pre-treated mice continued VEH treatment with loading, another VEH pre-treated group switched to receiving PTH, and the PTH pre-treated mice continued receiving PTH treatment. Based on the results of Aim 2, we hypothesized that the tensile region

would increase bone mass more in response to loading and PTH compared to the compressive region, with minimal changes in the neutral region. We also hypothesized that PTH pre-treatment would further enhance the anabolic response to loading.

Aim 4

Most osteoporosis-related fractures occur at cortico-cancellous sites, such as the hip and spine, highlighting the need to increase cancellous bone mass in osteoporosis patients to prevent fractures. Cancellous bone loses its ability to adapt to mechanical loads with age, therefore new strategies for enhancing the mechanoresponsiveness of cancellous bone are required. PTH is synergistically anabolic when combined with mechanical loading and may overcome this deficit. However, most studies investigating the combination of PTH and mechanical loading have been performed in normal bone mass mice and focused only on cortical bone. We performed tibial compression on 10- and 16-week-old female pOC-ERαKO and LC mice that received PTH or VEH to investigate the effects of low bone mass on the response to PTH and loading. To investigate whether pre-treating mice with PTH would prime osteoblasts prior to mechanical and enhance the anabolic effects, we pre-treated female C57Bl/6J with PTH or VEH as described in Aim 3. Bone mass and morphology at the metaphysis (cancellous and cortical) and diaphysis (cortical) were analyzed using microCT. Osteoblast and osteoclast activity at the cancellous metaphysis will be analyzed using immunohistochemistry. We hypothesized that pre-treating mice with PTH prior to initiating mechanical loading would increase the anabolic skeletal response, particularly in cancellous bone, and that low bone mass

pOC-ERαKO mice would respond to PTH differently than normal bone mass LC mice.

1.7 References

[1] National Osteoporosis Foundation, (2020). https://www.nof.org/.

[2] International Osteoporosis Foundation: Facts and Statistics, (2020). https://www.iofbonehealth.org/facts-statistics.

[3] J.A. Kanis, O. Johnell, C. De Laet, H. Johansson, A. Oden, P. Delmas, J. Eisman, S. Fujiwara, P. Garnero, H. Kroger, E. V. McCloskey, D. Mellstrom, L.J. Melton, H. Pols, J. Reeve, A. Silman, A. Tenenhouse, A meta-analysis of previous fracture and subsequent fracture risk, Bone. 35 (2004) 375–382. doi:10.1016/j.bone.2004.03.024.

[4] B.L. Riggs, Endocrine causes of age-related bone loss and osteoporosis, Novartis Found. Symp. 242 (2002) 247–264.

[5] O. of the S.G. U.S. Department of Health and Human Services, ed., Bone Health and Osteoporosis A Report of the Surgeon General, Rockville, MD, 2004.

[6] J. V. Pinkerton, S. Thomas, Use of SERMs for treatment in postmenopausal women, J. Steroid Biochem. Mol. Biol. 142 (2014) 142–154. doi:10.1016/j.jsbmb.2013.12.011.

[7] M.R. McClung, New management options for osteoporosis with emphasis on SERMs, Climacteric. 18 (2015) 56–61. doi:10.3109/13697137.2015.1104010doi.org/10.3109/13697137.2015.1104010.

[8] J.P. Brown, I.R. Reid, R.B. Wagman, D. Kendler, P.D. Miller, J.E.B. Jensen, M.A. Bolognese, N. Daizadeh, I. Valter, C.A.F. Zerbini, D.W. Dempster, Effects of Up to 5 years of denosumab treatment on bone histology and histomorphometry: The FREEDOM study extension, J. Bone Miner. Res. 29 (2014) 2051–2056. doi:10.1002/jbmr.2236.

[9] J.W. Mandema, J. Zheng, C. Libanati, J. Jose, P. Ruixo, Time Course of Bone Mineral Density Changes With Denosumab Compared With Other Drugs in Postmenopausal Osteoporosis : A Dose-Response-Based Meta-Analysis, J. Clin. Endocrinol. Metab. 99 (2014) 3746–3755. doi:10.1210/jc.2013-3795.

[10] L. Gennari, S. Rotatori, S. Bianciardi, R. Nuti, D. Merlotti, Treatment needs and current options for postmenopausal osteoporosis, Expert Opin. Pharmacother. 17 (2016) 1141–1152. doi:10.1080/14656566.2016.1176147.

[11] F. Cosman, Parathyroid hormone and abaloparatide treatment for osteoporosis, Curr. Opin. Endocr. Metab. Res. 3 (2018) 61–67. doi:10.1016/j.coemr.2018.02.005.

[12] M.N. Wein, H.M. Kronenberg, Regulation of bone remodeling by parathyroid hormone, Cold Spring Harb. Perspect. Med. 8 (2018). doi:10.1101/cshperspect.a031237.

[13] F. Cosman, D.B. Crittenden, J.D. Adachi, N. Binkley, E. Czerwinski, S. Ferrari, L.C. Hofbauer, E. Lau, E.M. Lewiecki, A. Miyauchi, C.A.F. Zerbini, C.E. Milmont, L. Chen, J. Maddox, P.D. Meisner, C. Libanati, A. Grauer, Romosozumab treatment in postmenopausal women with osteoporosis, N. Engl. J. Med. 375 (2016). doi:10.1056/NEJMoa1607948.

[14] F. Callewaert, M. Sinnesael, E. Gielen, S. Boonen, D. Vanderschueren, Skeletal sexual dimorphism: Relative contribution of sex steroids, GH-IGF1, and

mechanical loading, J. Endocrinol. 207 (2010) 127–134. doi:10.1677/JOE-10-0209.
[15] M. Almeida, M.R. Laurent, V. Dubois, F. Claessens, C.A. O'Brien, R. Bouillon, D. Vanderschueren, S.C. Manolagas, Estrogens and Androgens in Skeletal Physiology and Pathophysiology, Physiol. Rev. 97 (2017) 135–187. doi:10.1152/physrev.00033.2015.
[16] L.S. Richelson, H.W. Wahner, L.J. Melton III, B.L. Riggs, Relative contributions of aging and estrogen deficiency to postmenopausal bone loss, N. Engl. J. Med. 311 (1984) 1273–1275.
[17] S. Khosla, S. Amin, E. Orwoll, Osteoporosis in men, Endocr. Rev. 29 (2008) 441–464. doi:10.1210/er.2008-0002.
[18] F. Callewaert, S. Boonen, D. Vanderschueren, Sex steroids and the male skeleton: a tale of two hormones, Trends Endocrinol. Metab. 21 (2010) 89–95. doi:10.1016/j.tem.2009.09.002.
[19] M.L. Bouxsein, K.S. Myers, K.L. Shultz, L.R. Donahue, C.J. Rosen, W.G. Beamer, Ovariectomy-induced bone loss varies among inbred strains of mice, J. Bone Miner. Res. 20 (2005) 1085–1092. doi:10.1359/JBMR.050307.
[20] M. Li, Y. Shen, T.J. Wronski, Time course of femoral neck osteopenia in ovariectomized rats, Bone. 20 (1997) 55–61. doi:10.1016/S8756-3282(96)00317-1.
[21] T.J. Wronski, M. Cintron, L.M. Dann, Temporal relationship between bone loss and increased bone turnover in ovariectomized rats, Calcif. Tissue Int. 43 (1988) 179–183.
[22] T.J. Wronski, L.M. Dann, S.L. Horner, Time course of vertebral osteopenia in ovariectomized rats, Bone. 10 (1989) 295–301. doi:10.1016/8756-3282(89)90067-7.
[23] C.C. Danielsen, L. Mosekilde, B. Svenstrup, Cortical bone mass, composition, and mechanical properties in female rats in relation to age, long-term ovariectomy, and estrogen substitution, Calcif. Tissue Int. 52 (1993) 26–33. doi:10.1007/BF00675623.
[24] S. Kousteni, T. Bellido, L.I. Plotkin, C.A. O'Brien, D.L. Bodenner, L. Han, K. Han, G.B. DiGregorio, J.A. Katzenellenbogen, B.S. Katzenellenbogen, P.K. Roberson, R.S. Weinstein, R.L. Jilka, S.C. Manolagas, Nongenotropic, sex-nonspecific signaling through the estrogen or androgen receptors: Dissociation from transcriptional activity, Cell. 104 (2001) 719–730. doi:10.1016/s0092-8674(01)00268-9.
[25] S.H. Windahl, R. Galien, R. Chiusaroli, P. Clément-Lacroix, F. Morvan, L. Lepescheux, F. Nique, W.C. Horne, M. Resche-Rigon, R. Baron, Bone protection by estrens occurs through non-tissue-selective activation of the androgen receptor, J. Clin. Invest. 116 (2006) 2500–2509. doi:10.1172/JCI28809.
[26] D. Vanderschueren, L. Vandenput, S. Boonen, M.K. Lindberg, R. Bouillon, C. Ohlsson, Androgens and bone, Endocr. Rev. 25 (2004) 389–425. doi:10.1210/er.2003-0003.
[27] S. Bord, A. Horner, S. Beavan, J. Compston, Estrogen Receptors α and β Are Differentially Expressed in Developing Human Bone, J. Clin. Endocrinol.

Metab. 86 (2001) 2309–2314. doi:10.1210/jcem.86.5.7513.
[28] E.P. Smith, J. Boyd, G.R. Frank, H. Takahashi, R.M. Cohen, B. Specker, T.C. Williams, D.B. Lubahn, K.S. Korach, Estrogen resistance caused by a mutation in the estrogen-receptor gene in a man, N Engl J Med. 331 (1994) 1056–1061.
[29] L. Vico, J.M. Vanacker, Sex hormones and their receptors in bone homeostasis: Insights from genetically modified mouse models, Osteoporos. Int. 21 (2010) 365–372. doi:10.1007/s00198-009-0963-5.
[30] M.K. Lindberg, S.L. Alatalo, J.M. Halleen, S. Mohan, J.-Å. Gustafsson, C. Ohlsson, Estrogen receptor specificity in the regulation of the skeleton in female mice, J. Endocrinol. 171 (2001) 229–236.
[31] V. Parikka, Z. Peng, T. Hentunen, J. Risteli, T. Elo, H.K. Väänänen, P. Härkönen, Estrogen responsiveness of bone formation in vitro and altered bone phenotype in aged estrogen receptor-α-deficient male and female mice, Eur. J. Endocrinol. 152 (2005) 301–314. doi:10.1530/eje.1.01832.
[32] L.K. Saxon, G. Galea, L. Meakin, J. Price, L.E. Lanyon, Estrogen receptors α and β have different gender-dependent effects on the adaptive responses to load bearing in cancellous and cortical bone, Endocrinology. 153 (2012) 2254–2266. doi:10.1210/en.2011-1977.
[33] S. Yakar, H. Werner, C.J. Rosen, 40 years of IGF1: Insulin-like growth factors: Actions on the skeleton, J. Mol. Endocrinol. 61 (2018) T115–T137. doi:10.1530/JME-17-0298.
[34] E. Dolan, P.A. Swinton, C. Sale, A. Healy, J. O'Reilly, Influence of adipose tissue mass on bone mass in an overweight or obese population : systematic review and meta-analysis, Nutr. Clin. Care. 75 (2017) 858–870. doi:10.1093/nutrit/nux046.
[35] D.T. Felson, Y. Zhang, M.T. Hannan, J.J. Anderson, Effects of weight and body mass index on bone mineral density in men and women: The Framingham study, J. Bone Miner. Res. 8 (1993) 567–573. doi:10.1002/jbmr.5650080507.
[36] H. Jones, J. Priest, W. Hayes, C. Tichenor, D. Nagel, Humeral hypertrophy in response to exercise, J. Bone Jt. Surg. 59 (1977) 204–208.
[37] T. Cervinka, H. Sievänen, J. Hyttinen, J. Rittweger, Bone loss patterns in cortical, subcortical, and trabecular compartments during simulated microgravity., J. Appl. Physiol. 117 (2014) 80–8. doi:10.1152/japplphysiol.00021.2014.
[38] R.K. Fuchs, J.J. Bauer, C.M. Snow, Jumping improves hip and lumbar spine bone mass in prepubescent children: a randomized controlled trial., J. Bone Miner. Res. 16 (2001) 148–156. doi:10.1359/jbmr.2001.16.1.148.
[39] S. Kontulainen, H. Sievänen, P. Kannus, M. Pasanen, I. Vuori, Effect of long-term impact-loading on mass, size, and estimated strength of humerus and radius of female racquet-sports players: a peripheral quantitative computed tomography study between young and old starters and controls., J. Bone Miner. Res. 18 (2003) 352–359. doi:10.1359/jbmr.2003.18.2.352.
[40] A. Vainionpää, R. Korpelainen, J. Leppäluoto, T. Jämsä, Effects of high-impact exercise on bone mineral density: A randomized controlled trial in premenopausal women, Osteoporos. Int. 16 (2005) 191–197. doi:10.1007/s00198-004-1659-5.

[41] K.M. Winters-Stone, C.M. Snow, Site-specific response of bone to exercise in premenopausal women, Bone. 39 (2006) 1203–1209. doi:10.1016/j.bone.2006.06.005.
[42] D. Kerr, T. Ackland, B. Maslen, a Morton, R. Prince, Resistance training over 2 years increases bone mass in calcium-replete postmenopausal women., J. Bone Miner. Res. 16 (2001) 175–181. doi:10.1359/jbmr.2001.16.1.175.
[43] Z.F.G. Jaworski, M. Liskova-Kiar, H.K. Uhthoff, Effect of long-term immobilization on the pattern of bone loss in older dogs, J. Bone Jt. Surg. - Ser. B. 62 (1980) 104–110. doi:10.1302/0301-620x.62b1.6985912.
[44] V. Schneider, V. Oganov, A. LeBlanc, A. Rakmonov, L. Taggart, A. Bakulin, C. Huntoon, A. Grigoriev, L. Varonin, Bone and body mass changes during space flight, Acta Astronaut. 36 (1995) 463–466. doi:10.1016/0094-5765(95)00131-X.
[45] H.M. Frost, Bone's Mechanostat: A 2003 Update, Anat. Rec. - Part A Discov. Mol. Cell. Evol. Biol. 275 (2003) 1081–1101. doi:10.1002/ar.a.10119.
[46] C.H. Turner, M.P. Akhter, D.M. Raab, D.B. Kimmel, R.R. Recker, A noninvasive, in vivo model for studying strain adaptive bone modeling, Bone. 12 (1991) 73–79. doi:10.1016/8756-3282(91)90003-2.
[47] T.S. Gross, S. Srinivasan, C.C. Liu, T.L. Clemens, S.D. Bain, Noninvasive loading of the murine tibia: An in vivo model for the study of mechanotransduction, J. Bone Miner. Res. 17 (2002) 493–501. doi:10.1359/jbmr.2002.17.3.493.
[48] A.G. Torrance, J.R. Mosley, R.F.L. Suswillo, L.E. Lanyon, Noninvasive loading of the rat ulna in vivo induces a strain-related modeling response uncomplicated by trauma or periostal pressure, Calcif. Tissue Int. 54 (1994) 241–247. doi:10.1007/BF00301686.
[49] K.C.L. Lee, A. Maxwell, L.E. Lanyon, Validation of a technique for studying functional adaptation of the mouse ulna in response to mechanical loading, Bone. 31 (2002) 407–412. doi:10.1016/S8756-3282(02)00842-6.
[50] J.C. Fritton, E.R. Myers, T.M. Wright, M.C.H. Van Der Meulen, Loading induces site-specific increases in mineral content assessed by microcomputed tomography of the mouse tibia, Bone. 36 (2005) 1030–1038. doi:10.1016/j.bone.2005.02.013.
[51] R.L. De Souza, M. Matsuura, F. Eckstein, S.C.F. Rawlinson, L.E. Lanyon, A.A. Pitsillides, Non-invasive axial loading of mouse tibiae increases cortical bone formation and modifies trabecular organization: A new model to study cortical and cancellous compartments in a single loaded element, Bone. 37 (2005) 810–818. doi:10.1016/j.bone.2005.07.022.
[52] C.T. Rubin, L.E. Lanyon, Dynamic strain similarity in vertebrates; an alternative to allometric limb bone scaling, J. Theor. Biol. 107 (1984) 321–327. doi:10.1016/S0022-5193(84)80031-4.
[53] E.J. Bassey, M.C. Rothwell, J.J. Littlewood, D.W. Pye, Pre- and postmenopausal women have different bone mineral density responses to the same high-impact exercise., J. Bone Miner. Res. 13 (1998) 1805–1813. doi:10.1359/jbmr.1998.13.12.1805.
[54] K.-Z. Kim, A. Shin, J. Lee, S.-K. Myung, J. Kim, The Beneficial Effect of

Leisure-Time Physical Activity on Bone Mineral Density in Pre- and Postmenopausal Women, Calcif. Tissue Int. 91 (2012) 178–185. doi:10.1007/s00223-012-9624-3.
[55] N. Holguin, M.D. Brodt, M.E. Sanchez, M.J. Silva, Aging diminishes lamellar and woven bone formation induced by tibial compression in adult C57BL/6, Bone. 65 (2014) 83–91. doi:10.1016/j.bone.2014.05.006.
[56] B.M. Willie, A.I. Birkhold, H. Razi, T. Thiele, M. Aido, B. Kruck, A. Schill, S. Checa, R.P. Main, G.N. Duda, Diminished response to in vivo mechanical loading in trabecular and not cortical bone in adulthood of female C57Bl/6 mice coincides with a reduction in deformation to load, Bone. (2013). doi:10.1016/j.bone.2013.04.023.
[57] M.E. Lynch, R.P. Main, Q. Xu, T.L. Schmicker, M.B. Schaffler, T.M. Wright, M.C.H. van der Meulen, Tibial compression is anabolic in the adult mouse skeleton despite reduced responsiveness with aging, Bone. 49 (2011) 439–446. doi:10.1016/j.bone.2011.05.017.
[58] R.P. Main, M.E. Lynch, M.C.H. van der Meulen, Load-induced changes in bone stiffness and cancellous and cortical bone mass following tibial compression diminish with age in female mice., J. Exp. Biol. 217 (2014) 1775–83. doi:10.1242/jeb.085522.
[59] N. Holguin, M.D. Brodt, M.J. Silva, Activation of Wnt Signaling By Mechanical Loading Is Impaired in the Bone of Old Mice, J. Bone Miner. Res. 31 (2016) 2215–2226. doi:10.1002/jbmr.2900.
[60] G.L. Galea, L.B. Meakin, M.A. Harris, P.J. Delisser, L.E. Lanyon, S.E. Harris, J.S. Price, Old age and the associated impairment of bones' adaptation to loading are associated with transcriptomic changes in cellular metabolism, cell-matrix interactions and the cell cycle, Gene. 599 (2017). doi:10.1016/j.gene.2016.11.006.
[61] L.B. Meakin, G.L. Galea, T. Sugiyama, L.E. Lanyon, J.S. Price, Age-related impairment of bones' adaptive response to loading in mice is associated with sex-related deficiencies in osteoblasts but no change in osteocytes, J. Bone Miner. Res. 29 (2014) 1859–1871. doi:10.1002/jbmr.2222.
[62] C.H. Kim, E. Takai, H. Zhou, D. von Stechow, R. Müller, D.W. Dempster, X.E. Guo, Trabecular bone response to mechanical and parathyroid hormone stimulation: the role of mechanical microenvironment, J. Bone Miner. Res. 18 (2003) 2116–2125. doi:10.1359/jbmr.2003.18.12.2116.
[63] E.N. Cresswell, M.G. Goff, T.M. Nguyen, W.X. Lee, C.J. Hernandez, Spatial relationships between bone formation and mechanical stress within cancellous bone, J. Biomech. 49 (2016) 222–228. doi:10.1016/j.jbiomech.2015.12.011.
[64] Javaheri, H. Razi, S. Gohin, S. Wylie, Y.M. Chang, P. Salmon, P.D. Lee, A.A. Pitsillides, Lasting organ-level bone mechanoadaptation is unrelated to local strain, Sci. Adv. 6 (2020). doi:10.1126/sciadv.aax8301.
[65] Y. Lu, D. Zuo, J. Li, Y. He, Stochastic analysis of a heterogeneous micro-finite element model of a mouse tibia, Med. Eng. Phys. 63 (2019) 50–56. doi:10.1016/j.medengphy.2018.10.007.
[66] S.P. Kotha, Y.F. Hsieh, R.M. Strigel, R. Müller, M.J. Silva, Experimental and finite element analysis of the rat ulnar loading model - Correlations between

strain and bone formation following fatigue loading, J. Biomech. 37 (2004) 541–548. doi:10.1016/j.jbiomech.2003.08.009.
[67] T.K. Patel, M.D. Brodt, M.J. Silva, Experimental and finite element analysis of strains induced by axial tibial compression in young-adult and old female C57Bl/6 mice, J. Biomech. 47 (2014). doi:10.1016/j.jbiomech.2013.10.052.
[68] B.C. Silva, J.P. Bilezikian, Parathyroid hormone: Anabolic and catabolic actions on the skeleton, Curr. Opin. Pharmacol. 22 (2015) 41–50. doi:10.1016/j.coph.2015.03.005.
[69] D. Aslan, M.D. Andersen, L.B. Gede, T.K. de Franca, S.R. Jørgensen, P. Schwarz, N.R. Jørgensen, Mechanisms for the bone anabolic effect of parathyroid hormone treatment in humans, Scand. J. Clin. Lab. Investig. 72 (2012) 14–22. doi:10.3109/00365513.2011.624631.
[70] M.N. Wein, H.M. Kronenberg, Regulation of bone remodeling by parathyroid hormone, Cold Spring Harb. Perspect. Med. 8 (2018). doi:10.1101/cshperspect.a031237.
[71] G. Momsen, P. Schwarz, A mathematical/physiological model of parathyroid hormone secretion in response to blood-ionized calcium lowering in vivo, Scand. J. Clin. Lab. Invest. 57 (1997) 381–394. doi:10.3109/00365519709084585.
[72] M. Bastepe, S. Turan, Q. He, Heterotrimeric G proteins in the control of parathyroid hormone actions, J. Mol. Endocrinol. 58 (2017) R203–R224. doi:10.1530/JME-16-0221.
[73] R.W. Cheloha, S.H. Gellman, J.P. Vilardaga, T.J. Gardella, PTH receptor-1 signalling - Mechanistic insights and therapeutic prospects, Nat. Rev. Endocrinol. 11 (2015). doi:10.1038/nrendo.2015.139.
[74] T.M. Murray, L.G. Rao, P. Divieti, F.R. Bringhurst, Parathyroid hormone secretion and action: Evidence for discrete receptors for the carboxyl-terminal region and related biological actions of carboxyl-terminal ligands, Endocr. Rev. 26 (2005) 78–113. doi:10.1210/er.2003-0024.
[75] D. Yang, R. Singh, P. Divieti, J. Guo, M.L. Bouxsein, F.R. Bringhurst, Contributions of parathyroid hormone (PTH)/PTH-related peptide receptor signaling pathways to the anabolic effect of PTH on bone, Bone. 40 (2007) 1453–1461. doi:10.1016/j.bone.2007.02.001.
[76] J.C. Huang, T. Sakata, L.L. Pfleger, M. Bencsik, B.P. Halloran, D.D. Bikle, R.A. Nissenson, PTH Differentially Regulates Expression of RANKL and OPG, J. Bone Miner. Res. 19 (2004) 235–244. doi:10.1359/JBMR.0301226.
[77] H. Dobnig, R.T. Turner, Evidence that intermittent treatment with parathyroid hormone increases bone formation in adult rats by activation of bone lining cells, Endocrinology. 136 (1995) 3632–3638.
[78] J. Davies, T.J. Chambers, Parathyroid hormone activates adhesion in bone marrow stromal precursor cells, J. Endocrinol. 180 (2004) 505–513. doi:10.1677/joe.0.1800505.
[79] L.K. McCauley, A.J. Koh, C.A. Beecher, T.J. Rosol, Proto-oncogene c-fos is transcriptionally regulated by parathyroid hormone (PTH) and PTH-related protein in a cyclic adenosine monophosphate- dependent manner in osteoblastic cells, Endocrinology. 138 (1997) 5427–5433. doi:10.1210/endo.138.12.5587.

[80] T. Bellido, A.A. Ali, L.I. Plotkin, Q. Fu, I. Gubrij, P.K. Roberson, R.S. Weinstein, C.A. O'Brien, S.C. Manolagas, R.L. Jilka, Proteasomal degradation of Runx2 shortens parathyroid hormone-induced anti-apoptotic signaling in osteoblasts: A putative explanation for why intermittent administration is needed for bone anabolism, J. Biol. Chem. 278 (2003) 50259–50272. doi:10.1074/jbc.M307444200.
[81] N. Miyakoshi, Y. Kasukawa, T.A. Linkhart, D.J. Baylink, S. Mohan, Evidence that anabolic effects of PTH on bone require IGF-I in growing mice, Endocrinology. 142 (2001) 4349–4356. doi:10.1210/endo.142.10.8436.
[82] R.L. Jilka, R.S. Weinstein, T. Bellido, P. Roberson, A.M. Parfitt, S.C. Manolagas, Increased bone formation by prevention of osteoblast apoptosis with parathyroid hormone, J. Clin. Invest. 104 (1999) 439–446. doi:10.1172/JCI6610.
[83] S. V. Komarova, Mathematical model of paracrine interactions between osteoclasts and osteoblasts predicts anabolic action of parathyroid hormone on bone, Endocrinology. 146 (2005) 3589–3595. doi:10.1210/en.2004-1642.
[84] B. Langdahl, S. Ferrari, D.W. Dempster, Bone modeling and remodeling: potential as therapeutic targets for the treatment of osteoporosis, Ther. Adv. Musculoskelet. Dis. 8 (2016) 225–235. doi:10.1177/1759720X16670154.
[85] D.W. Dempster, H. Zhou, R.R. Recker, J.P. Brown, C.P. Recknor, E.M. Lewiecki, P.D. Miller, S.D. Rao, D.L. Kendler, R. Lindsay, J.H. Krege, J. Alam, K.A. Taylor, T.E. Melby, V.A. Ruff, Remodeling- and Modeling-Based Bone Formation With Teriparatide Versus Denosumab: A Longitudinal Analysis From Baseline to 3 Months in the AVA Study, J. Bone Miner. Res. 33 (2018) 298–306. doi:10.1002/jbmr.3309.
[86] H. Keller, M. Kneissel, SOST is a target gene for PTH in bone, Bone. 37 (2005) 148–158. doi:10.1016/j.bone.2005.03.018.
[87] U.H. Lerner, C. Ohlsson, The WNT system: Background and its role in bone, J. Intern. Med. 277 (2015). doi:10.1111/joim.12368.
[88] F. Cosman, G. Hattersley, M. Hu, G.C. Williams, L.A. Fitzpatrick, D.M. Black, Effects of Abaloparatide-SC on Fractures and Bone Mineral Density in Subgroups of Postmenopausal Women with Osteoporosis and Varying Baseline Risks, J Bone Min. Res. (2016) 1–19. doi:10.1002/jbmr.2991.
[89] F. Cosman, D.W. Dempster, J.W. Nieves, H. Zhou, M. Zion, C. Roimisher, Y. Houle, R. Lindsay, M. Bostrom, Effect of Teriparatide on Bone Formation in the Human Femoral Neck, J. Clin. Endocrinol. Metab. 101 (2016) 1498–1505. doi:10.1210/jc.2015-3698.
[90] R. Lindsay, H. Zhou, F. Cosman, J. Nieves, D.W. Dempster, A.B. Hodsman, Effects Of a One-Month Treatment With PTH(1-34) on Bone Formation on Cancellous, Endocortical, and Periosteal Surfaces of the Human Ilium, J. Bone Miner. Res. 22 (2007) 495–502. doi:10.1359/jbmr.070104.
[91] P.D. Miller, G. Hattersley, E. Lau, L.A. Fitzpatrick, A.G. Harris, G.C. Williams, M.Y. Hu, B.J. Riis, L. Russo, C. Christiansen, Bone mineral density response rates are greater in patients treated with abaloparatide compared with those treated with placebo or teriparatide: Results from the ACTIVE phase 3 trial, Bone. 120 (2019) 137–140. doi:10.1016/j.bone.2018.10.015.

[92] G. Hattersley, T. Dean, B.A. Corbin, H. Bahar, T.J. Gardella, Binding selectivity of abaloparatide for PTH-type-1-receptor conformations and effects on downstream signaling, Endocrinology. 157 (2016) 141–149. doi:10.1210/en.2015-1726.
[93] L.K. Saxon, C.H. Turner, Low-dose estrogen treatment suppresses periosteal bone formation in response to mechanical loading, Bone. 39 (2006) 1261–1267. doi:10.1016/j.bone.2006.06.030.
[94] T.L.N. Järvinen, P. Kannus, I. Pajamäki, T. Vuohelainen, J. Tuukkanen, M. Järvinen, H. Sievänen, Estrogen deposits extra mineral into bones of female rats in puberty, but simultaneously seems to suppress the responsiveness of female skeleton to mechanical loading, Bone. 32 (2003) 642–651. doi:10.1016/S8756-3282(03)00100-5.
[95] J.C. Tou, A. Foley, Y. V Yuan, S. Arnaud, C.E. Wade, M. Brown, The effect of ovariectomy combined with hindlimb unloading and reloading on the long bones of mature Sprague-Dawley rats., Menopause. 15 (2008) 494–502. doi:10.1097/gme.0b013e318148bbad.
[96] J.S. Price, T. Sugiyama, G.L. Galea, L.B. Meakin, A. Sunters, L.E. Lanyon, Role of endocrine and paracrine factors in the adaptation of bone to mechanical loading, Curr. Osteoporos. Rep. 9 (2011) 76–82. doi:10.1007/s11914-011-0050-7.
[97] E. Damien, J.S. Price, L.E. Lanyon, Mechanical strain stimulates osteoblast proliferation through the estrogen receptor in males as well as females., J. Bone Miner. Res. 15 (2000) 2169–2177. doi:10.1359/jbmr.2000.15.11.2169.
[98] E. Damien, J.S. Price, L.E. Lanyon, The estrogen receptor's involvement in osteoblasts' adaptive response to mechanical strain., J. Bone Miner. Res. 13 (1998) 1275–1282. doi:10.1359/jbmr.1998.13.8.1275.
[99] V.J. Armstrong, M. Muzylak, A. Sunters, G. Zaman, L.K. Saxon, J.S. Price, L.E. Lanyon, Wnt/β-catenin signaling is a component of osteoblastic bone cell early responses to load-bearing and requires estrogen receptor α, J. Biol. Chem. 282 (2007) 20715–20727. doi:10.1074/jbc.M703224200.
[100] G.L. Galea, L.B. Meakin, T. Sugiyama, N. Zebda, A. Sunters, H. Taipaleenmaki, G.S. Stein, A.J. Van Wijnen, L.E. Lanyon, J.S. Price, Estrogen receptor α mediates proliferation of osteoblastic cells stimulated by estrogen and mechanical strain, but their acute down-regulation of the Wnt antagonist Sost is mediated by estrogen receptor β, J. Biol. Chem. 288 (2013) 9035–9048. doi:10.1074/jbc.M112.405456.
[101] H.L. Jessop, R.F.L. Suswillo, S.C.F. Rawlinson, G. Zaman, K. Lee, V. Das-Gupta, A. a Pitsillides, L.E. Lanyon, Osteoblast-like cells from estrogen receptor alpha knockout mice have deficient responses to mechanical strain., J. Bone Miner. Res. 19 (2004) 938–946. doi:10.1359/JBMR.
[102] G. Zaman, M.Z. Cheng, H.L. Jessop, R. White, L.E. Lanyon, Mechanical strain activates estrogen response elements in bone cells, Bone. 27 (2000) 233–239. doi:10.1016/S8756-3282(00)00324-0.
[103] K.C.L. Lee, H. Jessop, R. Suswillo, G. Zaman, L.E. Lanyon, The adaptive response of bone to mechanical loading in female transgenic mice is deficient in the absence of oestrogen receptor-alpha and -beta., J. Endocrinol. 182 (2004)

193–201. doi:15283680.
[104] K. Lee, H. Jessop, R. Suswillo, G. Zaman, L. Lanyon, Bone adaptation requires oestrogen receptor-alpha, Nature. 424 (2003) 389.
[105] J.W. Chow, S. Fox, C.J. Jagger, T.J. Chambers, Role for parathyroid hormone in mechanical responsiveness of rat bone., Am. J. Physiol. 274 (1998) E146–E154.
[106] J.D. Gardinier, C. Daly-Seiler, N. Rostami, S. Kundal, C. Zhang, Loss of the PTH/PTHrP receptor along the osteoblast lineage limits the anabolic response to exercise, PLoS One. 14 (2019) e0211076. doi:10.1371/journal.pone.0211076.
[107] J. Delgado-Calle, X. Tu, R. Pacheco-Costa, K. McAndrews, R. Edwards, G.G. Pellegrini, K. Kuhlenschmidt, N. Olivos, A. Robling, M. Peacock, L.I. Plotkin, T. Bellido, Control of Bone Anabolism in Response to Mechanical Loading and PTH by Distinct Mechanisms Downstream of the PTH Receptor, J. Bone Miner. Res. 32 (2017) 522–535. doi:10.1002/jbmr.3011.
[108] K.D. Ryder, R.L. Duncan, Parathyroid hormone modulates the response of osteoblast-like cells to mechanical stimulation, Calcif. Tissue Int. 67 (2000) 241–246. doi:10.1007/s002230001115.
[109] Y. Ma, W.S. Jee, Z. Yuan, W. Wei, H. Chen, S. Pun, H. Liang, C. Lin, Parathyroid hormone and mechanical usage have a synergistic effect in rat tibial diaphyseal cortical bone., J. Bone Miner. Res. 14 (1999) 439–48. doi:10.1359/jbmr.1999.14.3.439.
[110] H. Hagino, T. Okano, M.P. Akhter, M. Enokida, R. Teshima, Effect of parathyroid hormone on cortical bone response to in vivo external loading of the rat tibia, J. Bone Miner. Metab. 19 (2001) 244–250. doi:10.1007/s007740170027.
[111] M.D. Roberts, T.J. Santner, R.T. Hart, Local bone formation due to combined mechanical loading and intermittent hPTH-(1-34) treatment and its correlation to mechanical signal distributions, J. Biomech. 42 (2009) 2431–2438. doi:10.1016/j.jbiomech.2009.08.030.
[112] T. Sugiyama, L.K. Saxon, G. Zaman, A. Moustafa, A. Sunters, J.S. Price, L.E. Lanyon, Mechanical loading enhances the anabolic effects of intermittent parathyroid hormone (1-34) on trabecular and cortical bone in mice, Bone. 43 (2008) 238–248. doi:10.1016/j.bone.2008.04.012.
[113] L.B. Meakin, H. Todd, P.J. Delisser, G.L. Galea, A. Moustafa, L.E. Lanyon, S.H. Windahl, J.S. Price, Parathyroid hormone's enhancement of bones' osteogenic response to loading is affected by ageing in a dose- and time-dependent manner, Bone. 98 (2017) 59–67. doi:10.1016/j.bone.2017.02.009.
[114] D.B. Jepsen, J. Ryg, S. Hansen, N.R. Jørgensen, J. Gram, T. Masud, The combined effect of Parathyroid hormone (1–34) and whole-body Vibration exercise in the treatment of postmenopausal OSteoporosis (PaVOS study): a randomized controlled trial, Osteoporos. Int. 30 (2019) 1827–1836. doi:10.1007/s00198-019-05029-z.
[115] A. Miyauchi, K. Notoya, Y. Mikuni-Takagaki, Y. Takagi, M. Goto, Y. Miki, T. Takano-Yamamoto, K. Jinnai, K. Takahashi, M. Kumegawa, K. Chihara, T. Fujita, Parathyroid hormone-activated volume-sensitive calcium influx

pathways in mechanically loaded osteocytes, J. Biol. Chem. 275 (2000) 3335–3342. doi:10.1074/jbc.275.5.3335.
[116] J. Li, R.L. Duncan, D.B. Burr, V.H. Gattone, C.H. Turner, Parathyroid hormone enhances mechanically induced bone formation, possibly involving L-type voltage-sensitive calcium channels, Endocrinology. 144 (2003) 1226–1233. doi:10.1210/en.2002-220821.
[117] K.M. Melville, N.H. Kelly, G. Surita, D.B. Buchalter, J.C. Schimenti, R.P. Main, F.P. Ross, M.C.H. Van Der Meulen, Effects of Deletion of ERα in Osteoblast-Lineage Cells on Bone Mass and Adaptation to Mechanical Loading Differ in Female and Male Mice, J. Bone Miner. Res. 30 (2015) 1468–1480. doi:10.1002/jbmr.2488.

Chapter 2

MOUSE MODELS TO EVALUATE THE ROLE OF ESTROGEN RECEPTOR ALPHA IN SKELETAL MAINTENANCE AND ADAPTATION

The following chapter is published in the *Annals of the New York Academy of Sciences* and reprinted here with permission. The reference to the published work is:

A.M. Rooney, M.C.H. van der Meulen, Mouse models to evaluate the role of estrogen receptor α in skeletal maintenance and adaptation, Ann. N. Y. Acade. Sci. 1410 (2017) 85-92. doi:10.1111/nyas.13523.

2.1 Introduction

Bone mass and strength are influenced by a complex network of factors throughout life. Estrogen signaling and mechanical loading are two key skeletal regulators. Estrogen signaling during puberty regulates skeletal growth, limiting endocortical resorption and periosteal expansion in females and contributing to radial expansion in males [1,2]. Later in life, decreasing levels of bioavailable estrogen with age cause reductions in bone mass that often lead to osteoporosis and increased risk of fracture [3–6]. Women are particularly affected at the onset of menopause, when the loss of estrogen leads to increased bone turnover, disproportionately increased levels of resorption, and deteriorated skeletal structure, changes that can be attenuated by estrogen supplementation [3].

In addition to estrogen signaling, skeletal homeostasis is maintained by mechanical loading. Bone tissue senses and adapts to its mechanical environment,

increasing mass in response to dynamic loading and decreasing mass in response to disuse in adults [7,8]. In humans, mechanical loading through exercise increases bone mass [9–12]. Understanding the mechanisms responsible for the anabolic skeletal response to loading may provide new targets for drug therapies to treat diseases such as osteoporosis.

The interaction of estrogen signaling and mechanical loading also affects bone mass. In clinical studies, pre- and postmenopausal women have different skeletal responses to exercise that are further influenced by estrogen supplementation. Postmenopausal women had negligible changes in bone mass following exercise, whereas exercise significantly increased the bone mass of premenopausal women [13,14]. However, because mechanical responsiveness decreases with age [15,16], determining whether these differences were due solely to estrogen status is difficult. Estrogen treatment and exercise increased bone mass more than exercise alone among postmenopausal women, but how these differences compare to premenopausal women is unclear [17].

Animal models of menopause and hormone depletion are useful tools for studying the role of estrogen and other hormones in mechanical adaptation, and include ovariectomy (OVX) and orchidectomy (ORX). In rats, for instance, estrogen treatment reduced skeletal responsiveness to exercise and mechanical loading [18], and OVX-induced estrogen loss increased responsiveness [19,20]. Female mice that underwent OVX had similar anabolic responses to loading as their intact controls [21], and loading rescued ORX-induced bone loss in male mice [22]. Although estrogen receptor-beta (ERβ) contributes to skeletal maintenance, alone and in conjunction with

ERα [23,24], estrogen signaling through ERα in particular has been implicated in regulating the *in vivo* response to loading in bone [25,26].

Many *in vitro* studies have investigated the role of ERα in bone cell function and response to mechanical loading [27]. Cultured osteoblasts from wild-type animals exposed to ER modulators had a reduced or absent proliferative response to mechanical stimulation [28–31], as did cells obtained from global ERα knockout mice [30,32]. *In vitro* ERα regulated osteoclast function and lifespan rather than differentiation [33]. Although *in vitro* mechanical loading studies provide valuable signaling information, the findings do not always capture the responses seen *in vivo*. *In vivo* adaptation to mechanical loading can be reduced [21,34], increased [35–37], or unchanged [38,39] depending on the ERα model used. Therefore, genetic mouse models have become an important tool for studying specific roles of ERα and bone adaptation *in vivo*.

Initially, estrogen signaling was studied using mice with global deletion of ERα [40,41]. Female global knockout mice had increased cortical and cancellous bone mass and a reduced response to loading, and male global knockout mice had an increased response to loading [34,35,42,43]. These results did not replicate the bone loss caused by disrupted estrogen signaling seen clinically in postmenopausal women. Global ERα deletion resulted in compensatory increases in body weight and serum estrogen levels and decreases in serum IGF-1 levels, all of which independently regulate bone mass [35,42,44]. These confounding effects may explain the discrepancies between mouse models and postmenopausal women. In contrast, bone-specific conditional knockout mice have fewer confounding systemic changes and

better model human effects of estrogen loss. The effects of global ERα deletion have been reviewed elsewhere [45]. Here, we will review insights gained from animal models concerning the function of ERα, focusing on cell-specific ERα knockout (ERαKO) mice and their response to mechanical loading.

2.2 Changes in Skeletal Phenotype with Cell-Specific ERα Deletion

Given the well-established confounding systemic skeletal effects with germline ERαKO mice, cell-specific ERαKO mice were developed to isolate the effects of ERα on bone. Cell-specific knockouts rely on the Cre-lox system [40,46], in which the ERα gene is only deleted from cells expressing a specified promoter [2]. Using cell-specific promoters, ERα has been deleted from mesenchymal progenitors via the *Prx1* promoter (Prx1-ERαKO) [47], osteoblast progenitors via the *Osx1* promoter (Osx1-ERαKO) [47], osteoblasts via the *Col1a1* promoter (Col1a1-ERαKO) [47], mature osteoblasts via the *OC* promoter (OC-ERαKO) [36,38,48–50], osteocytes using the

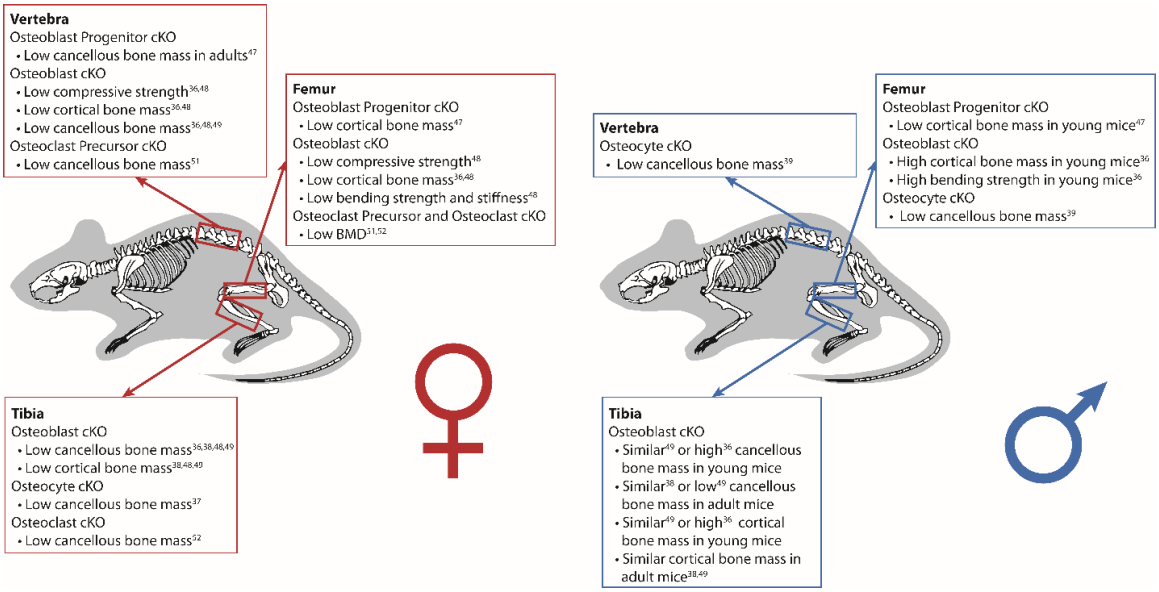

Figure 2.1 The *in vivo* skeletal effects of cell-specific ERα gene deletion in mice by anatomical location in females and males. ckO, conditional knockout.

Dmp1 promoter (Dmp1-ERαKO) [37,39], osteoclast precursors via the *LysM* promoter (LysM-ERαKO) [51], and osteoclasts via the *Ctsk* promoter (Ctsk-ERαKO) [52]. The skeletal phenotype of these deletions depends on the stage at which ERα was deleted, and skeletal location of interest (Table 2.1, Figure 2.1).

Table 2.1 In vivo skeletal effects of cell-specific ERα deletion in mice

Cell Type and Promoter	Sex	Age	Cortical Bone Mass	Cancellous Bone Mass	Response to Loading	Reference(s)
Osteoblast progenitors						
Prx1	F	2m	↓	=		47
		6m	↓	=		47
	M	2m	↓	=		47
		4m	=	=		47
Osx1	F	6m	↓	=		47
Osteoblasts						
Col1a1	F	3m	=	=		47
		6m	=	=		47
OC	F	3m	↓	↓	↑	36,48,49
		6m	↓ or =	↓	=	38,49
		12m	↓	↓		49
	M	3m	= or ↑	= or ↑	=	36,49
		6m	=	↓ or =	=	38,49
		12m	=	=		49
Osteocytes						
Dmp1	F	3m	=	↓ or =	= (Ct) or ↑ (Cn)	37,39
	M	3m	=	↓ or =		37,39
Osteoclast precursors						
LysM	F	3m	=	=		51
		6m	=	↓		51
Osteoclasts						
Ctsk	F	3m	=	↓		52
	M	3m	=	=		52
Neurons						
Nestin	F	3m	↑	↑		56,57
		6m	↑	↑		56,57

↓, lower in ERα gene knockout mice; ↑, higher in ERα knockout mice; =, no difference in ERα knockout mice; Ct, cortical bone; Cn, cancellous bone.

ERα in osteoblast-lineage cells did not appear to play an integral role in the maintenance of cancellous bone until the cells were further differentiated, but was required for cortical bone maintenance in early stage osteoblasts. However, these effects were sex-dependent. ERα in mature osteoblasts maintained cortical and cancellous bone mass during growth and into adulthood in female mice, but had a less clear role in male mice. Adult male mice likely do not require ERα to maintain normal bone mass, and ERα may inhibit bone growth in young male mice.

Deletion of ERα from osteoblast progenitors caused skeletal changes in both male and female mice. Cancellous bone mass was not different in growing Prx1-ERαKO males or females at 8 weeks of age, but cortical thickness was reduced for both sexes [47]. In female conditional knockout mice, the thinner cortex resulted from decreased periosteal mineral apposition rates rather than the extent of mineralizing surface. Aging caused sex-dependent phenotypic changes in Prx1-ERαKO mice. At 18 weeks, skeletally mature male Prx1-ERαKO male mice had similar cortical and cancellous bone mass compared to their controls. Female Prx1-ERαKO mice, on the other hand, continued to display reduced cortical thickness up to 28 weeks of age. Similarly, adult female Osx1-ERαKO mice had reduced cortical thickness but similar cancellous bone mass as their controls [47]. Thus, ERα in osteoblast progenitors may be important in maintaining cortical bone but not cancellous bone, with only a temporary role in males during growth.

Two promoters, *Col1a1* and *OC*, are available to delete ERα from osteoblasts at different stages of maturation and produce different phenotypes. Deletion via the *Col1a1* promoter did not result in any differences in cortical or cancellous bone mass

in mice of either sex up to 12 weeks of age, or in 26-week-old female mice [47]. However, female mice with increased levels of ERα through constitutively active expression under the *Col1a1* promoter had increased femoral BMD and increased tibial cancellous bone mass at 15 weeks of age [53]. In contrast, growing 12-week-old female OC-ERαKO lacking ERα in mature osteoblasts had decreased cortical and cancellous bone mass [36,48,49]. Cancellous bone mass at the tibial metaphysis was reduced in young female OC-ERαKO mice due to increased trabecular separation, reduced trabecular number, and similar or reduced trabecular thickness [36,49]. In addition to decreased cortical bone mass [48], bone turnover measures were also reduced in young female OC-ERαKO mice. Female conditional knockout mice had fewer active osteoblasts and osteoclasts in the vertebrae, and fewer osteoblasts in the proximal tibia [48,49]. These reductions in bone mass resulted in decreased femoral and vertebral whole bone strength in female OC-ERαKO mice [36,48]. Skeletally mature 18-week-old and 26-week-old female OC-ERαKO mice had skeletal alterations similar to growing knockout mice, including lower cortical and cancellous bone mass than control mice [38,48,49]. At 12 months of age, however, cortical thickness was reduced in knockout female mice, but cancellous bone mass was unaffected [49].

Male OC-ERαKO mice had a different skeletal phenotype than female conditional knockout mice at multiple ages, although conflicting phenotypes have been reported. Growing (12-week-old) male OC-ERαKO mice had similar or greater cortical and cancellous bone mass than controls, which led to greater bending strength of the femur [36,49]. In addition, male conditional knockout mice had lower tibial

endocortical mineralizing surface than controls [36]. Adult (26-week-old) male OC-ERαKO mice had similar cortical bone mass, and similar or decreased cancellous bone mass compared to control mice [38,49]. Decreased cancellous bone mass in 26-week-old male knockout mice was caused by reduced trabecular number and increased trabecular separation [49]. In 12-month-old male OC-ERαKO mice cancellous and cortical bone mass were not different from controls [49].

When ERα is removed from osteocytes in Dmp1-ERαKO mice, the effects were primarily limited to cancellous bone. Growing 11- and 12-week-old female and male Dmp1-ERαKO mice had similar or decreased cancellous bone mass compared to their controls, while maintaining normal cortical bone mass [37,39]. In reports of reduced cancellous bone mass in males and females, the reduction was accompanied by fewer or less active osteoblasts and subsequent decreases in mineral apposition rate, mineralized surface, and bone formation rate [37,39]. However, measures of osteoclast function were unchanged by osteocyte ERα deletion, indicating that cancellous bone loss resulting from Dmp1-ERαKO was caused by reduced formation rather than increased resorption [37,39].

In addition to its role in osteoblast-lineage cells, ERα influences bone mass through osteoclasts and their precursors. Female osteoclast precursor ERα knockout mice, LysM-ERαKO, had increased osteoclast numbers in vertebral cancellous bone in growing (12-week-old) mice and adult (28-week-old) mice, and decreased cancellous bone mass at 28 weeks of age [51]. The reduced bone mass was due to decreased trabecular width and number, and increased trabecular separation. Measures of osteoblast number and activity were not different between LysM-ERαKO females and

their controls [51], suggesting that the cancellous bone deficiency was due to the increased number of osteoclasts rather than insufficient formation. Loss of ERα in osteoclast precursors did not affect cortical bone mass [51]. ERα deletion from mature osteoclasts caused similar skeletal effects in Ctsk-ERαKO mice. Growing (12-week-old) female Ctsk-ERαKO mice had reduced tibial cancellous bone mass and increased eroded surface and osteoclast number [52]. Osteoblast number and mineralizing surface were not affected by the conditional knockout, although mineral apposition rate and bone formation rate were both greater in Ctsk-ERαKO animals. In contrast, 12-week-old male Ctsk-ERαKO mice had skeletal phenotypes and bone cell activity levels similar to their wild type controls [52]. One mechanism whereby ERα in osteoclasts may regulate bone mass is through HIF1α destabilization. HIF1α stabilization in osteoclasts following estrogen loss promotes osteoclast activation and leads to decreased bone mass [54]. The decreased cancellous bone mass and increased osteoclastogenesis in female Ctsk-ERαKO mice was rescued when HIF1α was also conditionally deleted from osteoclasts, indicating that HIF1α is critical to the mechanism of ERα-related skeletal maintenance [55]. Overall, ERα in osteoclast-lineage cells may regulate cancellous but not cortical bone mass in females by limiting bone resorption via HIF1α destabilization, and may not influence bone mass in males at all.

Interestingly, bone mass is also regulated by ERα in non-skeletal cells. Recently, ERα deletion from hypothalamic proopiomelanocortin (POMC) neurons in 3- and 6-month-old female mice using nestin-Cre (nestin-ERαKO) increased cortical and cancellous bone mass at the femur, tibia, and vertebrae, and mechanical strength

in the femur [56,57]. Following OVX, cancellous bone loss was greater in nestin-ERαKO mice than that of OVX control mice, as was the anabolic response to estrogen treatment. Therefore, ERα may also influence bone mass via signaling from the central nervous system.

ERα has a variable effect on the skeleton depending on the lineage and stage of development of the cell lineage of interest. ERα in osteoclasts and their precursors helps regulate cancellous bone mass in females. Osteoblast progenitors require ERα to maintain cortical bone mass, mature osteoblasts require ERα to maintain cortical and cancellous bone mass, and osteocytes require ERα to maintain cancellous bone mass.

2.3 Adaptation to Mechanical Loading in Cell-Specific ERα Knockout Mice

While more data are emerging about the phenotypic changes that occur with ERα deletion at the different stages of bone cell lineage, less is known about how cell-specific ERα deletion affects mechanical adaptation of bone. To date, *in vivo* mechanical loading studies on cell-specific ERαKO mice have been limited to osteoblast-specific knockout mice and osteocyte-specific knockout mice (Table 2.1) [36–39,50].

Although growing female osteoblast-specific OC-ERαKO mice had reduced bone mass [36,48,49], these animals responded more robustly to mechanical loading compared to their littermate controls. Following two weeks of cyclic tibial compression, young female OC-ERαKO showed greater increases in both cancellous and cortical bone mass, specifically metaphyseal cancellous bone volume fraction and trabecular thickness, metaphyseal cortical shell thickness and minimum moment of

inertia, and midshaft cortical area, maximum and minimum moment of inertia [36]. The loading-induced structural changes in young female OC-ERαKO mice corresponded to greater loading-induced increases in cancellous mineralizing surface and mineral apposition rate, although changes in cortical bone cell activity were not affected by ERα deletion [36]. A contributing factor to the cancellous-specific loading-induced bone cell activity changes may have been differences in transcriptional response by bone envelope. RNA sequencing following a single session of cyclic tibial compression revealed that 10-week-old female OC-ERαKO mice had more genes differentially expressed in cancellous bone, but fewer genes differentially expressed in cortical bone compared to control mice [50]. In cancellous bone, more genes involved in the Wnt signaling pathway were differentially expressed in OC-ERαKO mice than controls, including upregulation of *Rspo4* and *Wnt7b*. Greater cancellous transcriptional response of the Wnt pathway may explain why loading increased bone mass to a greater extent in OC-ERαKO female mice, particularly in cancellous bone. In contrast with 10-week-old female OC-ERαKO mice, 10-week-old male and 26-week-old male and female OC-ERαKO mice had similar responses to tibial mechanical loading as control mice [36,38], indicating an age- and sex-dependent role for osteoblast ERα in mechanical adaptation.

Deletion of ERα from osteocytes in 3-month-old female Dmp1-ERαKO mice also had a more pronounced effect on the response to loading in cancellous bone than cortical bone. Two weeks of cyclic tibial loading resulted in similar cortical anabolic responses in Dmp1-ERαKO and wild type mice at the tibial midshaft [39]. Similarly, four weeks of unloading via hindlimb suspension beginning at eight weeks of age led

to similar decreases in bone area and Ct.Th at the femoral midshaft in female mice, although cortical volumetric BMD decreased less in Dmp1-ERαKO mice [37]. In cancellous bone at the distal metaphysis of the femur however, osteocyte-specific knockout female mice had greater decreases in bone mass with hindlimb unloading than wild type controls.

Taken together, ERα in osteoblasts and osteocytes may either suppress the skeletal response to mechanical loading, particularly in cancellous bone, or may not be required for functional adaptation. Although global ERα knockout mice had a reduced cortical response to loading in female mice, indicating a positive role of ERα in adaptation, it is uncertain whether this result was driven by ERα deletion from bone cells or one of the many confounding factors discussed previously [34,35,43]. To obtain a clearer understanding of the role of ERα in skeletal adaptation, further work needs to be done in bone cell and other cell-specific ERα knockout mice.

2.4 Conclusions & Future Directions

ERα has an important role in both skeletal maintenance and adaptation to mechanical loading. The precise nature of these roles is still unclear, but genetic mouse models have helped elucidate how ERα functions in bone cells. Bone cell-specific ERα knockout mice isolate the effects of disrupted ERα signaling to bone, eliminating confounding systemic factors present in global ERα knockout models. Through these animal models we have discovered that ERα plays a particularly important role in maintaining cancellous bone mass, especially in females, and may reduce the skeleton's ability to adapt to mechanical loads.

However, much still remains unknown about the role of estrogen signaling in bone health. More work is needed to understand the effects of disrupted ERα signaling on mechanical adaptation in both males and females of all ages. Furthermore, the molecular mechanisms behind these changes are largely unknown. Many previous mechanistic studies have focused on functional adaptation and ERα signaling *in vitro*, and although these experiments provide an excellent starting point for identifying molecular targets, they need to be expanded to more applicable *in vivo* models to be verified. Recent *in vivo* investigations have provided useful information regarding the estrogenic responses of ERα [58,59], however the mechanism whereby ERα alters responses during skeletal adaptation is still unclear.

Investigating relevant signaling pathways and molecules in cell-specific ERα knockout mice will provide valuable insights into potential treatments for osteoporosis, such as selective estrogen receptor modulators (SERMs). Clinically, SERMs have been used extensively to prevent and treat osteoporosis, breast cancer, and other postmenopausal health concerns. Individual SERMs can act as estrogen agonists or antagonists in different tissues, most likely due to differences in receptor complex conformational changes [60,61]. Although the relationship between SERMs and ERα has been extensively investigated [62–64], understanding the molecular mechanisms that result in these drug- and tissue-specific effects could benefit from the use of conditional ERα knockout mice. Tissue-specific mouse models can help screen potential new therapies that provide bone-specific benefits with reduced off-target effects. Additionally, *in vivo* mechanical loading in these models will provide

important data on potential synergistic benefits of combining exercise with SERM treatments during menopause.

Conditional knockout models provide a valuable experimental platform that can be expanded into many areas of research, including prevention, development, and treatment of diseases such as osteoporosis. The results to date demonstrate the importance of ERα signaling to the acquisition of bone mass and will provide valuable mechanistic insights for future therapies.

2.5 References

[1] F. Callewaert, M. Sinnesael, E. Gielen, S. Boonen, D. Vanderschueren, Skeletal sexual dimorphism: Relative contribution of sex steroids, GH-IGF1, and mechanical loading, J. Endocrinol. 207 (2010) 127–134. doi:10.1677/JOE-10-0209.

[2] M. Almeida, M.R. Laurent, V. Dubois, F. Claessens, C.A. O'Brien, R. Bouillon, D. Vanderschueren, S.C. Manolagas, Estrogens and Androgens in Skeletal Physiology and Pathophysiology, Physiol. Rev. 97 (2017) 135–187. doi:10.1152/physrev.00033.2015.

[3] B.L. Riggs, Endocrine causes of age-related bone loss and osteoporosis, Novartis Found. Symp. 242 (2002) 247–264.

[4] L.S. Richelson, H.W. Wahner, L.J. Melton III, B.L. Riggs, Relative contributions of aging and estrogen deficiency to postmenopausal bone loss, N. Engl. J. Med. 311 (1984) 1273–1275.

[5] S. Khosla, S. Amin, E. Orwoll, Osteoporosis in men, Endocr. Rev. 29 (2008) 441–464. doi:10.1210/er.2008-0002.

[6] F. Callewaert, S. Boonen, D. Vanderschueren, Sex steroids and the male skeleton: a tale of two hormones, Trends Endocrinol. Metab. 21 (2010) 89–95. doi:10.1016/j.tem.2009.09.002.

[7] H. Jones, J. Priest, W. Hayes, C. Tichenor, D. Nagel, Humeral hypertrophy in response to exercise, J. Bone Jt. Surg. 59 (1977) 204–208.

[8] T. Cervinka, H. Sievänen, J. Hyttinen, J. Rittweger, Bone loss patterns in cortical, subcortical, and trabecular compartments during simulated microgravity., J. Appl. Physiol. 117 (2014) 80–8. doi:10.1152/japplphysiol.00021.2014.

[9] R.K. Fuchs, J.J. Bauer, C.M. Snow, Jumping improves hip and lumbar spine bone mass in prepubescent children: a randomized controlled trial., J. Bone Miner. Res. 16 (2001) 148–156. doi:10.1359/jbmr.2001.16.1.148.

[10] S. Kontulainen, H. Sievänen, P. Kannus, M. Pasanen, I. Vuori, Effect of long-term impact-loading on mass, size, and estimated strength of humerus and radius of female racquet-sports players: a peripheral quantitative computed tomography study between young and old starters and controls., J. Bone Miner. Res. 18 (2003) 352–359. doi:10.1359/jbmr.2003.18.2.352.

[11] A. Vainionpää, R. Korpelainen, J. Leppäluoto, T. Jämsä, Effects of high-impact exercise on bone mineral density: A randomized controlled trial in premenopausal women, Osteoporos. Int. 16 (2005) 191–197. doi:10.1007/s00198-004-1659-5.

[12] K.M. Winters-Stone, C.M. Snow, Site-specific response of bone to exercise in premenopausal women, Bone. 39 (2006) 1203–1209. doi:10.1016/j.bone.2006.06.005.

[13] E.J. Bassey, M.C. Rothwell, J.J. Littlewood, D.W. Pye, Pre- and postmenopausal women have different bone mineral density responses to the same high-impact exercise., J. Bone Miner. Res. 13 (1998) 1805–1813. doi:10.1359/jbmr.1998.13.12.1805.

[14] K.-Z. Kim, A. Shin, J. Lee, S.-K. Myung, J. Kim, The Beneficial Effect of

Leisure-Time Physical Activity on Bone Mineral Density in Pre- and Postmenopausal Women, Calcif. Tissue Int. 91 (2012) 178–185. doi:10.1007/s00223-012-9624-3.
[15] N. Holguin, M.D. Brodt, M.E. Sanchez, M.J. Silva, Aging diminishes lamellar and woven bone formation induced by tibial compression in adult C57BL/6, Bone. 65 (2014) 83–91. doi:10.1016/j.bone.2014.05.006.
[16] M.E. Lynch, R.P. Main, Q. Xu, T.L. Schmicker, M.B. Schaffler, T.M. Wright, M.C.H. van der Meulen, Tibial compression is anabolic in the adult mouse skeleton despite reduced responsiveness with aging, Bone. 49 (2011) 439–446. doi:10.1016/j.bone.2011.05.017.
[17] R. Zhao, Z. Xu, M. Zhao, Effects of Oestrogen Treatment on Skeletal Response to Exercise in the Hips and Spine in Postmenopausal Women: A Meta-Analysis, Sport. Med. 45 (2015) 1163–1173. doi:10.1007/s40279-015-0338-3.
[18] L.K. Saxon, C.H. Turner, Low-dose estrogen treatment suppresses periosteal bone formation in response to mechanical loading, Bone. 39 (2006) 1261–1267. doi:10.1016/j.bone.2006.06.030.
[19] T.L.N. Järvinen, P. Kannus, I. Pajamäki, T. Vuohelainen, J. Tuukkanen, M. Järvinen, H. Sievänen, Estrogen deposits extra mineral into bones of female rats in puberty, but simultaneously seems to suppress the responsiveness of female skeleton to mechanical loading, Bone. 32 (2003) 642–651. doi:10.1016/S8756-3282(03)00100-5.
[20] J.C. Tou, A. Foley, Y. V Yuan, S. Arnaud, C.E. Wade, M. Brown, The effect of ovariectomy combined with hindlimb unloading and reloading on the long bones of mature Sprague-Dawley rats., Menopause. 15 (2008) 494–502. doi:10.1097/gme.0b013e318148bbad.
[21] S.H. Windahl, L. Saxon, A.E. Börjesson, M.K. Lagerquist, B. Frenkel, P. Henning, U.H. Lerner, G.L. Galea, L.B. Meakin, C. Engdahl, K. Sjögren, M.C. Antal, A. Krust, P. Chambon, L.E. Lanyon, J.S. Price, C. Ohlsson, Estrogen receptor-α is required for the osteogenic response to mechanical loading in a ligand-independent manner involving its activation function 1 but not 2, J. Bone Miner. Res. 28 (2013) 291–301. doi:10.1002/jbmr.1754.
[22] J.C. Fritton, E.R. Myers, T.M. Wright, M.C. van der Meulen, Bone Mass Is Preserved and Cancellous Architecture Altered Due to Cyclic Loading of the Mouse Tibia After Orchidectomy, J. Bone Miner. Res. 23 (2008) 663–671. doi:10.1359/jbmr.080104.
[23] K.M. Nicks, K. Fujita, D. Fraser, U. McGregor, M.T. Drake, M.E. McGee-Lawrence, J.J. Westendorf, D.G. Monroe, S. Khosla, Deletion of Estrogen Receptor Beta in Osteoprogenitor Cells Increases Trabecular but Not Cortical Bone Mass in Female Mice, J. Bone Miner. Res. 31 (2016) 606–614. doi:10.1002/jbmr.2723.
[24] A.B. Khalid, S.A. Krum, Estrogen receptors alpha and beta in bone, Bone. 87 (2016) 130–135. doi:10.1016/j.bone.2016.03.016.
[25] K. Lee, L. Lanyon, Mechanical loading influences bone mass through estrogen receptor α, Exerc. Sport Sci. Rev. 32 (2004) 64–68. http://discovery.ucl.ac.uk/183482/.
[26] P.J. Ehrlich, B.S. Noble, H.L. Jessop, H.Y. Stevens, J.R. Mosley, L.E. Lanyon,

The effect of in vivo mechanical loading on estrogen receptor alpha expression in rat ulnar osteocytes, J Bone Min. Res. 17 (2002) 1646–1655. doi:10.1359/jbmr.2002.17.9.1646.

[27] J.S. Price, T. Sugiyama, G.L. Galea, L.B. Meakin, A. Sunters, L.E. Lanyon, Role of endocrine and paracrine factors in the adaptation of bone to mechanical loading, Curr. Osteoporos. Rep. 9 (2011) 76–82. doi:10.1007/s11914-011-0050-7.

[28] E. Damien, J.S. Price, L.E. Lanyon, Mechanical strain stimulates osteoblast proliferation through the estrogen receptor in males as well as females., J. Bone Miner. Res. 15 (2000) 2169–2177. doi:10.1359/jbmr.2000.15.11.2169.

[29] E. Damien, J.S. Price, L.E. Lanyon, The estrogen receptor's involvement in osteoblasts' adaptive response to mechanical strain., J. Bone Miner. Res. 13 (1998) 1275–1282. doi:10.1359/jbmr.1998.13.8.1275.

[30] V.J. Armstrong, M. Muzylak, A. Sunters, G. Zaman, L.K. Saxon, J.S. Price, L.E. Lanyon, Wnt/β-catenin signaling is a component of osteoblastic bone cell early responses to load-bearing and requires estrogen receptor α, J. Biol. Chem. 282 (2007) 20715–20727. doi:10.1074/jbc.M703224200.

[31] G.L. Galea, L.B. Meakin, T. Sugiyama, N. Zebda, A. Sunters, H. Taipaleenmaki, G.S. Stein, A.J. Van Wijnen, L.E. Lanyon, J.S. Price, Estrogen receptor α mediates proliferation of osteoblastic cells stimulated by estrogen and mechanical strain, but their acute down-regulation of the Wnt antagonist Sost is mediated by estrogen receptor β, J. Biol. Chem. 288 (2013) 9035–9048. doi:10.1074/jbc.M112.405456.

[32] H.L. Jessop, R.F.L. Suswillo, S.C.F. Rawlinson, G. Zaman, K. Lee, V. Das-Gupta, A. a Pitsillides, L.E. Lanyon, Osteoblast-like cells from estrogen receptor alpha knockout mice have deficient responses to mechanical strain., J. Bone Miner. Res. 19 (2004) 938–946. doi:10.1359/JBMR.

[33] Y. Imai, M.Y. Youn, S. Kondoh, T. Nakamura, A. Kouzmenko, T. Matsumoto, I. Takada, K. Takaoka, S. Kato, Estrogens maintain bone mass by regulating expression of genes controlling function and life span in mature osteoclasts, Ann. N. Y. Acad. Sci. 1173 (2009) 31–39. doi:10.1111/j.1749-6632.2009.04954.x.

[34] K.C.L. Lee, H. Jessop, R. Suswillo, G. Zaman, L.E. Lanyon, The adaptive response of bone to mechanical loading in female transgenic mice is deficient in the absence of oestrogen receptor-alpha and -beta., J. Endocrinol. 182 (2004) 193–201. doi:15283680.

[35] L.K. Saxon, G. Galea, L. Meakin, J. Price, L.E. Lanyon, Estrogen receptors α and β have different gender-dependent effects on the adaptive responses to load bearing in cancellous and cortical bone, Endocrinology. 153 (2012) 2254–2266. doi:10.1210/en.2011-1977.

[36] K.M. Melville, N.H. Kelly, G. Surita, D.B. Buchalter, J.C. Schimenti, R.P. Main, F.P. Ross, M.C.H. Van Der Meulen, Effects of Deletion of ERα in Osteoblast-Lineage Cells on Bone Mass and Adaptation to Mechanical Loading Differ in Female and Male Mice, J. Bone Miner. Res. 30 (2015) 1468–1480. doi:10.1002/jbmr.2488.

[37] S. Kondoh, K. Inoue, K. Igarashi, H. Sugizaki, Y. Shirode-Fukuda, E. Inoue, T.

Yu, J.K. Takeuchi, J. Kanno, L.F. Bonewald, Y. Imai, Estrogen receptor α in osteocytes regulates trabecular bone formation in female mice, Bone. 60 (2014) 68–77. doi:10.1016/j.bone.2013.12.005.
[38] A.M. Rooney, O.O. Adebayo, N.H. Kelly, J.C. Schimenti, F.P. Ross, M.C.H. Van Der Meulen, Gender-Dependent Effects of ERα Deletion from Mature Osteoblasts on Bone Adaptation in Adult Mice, Trans Orthop Res Soc. 42 (2017) 1671.
[39] S.H. Windahl, A.E. Börjesson, H.H. Farman, C. Engdahl, S. Movérare-Skrtic, K. Sjögren, M.K. Lagerquist, J.M. Kindblom, A. Koskela, J. Tuukkanen, P. Divieti Pajevic, J.Q. Feng, K. Dahlman-Wright, P. Antonson, J.-Å. Gustafsson, C. Ohlsson, Estrogen receptor-α in osteocytes is important for trabecular bone formation in male mice., Proc. Natl. Acad. Sci. U. S. A. 110 (2013) 2294–9. doi:10.1073/pnas.1220811110.
[40] S. Dupont, A. Krust, A. Gansmuller, A. Dierich, P. Chambon, M. Mark, Effect of single and compound knockouts of estrogen receptors alpha (ERalpha) and beta (ERbeta) on mouse reproductive phenotypes., Development. 127 (2000) 4277–4291.
[41] D.B. Lubahn, J.S. Moyer, T.S. Golding, J.F. Couse, K.S. Korach, O. Smithies, Alteration of reproductive function but not prenatal sexual development after insertional disruption of the mouse estrogen receptor gene., Proc. Natl. Acad. Sci. U. S. A. 90 (1993) 11162–6. doi:10.1073/pnas.90.23.11162.
[42] M.K. Lindberg, S.L. Alatalo, J.M. Halleen, S. Mohan, J.-Å. Gustafsson, C. Ohlsson, Estrogen receptor specificity in the regulation of the skeleton in female mice, J. Endocrinol. 171 (2001) 229–236.
[43] K. Lee, H. Jessop, R. Suswillo, G. Zaman, L. Lanyon, Bone adaptation requires oestrogen receptor-alpha, Nature. 424 (2003) 389.
[44] V. Parikka, Z. Peng, T. Hentunen, J. Risteli, T. Elo, H.K. Väänänen, P. Härkönen, Estrogen responsiveness of bone formation in vitro and altered bone phenotype in aged estrogen receptor-α-deficient male and female mice, Eur. J. Endocrinol. 152 (2005) 301–314. doi:10.1530/eje.1.01832.
[45] L. Vico, J.M. Vanacker, Sex hormones and their receptors in bone homeostasis: Insights from genetically modified mouse models, Osteoporos. Int. 21 (2010) 365–372. doi:10.1007/s00198-009-0963-5.
[46] P.C. Orban, D. Chui, J.D. Marth, Tissue- and site-specific DNA recombination in transgenic mice., Proc. Natl. Acad. Sci. U. S. A. 89 (1992) 6861–5. doi:10.1073/pnas.89.15.6861.
[47] M. Almeida, S. Iyer, M. Martin-Millan, S.M. Bartell, L. Han, E. Ambrogini, M. Onal, J. Xiong, R.S. Weinstein, R.L. Jilka, C.A. O'Brien, S.C. Manolagas, Estrogen receptor-α signaling in osteoblast progenitors stimulates cortical bone accrual, J. Clin. Invest. 123 (2013) 394–404. doi:10.1172/JCI65910.
[48] K.M. Melville, N.H. Kelly, S. a Khan, J.C. Schimenti, F.P. Ross, R.P. Main, M.C. van der Meulen, Female mice lacking estrogen receptor-alpha in osteoblasts have compromised bone mass and strength, J Bone Min. Res. 29 (2014) 370–379. doi:10.1002/jbmr.2082.
[49] J.A. Määttä, K.G. Büki, G. Gu, M.H. Alanne, J. Vääräniemi, H. Liljenbäck, M. Poutanen, P. Härkönen, K. Väänänen, Inactivation of estrogen receptor α in

bone-forming cells induces bone loss in female mice, FASEB J. 27 (2013) 478–488. doi:10.1096/fj.12-213587.

[50] N.H. Kelly, J.C. Schimenti, F.P. Ross, M.C.H. van der Meulen, Female mice lacking estrogen receptor alpha in mature osteoblasts have an increased transcriptional response to mechanical loading in cancellous but not cortical bone, Trans Orthop Res Soc. 42 (2017) 776.

[51] M. Martin-Millan, M. Almeida, E. Ambrogini, L. Han, H. Zhao, R.S. Weinstein, R.L. Jilka, C. a O'Brien, S.C. Manolagas, The estrogen receptor-alpha in osteoclasts mediates the protective effects of estrogens on cancellous but not cortical bone., Mol. Endocrinol. 24 (2010) 323–34. doi:10.1210/me.2009-0354.

[52] T. Nakamura, Y. Imai, T. Matsumoto, S. Sato, K. Takeuchi, K. Igarashi, Y. Harada, Y. Azuma, A. Krust, Y. Yamamoto, H. Nishina, S. Takeda, H. Takayanagi, D. Metzger, J. Kanno, K. Takaoka, T.J. Martin, P. Chambon, S. Kato, Estrogen Prevents Bone Loss via Estrogen Receptor α and Induction of Fas Ligand in Osteoclasts, Cell. 130 (2007) 811–823. doi:10.1016/j.cell.2007.07.025.

[53] K. Ikeda, T. Tsukui, K. Horie-Inoue, S. Inoue, Conditional expression of constitutively active estrogen receptor α in osteoblasts increases bone mineral density in mice, FEBS Lett. 585 (2011) 1303–1309. doi:10.1016/j.febslet.2011.03.038.

[54] T. Miyamoto, Mechanism underlying post-menopausal osteoporosis: HIF1α is required for osteoclast activation by estrogen deficiency, Keio J. Med. 64 (2015) 44–47. doi:10.2302/kjm.2015-0003-RE.

[55] Y. Miyauchi, Y. Sato, T. Kobayashi, S. Yoshida, T. Mori, H. Kanagawa, E. Katsuyama, A. Fujie, W. Hao, K. Miyamoto, T. Tando, H. Morioka, M. Matsumoto, P. Chambon, R.S. Johnson, S. Kato, Y. Toyama, T. Miyamoto, HIF1α is required for osteoclast activation by estrogen deficiency in postmenopausal osteoporosis, Proc. Natl. Acad. Sci. 110 (2013) 16568–16573. doi:10.1073/pnas.1308755110/-/DCSupplemental.www.pnas.org/cgi/doi/10.1073/pnas.1308755110.

[56] H.H. Farman, S.H. Windahl, L. Westberg, H. Isaksson, E. Egecioglu, E. Schele, H. Ryberg, J.O. Jansson, J. Tuukkanen, A. Koskela, S.K. Xie, L. Hahner, J. Zehr, D.J. Clegg, M.K. Lagerquist, C. Ohlsson, Female mice lacking estrogen receptor-α in hypothalamic proopiomelanocortin (POMC) neurons display enhanced estrogenic response on cortical bone mass, Endocrinology. 157 (2016) 3242–3252. doi:10.1210/en.2016-1181.

[57] C. Ohlsson, C. Engdahl, A.E. Börjesson, S.H. Windahl, E. Studer, L. Westberg, E. Eriksson, A. Koskela, J. Tuukkanen, A. Krust, P. Chambon, H. Carlsten, M.K. Lagerquist, Estrogen receptor-α expression in neuronal cells affects bone mass., Proc. Natl. Acad. Sci. U. S. A. 109 (2012) 983–8. doi:10.1073/pnas.1111436109.

[58] H.H. Farman, J. Wu, K.L. Gustafsson, S.H. Windahl, S.H. Kim, J.A. Katzenellenbogen, C. Ohlsson, M.K. Lagerquist, Extra-nuclear effects of estrogen on cortical bone in males require ERαAF-1, J. Mol. Endocrinol. 58 (2017) 105–111. doi:10.1530/JME-16-0209.

[59] K.L. Gustafsson, H. Farman, P. Henning, V. Lionikaite, S. Movérare-Skrtic, J. Wu, H. Ryberg, A. Koskela, J.-Å. Gustafsson, J. Tuukkanen, E.R. Levin, C. Ohlsson, M.K. Lagerquist, The role of membrane ERα signaling in bone and other major estrogen responsive tissues., Sci. Rep. 6 (2016) 29473. doi:10.1038/srep29473.

[60] J. V. Pinkerton, S. Thomas, Use of SERMs for treatment in postmenopausal women, J. Steroid Biochem. Mol. Biol. 142 (2014) 142–154. doi:10.1016/j.jsbmb.2013.12.011.

[61] M.R. McClung, New management options for osteoporosis with emphasis on SERMs, Climacteric. 18 (2015) 56–61. doi:10.3109/13697137.2015.1104010doi.org/10.3109/13697137.2015.1104010.

[62] A.E. Börjesson, M.K. Lagerquist, S.H. Windahl, C. Ohlsson, The role of estrogen receptor α in the regulation of bone and growth plate cartilage, Cell. Mol. Life Sci. 70 (2013) 4023–4037. doi:10.1007/s00018-013-1317-1.

[63] A.E. Börjesson, H.H. Farman, S. Movérare-Skrtic, C. Engdahl, M.C. Antal, A. Koskela, J. Tuukkanen, H. Carlsten, A. Krust, P. Chambon, K. Sjögren, M.K. Lagerquist, S.H. Windahl, C. Ohlsson, SERMs have substance-specific effects on bone, and these effects are mediated via ERαAF-1 in female mice., Am. J. Physiol. Endocrinol. Metab. 310 (2016) E912-8. doi:10.1152/ajpendo.00488.2015.

[64] S.J. Han, K. Begum, C.E. Foulds, R.A. Hamilton, S. Bailey, A. Malovannaya, D. Chan, J. Qin, B.W. O'Malley, The Dual Estrogen Receptor α Inhibitory Effects of the Tissue-Selective Estrogen Complex for Endometrial and Breast Safety, Mol. Pharmacol. 89 (2016) 14–26. doi:10.1124/mol.115.100925.

Chapter 3

LACK OF ERα IN MATURE OSTEOBLASTS ALTERS BONE MASS AND ADAPTATION TO MECHANICAL LOADING IN ADULT FEMALE BUT NOT MALE MICE

3.1 Introduction

Estrogen signaling via estrogen receptors (ERs) is an important regulator of bone mass throughout life in both men and women [1,2]. During puberty, estrogen limits endocortical resorption and periosteal expansion in females and may contribute to radial expansion in males [3,4]. Age-related decreases in bioavailable estrogen in women and men result in reduced bone mass and strength that often lead to osteoporosis and an increased risk of fracture [5–8].

Estrogen acts through ERα and ERβ in bone tissue, although ERα in particular influences skeletal homeostasis in both males and females [9,10]. Global knockout of ERα in mouse models causes systemic changes, including altered hormone levels and body mass differences that produce independent skeletal effects and increase bone mass, contradicting the known effects of estrogen loss [11]. Cell-specific ERα knockout mice overcome this limitation and demonstrate varying effects of ERα across age, sex, tissue, and cell type [12]. When ERα was deleted from osteoblast progenitors and precursors, cortical bone mass was reduced in young male and female animals but cancellous bone mass was unchanged [13]. Young female mice lacking ERα in mature osteoblasts had lower cortical and cancellous bone mass, whereas young males had similar or greater bone mass compared to littermate controls [14,15].

However, skeletally-mature adult mice had lower cancellous bone mass in both females and males [15]. Finally, cortical bone was unaffected in young mice lacking ERα in osteocytes, but cancellous bone mass was lower in males and similar or lower in females [16,17]. These somewhat conflicting data provide an incomplete understanding of the function of ERα in skeletal health. Most studies in cell-specific ERα knockout mice focused only on females or young, growing animals. However, confounding effects from longitudinal growth prior to skeletal maturity and sex-based differences in the role of estrogen on skeletal health underscore the need for further investigation into the role of ERα in skeletally-mature animals of both sexes.

The adult skeleton responds to its mechanical environment, increasing bone mass with dynamic loading and decreasing bone mass with disuse [18,19]. ERα has been implicated in the anabolic response of bone to mechanical loading [20–22], but the interaction between loading and ERα has been examined predominantly *in vitro* [23–25], with *in vivo* studies focusing mainly on cortical bone and global knockout models [26–29]. Mechanical adaptation in cell-specific knockout models is still not well understood. Mechanically-induced cortical bone formation was unchanged when ERα was removed at the osteocyte stage in young female mice, but cancellous adaptation was increased [16,17]. ERα deletion from mature osteoblasts increased the response to mechanical loading in young female mice and did not affect the response in young male mice [14]. Of note, these studies were performed on young, growing animals. Clinical evidence suggests that responsiveness to bioavailable estrogen and mechanical loading decreases in adult and elderly individuals [6,30]. Preclinical models also demonstrate decreased mechanical adaptation with age [31–33], and this

loss of responsiveness may alter the roles of ERα and mechanical adaptation in the elderly population most at risk for osteoporosis. However, the relationship between ERα and functional adaptation has not been investigated in skeletally-mature adult animals.

In the present study, we sought to elucidate the role of ERα in bone adaptation to mechanical loading in skeletally-mature adult male and female mice by using mice lacking ERα in mature osteoblasts and osteocytes via the osteocalcin promoter (pOC-ERαKO). Based on our previous results in young mice [14,34], we hypothesized that skeletally-mature adult female pOC-ERαKO mice would have reduced bone mass but a greater response to mechanical loading compared to littermate controls (LC), whereas adult male pOC-ERαKO mice would have greater bone mass and a normal response to mechanical loading. We also hypothesized that greater peak load magnitudes would elicit greater anabolic responses in adult female mice. We subjected 26-week-old male and female mice to 2 weeks of *in vivo* cyclic mechanical loading and analyzed bone mass and architecture using microcomputed tomography (microCT). We found that ERα deletion reduced bone mass in adult female but not male mice, and increased adaptation to loading in females loaded at a high-magnitude peak load level.

3.2 Methods

3.2.1 Generation of osteoblast-specific ERαKO mice (pOC-ERαKO)

Osteoblast-specific ERα knockout and littermate control (LC) mice were generated as previously described [34]. Briefly, mice with loxP sequences flanking

exon 3 of the DNA-binding domain of the ERα gene (*Esr1*) (*ERα*$^{fl/fl}$, provided by Dr. Sohaib Kahn, University of Cincinnati, Cincinnati, OH, USA) [35] were crossed with mice containing a transgene encoding *Cre* recombinase driven by the human osteocalcin promoter (*OC-Cre*, provided by Dr. Thomas Clemens, The Johns Hopkins University, Baltimore, MD, USA) [36,37]. *ERα*$^{fl/fl}$ mice were inbred to be >99% pure C57Bl/6 by speed congenics (DartMouse Speed Congenic Core Facility, Geisel School of Medicine at Dartmouth, Hanover, NH, USA) prior to crossing with *OC-Cre* mice that had previously been inbred to the C57Bl/6 strain. Mice were genotyped using lysed tail PCR as described [34]. Mice were housed 3 to 5 per cage, but males were separated after 2 days due to fighting and housed individually to avoid confounding loading effects [38]. Mice had *ad libitum* access to food and water. All animal procedures were approved by Cornell University's IACUC.

3.2.2 In vivo tibial mechanical loading

The applied peak loads were based on the *in vivo* strains measured in each genotype. At 26 weeks of age, single-element strain gauges (EA-06-015LA-120, Micro-Measurements, Wendell, NC, USA) were surgically attached to the anteromedial surface of the tibial midshafts of a small subset of female and male LC and pOC-ERαKO mice (n=4-5 per genotype). Axial cyclic compressive loads with peak load magnitudes ranging from -2 to -13N were applied to the left and right tibiae in our custom tibial loading device [39,40]. Mice were immediately euthanized following data collection. Using the load and strain data, bone stiffness and the peak load required to induce +1000 microstrain (με) on the anteromedial surface of the

tibial midshaft were calculated as previously described [40]. Bone stiffness was similar between LC and pOC-ERαKO mice within each sex and different between males and females (0.00677 ± 0.0028N/με LC females, 0.00705 ± 0.0043N/με pOC-ERαKO females, 0.0118 ± 0.0045N/με LC males, 0.0149 ± 0.0075N/με pOC-ERαKO males; mean ± SD). Based on the lower female stiffness, peak loads of -6.5N and -13.0N were applied to female and male mice, respectively. To investigate the influence of load magnitude in female adult animals, a second group of 26-week-old female LC and pOC-ERαKO mice were loaded at a -9.0N peak load (n=6 per genotype) to match the load magnitude applied in our previous work in young female mice [14]. Female mice loaded at -6.5N will be referred to as moderate-magnitude and -9.0N will be referred to as high-magnitude.

The left tibiae of 26-week-old male and female LC and pOC-ERαKO mice (n=8-9 per group) were loaded in cyclic compression *in vivo* for 2 weeks, as previously described [40]. Compressive loading was applied at a rate of 4Hz for 1200 cycles per day, 5 days per week, in a triangular waveform with peak loads of -6.5N, -9.0N, or -13.0N described above. A dwell of 100ms at -0.5N was maintained between successive load cycles, and the dwell-to-peak time was 75ms. The right limb served as a contralateral control. Three days after the last session of *in vivo* tibial compression (day 15), mice were euthanized via isoflurane overdose and cardiac puncture.

3.2.3 Microcomputed tomography

Bone morphology was examined using microCT. At euthanasia, left and right tibiae were stored in 4% paraformaldehyde overnight and later scanned in 70%

ethanol at 10μm and 15μm voxel resolution at the metaphysis and diaphysis, respectively (μCT35, Scanco Medical AG; 55kVp, 145μA, 600ms integration time). The metaphysis volume of interest (VOI) was defined as 10% of total tibial length beginning 50μm distal to the growth plate, and the diaphysis VOI was defined as 2.5% of total tibial length centered at the midshaft [34]. Within the metaphysis, the cancellous core and cortical shell were segmented manually and analyzed separately. Outcome measures for cancellous bone were bone volume fraction (BV/TV), trabecular thickness (Tb.Th), separation (Tb.Sp), and number (Tb.N), and cancellous tissue mineral density (cn.TMD). Outcome measures for cortical bone were cortical area (Ct.Ar), marrow area (Ma.Ar, diaphysis only), cortical thickness (Ct.Th), maximum and minimum moment of inertia (I_{MAX} and I_{MIN}), and cortical tissue mineral density (ct.TMD).

3.2.4 Statistics

Effects of genotype and loading: The effects of genotype and loading in adult male and moderate-magnitude female mice (-13N and -6.5N for male and female mice respectively) were tested using a linear mixed-effects model with genotype, loading, and their interaction as fixed effects. A random mouse effect was included to account for the repeated measure (loaded and control limbs) within each animal. A Tukey HSD post-hoc test was performed when the interaction term was significant. Male and female mice were analyzed separately.

Effect of load magnitude: The effect of load magnitude in adult female mice was tested using an ANOVA. Limb differences [Loaded-Control] within each animal

were analyzed for genotype, load magnitude, and their interaction. Individual limbs were also analyzed using a linear mixed-effects model with genotype, loading, load magnitude, and their interactions as fixed effects with a random mouse effect. Differences between loaded and control limbs were determined to be different from zero when the loading×load magnitude cross term from the analysis on the individual limbs showed differences between the control and loaded limbs. Significance was set at $p<0.05$, and all results are statistically significant unless stated otherwise.

3.3 Results

3.3.1 Female pOC-ERαKO mice had reduced bone mass compared to LC

Control limbs of adult female pOC-ERαKO mice exhibited reduced cancellous and cortical bone mass in the metaphysis and mid-diaphysis compared to LC mice (Table 3.1a). At the metaphysis, cancellous BV/TV was 22% lower in female pOC-ERαKO mice due to increased Tb.Sp (+45%) and reduced Tb.N (-30%) (Fig. 3.1a,c). Lack of ERα in mature osteoblasts and osteocytes did not affect Tb.Th or cn.TMD in adult female mice. Cortical bone mass was also reduced in adult female pOC-ERαKO mice compared to LC mice. Reductions in Ct.Ar and Ct.Th (-9.1% and -8.7%, respectively) at the metaphyseal shell in knockout mice were accompanied by lower I_{MAX} (-7.6%), I_{MIN} (-14%), and ct.TMD (-3.7%) (Fig. 3.1a,c). In control limbs, midshaft Ct.Ar and Ct.Th also were lower in pOC-ERαKO mice (Ct.Ar: -8.9%; Ct.Th: -7.7%), although Ma.Ar was not different between genotypes (Fig. 3.2a,c). In addition to reduced bone mass, female pOC-ERαKO mice also had lower diaphyseal I_{MAX} (-10%), I_{MIN} (-13%), and ct.TMD (-1.8%) than female LC mice (Fig. 3.2a,c).

Table 3.1 Adult female pOC-ERαKO mice had lower bone mass and male pOC-ERαKO mice had similar bone mass compared to their respective LCs. Moderate-magnitude tibial loading increased cortical bone mass in adult female mice, and metaphyseal cortical and cancellous bone mass in adult male mice. Data are mean ± SD.

[#]pOC-ERαKO different from LC, [†]Loaded limb different from Control, $p < 0.05$ by linear mixed-effects model with random animal effect for each sex.

[a,b,c] Groups not sharing the same letter are significantly different by Tukey HSD post-hoc, where a > b > c. Post-hoc was performed when interaction term was significant.

a

	Female (Moderate-magnitude)			
	LC		pOC-ERαKO	
	Control	Loaded	Control	Loaded
Cancellous Metaphysis				
BV/TV	0.0645 ± 0.012	0.0584 ± 0.011	0.0482 ± 0.0066[#]	0.0479 ± 0.015[#]
Tb.Th (mm)	0.0500 ± 0.0020[c]	0.0532 ± 0.0038[†,b]	0.0527 ± 0.0029[#,bc]	0.062 ± 0.0033[#,†,a]
Tb.Sp (mm)	0.388 ± 0.048	0.432 ± 0.059	0.589 ± 0.096[#]	0.603 ± 0.11[#]
Tb.N (1/mm)	2.61 ± 0.30	2.36 ± 0.32[†]	1.75 ± 0.32[#]	1.73 ± 0.36[#,†]
cn.TMD (mg HA/cc)	891 ± 34	893 ± 15	876 ± 21	887 ± 23
Cortical shell metaphysis				
Ct.Ar (mm^2)	0.929 ± 0.044	0.999 ± 0.027[†]	0.818 ± 0.018[#]	0.934 ± 0.058[#,†]
Ct.Th (mm)	0.156 ± 0.0076	0.159 ± 0.010[†]	0.139 ± 0.0070[#]	0.149 ± 0.0094[#,†]
I_{MAX} (mm^4)	0.333 ± 0.046	0.375 ± 0.019[†]	0.292 ± 0.026[#]	0.362 ± 0.038[#,†]
I_{MIN} (mm^4)	0.249 ± 0.035	0.282 ± 0.024[†]	0.212 ± 0.021[#]	0.243 ± 0.018[#,†]
ct.TMD (mg HA/cc)	1051 ± 20	1041 ± 17[†]	1016 ± 16[*]	998 ± 25[#,†]
Cortical midshaft				
Ct.Ar (mm^2)	0.663 ± 0.028	0.695 ± 0.062[†]	0.595 ± 0.027[#]	0.642 ± 0.038[#,†]
Ma.Ar (mm^2)	0.380 ± 0.031	0.399 ± 0.051	0.392 ± 0.028	0.403 ± 0.014
Ct.Th (mm)	0.222 ± 0.012	0.225 ± 0.011[†]	0.202 ± 0.0057[#]	0.211 ± 0.0099[#,†]
I_{MAX} (mm^4)	0.0838 ± 0.0072	0.0970 ± 0.018[†]	0.0748 ± 0.0085[#]	0.0870 ± 0.0098[#,†]
I_{MIN} (mm^4)	0.0694 ± 0.0042	0.0751 ± 0.016	0.0593 ± 0.0061[#]	0.0666 ± 0.0059[#]
ct.TMD (mg HA/cc)	1078 ± 15	1075 ± 14	1055 ± 9.6[#]	1059 ± 13[#]

b

	Male			
	LC		pOC-ERαKO	
	Control	Loaded	Control	Loaded
Cancellous Metaphysis				
BV/TV	0.126 ± 0.019	0.144 ± 0.028[†]	0.140 ± 0.0097	0.150 ± 0.016[†]
Tb.Th (mm)	0.0429 ± 0.0047	0.0520 ± 0.0043[†]	0.0458 ± 0.0060	0.0516 ± 0.0020[†]
Tb.Sp (mm)	0.233 ± 0.022	0.236 ± 0.031	0.231 ± 0.016	0.233 ± 0.016
Tb.N (1/mm)	4.17 ± 0.33	4.08 ± 0.42[†]	4.20 ± 0.26	4.10 ± 0.26[†]
cn.TMD (mg HA/cc)	884 ± 21	895 ± 15	886 ± 25	888 ± 10
Cortical shell metaphysis				
Ct.Ar (mm^2)	0.976 ± 0.037	1.16 ± 0.057[†]	0.987 ± 0.029	1.17 ± 0.082[†]
Ct.Th (mm)	0.139 ± 0.0076	0.151 ± 0.013[†]	0.142 ± 0.0063	0.152 ± 0.0081[†]
I_{MAX} (mm^4)	0.464 ± 0.030	0.574 ± 0.057[†]	0.459 ± 0.021	0.567 ± 0.043[†]
I_{MIN} (mm^4)	0.322 ± 0.026	0.391 ± 0.035[†]	0.324 ± 0.017	0.400 ± 0.044[†]
ct.TMD (mg HA/cc)	995 ± 10	976 ± 12[†]	996 ± 10	968 ± 8.9[†]
Cortical midshaft				
Ct.Ar (mm^2)	0.824 ± 0.055	0.855 ± 0.057	0.841 ± 0.047	0.840 ± 0.051
Ma.Ar (mm^2)	0.641 ± 0.13	0.591 ± 0.10[†]	0.611 ± 0.08	0.567 ± 0.05[†]
Ct.Th (mm)	0.218 ± 0.014	0.234 ± 0.016[†]	0.224 ± 0.019	0.231 ± 0.0068[†]
I_{MAX} (mm^4)	0.180 ± 0.037	0.177 ± 0.027	0.191 ± 0.023	0.179 ± 0.034
I_{MIN} (mm^4)	0.116 ± 0.026	0.117 ± 0.020	0.110 ± 0.012	0.106 ± 0.012
ct.TMD (mg HA/cc)	1047 ± 15	1068 ± 8.1[†]	1044 ± 19	1054 ± 18[†]

BV/TV = bone volume fraction; Tb.Th = trabecular thickness; Tb.Sp = trabecular separation; Tb.N = trabecular number; cn.TMD = cancellous tissue mineral density; Ct.Ar = cortical area; Ma.Ar = marrow area; Ct.Th = cortical thickness; I_{MAX} and I_{MIN} = maximum and minimum moments of inertia; ct.TMD = cortical tissue mineral density.

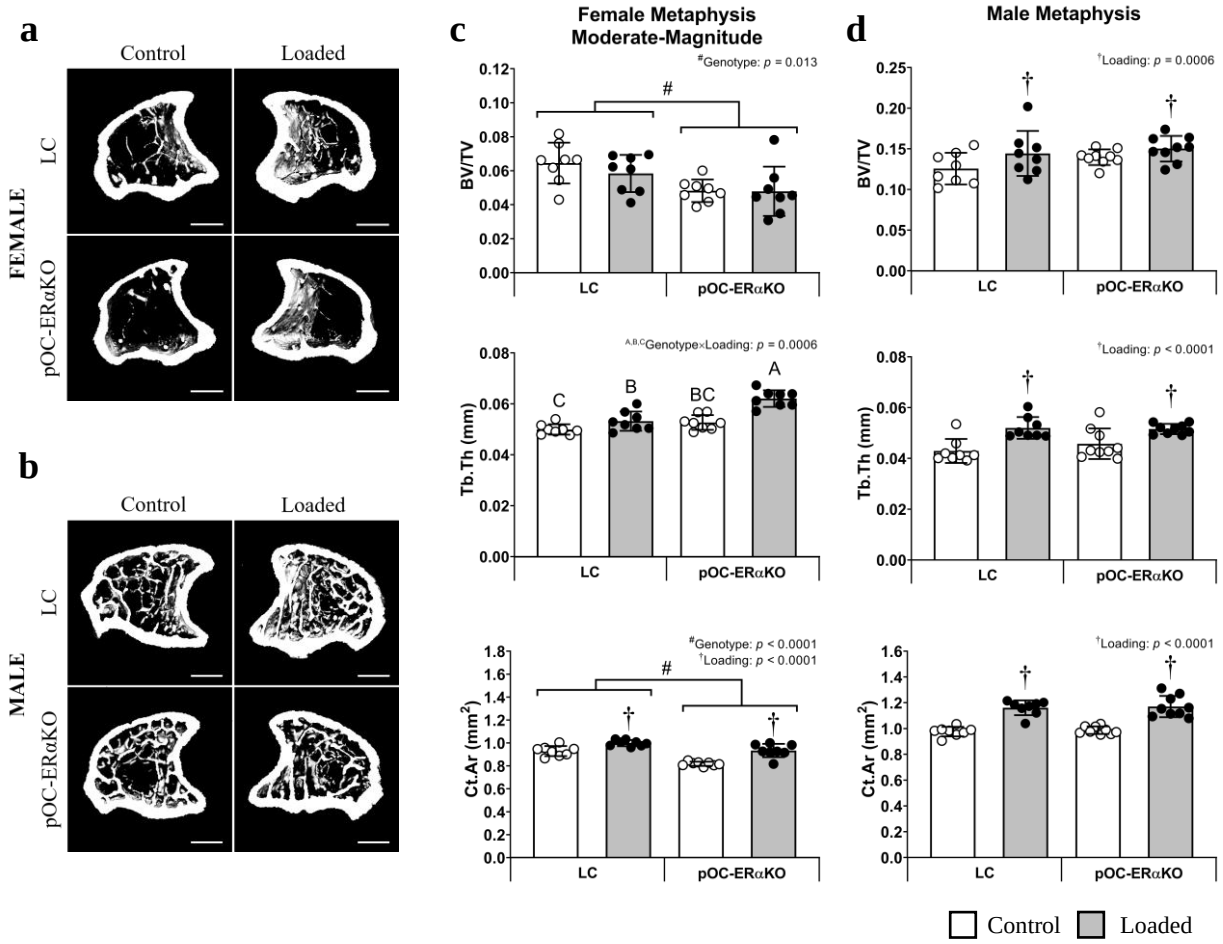

Figure 3.1 Female pOC-ERαKO mice had lower metaphyseal bone mass compared to their respective LCs. Moderate-magnitude tibial loading increased cortical shell mass in females, and cancellous and cortical shell mass in males. (a,b) Representative 3D microCT reconstructions of the tibial metaphysis after 2 weeks of mechanical loading. (c) Moderate-magnitude mechanical loading increased Tb.Th in female pOC-ERαKO mice more than in female LC mice, although BV/TV was unchanged by loading in both genotypes. Moderate-magnitude loading increased female metaphyseal Ct.Ar in both genotypes, although pOC-ERαKO mice had lower Ct.Ar than LC. (d) Loading increased BV/TV, Tb.Th, and metaphyseal Ct.Ar in males. There were no differences between pOC-ERαKO and LC male mice. Data are mean ± SD. #pOC-ERαKO different from LC. †Loaded limb different from Control. A > B > C, groups not sharing the same letter are different by Tukey post-hoc, performed only when the interaction term (genotype×loading) was significant. Statistical *p*-values shown for a linear mixed-effects model with a random animal effect for each sex. Scale bars = 500μm.

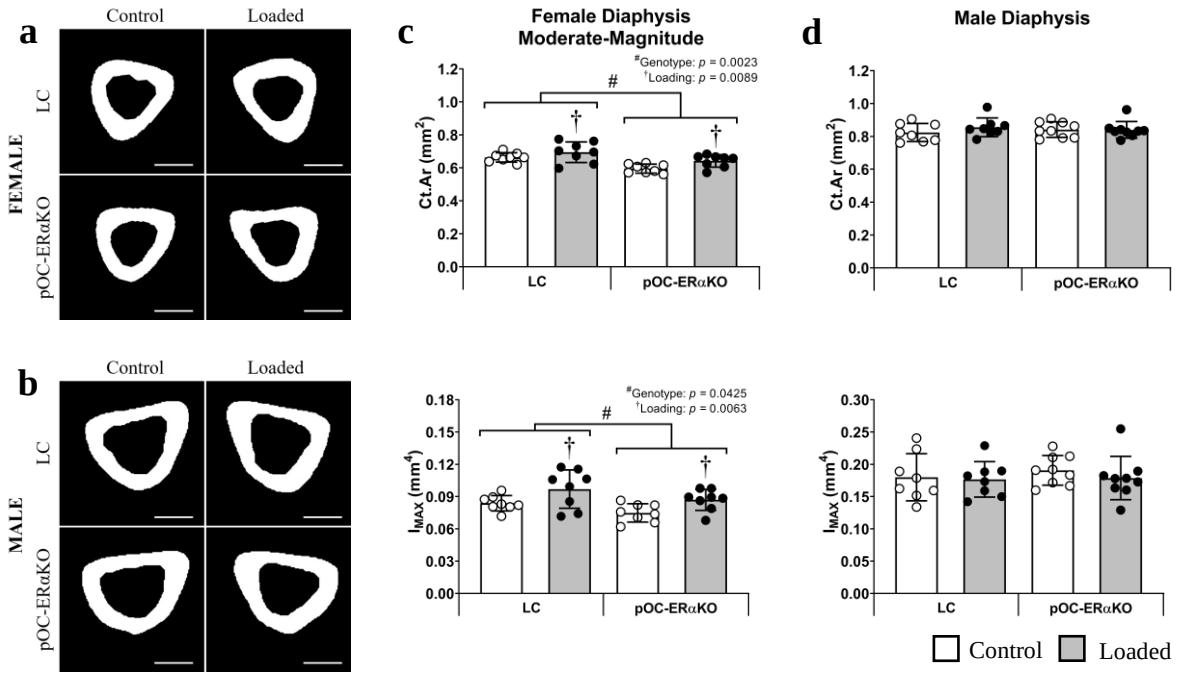

Figure 3.2 Female pOC-ERαKO mice had lower diaphyseal cortical bone mass than LC mice, and both genotypes increased bone mass with loading. (a,b) Representative 3D microCT reconstructions of the tibial midshaft after 2 weeks of mechanical loading. (c) Female pOC-ERαKO mice had lower Ct.Ar and I_{MAX} than LC, but moderate-magnitude loading increased Ct.Ar and I_{MAX} similarly in both genotypes. (d) Ct.Ar and I_{MAX} in male mice were similar between genotypes and were unaffected by mechanical loading. Data are mean ± SD. #pOC-ERαKO different from LC, †Loaded limb different from Control. Statistical *p*-values shown for a linear mixed-effects model with a random animal effect for each sex. Scale bars = 500μm.

3.3.2 Bone mass was unchanged in male pOC-ERαKO mice compared to LC

Removing ERα from mature osteoblasts and osteocytes did not affect the skeletal phenotype of adult male mice (Table 3.1b). Metaphyseal cancellous BV/TV, Tb.Th, Tb.Sp, Tb.N, and cn.TMD were similar between pOC-ERαKO and LC males (Fig. 3.1b,d). At the metaphyseal shell and midshaft Ct.Ar, Ct.Th, I_{MAX}, I_{MIN}, and ct.TMD were not different between genotypes, and diaphyseal Ma.Ar was also unaffected by ERα deletion (Figs. 3.1b,d & 3.2b,d).

3.3.3 Female pOC-ERαKO and LC mice had similar but limited adaptation to moderate-magnitude mechanical loading

Cancellous bone mass at the tibial metaphysis of adult females had little adaptation to moderate-magnitude compressive loading (Fig. 3.1a,c). Moderate-magnitude loading increased Tb.Th more in pOC-ERαKO females (+18%) compared to LC females (+6.5%). However, a concurrent reduction in Tb.N with loading (-6.4%) resulted in no change in BV/TV in either genotype. In contrast, the cortical shell responded to mechanical stimulation, and the responses were similar for both genotypes. Moderate-magnitude loading increased Ct.Ar (+11%), Ct.Th (+4.6%), I_{MAX} (+18%), and I_{MIN} (+14%), and decreased ct.TMD (-1.4%) in female mice. Likewise, moderate-magnitude loading increased Ct.Ar (+6.2%), Ct.Th (+2.8%), and I_{MAX} (+16%) at the cortical midshaft similarly in both genotypes (Fig. 3.2a,c).

3.3.4 High-magnitude loading in female mice was not sufficient to produce an anabolic cancellous response but produced a dose-dependent response in cortical bone

To investigate whether increased load magnitude could overcome the decreased mechanoadaptation in adult female mice, we compared the limb differences [Loaded-Control] following moderate-magnitude (6.5N) and high-magnitude (9.0N) tibial compression (Table 3.2, Fig. 3.3). The effect of loading on metaphyseal BV/TV was greater with high-magnitude compared to moderate-magnitude loading, although neither increased BV/TV. However, Tb.Th did increase with loading. Loading-

induced differences in Tb.Th were greater in pOC-ERαKO than LC mice (+150%) and were increased with higher load magnitude (+135%). A trend (p=0.0887) was evident toward a greater difference between pOC-ERαKO and LC mice with high-magnitude compared to moderate-magnitude loading (Fig. 3.3a). Increased Tb.Sp and decreased Tb.N with loading counteracted the load-induced increase in Tb.Th, but these responses were not affected by load magnitude or genotype. Loading at either load magnitude did not affect cn.TMD.

Table 3.2 Tibial loading effects on female mice measured by limb differences [Loaded-Control]. High-magnitude loading had a greater anabolic effect than moderate-magnitude loading, but was not sufficient to increase cancellous bone mass. pOC-ERαKO mice had greater loading responses at the metaphyseal shell and diaphysis than LC mice. Data are mean ± SD of the limb differences within each animal [Loaded-Control].

$^{\#}$pOC-ERαKO different from LC, †[Loaded-Control] different from zero, §High-magnitude different from Moderate-magnitude, $p < 0.05$ by ANOVA for genotype, load magnitude, and their interaction.

^{a,b,c} Groups not sharing the same letter are significantly different by Tukey HSD post-hoc, where a > b > c. Post-hoc performed when the interaction term was significant.

	Female			
	Moderate-magnitude (6.5N)		High-magnitude (9N)	
	LC	pOC-ERαKO	LC	pOC-ERαKO
Cancellous Metaphysis				
ΔBV/TV	-0.00614 ± 0.014	-0.000300 ± 0.011	0.00587 ± 0.013§	0.0150 ± 0.013§
ΔTb.Th (mm)	0.00325 ± 0.0034†	0.00936 ± 0.0020$^{\#,\dagger}$	0.00893 ± 0.0042†,§	0.0207 ± 0.0067*,†,§
ΔTb.Sp (mm)	0.00439 ± 0.037†	0.0143 ± 0.089†	0.0221 ± 0.048†	0.0579 ± 0.097†
ΔTb.N (1/mm)	-0.253 ± 0.24†	-0.0254 ± 0.25†	-0.186 ± 0.32†	-0.137 ± 0.24†
Δcn.TMD (mg HA/cc)	2.95 ± 36	11.3 ± 38	2.67 ± 19	11.1 ± 15
Cortical shell metaphysis				
ΔCt.Ar (mm^2)	0.0697 ± 0.044†	0.116 ± 0.064$^{\#,\dagger}$	0.179 ± 0.065†,§	0.284 ± 0.037$^{\#,\dagger,\S}$
ΔCt.Th (mm)	0.00325 ± 0.0082^{†,c}	0.0103 ± 0.0093$^{\#,\dagger,bc}$	0.0163 ± 0.0083^{†,§,b}	0.0372 ± 0.0021$^{\#,\dagger,\S,a}$
ΔI_{MAX} (mm^4)	0.0417 ± 0.029†	0.704 ± 0.059†	0.108 ± 0.055†,§	0.143 ± 0.029†,§
ΔI_{MIN} (mm^4)	0.0326 ± 0.017†	0.0312 ± 0.025†	0.0531 ± 0.030†,§	0.0681 ± 0.023†,§
Δct.TMD (mg HA/cc)	-10.5 ± 16†	-18.2 ± 29†	-40.8 ± 15†,§	-33.8 ± 7.4†,§
Cortical midshaft				
ΔCt.Ar (mm^2)	0.0313 ± 0.053^{†,b}	0.0468 ± 0.050$^{\#,\dagger,b}$	0.0559 ± 0.027^{†,§,b}	0.147 ± 0.029$^{\#,\dagger,\S,a}$
ΔMa.Ar (mm^2)	0.0189 ± 0.045	0.0107 ± 0.034	-0.0184 ± 0.021	-0.00477 ± 0.056
ΔCt.Th (mm)	0.00288 ± 0.010	0.00913 ± 0.010$^{\#}$	0.0194 ± 0.010†,§	0.0407 ± 0.015$^{\#,\dagger,\S}$
ΔI_{MAX} (mm^4)	0.0132 ± 0.016†	0.0121 ± 0.015†	0.0132 ± 0.0069†,§	0.0310 ± 0.0080†,§
ΔI_{MIN} (mm^4)	0.00571 ± 0.015†	0.00732 ± 0.0096†	0.00202 ± 0.0036†	0.0161 ± 0.0045†
Δct.TMD (mg HA/cc)	-2.72 ± 19	3.94 ± 15	-0.273 ± 18	-11.0 ± 18

BV/TV = bone volume fraction; Tb.Th = trabecular thickness; Tb.Sp = trabecular separation; Tb.N = trabecular number; cn.TMD = cancellous tissue mineral density; Ct.Ar = cortical area; Ma.Ar = marrow area; Ct.Th = cortical thickness; I_{MAX} and I_{MIN} = maximum and minimum moments of inertia; ct.TMD = cortical tissue mineral density; pOC-ERαKO = estrogen receptor-α knockout; LC = littermate control; Δ = [Loaded – Control].

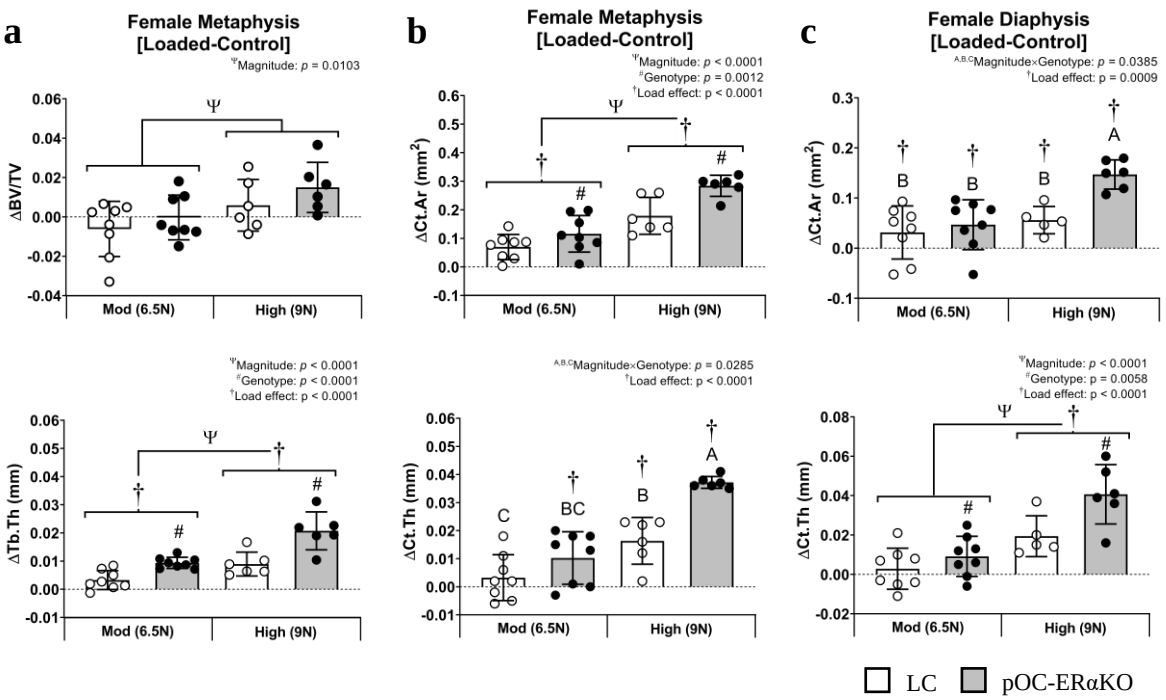

Figure 3.3 The skeletal response to moderate-magnitude tibial loading was less than high-magnitude loading in female mice as measured by limb differences within each animal [Loaded – Control]. (a) Neither load magnitude increased metaphyseal BV/TV, but the difference between loaded and control limbs was greater with high-magnitude loading. Tb.Th was increased to a greater extent with high-magnitude than moderate-magnitude loading. Female pOC-ERαKO mice had greater loading-induced increases in Tb.Th than LC. (b) Loading increased metaphyseal shell Ct.Ar more with high-magnitude loading, with greater increases in pOC-ERαKO mice. Loading only increased metaphyseal shell Ct.Th in pOC-ERαKO mice at the moderate-magnitude. High-magnitude loading increased Ct.Th in both genotypes, but the increase was greater in pOC-ERαKO mice. (c) At the diaphysis, Ct.Ar was increased more in pOC-ERαKO mice with high-magnitude loading. Ct.Th was only increased with high-magnitude loading. Loading increased Ct.Th more in pOC-ERαKO than LC mice. Data are mean ± SD. Δ represents the difference between loaded and control limbs [Loaded-Control]. $^{\Psi}$Low-magnitude different from High-magnitude. $^{\#}$pOC-ERαKO different from LC, †[Loaded-Control] different from zero. A > B > C, groups not sharing the same letter are different by Tukey post-hoc. Statistical *p*-values shown for an ANOVA for genotype, load magnitude, and their interaction.

Although cortical bone mass increased with moderate-magnitude loading, high-magnitude loading produced a more effective anabolic response. At the cortical metaphyseal shell, high-magnitude loading caused a larger increase in Ct.Ar (+149%) than moderate-magnitude loading, and the response was greater in pOC-ERαKO mice

(+61%). Ct.Th also increased the most in pOC-ERαKO mice with high-magnitude loading, but moderate-magnitude loading was not sufficiently anabolic to differentiate between genotypes (Fig. 3.3b). Both I_{MAX} and I_{MIN} were increased to a greater extent with high-magnitude loading (I_{MAX}: +125%; I_{MIN}: +90%), and I_{MAX} had a trend toward a greater anabolic loading effect in pOC-ERαKO mice (p=0.0817, +44%). Additionally, high-magnitude loading caused a greater decrease in ct.TMD than moderate-magnitude loading (+160%).

At the diaphysis, similar to the metaphyseal shell, high-magnitude loading was more anabolic than moderate-magnitude loading. High-magnitude loading caused a greater increase in Ct.Ar only in pOC-ERαKO mice (+241%), while the loading response in LC mice was not affected by the increased load magnitude (Fig. 3.3c). Ct.Th and I_{MAX} increased to a greater extent with high-magnitude loading (Ct.Th: +417%; I_{MAX}: +81%). Similarly to Ct.Ar, I_{MAX} trended toward a greater loading response in high-magnitude loaded pOC-ERαKO mice compared to the other groups (p=0.0816, +143%). Ct.Th increased more in pOC-ERαKO mice regardless of load magnitude (+145%), and I_{MIN} also trended toward a greater anabolic response in pOC-ERαKO mice (p=0.0628, +159%). Both Ma.Ar and ct.TMD were unaffected by loading at either load magnitude.

3.3.5 Loading induced similar anabolic bone responses in male pOC-ERαKO and LC mice

Unlike in female mice, two weeks of mechanical loading was anabolic for cancellous bone at the metaphysis of male mice when similar *in vivo* strains were

induced (Fig. 3.1b,d). BV/TV was increased with loading in both genotypes (+11%), due to an increase in Tb.Th (+17%) that overcame a decrease in Tb.N (-2.2%). Mechanical loading was also anabolic in the metaphyseal shell of adult male mice, increasing Ct.Ar by 19%. In combination with a loading-induced increase in Ct.Th (+8.0%), both genotypes had greater I_{MAX} (+24%) and I_{MIN} (+23%) following loading. Loading decreased ct.TMD in both genotypes (-2.3%). Adaptation to mechanical loading was less pronounced at the tibial midshaft than at the metaphysis (Fig. 3.2b,d). Additionally, loading increased Ct.Th (5.2%) and decreased Ma.Ar (-7.4%), but did not affect Ct.Ar or moment of inertia. Loading also increased ct.TMD by 1.4%. All responses to loading in adult male mice were independent of genotype.

3.4 Discussion

Compared to littermate controls, 26-week-old adult female mice lacking ERα in mature osteoblasts and osteocytes had reduced bone mass; in contrast, bone mass in their adult male counterparts was similar to controls. Mechanical loading increased metaphyseal cortical and cancellous bone mass in male mice similarly in both genotypes. Moderate-magnitude loading in female mice had limited anabolic effects in metaphyseal and diaphyseal cortical bone, irrespective of genotype. High-magnitude loading increased the cortical response and was more anabolic in pOC-ERαKO mice, but was insufficient to restore the loading response to the level of young mice.

Our results demonstrate the importance of ERα in determining female bone mass in adulthood. Määttä and colleagues found similar reductions in cancellous bone mass in 6-month-old osteoblast- and osteocyte-specific female pOC-ERαKO mice and

also reported that genotype did not affect cortical bone mass in adult males [15]. In their study, however, cortical bone mass was not different in female pOC-ERαKO mice compared to littermate controls, and cancellous bone mass was reduced in adult male pOC-ERαKO mice. Genetic variation across inbred mouse strains produces differences in bone density and geometry that may explain these discrepancies in skeletal phenotype [41,42]. Our mice were fully backcrossed to a C57Bl/6 background, while the genetic background was not reported by Määttä and colleagues.

The skeletal phenotypes of adult pOC-ERαKO mice differed between males and females. Adult female pOC-ERαKO mice had low bone mass compared to controls, but male mice were unaffected by ERα deletion. We previously reported that young female pOC-ERαKO mice had low bone mass and young male pOC-ERαKO mice had high bone mass compared to LC mice [14]. Here, adult female pOC-ERαKO mice had an exacerbated low bone mass phenotype compared to their young counterparts, whereas adult male pOC-ERαKO mice lost the high bone mass phenotype of young males (Supp. Table 3.1). In female mice, lack of ERα signaling in mature osteoblasts and osteocytes during puberty may have caused a reduction in the stimulatory effects of estrogen on female bone growth. Continued estrogen-signaling deficiency into adulthood led to a sex-based phenotypic divergence that may have been further enhanced by age-related reductions in estrogen [43]. In growing males, impaired estrogen signaling, directly or in combination with other indirect effects, was anabolic and increased bone mass in young pOC-ERαKO mice. However, the skeletal phenotype of adult male pOC-ERαKO mice was similar to their littermate controls, potentially suggesting that lack of ERα caused male mice to reach peak bone mass

sooner than control mice rather than increasing their achieved peak bone mass.

ERα deletion altered adaptation to mechanical loading only in female mice loaded at a high-magnitude peak load. Male pOC-ERαKO mice had the same anabolic response to loading as their controls, and moderate-magnitude loading in female pOC-ERαKO mice was not sufficiently anabolic to detect substantial differences in the loading response of pOC-ERαKO mice. High-magnitude loading overcame some of the reduced mechanoresponsiveness with age in female mice in cortical bone and demonstrated that adult pOC-ERαKO female mice responded to mechanical loading to a greater extent than control mice. These results are consistent with our previous data for growing mice. Young female pOC-ERαKO mice had a greater anabolic response to loading in cancellous and diaphyseal cortical bone [14]. Similarly, Kondoh and colleagues found that when ERα was removed at the osteocyte stage using Dmp1-Cre, cancellous bone loss due to hindlimb unloading was exacerbated [17]. Together with our results, this finding suggests that ERα may modulate mechanoadaptation or mechanosensitivity in female mice.

Adult female mice had greatly diminished load-induced increases in bone mass compared to our previous work in young mice, but mechanical loading was similarly anabolic in adult and young male mice (Fig. 3.4, Supp. Table 3.2) [14]. Moderate-magnitude and high-magnitude loading in adult female mice were still able to produce an anabolic response in cortical bone at the metaphysis and diaphysis, but both levels of loading produced a lower response than that of young mice (Fig. 4). Additionally, even high-magnitude loading was unable to increase cancellous bone mass at the metaphysis in adult female mice. The threshold for mechanically-induced bone

anabolism increases with age [44], and 9N peak loads may not have been sufficient to reach that increased threshold in cancellous bone in adult female mice. Additionally, the lack of cancellous adaptation may have been due to lower cancellous bone mass and connectivity reducing load transfer from the cortical shell, resulting in reduced tissue strains in the trabeculae of adult mice compared to young mice during tibial loading [45]. Adult male LC mice had a slight increase in cancellous bone mass with loading that was not present in young mice. Cancellous bone mass did not decrease with age in male mice unlike in female mice, so the strain levels in their trabeculae may not have been as affected by age-related changes in load-sharing with the cortical shell, allowing for load-induced adaptation during adulthood. In contrast to female mice, adult male mice had the same level of cortical loading response at the metaphyseal shell and diaphysis as young males.

The reduced or absent mechanoresponsiveness in adult female mice and the diaphysis of adult male mice may have had several contributing factors. In mice, aging reduces Wnt signaling in bone [46], a primary pathway activated by ERα following mechanical stimulation to promote bone formation [29,47]. Therefore, we speculate that reduced Wnt signaling with age may have reduced the impact of ERα on the response to moderate-magnitude loading in adult female mice, and that the overall reduced response to mechanical loading could reflect the loss of Wnt signaling with age [31–33,48].

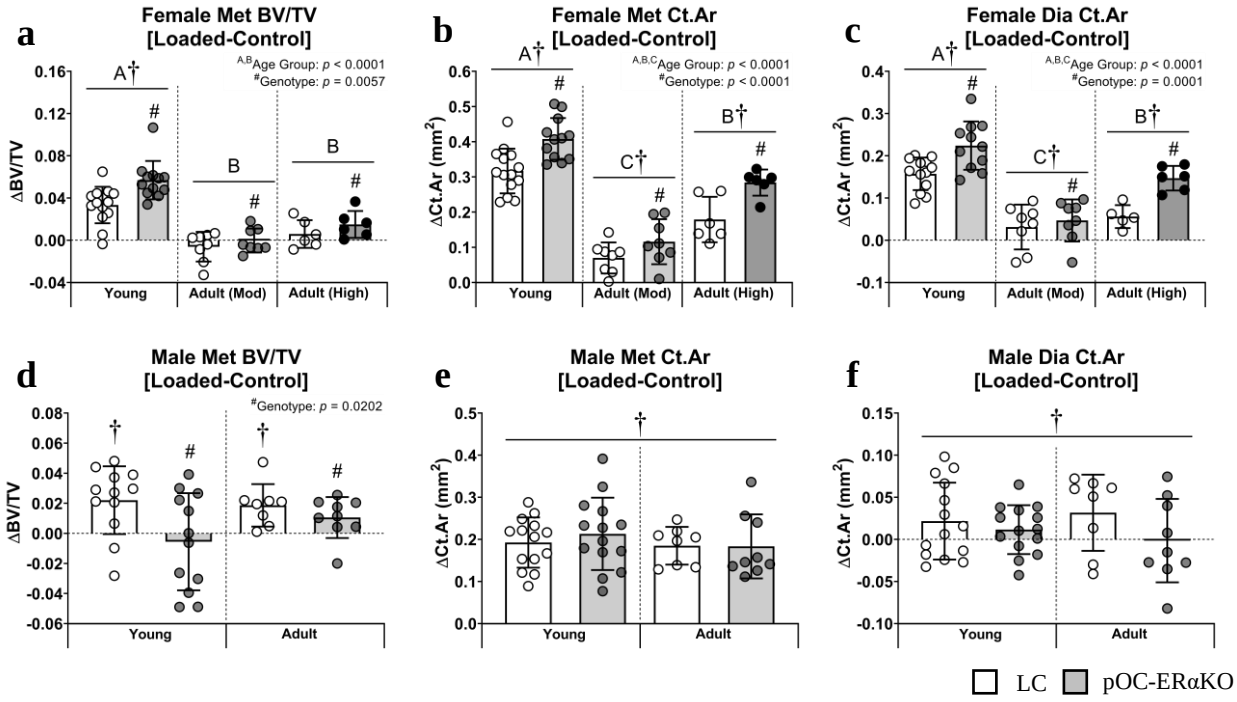

Figure 3.4 Adult female mice responded less to tibial loading than young mice. Overall, age did not affect the response to loading in male mice. (a) Unlike young female mice, adults did not increase BV/TV with loading. (b,c) Adult female metaphyseal (Met) shell Ct.Ar and diaphyseal (Dia) Ct.Ar increased with loading, but not to the extent as in young female mice. The effect of loading was greater in pOC-ERαKO mice. (d) BV/TV only increased with loading in LC male mice. (e,f) Loading increased Ct.Ar at the metaphysis and diaphysis regardless of age or genotype. Data for young mice are from Ref. [14]. Data are mean ± SD. Δ represents the difference between loaded and control limbs [Loaded-Control]. #pOC-ERαKO different from LC, †[Loaded-Control] different from zero. A > B > C, groups not sharing the same letter are different by Tukey post-hoc. Statistical *p*-values shown for an ANOVA for genotype, age group, and their interaction.

We showed previously that reduced adaptation to mechanical loading with age was significant in cancellous bone but not cortical bone when load magnitudes were matched in adult female mice [31]. However, the 11.3N peak load magnitude used previously was greater than the 9N peak load applied to the young mice [14] and high-magnitude loading group here. The peak load for moderate-magnitude loading in females and adult male mice used here were chosen to induce +1000με at the midshaft, while our previous studies induced +1200με. We chose to reduce the target

strain value to reduce the formation of woven bone at the midshaft. Additionally, the 13N peak load used for adult male mice to produce +1000με caused some swelling at the ankles. Therefore, we did not include higher magnitude loading for the adult male mice to avoid injury.

Understanding the complex relationship between sex, estrogen signaling, and mechanical loading in the adult skeleton is critical for preventing and treating osteoporosis in the increasingly elderly population. Using a bone cell-specific ERα knockout mouse model, we demonstrated significant differences between adult male and female mice in the response to loading with and without ERα signaling. Adult female mice had attenuated loading responses compared to young females, but males retained most of their loading responses with age. Our data provide important information for the first time on *in vivo* adaptation of both cortical and cancellous bone in both sexes of adult animals, whereas previous studies have focused solely on cortical bone or growing animals. In addition, we report the responses of both tissue types at a single location, the tibial metaphysis, allowing more direct comparisons between cortical and cancellous bone tissue. Future studies investigating the signaling pathways and transcriptional changes responsible for these tissue-level changes may uncover new targets for therapies to treat osteoporosis.

3.5 References

[1] S. Khosla, M.J. Oursler, D.G. Monroe, Estrogen and the skeleton, Trends Endocrinol. Metab. 23 (2012) 576–581. doi:10.1016/j.tem.2012.03.008.

[2] S.H. Windahl, G. Andersson, J.-A. Gustafsson, Elucidation of estrogen receptor function in bone with the use of mouse models., Trends Endocrinol. Metab. 13 (2002) 195–200. doi:10.1016/S1043-2760(02)00594-5.

[3] F. Callewaert, M. Sinnesael, E. Gielen, S. Boonen, D. Vanderschueren, Skeletal sexual dimorphism: Relative contribution of sex steroids, GH-IGF1, and mechanical loading, J. Endocrinol. 207 (2010) 127–134. doi:10.1677/JOE-10-0209.

[4] M. Almeida, M.R. Laurent, V. Dubois, F. Claessens, C.A. O'Brien, R. Bouillon, D. Vanderschueren, S.C. Manolagas, Estrogens and Androgens in Skeletal Physiology and Pathophysiology, Physiol. Rev. 97 (2017) 135–187. doi:10.1152/physrev.00033.2015.

[5] L.S. Richelson, H.W. Wahner, L.J. Melton III, B.L. Riggs, Relative contributions of aging and estrogen deficiency to postmenopausal bone loss, N. Engl. J. Med. 311 (1984) 1273–1275.

[6] B.L. Riggs, Endocrine causes of age-related bone loss and osteoporosis, Novartis Found. Symp. 242 (2002) 247–264.

[7] S. Khosla, S. Amin, E. Orwoll, Osteoporosis in men, Endocr. Rev. 29 (2008) 441–464. doi:10.1210/er.2008-0002.

[8] F. Callewaert, S. Boonen, D. Vanderschueren, Sex steroids and the male skeleton: a tale of two hormones, Trends Endocrinol. Metab. 21 (2010) 89–95. doi:10.1016/j.tem.2009.09.002.

[9] L. Vico, J.M. Vanacker, Sex hormones and their receptors in bone homeostasis: Insights from genetically modified mouse models, Osteoporos. Int. 21 (2010) 365–372. doi:10.1007/s00198-009-0963-5.

[10] S. Bord, A. Horner, S. Beavan, J. Compston, Estrogen Receptors α and β Are Differentially Expressed in Developing Human Bone, J. Clin. Endocrinol. Metab. 86 (2001) 2309–2314. doi:10.1210/jcem.86.5.7513.

[11] M.K. Lindberg, S.L. Alatalo, J.M. Halleen, S. Mohan, J.-Å. Gustafsson, C. Ohlsson, Estrogen receptor specificity in the regulation of the skeleton in female mice, J. Endocrinol. 171 (2001) 229–236.

[12] A.M. Rooney, M.C.H. van der Meulen, Mouse models to evaluate the role of estrogen receptor α in skeletal maintenance and adaptation, Ann. N. Y. Acad. Sci. 1410 (2017) 85–92. doi:10.1111/nyas.13523.

[13] M. Almeida, S. Iyer, M. Martin-Millan, S.M. Bartell, L. Han, E. Ambrogini, M. Onal, J. Xiong, R.S. Weinstein, R.L. Jilka, C.A. O'Brien, S.C. Manolagas, Estrogen receptor-α signaling in osteoblast progenitors stimulates cortical bone accrual, J. Clin. Invest. 123 (2013) 394–404. doi:10.1172/JCI65910.

[14] K.M. Melville, N.H. Kelly, G. Surita, D.B. Buchalter, J.C. Schimenti, R.P. Main, F.P. Ross, M.C.H. Van Der Meulen, Effects of Deletion of ERα in Osteoblast-Lineage Cells on Bone Mass and Adaptation to Mechanical Loading Differ in Female and Male Mice, J. Bone Miner. Res. 30 (2015) 1468–1480. doi:10.1002/jbmr.2488.

[15] J.A. Määttä, K.G. Büki, G. Gu, M.H. Alanne, J. Vääräniemi, H. Liljenbäck, M. Poutanen, P. Härkönen, K. Väänänen, Inactivation of estrogen receptor α in bone-forming cells induces bone loss in female mice, FASEB J. 27 (2013) 478–488. doi:10.1096/fj.12-213587.
[16] S.H. Windahl, A.E. Börjesson, H.H. Farman, C. Engdahl, S. Movérare-Skrtic, K. Sjögren, M.K. Lagerquist, J.M. Kindblom, A. Koskela, J. Tuukkanen, P. Divieti Pajevic, J.Q. Feng, K. Dahlman-Wright, P. Antonson, J.-Å. Gustafsson, C. Ohlsson, Estrogen receptor-α in osteocytes is important for trabecular bone formation in male mice., Proc. Natl. Acad. Sci. U. S. A. 110 (2013) 2294–9. doi:10.1073/pnas.1220811110.
[17] S. Kondoh, K. Inoue, K. Igarashi, H. Sugizaki, Y. Shirode-Fukuda, E. Inoue, T. Yu, J.K. Takeuchi, J. Kanno, L.F. Bonewald, Y. Imai, Estrogen receptor α in osteocytes regulates trabecular bone formation in female mice, Bone. 60 (2014) 68–77. doi:10.1016/j.bone.2013.12.005.
[18] H. Jones, J. Priest, W. Hayes, C. Tichenor, D. Nagel, Humeral hypertrophy in response to exercise, J. Bone Jt. Surg. 59 (1977) 204–208.
[19] T. Cervinka, H. Sievänen, J. Hyttinen, J. Rittweger, Bone loss patterns in cortical, subcortical, and trabecular compartments during simulated microgravity., J. Appl. Physiol. 117 (2014) 80–8. doi:10.1152/japplphysiol.00021.2014.
[20] K. Lee, L. Lanyon, Mechanical loading influences bone mass through estrogen receptor α, Exerc. Sport Sci. Rev. 32 (2004) 64–68. http://discovery.ucl.ac.uk/183482/.
[21] P.J. Ehrlich, B.S. Noble, H.L. Jessop, H.Y. Stevens, J.R. Mosley, L.E. Lanyon, The effect of in vivo mechanical loading on estrogen receptor alpha expression in rat ulnar osteocytes, J Bone Min. Res. 17 (2002) 1646–1655. doi:10.1359/jbmr.2002.17.9.1646.
[22] G.L. Galea, J.S. Price, L.E. Lanyon, Estrogen receptors' roles in the control of mechanically adaptive bone (re)modeling, Bonekey Rep. 2 (2013) 413. doi:10.1038/bonekey.2013.147.
[23] E. Damien, J.S. Price, L.E. Lanyon, The estrogen receptor's involvement in osteoblasts' adaptive response to mechanical strain., J. Bone Miner. Res. 13 (1998) 1275–1282. doi:10.1359/jbmr.1998.13.8.1275.
[24] E. Damien, J.S. Price, L.E. Lanyon, Mechanical strain stimulates osteoblast proliferation through the estrogen receptor in males as well as females., J. Bone Miner. Res. 15 (2000) 2169–2177. doi:10.1359/jbmr.2000.15.11.2169.
[25] H.L. Jessop, R.F.L. Suswillo, S.C.F. Rawlinson, G. Zaman, K. Lee, V. Das-Gupta, A. a Pitsillides, L.E. Lanyon, Osteoblast-like cells from estrogen receptor alpha knockout mice have deficient responses to mechanical strain., J. Bone Miner. Res. 19 (2004) 938–946. doi:10.1359/JBMR.
[26] L.K. Saxon, G. Galea, L. Meakin, J. Price, L.E. Lanyon, Estrogen receptors α and β have different gender-dependent effects on the adaptive responses to load bearing in cancellous and cortical bone, Endocrinology. 153 (2012) 2254–2266. doi:10.1210/en.2011-1977.
[27] K. Lee, H. Jessop, R. Suswillo, G. Zaman, L. Lanyon, Bone adaptation requires oestrogen receptor-alpha, Nature. 424 (2003) 389.

[28] K.C.L. Lee, H. Jessop, R. Suswillo, G. Zaman, L.E. Lanyon, The adaptive response of bone to mechanical loading in female transgenic mice is deficient in the absence of oestrogen receptor-alpha and -beta., J. Endocrinol. 182 (2004) 193–201. doi:15283680.
[29] H. Todd, G.L. Galea, L.B. Meakin, P.J. Delisser, L.E. Lanyon, S.H. Windahl, J.S. Price, Wnt16 is associated with age-related bone loss and estrogen withdrawal in murine bone, PLoS One. 10 (2015) 1–16. doi:10.1371/journal.pone.0140260.
[30] E.J. Bassey, M.C. Rothwell, J.J. Littlewood, D.W. Pye, Pre- and postmenopausal women have different bone mineral density responses to the same high-impact exercise., J. Bone Miner. Res. 13 (1998) 1805–1813. doi:10.1359/jbmr.1998.13.12.1805.
[31] M.E. Lynch, R.P. Main, Q. Xu, T.L. Schmicker, M.B. Schaffler, T.M. Wright, M.C.H. van der Meulen, Tibial compression is anabolic in the adult mouse skeleton despite reduced responsiveness with aging, Bone. 49 (2011) 439–446. doi:10.1016/j.bone.2011.05.017.
[32] R.P. Main, M.E. Lynch, M.C.H. van der Meulen, Load-induced changes in bone stiffness and cancellous and cortical bone mass following tibial compression diminish with age in female mice., J. Exp. Biol. 217 (2014) 1775–83. doi:10.1242/jeb.085522.
[33] N. Holguin, M.D. Brodt, M.E. Sanchez, M.J. Silva, Aging diminishes lamellar and woven bone formation induced by tibial compression in adult C57BL/6, Bone. 65 (2014) 83–91. doi:10.1016/j.bone.2014.05.006.
[34] K.M. Melville, N.H. Kelly, S. a Khan, J.C. Schimenti, F.P. Ross, R.P. Main, M.C. van der Meulen, Female mice lacking estrogen receptor-alpha in osteoblasts have compromised bone mass and strength, J Bone Min. Res. 29 (2014) 370–379. doi:10.1002/jbmr.2082.
[35] Y. Feng, D. Manka, K.-U. Wagner, S.A. Khan, Estrogen receptor-alpha expression in the mammary epithelium is required for ductal and alveolar morphogenesis in mice., Proc. Natl. Acad. Sci. U. S. A. 104 (2007) 14718–23. doi:10.1073/pnas.0706933104.
[36] T.L. Clemens, H. Tang, S. Maeda, R. a Kesterson, F. Demayo, J.W. Pike, C.M. Gundberg, Analysis of osteocalcin expression in transgenic mice reveals a species difference in vitamin D regulation of mouse and human osteocalcin genes., J. Bone Miner. Res. 12 (1997) 1570–6. doi:10.1359/jbmr.1997.12.10.1570.
[37] M. Zhang, S. Xuan, M.L. Bouxsein, D. Von Stechow, N. Akeno, M.C. Faugere, H. Malluche, G. Zhao, C.J. Rosen, A. Efstratiadis, T.L. Clemens, Osteoblast-specific knockout of the insulin-like growth factor (IGF) receptor gene reveals an essential role of IGF signaling in bone matrix mineralization, J. Biol. Chem. 277 (2002) 44005–44012. doi:10.1074/jbc.M208265200.
[38] L.B. Meakin, T. Sugiyama, G.L. Galea, W.J. Browne, L.E. Lanyon, J.S. Price, Male mice housed in groups engage in frequent fighting and show a lower response to additional bone loading than females or individually housed males that do not fight, Bone. 54 (2013) 113–117. doi:10.1016/j.bone.2013.01.029.
[39] J.C. Fritton, E.R. Myers, T.M. Wright, M.C.H. Van Der Meulen, Loading

induces site-specific increases in mineral content assessed by microcomputed tomography of the mouse tibia, Bone. 36 (2005) 1030–1038. doi:10.1016/j.bone.2005.02.013.
[40] M.E. Lynch, R.P. Main, Q. Xu, D.J. Walsh, M.B. Schaffler, T.M. Wright, M.C.H. van der Meulen, Cancellous bone adaptation to tibial compression is not sex dependent in growing mice., J. Appl. Physiol. 109 (2010) 685–691. doi:10.1152/japplphysiol.00210.2010.
[41] W.G. Beamer, L.R. Donahue, I.C.J. Rosen, D.J. Baylink, Genetic Variability in Adult Bone Density Among Inbred Strains of Mice, Bone. 18 (1996) 397–3. doi:10.1016/8756-3282(96)00047-6.
[42] J.E. Wergedal, M.H.C. Sheng, C.L. Ackert-Bicknell, W.G. Beamer, D.J. Baylink, Genetic variation in femur extrinsic strength in 29 different inbred strains of mice is dependent on variations in femur cross-sectional geometry and bone density, Bone. 36 (2005) 111–122. doi:10.1016/j.bone.2004.09.012.
[43] J.F. Nelson, L.S. Felicio, H.H. Osterburg, C.E. Finch, Altered Profiles of Estradiol and Progesterone Associated with Prolonged Estrous Cycles and Persistent Vaginal Cornification in Aging C57BL/6J Mice, Biol. Reprod. 24 (1981) 784–794. doi:10.1095/biolreprod24.4.784.
[44] B. Javaheri, A. Carriero, M. Wood, R. De Souza, P.D. Lee, S. Shefelbine, A.A. Pitsillides, Transient peak-strain matching partially recovers the age-impaired mechanoadaptive cortical bone response, Sci. Rep. 8 (2018) 2–13. doi:10.1038/s41598-018-25084-6.
[45] H. Razi, A.I. Birkhold, P. Zaslansky, R. Weinkamer, G.N. Duda, B.M. Willie, S. Checa, Skeletal maturity leads to a reduction in the strain magnitudes induced within the bone: A murine tibia study, Acta Biomater. 13 (2015). doi:10.1016/j.actbio.2014.11.021.
[46] N. Holguin, M.D. Brodt, M.J. Silva, Activation of Wnt Signaling By Mechanical Loading Is Impaired in the Bone of Old Mice., J. Bone Miner. Res. 31 (2016) 2215–2226. doi:10.1002/jbmr.2900.
[47] V.J. Armstrong, M. Muzylak, A. Sunters, G. Zaman, L.K. Saxon, J.S. Price, L.E. Lanyon, Wnt/β-catenin signaling is a component of osteoblastic bone cell early responses to load-bearing and requires estrogen receptor α, J. Biol. Chem. 282 (2007) 20715–20727. doi:10.1074/jbc.M703224200.
[48] L.B. Meakin, G.L. Galea, T. Sugiyama, L.E. Lanyon, J.S. Price, Age-related impairment of bones' adaptive response to loading in mice is associated with sex-related deficiencies in osteoblasts but no change in osteocytes, J. Bone Miner. Res. 29 (2014) 1859–1871. doi:10.1002/jbmr.2222.

3.6 Chapter 3 Supplemental Information

Supplemental Table 3.1 Young female pOC-ERαKO mice had lower bone mass than LC, and this difference was exacerbated in adult animals. Young male pOC-ERαKO mice had higher bone mass than LC, but this difference was lost with age. Data for young mice are from Ref. [14]. **Bold** indicates pOC-ERαKO greater than LC; = indicates no difference between pOC-ERαKO and LC.

		Female		Male	
		Young	Adult (Moderate)	Young	Adult
Cancellous metaphysis	BV/TV	pOC-ERαKO < LC	pOC-ERαKO < LC	**pOC-ERαKO > LC**	=
	Tb.Th	=	=	**pOC-ERαKO > LC**	=
	Tb.Sp	**pOC-ERαKO > LC**	**pOC-ERαKO > LC**	=	=
	Tb.N	pOC-ERαKO < LC	pOC-ERαKO < LC	=	=
	cn.TMD	=	=	=	=
Cortical shell metaphysis	Ct.Ar	=	pOC-ERαKO < LC	=	=
	Ct.Th	pOC-ERαKO < LC	pOC-ERαKO < LC	=	=
	I_{MAX}	=	pOC-ERαKO < LC	**pOC-ERαKO > LC**	=
	I_{MIN}	pOC-ERαKO < LC	pOC-ERαKO < LC	=	=
	ct.TMD	=	pOC-ERαKO < LC	=	=
Cortical midshaft	Ct.Ar	=	pOC-ERαKO < LC	**pOC-ERαKO > LC**	=
	Ma.Ar	=	=	**pOC-ERαKO > LC**	=
	Ct.Th	=	pOC-ERαKO < LC	=	=
	I_{MAX}	=	pOC-ERαKO < LC	**pOC-ERαKO > LC**	=
	I_{MIN}	=	pOC-ERαKO < LC	**pOC-ERαKO > LC**	=
	ct.TMD	=	pOC-ERαKO < LC	=	=

BV/TV = bone volume fraction; Tb.Th = trabecular thickness; Tb.Sp = trabecular separation; Tb.N = trabecular number; cn.TMD = cancellous tissue mineral density; Ct.Ar = cortical area; Ma.Ar = marrow area; Ct.Th = cortical thickness; I_{MAX} and I_{MIN} = maximum and minimum moments of inertia; ct.TMD = cortical tissue mineral density.

Supplemental Table 3.2 Adult female mice had a limited response to moderate-magnitude loading that was similar between genotypes, whereas young female mice had a robust response to loading that was greater in pOC-ERαKO mice. Loading increased cancellous bone mass in adult male mice but not young male mice. Data for young mice are from Ref. [14]. Light green + indicates an increase with loading; Dark green ++ indicates a greater increase with loading compared across genotype; Red – indicates a decrease with loading; White = indicates no change with loading.

		Female						Male			
		Young		Adult (Mod)		Adult (High)		Young		Adult	
		LC	pOC-ERαKO	LC	pOC-ERαKO	LC	pOC-ERαKO	LC	pOC-ERαKO	LC	pOC-ERαKO
Cancellous metaphysis	BV/TV	+	++	=	=	+	+	=	=	+	+
	Tb.Th	+	++	+	++	+	++	++	+	+	+
	Tb.Sp	=	=	=	=	=	=	=	=	=	=
	Tb.N	=	=	–	–	=	=	=	=	–	–
	cn.TMD	+	+	=	=	=	=	+	+	=	=
Cortical shell metaphysis	Ct.Ar	+	+	+	+	+	++	+	+	+	+
	Ct.Th	+	++	+	+	+	++	+	+	+	+
	I_{MAX}	+	+	+	+	+	+	+	+	+	+
	I_{MIN}	+	++	+	+	+	+	+	+	+	+
	ct.TMD	+	+	–	–	–	–	=	=	–	–
Cortical midshaft	Ct.Ar	+	++	+	+	+	++	+	+	=	=
	Ma.Ar	–	–	=	=	=	=	=	=	–	–
	Ct.Th	+	+	+	+	+	++	=	=	+	+
	I_{MAX}	+	++	+	+	+	++	+	+	=	=
	I_{MIN}	+	+	=	=	=	+	+	+	=	=
	ct.TMD	–	–	=	=	=	=	=	=	+	+

BV/TV = bone volume fraction; Tb.Th = trabecular thickness; Tb.Sp = trabecular separation; Tb.N = trabecular number; cn.TMD = cancellous tissue mineral density; Ct.Ar = cortical area; Ma.Ar = marrow area; Ct.Th = cortical thickness; I_{MAX} and I_{MIN} = maximum and minimum moments of inertia; ct.TMD = cortical tissue mineral density.

Chapter 4

LOADING MODALITY AND AGE INFLUENCE TERIPARATIDE-INDUCED BONE FORMATION IN THE HUMAN FEMORAL NECK

The following chapter is published in *Bone* and reprinted here with permission. The reference to the published work is:

A.M. Rooney, M.P.G. Bostrom, D.W. Dempster, J.W. Nieves, H. Zhou, F. Cosman, Loading modality and age influence teriparatide-induced bone formation in the human femoral neck, Bone 136 (2020). doi: 10.1016/j.bone.2020.115373.

4.1 Introduction

Teriparatide (TPTD), an analog of parathyroid hormone (PTH), has an anabolic effect on the skeleton when administered daily to treat osteoporosis. PTH analogs stimulate osteoblast activity and differentiation, increasing bone mass and improving microarchitecture [1,2]. TPTD and PTH produce a rapid increase in bone formation markers and a slower increase in bone resorption markers [3,4]. Iliac crest bone biopsy findings suggest that both modeling-based bone formation and remodeling-based bone formation are stimulated by TPTD, although the remodeling-based effect is responsible for most of the bone formed [5,6]. Much less is known about cellular activity in the femoral neck (FN), although we have shown previously that TPTD stimulates bone formation rapidly in endocortical and cancellous bone envelopes of the FN in patients undergoing total hip arthroplasty for osteoarthritis [7].

Mechanical loading also has an anabolic effect on the skeleton. Clinical studies have shown that mechanical loading through exercise increases bone mineral density (BMD) [8–11]. However, the skeleton's ability to adapt to its mechanical environment decreases with age, limiting the effectiveness of exercise in older populations that represent a large portion of osteoporosis patients [12,13]. In animal models, TPTD has been shown to have a synergistic effect when combined with mechanical loading, increasing bone mass to a greater extent than the additive benefits of either treatment alone [14–16]. Combining these two treatments may provide an opportunity to overcome the decline in mechanoadaptation with age and increase the anabolic effects of TPTD.

Mechanical loading may also help explain the site-specific limitations of TPTD in treating osteoporosis. Clinically, TPTD is most effective at increasing BMD in the spine, produces a moderate increase at the hip, and actually reduces BMD of the radius [17,18]. Many osteoporosis treatments are more effective at the spine, potentially due to the predominance of cancellous bone at this location compared to the hip and radius. However, in preclinical studies in mice, PTH was more effective at increasing BMD in the tibia and femur, and less effective in the spine [19]. These data suggest that locations experiencing mechanical loading, the spine in humans and the tibia and femur in mice, respond more to PTH treatment than those that do not, regardless of the amount of cancellous bone present. However, the hip in adult humans does not respond as well to TPTD, as measured by areal dual-energy X-ray absorptiometry BMD, despite undergoing mechanical loading during daily activities, indicating a more complex relationship.

One factor that may influence this relationship is the modality of mechanical loading the skeleton experiences. In a preclinical study, PTH and mechanical loading produced a synergistic increase in bone formation rate (BFR) on the tensile periosteal surface of rat tibias that underwent four-point bending, but PTH had no effect on the compressive surface [16]. In humans, bending in the femoral neck produces tension on one side and compression on the other [20]. In this study, we sought to compare the anabolic effects of TPTD at one skeletal site that experiences both loading conditions. We analyzed femoral neck samples obtained from patients undergoing total hip replacements for differences in formation indices in the tensile and compressive regions following TPTD treatment.

4.2 Methods

4.2.1 Patients

Forty postmenopausal women and men aged 60-89 years of age requiring a total hip replacement due to severe osteoarthritis (OA) were recruited and selected from two NY hospitals (Helen Hayes Hospital, West Haverstraw, NY; Hospital for Special Surgery, New York, NY) for this study as previously described, with thirty-eight patients completing the study [7]. Exclusion criteria were tetracycline allergy, diagnosis of rheumatologic disease other than OA, severe renal dysfunction (estimated glomerular filtration rate <30mL/min), uncorrected vitamin D deficiency (≤25ng/mL), recent use of glucocorticoids or osteoporosis medication (within 3 months), use of bisphosphonates within the past year, and all contraindications to the use of teriparatide (Paget's disease of bone, unexplained elevations in alkaline phosphatase,

hypercalcemia, hyperparathyroidism, metabolic bone disease other than osteoporosis, history of bone irradiation, or history of bone cancer), any active cancer other than skin, and history of multiple or recent renal calculi. Patients were excluded if they had used bisphosphonates within the prior year. Use before that period was n=5 in the TPTD group and n=4 in the placebo group. The study was approved by the institutional review boards of both hospitals and all participants provided informed consent. A National Institutes of Health-appointed data safety monitoring board supervised study progress.

4.2.2 Protocols and procedures

Patients were randomized to receive daily subcutaneous injections of TPTD (20mcg, n=21) or identically appearing placebo (PBO, n=18) prior to surgery. The mean treatment duration for the TPTD group was 41 days, with all but one patient receiving treatment for 25-56 days. One patient was treated for 84 days due to an unrelated delay in surgery. The mean treatment duration for the PBO group was 39 days, ranging from 27-56 days. Double tetracycline labeling for new bone formation was administered starting 21 days prior to surgery, following a standard protocol (250 mg tetracycline 4 times daily for 3 days, 10 days off, 150 mg demeclocycline 4 times daily for 3 days, and 5 days off before surgery).

During surgery, a 1.0-1.5 cm thick sample of the mid-femoral neck was removed, fixed in 10% formalin, and embedded following standard protocol for undecalcified iliac crest biopsies [1,7]. As previously described, three sections, one 20 µm thick and two 7 µm thick, were obtained from two locations 100 µm apart. The 20

μm thick sections from both locations were mounted unstained, and one 7 μm thick section from each location was stained with Goldner trichrome and the other with toluidine blue [7].

Histomorphometric analysis was performed using OsteoMeasure version 3.0 (OsteoMetrics, Inc.) [1]. The tensile and compressive regions were analyzed separately. Based on finite element models [20], the tensile region was defined as the superior and superior-posterior octants, and the compressive region was defined as the inferior and inferior-anterior octants (Fig. 4.1). Goldner trichrome-stained sections were analyzed for cortical width (Ct.Wi) and porosity (Ct.Po.Ar), and eroded surface (ES/BS). Toluidine blue sections were analyzed for osteoclast number (Oc.N/BS). Unstained sections were analyzed for mineralized surface (MS/BS), mineral apposition rate (MAR), and bone formation rate (BFR/BS). MS/BS, MAR, and BFR/BS were analyzed on both the endocortical (Ec) and periosteal (Ps) surfaces. Oc.N/BS and ES/BS were analyzed only on the endocortical surface. Femoral neck angle and offset were measured from pre-operative radiographs.

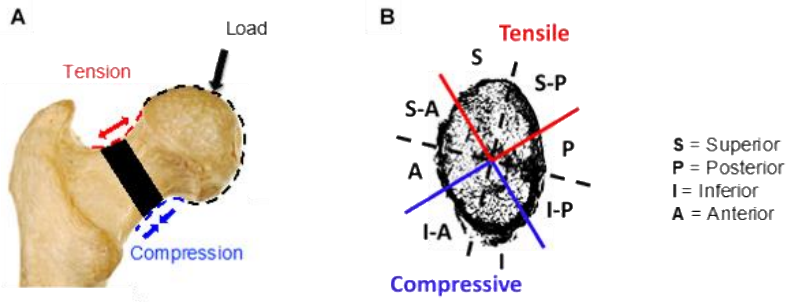

Figure 4.1 Sample location and definition of loading modality regions. (A) Samples were taken from the mid-femoral neck, shown in black. (B) Daily activity produces tension in the superior and superior-posterior regions (S, S-P) and compression in the inferior and inferior-anterior regions (I, I-A), as shown in the representative FN cross section.

4.2.3 Statistical analyses

Differences in FN angle and offset by treatment group were tested using Student *t* tests. The effects of treatment (TPTD vs. PBO) and loading modality (Tensile vs. Compressive) were tested using a linear mixed effects model with treatment, loading modality, and their interaction as fixed effects. A random patient effect was included to account for intra-patient variability. Significance was set at $p<0.05$.

Multiple regression analyses were conducted using linear mixed effects models with a random patient effect to account for multiple measurements within a single patient. The relationships between intrinsic anatomical parameters (age, sex, body mass index [BMI], body weight [BW], femoral neck angle and offset, Ct.Wi, Ct.Po.Ar, loading modality, treatment) and bone remodeling parameters (MS/BS, MAR, BFR/BS, Oc.N/BS, ES/BS) were examined. Multiple regression models for bone remodeling measures included loading modality, treatment, and one other anatomical parameter as fixed effects. Models were constructed through stepwise regression of variables. The exclusion criteria for the highest order term in the model was $p>0.10$.

4.3 Results

4.3.1 Patient characteristics

As previously reported, there were no statistical differences in patient demographics between groups [7], including age (PBO 69.2±5.8y, TPTD 71.6±9.3y), height (PBO 65.7±4.0in, TPTD 65.1±4.7in), weight (PBO 186±44lb, TPTD

166±42lb), BMI (PBO 30.2±6.1kg/m^2, TPTD 27.4±5.5kg/m^2), and male to female ratio (PBO 6M/11F, TPTD 8M/13F). There were also no differences in Ct.Wi, Ct.Po.Ar, FN angle and offset between the TPTD and PBO groups (Table 4.1). However, Ct.Wi was thinner in the tensile compared to compressive region for both treatments.

Table 4.1 Histomorphometric data by loading modality and treatment

	Teriparatide (n=21)		Placebo (n=17)	
	Tensile	Compressive	Tensile	Compressive
Endocortical Surface				
MS/BS (%)	19.0±3.0†,*	13.2±2.0*	11.0±2.5†	7.02±1.3
MAR (μm/d)	0.663±0.033	0.652±0.029	0.617±0.033	0.660±0.033
BFR/BS ($mm^3/mm^2/y$)	0.054±0.008†,*	0.036±0.006*	0.030±0.007†	0.023±0.005
ES/BS (%)	4.78±0.81	4.74±0.64	3.79±0.63	7.00±1.6
Oc.N/BS (#/mm)	0.135±0.033	0.0906±0.020	0.0873±0.024	0.0899±0.026
Periosteal Surface				
MS/BS (%)	19.1±3.3†	24.4±3.8	12.8±2.0†	25.0±5.0
MAR (μm/d)	0.820±0.067	0.916±0.070	0.846±0.10	0.867±0.063
BFR/BS ($mm^3/mm^2/y$)	0.067±0.01†	0.096±0.02	0.057±0.01†	0.101±0.02
Ct.Wi (μm)	684±73†	1227±128	609±59†	1369±128
Ct.Po.Ar (%)	10.6±0.73	10.3±0.80	9.44±0.75	9.38±1.0
FN Offset (mm)	39.0±2.0		39.1±1.4	
FN Angle (°)	137±1.4		135±1.1	

Data are Mean±SEM; $p < 0.05$
† Tensile different from Compressive
* TPTD different from PBO

4.3.2 Endocortical surface

Dynamic bone formation parameters on the endocortical surface were different by treatment and loading modality (Table 4.1). The TPTD group exhibited higher MS/BS (+79%) and BFR/BS (+75%) compared to PBO in both tensile and compressive regions (Fig. 4.2A,C). MS/BS and BFR/BS were greater in the tensile region compared to the compressive region in both TPTD and PBO groups (+48%

MS/BS, +43% BFR/BS), although there was no difference in TPTD effect by region. Eroded surface was greater in the compressive compared to the tensile region of the PBO group and compared to both the tensile and compressive regions in the TPTD group (+56%, p=0.087) (Fig. 4.2D). MAR and Oc.N/BS were not affected by treatment or loading modality (Fig. 4.2B,E).

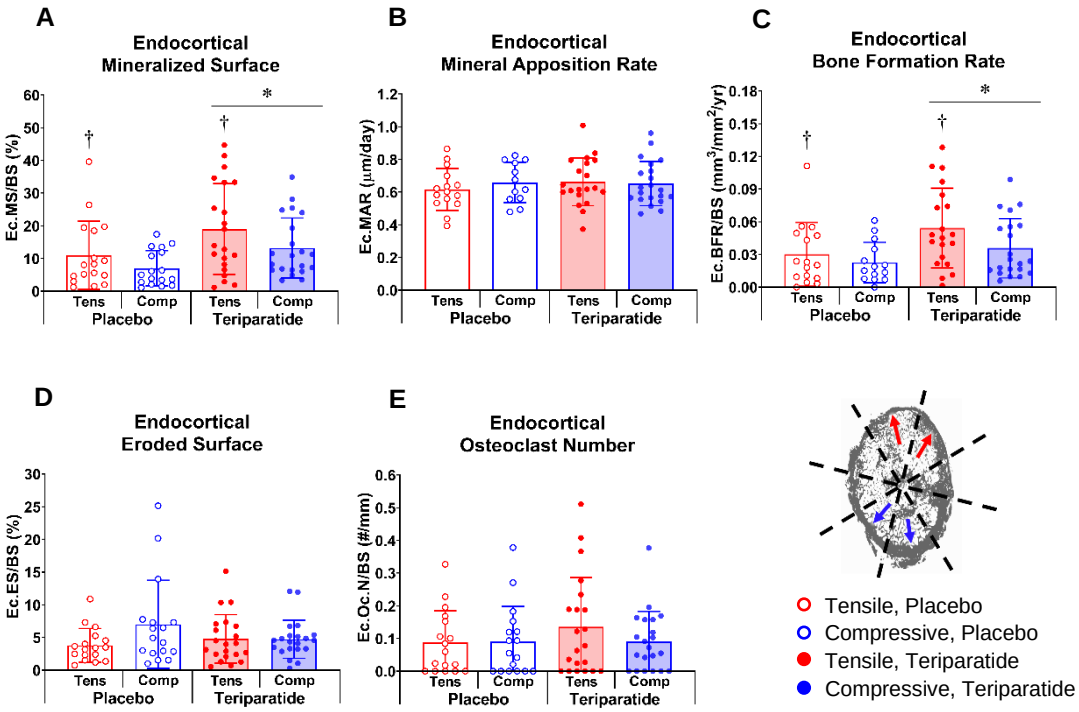

Figure 4.2 Dynamic formation indices on the endocortical surface were greater in the TPTD group and differed by loading modality. (A,C) The TPTD group had greater endocortical MS/BS and BFR/BS compared to the PBO group. MS/BS and BFR/BS were greater on the tensile (Tens) surface than the compressive (Comp) surface. (B,D,E) Endocortical MAR, ES/BS, and Oc.N/BS were not statistically different by treatment group or loading modality. ES/BS in the compressive region of the PBO group trended higher than the tensile region and both regions of the TPTD group (p = 0.087). * TPTD different from PBO, † Tensile different from Compressive, $p < 0.05$ by a linear mixed effects model with a random patient effect.

In order to account for some of the variability in the broad patient population, we examined multiple linear regression models for bone remodeling measures.

Loading modality, treatment, and age best explained the variability in endocortical MS/BS (R^2_{adj}=0.283, Fig. 4.3A) and BFR/BS (R^2_{adj}=0.225, Supp. Table 4.1). The models predicted a greater effect of TPTD in increasing MS/BS in older patients compared to younger patients (Fig. 4.3B). BFR/BS was predicted to increase with age, but TPTD was predicted to increase BFR/BS similarly for all ages. Variability in endocortical MS/BS (R^2_{adj}=0.245, Fig. 4.4A), BFR/BS (R^2_{adj}=0.213, Supp. Table 4.1), and Oc.N/BS (R^2_{adj}=0.247, Fig. 4.4B) was also greatly explained by patient sex. TPTD was predicted to increase MS/BS and BFR/BS in females but not males (Fig. 4.4C). The models also predicted that TPTD would not have an effect on Oc.N/BS in the compressive region, and would increase Oc.N/BS in the tensile region in females but decrease Oc.N/BS in the tensile region in males (Fig. 4.4D). Increased body weight was associated with decreased Oc.N/BS (R^2_{adj}=0.132, Supp. Table 4.1). FN angle and offset were not significant in any of the endocortical regression models.

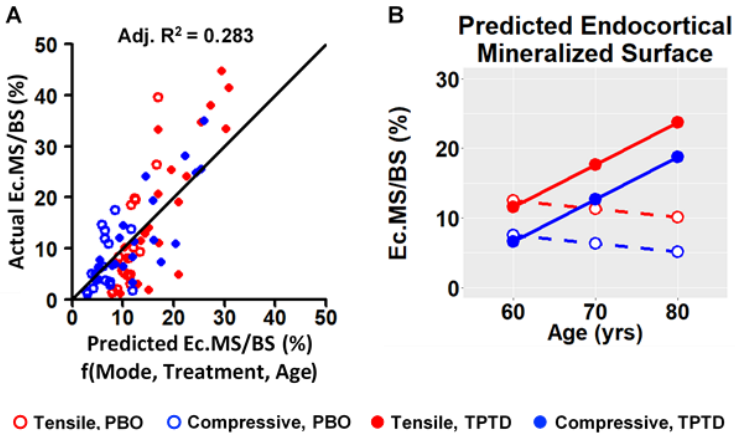

Figure 4.3 Age had the most explanatory power over the variability in endocortical formation indices. (A) Multivariable linear mixed effects model shown as predicted endocortical MS/BS versus measured values. Variations in endocortical MS/BS were best explained by loading modality, treatment, and patient age. (B) Model prediction based on varying patient data. The beneficial effect of TPTD on endocortical MS/BS was predicted to increase with age for the compressive and tensile regions.

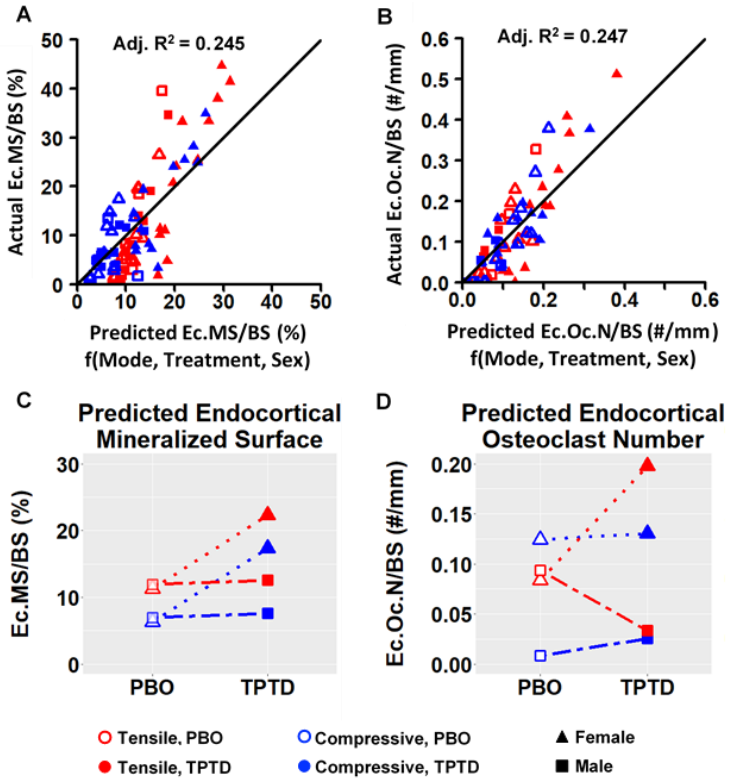

Figure 4.4 Patient sex had a high explanatory power over the variability in endocortical formation indices. (A,B) Multivariable linear mixed effects models shown as predicted versus measured values. Variations in endocortical MS/BS and Oc.N/BS were well explained by loading modality, treatment, and patient sex. (C,D) Model predictions based on varying patient data. TPTD was predicted to increase endocortical MS/BS in females but not males. Endocortical Oc.N/BS in the tensile region was predicted to increase in females and decrease in males with TPTD, but the compressive region was predicted to be unaffected by TPTD.

4.3.3 Periosteal surface

Unlike the endocortical surface, TPTD did not affect bone formation on the periosteal surface (Table 4.1). Also in contrast to the endocortical surface, MS/BS and BFR/BS were lower in the tensile region compared to the compressive region (-52% MS/BS, -58% BFR/BS) (Fig. 4.5A,C). MAR was again unaffected by treatment and loading modality (Fig. 4.5B). ES/BS and Oc.N/BS were not analyzed on the periosteal

surface as there is minimal periosteal remodeling in adults and modeling-based resorption typically only occurs during bone growth.

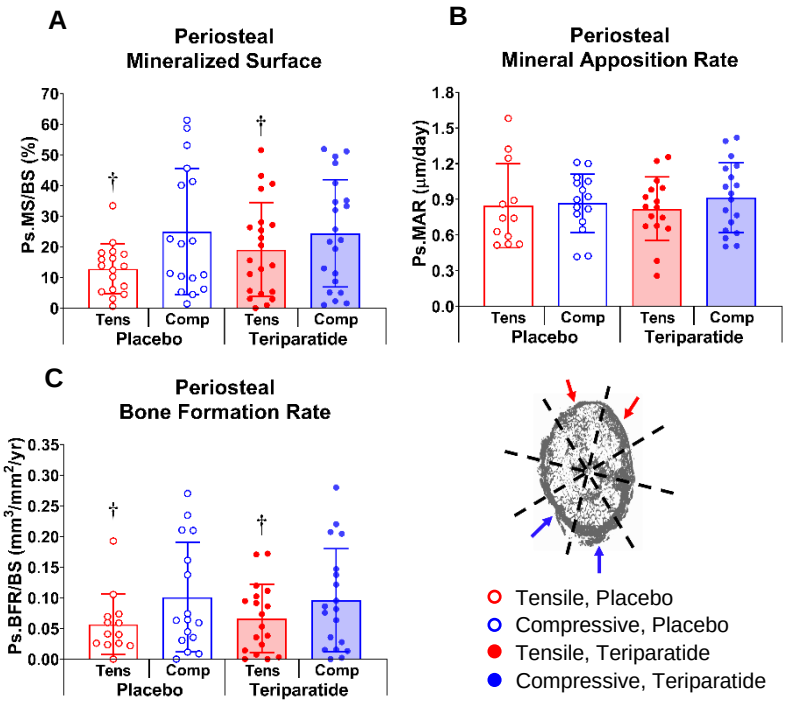

Figure 4.5 On the periosteal surface, TPTD had no effect on dynamic bone formation indices. (A,C) MS/BS and BFR/BS were greater on the compressive (Comp) surface compared to the tensile (Tens) surface. (B) MAR was unaffected by treatment or loading modality. † Tensile different from Compressive, $p < 0.05$ by a linear mixed effects model with a random patient effect.

The variability in periosteal bone formation parameters was best explained by body weight or BMI, patient sex, and Ct.Wi. Periosteal bone measures may also have been altered due to the presence of severe osteoarthritis in the joint. Thicker cortices were associated with increased MS/BS (Supp. Table 4.1). Interactions between loading modality, treatment, and patient BMI (R^2_{adj}=0.126, Fig. 4.6A) or sex (R^2_{adj}=0.153, Fig. 4.7A) best explained the variability in MS/BS, and interactions between loading modality, treatment, and body weight best explained the variability in BFR/BS (R^2_{adj}=0.167, Fig. 4.6B). In females, TPTD was predicted to increase

periosteal MS/BS in the tensile but not the compressive region (Fig. 4.7B). TPTD was predicted to have limited effects on periosteal MS/BS in males (Fig. 4.7B). In general, TPTD had a greater effect on bone formation in patients with lower body weight and BMI than in larger patients (Fig. 4.6C,D). The models predicted that TPTD would increase MS/BS and BFR/BS in the tensile region and decrease bone formation indices in the compressive region for smaller patients. Age, FN angle and offset, and Ct.Po.Ar were not significant in any of the periosteal regression models.

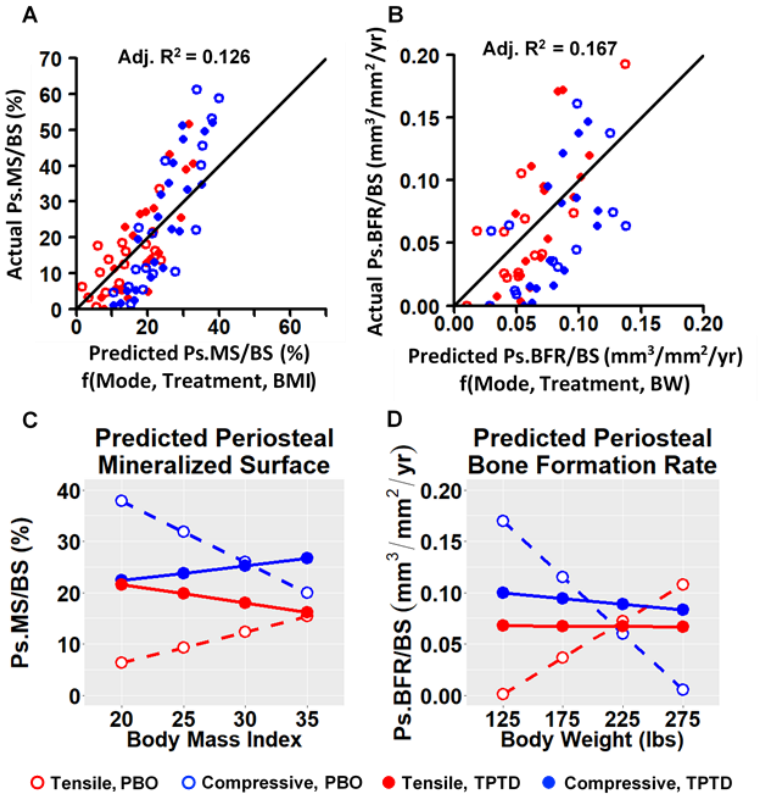

Figure 4.6 Patient BMI and body weight (BW) accounted for a high amount of variability in periosteal formation indices. (A,B) Multivariable linear mixed effects models shown as predicted versus measured values. Variations in periosteal MS/BS and BFR/BS were well explained by loading modality, treatment, and patient BMI or BW. (C,D) Model predictions based on varying patient data. TPTD was predicted to have greater effects on the periosteal surface in patients with lower BMI and BW, reducing formation in the compressive region and increasing formation in the tensile region.

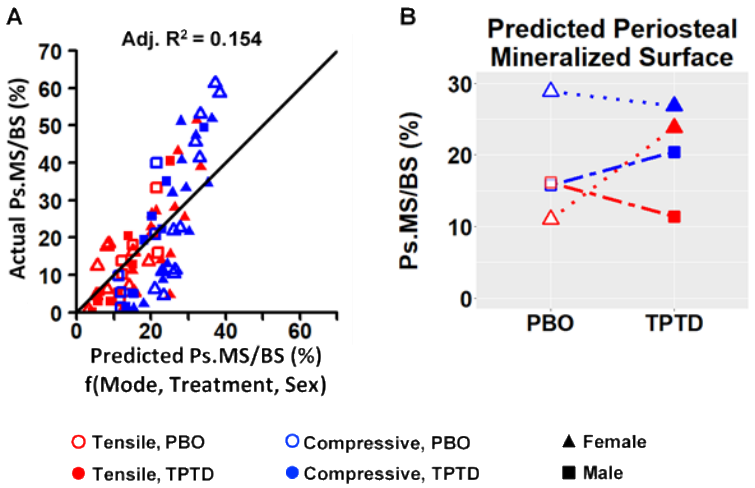

Figure 4.7 Patient sex accounted for a high amount of variability in periosteal formation indices. (A) Multivariable linear mixed effects model shown as predicted versus measured values. Variations in periosteal MS/BS were greatly explained by loading modality, treatment, and patient sex. (B) Model prediction based on varying patient data. TPTD was predicted to increase periosteal BFR/BS in the tensile region in females but not males. TPTD was predicted to have limited effects in the compressive region of males and females.

4.4 Discussion

Although these patients were treated for a short duration and presented with osteoarthritis but not osteoporosis, these data provide important insights into the effect of teriparatide at a clinically relevant fracture site. TPTD increased bone formation on the endocortical surface but not the periosteal surface of the femoral neck. Regardless of treatment, the tensile region exhibited greater bone formation than the compressive region on the endocortical surface. In contrast, on the periosteal surface there was less bone formation in the tensile compared with the compressive region.

These data represent the first direct comparison of two loading modalities and their impact on teriparatide-induced bone formation parameters in humans. Roberts and colleagues analyzed the effect of PTH on the endocortical surfaces of rat tibias

subjected to *in vivo* four-point bending by circumferential location [21]. They found that PTH enhanced the anabolic effects of the applied mechanical loading on the tensile and compressive locations similarly. Hagino and colleagues performed a similar tibial four-point bending experiment in PTH-treated rats and analyzed the tensile and compressive periosteal surfaces [16]. They found that PTH enhanced the load-induced increase in bone formation on the tensile surface but not the compressive surface. However, the strain magnitudes on the tensile surface were higher than those on the compressive surface, and there was no direct comparison between these two surfaces.

Here, we found greater bone formation in the tensile region on the endocortical surface and greater bone formation in the compressive region on the periosteal surface regardless of TPTD treatment. The cortical widths of the superior and superior-posterior octants that comprised the tensile region were thinner than the inferior and inferior-anterior octants that comprised the compressive region. This anatomical difference may have contributed to these baseline differences in dynamic bone formation, as thicker cortices in the iliac crest have been associated with greater dynamic formation indices in patients treated with TPTD [22]. Increased bone formation with TPTD was due to increased MS/BS rather than increased MAR, consistent with some previous studies [1,23]. Although other studies have shown increased cancellous [2,24] or endocortical [25] MAR at the iliac crest with TPTD treatment in postmenopausal women, our more diverse patient population and different site of analysis may account for these differences.

There were no statistically significant differences in the response to teriparatide by loading modality alone, but some trends emerged. Endocortical eroded surface was decreased with TPTD only in the compressive region. On the periosteal surface, MS/BS and BFR/BS were predicted to increase with teriparatide in the tensile region but decrease with teriparatide in the compressive region for smaller patients. Additionally, TPTD was predicted to increase endocortical Oc.N/BS and periosteal MS/BS only in the tensile region in females. It is important to note that in this study females had lower body weight ($p<0.05$, Student t test) and BMI ($p=0.07$, Student t test) than males. Therefore, it is difficult to determine whether low body mass or patient sex was the driving factor for this increase in TPTD effect in the tensile region. Together these data suggest an increased ratio of formation to resorption particularly in the tensile regions of the femoral neck with teriparatide. However, the wide range of patient demographics and small sample size led to highly variable data that may have obscured some of the interactions between treatment and loading modality.

Unlike previous preclinical studies, patients in this study were not subjected to external mechanical loading. Our study took advantage of the physiological loading environment of the femoral neck during normal daily activity. However, these patients had osteoarthritis severe enough to require a total hip replacement and were likely in enough pain to limit their daily activity. Therefore, the effects of loading modality may have been underestimated or obscured by the reduction in overall mechanical loading. The presence of severe osteoarthritis at the hip also may have altered the environment of the joint, influencing baseline dynamic measurements and their response to teriparatide [26]. This altered periosteal environment due to osteoarthritis

may help explain the lack of a TPTD effect in the periosteal envelope that has been previously shown in other studies [6,23]. Additionally, the short treatment time course in this study, typically ranging from 4 to 8 weeks, may have underestimated the effects of teriparatide. A longer time course may have produced greater differences between treatment groups, and potentially revealed differences by loading modality. In fact, in clinical trials, there is a greater rate of BMD increase in the FN during the last 6 months of a 2 year TPTD treatment course [27,28]. However, the surgeries could not be delayed to increase the treatment time for ethical reasons.

Our data predict that endocortical bone formation is increased with TPTD more in older compared to younger patients. Preclinical studies have shown similar results when comparing the response to PTH in aged and young mice [29] and rats [30]. Aged animals demonstrated a greater increase in bone formation with PTH treatment than young animals. However, a meta-analysis of clinical studies performed by Schwarz and colleagues found that patient age did not correlate to total hip BMD changes with PTH, and was negatively correlated with BMD changes in the spine [31]. It is possible that the age-related increase in teriparatide response we found here was isolated to the endocortical surface of the femoral neck, and therefore would not be detectable in a total hip BMD measurement. Further investigation into the role of age on teriparatide efficacy in a larger population is required to fully understand this association.

Endocortical bone formation was also predicted to increase with TPTD in females but not males. However, as previously mentioned, body weight and BMI were lower in females than males and BMI was also a significant predictor of endocortical

MS/BS (Supp. Table 4.1). TPTD was predicted to increase endocortical MS/BS the most in the tensile region of patients with lower BMI (Supp. Fig 4.1). The difference in predicted TPTD efficacy in endocortical MS/BS may be due to the lower body mass associated with females in this study rather than inherent differences by sex. Additionally, there were fewer men than women in both treatment groups which may have limited the statistical power to detect changes with treatment in men.

The relationship between body mass and skeletal health is complicated and not well defined [32]. It has long been known that increased body mass produces greater mechanical loads on the skeleton, which increases bone mass [33,34]. However, metabolic changes associated with obesity may counteract these benefits and cause reductions in bone mass [35,36]. Our data show a similarly complicated relationship, with the effect of body mass on predicted periosteal bone formation differing based on loading modality and treatment. In placebo treated patients, increased body mass was predicted to decrease MS/BS and BFR/BS in the compressive region but increase MS/BS and BFR/BS in the tensile region. Teriparatide was not predicted to alter periosteal bone formation in larger patients but was predicted to increase mineralized surface in the tensile region and decrease mineralized surface in the compressive region in smaller patients. Differences in formation on the tensile and compressive surfaces in the PBO group may be due to baseline anatomical differences. Ct.Wi is different in these two locations, which may provide a different loading environment and baseline cellular activity. In non-obese patients (BMI < 30; PBO n=7, TPTD n=14), the predicted effect of TPTD was different in the tensile and compressive regions, indicating a role of loading modality in the efficacy of TPTD that should be

explored further. In obese patients (BMI > 30; PBO n=10, TPTD n=7), the predicted periosteal effect of TPTD was minimal. This may be due to confounding metabolic factors preventing or counteracting the effects of TPTD.

These data represent the first dynamic comparison of teriparatide treatment under two loading modalities in human samples. The femoral neck is a clinically relevant osteoporotic fracture site and allows the comparison of two loading modalities at a single location in a patient. We found that the level of bone formation was different in the tensile and compressive regions of both the endocortical and periosteal envelopes. There was also a trend toward decreased eroded surface with teriparatide in the compressive region, indicating a potential loading modality specific effect of teriparatide. Future work could determine whether specific hip loading interventions could amplify the benefits of teriparatide on the hip in clinical settings.

4.5 References

[1] D.W. Dempster, F. Cosman, E.S. Kurland, H. Zhou, J. Nieves, L. Woelfert, E. Shane, K. Plavetić, R. Müller, J. Bilezikian, R. Lindsay, Effects of daily treatment with parathyroid hormone on bone microarchitecture and turnover in patients with osteoporosis: a paired biopsy study., J. Bone Miner. Res. 16 (2001) 1846–53. doi:10.1359/jbmr.2001.16.10.1846.

[2] R. Lindsay, H. Zhou, F. Cosman, J. Nieves, D.W. Dempster, A.B. Hodsman, Effects Of a One-Month Treatment With PTH(1-34) on Bone Formation on Cancellous, Endocortical, and Periosteal Surfaces of the Human Ilium, J. Bone Miner. Res. 22 (2007) 495–502. doi:10.1359/jbmr.070104.

[3] F. Cosman, Parathyroid hormone and abaloparatide treatment for osteoporosis, Curr. Opin. Endocr. Metab. Res. 3 (2018) 61–67. doi:10.1016/j.coemr.2018.02.005.

[4] F. Cosman, J. Nieves, M. Zion, L. Woelfert, M. Luckey, R. Lindsay, Daily and cyclic parathyroid hormone in women receiving alendronate, N. Engl. J. Med. 353 (2005) 566–575.

[5] D.W. Dempster, H. Zhou, V.A. Ruff, T.E. Melby, J. Alam, K.A. Taylor, Longitudinal Effects of Teriparatide or Zoledronic Acid on Bone Modeling- and Remodeling-Based Formation in the SHOTZ Study, J. Bone Miner. Res. 33 (2018) 627–633. doi:10.1002/jbmr.3350.

[6] D.W. Dempster, H. Zhou, R.R. Recker, J.P. Brown, C.P. Recknor, E.M. Lewiecki, P.D. Miller, S.D. Rao, D.L. Kendler, R. Lindsay, J.H. Krege, J. Alam, K.A. Taylor, T.E. Melby, V.A. Ruff, Remodeling- and Modeling-Based Bone Formation With Teriparatide Versus Denosumab: A Longitudinal Analysis From Baseline to 3 Months in the AVA Study, J. Bone Miner. Res. 33 (2018) 298–306. doi:10.1002/jbmr.3309.

[7] F. Cosman, D.W. Dempster, J.W. Nieves, H. Zhou, M. Zion, C. Roimisher, Y. Houle, R. Lindsay, M. Bostrom, Effect of Teriparatide on Bone Formation in the Human Femoral Neck, J. Clin. Endocrinol. Metab. 101 (2016) 1498–1505. doi:10.1210/jc.2015-3698.

[8] R.K. Fuchs, J.J. Bauer, C.M. Snow, Jumping improves hip and lumbar spine bone mass in prepubescent children: a randomized controlled trial., J. Bone Miner. Res. 16 (2001) 148–156. doi:10.1359/jbmr.2001.16.1.148.

[9] S. Kontulainen, H. Sievänen, P. Kannus, M. Pasanen, I. Vuori, Effect of long-term impact-loading on mass, size, and estimated strength of humerus and radius of female racquet-sports players: a peripheral quantitative computed tomography study between young and old starters and controls., J. Bone Miner. Res. 18 (2003) 352–359. doi:10.1359/jbmr.2003.18.2.352.

[10] A. Vainionpää, R. Korpelainen, J. Leppäluoto, T. Jämsä, Effects of high-impact exercise on bone mineral density: A randomized controlled trial in premenopausal women, Osteoporos. Int. 16 (2005) 191–197. doi:10.1007/s00198-004-1659-5.

[11] K.M. Winters-Stone, C.M. Snow, Site-specific response of bone to exercise in premenopausal women, Bone. 39 (2006) 1203–1209. doi:10.1016/j.bone.2006.06.005.

[12] M.E. Lynch, R.P. Main, Q. Xu, T.L. Schmicker, M.B. Schaffler, T.M. Wright, M.C.H. van der Meulen, Tibial compression is anabolic in the adult mouse skeleton despite reduced responsiveness with aging, Bone. 49 (2011) 439–446. doi:10.1016/j.bone.2011.05.017.
[13] E.J. Bassey, M.C. Rothwell, J.J. Littlewood, D.W. Pye, Pre- and postmenopausal women have different bone mineral density responses to the same high-impact exercise., J. Bone Miner. Res. 13 (1998) 1805–1813. doi:10.1359/jbmr.1998.13.12.1805.
[14] Y. Ma, W.S. Jee, Z. Yuan, W. Wei, H. Chen, S. Pun, H. Liang, C. Lin, Parathyroid hormone and mechanical usage have a synergistic effect in rat tibial diaphyseal cortical bone., J. Bone Miner. Res. 14 (1999) 439–48. doi:10.1359/jbmr.1999.14.3.439.
[15] T. Sugiyama, L.K. Saxon, G. Zaman, A. Moustafa, A. Sunters, J.S. Price, L.E. Lanyon, Mechanical loading enhances the anabolic effects of intermittent parathyroid hormone (1-34) on trabecular and cortical bone in mice, Bone. 43 (2008) 238–248. doi:10.1016/j.bone.2008.04.012.
[16] H. Hagino, T. Okano, M.P. Akhter, M. Enokida, R. Teshima, Effect of parathyroid hormone on cortical bone response to in vivo external loading of the rat tibia, J. Bone Miner. Metab. 19 (2001) 244–250. doi:10.1007/s007740170027.
[17] F. Cosman, Anabolic and Antiresorptive Therapy for Osteoporosis : Combination and Sequential Approaches, Curr. Osteoporos. Rep. (2014) 385–395. doi:10.1007/s11914-014-0237-9.
[18] J.W. Mandema, J. Zheng, C. Libanati, J. Jose, P. Ruixo, Time Course of Bone Mineral Density Changes With Denosumab Compared With Other Drugs in Postmenopausal Osteoporosis : A Dose-Response-Based Meta-Analysis, J. Clin. Endocrinol. Metab. 99 (2014) 3746–3755. doi:10.1210/jc.2013-3795.
[19] A. Iida-Klein, H. Zhou, S.S. Lu, L.R. Levine, M. Ducayen-Knowles, D.W. Dempster, J. Nieves, R. Lindsay, Anabolic action of parathyroid hormone is skeletal site specific at the tissue and cellular levels in mice, J. Bone Miner. Res. 17 (2002) 808–816. doi:10.1359/jbmr.2002.17.5.808.
[20] S. Nawathe, B.P. Nguyen, N. Barzanian, H. Akhlaghpour, M.L. Bouxsein, T.M. Keaveny, Cortical and trabecular load sharing in the human femoral neck, J. Biomech. 48 (2015) 816–822. doi:10.1016/j.jbiomech.2014.12.022.
[21] M.D. Roberts, T.J. Santner, R.T. Hart, Local bone formation due to combined mechanical loading and intermittent hPTH-(1-34) treatment and its correlation to mechanical signal distributions, J. Biomech. 42 (2009) 2431–2438. doi:10.1016/j.jbiomech.2009.08.030.
[22] Y.L. Ma, F. Marin, J. Stepan, S. Ish-Shalom, R. Möricke, F. Hawkins, G. Kapetanos, M.P. de la Peña, J. Kekow, G. Martínez, J. Malouf, Q.Q. Zeng, X. Wan, R.R. Recker, Comparative effects of teriparatide and strontium ranelate in the periosteum of iliac crest biopsies in postmenopausal women with osteoporosis, Bone. 48 (2011) 972–978. doi:10.1016/j.bone.2011.01.012.
[23] Y.L. Ma, Q.Q. Zeng, A.Y. Chiang, D. Burr, J. Li, H. Dobnig, A. Fahrleitner-Pammer, D. Michalská, F. Marin, I. Pavo, J.J. Stepan, Effects of teriparatide on cortical histomorphometric variables in postmenopausal women with or without

prior alendronate treatment, Bone. 59 (2014) 139–147. doi:10.1016/j.bone.2013.11.011.
[24] A.B. Hodsman, M. Kisiel, J.D. Adachi, L.J. Fraher, P.H. Watson, Histomorphometric evidence for increased bone turnover without change in cortical thickness or porosity after 2 years of cyclical hPTH(1-34) therapy in women with severe osteoporosis, Bone. 27 (2000) 311–318. doi:10.1016/S8756-3282(00)00316-1.
[25] R. Lindsay, F. Cosman, H. Zhou, M.P. Bostrom, V.W. Shen, J.A.D. Cruz, J.W. Nieves, D.W. Dempster, A novel tetracycline labeling schedule for longitudinal evaluation of the short-term effects of anabolic therapy with a single iliac crest bone biopsy: Early actions of teriparatide, J. Bone Miner. Res. 21 (2006) 366–373. doi:10.1359/JBMR.051109.
[26] G.R. Jordan, N. Loveridge, J. Power, M.T. Clarke, J. Reeve, Increased cancellous bone in the femoral neck of patients with coxarthrosis (hip osteoarthritis): a positive remodeling imbalance favoring bone formation, Osteoporos. Int. 14 (2003) 160–165. doi:10.1007/s00198-002-1351-6.
[27] B.Z. Leder, J.N. Tsai, A. V. Uihlein, S.A.M. Burnett-Bowie, Y. Zhu, K. Foley, H. Lee, R.M. Neer, Two years of denosumab and teriparatide administration in postmenopausal women with osteoporosis (The DATA Extension Study): A randomized controlled trial, J. Clin. Endocrinol. Metab. 99 (2014) 1694–1700. doi:10.1210/jc.2013-4440.
[28] B.M. Obermayer-Pietsch, F. Marin, E. V. McCloskey, P. Hadji, J. Farrerons, S. Boonen, M. Audran, C. Barker, A.D. Anastasilakis, W.D. Fraser, T. Nickelsen, Effects of two years of daily teriparatide treatment on BMD in postmenopausal women with severe osteoporosis with and without prior antiresorptive treatment, J. Bone Miner. Res. 23 (2008) 1591–1600. doi:10.1359/jbmr.080506.
[29] R.L. Jilka, M. Almeida, E. Ambrogini, L. Han, P.K. Roberson, R.S. Weinstein, S.C. Manolagas, Decreased oxidative stress and greater bone anabolism in the aged, when compared to the young, murine skeleton with parathyroid hormone administration, Aging Cell. 9 (2010) 851–867. doi:10.1111/j.1474-9726.2010.00616.x.
[30] G. Friedl, R.T. Turner, G.L. Evans, H. Dobnig, Intermittent Parathyroid Hormone (PTH) Treatment and Age-Dependent Effects on Rat Cancellous Bone and Mineral Metabolism, J. Orthop. Res. 25 (2007) 1454–1464. doi:10.1002/jor.
[31] P. Schwarz, N.R. Jørgensen, L. Mosekilde, P. Vestergaard, Effects of Increasing Age, Dosage, and Duration of PTH Treatment on BMD Increase — A Meta-analysis, Calcif. Tissue Int. 90 (2012) 165–173. doi:10.1007/s00223-011-9564-3.
[32] E. Dolan, P.A. Swinton, C. Sale, A. Healy, J. O'Reilly, Influence of adipose tissue mass on bone mass in an overweight or obese population : systematic review and meta-analysis, Nutr. Clin. Care. 75 (2017) 858–870. doi:10.1093/nutrit/nux046.
[33] D.T. Felson, Y. Zhang, M.T. Hannan, J.J. Anderson, Effects of weight and body mass index on bone mineral density in men and women: The Framingham study, J. Bone Miner. Res. 8 (1993) 567–573. doi:10.1002/jbmr.5650080507.

[34] P. Ravn, G. Cizza, N.H. Bjarnason, D. Thompson, M. Daley, R.D. Wasnich, M. McClung, D. Hosking, A.J. Yates, C. Christiansen, Low Body Mass Index Is an Important Risk Factor for Low Bone Mass and Increased Bone Loss in Early Postmenopausal Women, J. Bone Miner. Res. 14 (1999) 1622–1627. doi:10.1359/jbmr.1999.14.9.1622.
[35] S.A. Shapses, L.C. Pop, Y. Wang, Obesity is a concern for bone health with aging, Nutr. Res. 39 (2017) 1–13. doi:10.1016/j.nutres.2016.12.010.
[36] J.J. Cao, Effects of obesity on bone metabolism, J. Orthop. Surg. Res. 6 (2011) 1–7.

4.6 Chapter 4 Supplemental Information

Supplemental Table 4.1 Statistically significant linear mixed-effects models

Dependent Variable	Independent Variables	Adjusted R^2
Ec.MS/BS	Loading Modality, Treatment, Age, Treatment×Age	0.283
	Loading Modality, Treatment, Sex, Treatment×Sex	0.245
	Loading Modality, Treatment, Ct.Po.Ar, Treatment×Ct.Po.Ar	0.200
	Loading Modality*Treatment*BMI	0.178
	Loading Modality, BW	0.127
Ec.BFR/BS	Loading Modality, Treatment, Age	0.225
	Loading Modality, Treatment, Sex, Treatment×Sex	0.213
	Loading Modality*Treatment*Ct.Wi	0.172
	Loading Modality, BW	0.107
Ec.ES/BS	Loading Modality, Treatment, Loading Modality×Treatment	0.0667
Ec.Oc.N/BS	Loading Modality*Treatment*Sex	0.247
	Body Weight	0.132
Ps.MS/BS	Loading Modality*Treatment*Sex	0.154
	Loading Modality*Treatment*BMI	0.126
	Ct.Wi	0.0774
Ps.BFR/BS	Loading Modality*Treatment*BW	0.167
	Loading Modality, Sex	0.104

* Indicates full factorial model, all single and cross terms included
× Indicates individual cross term

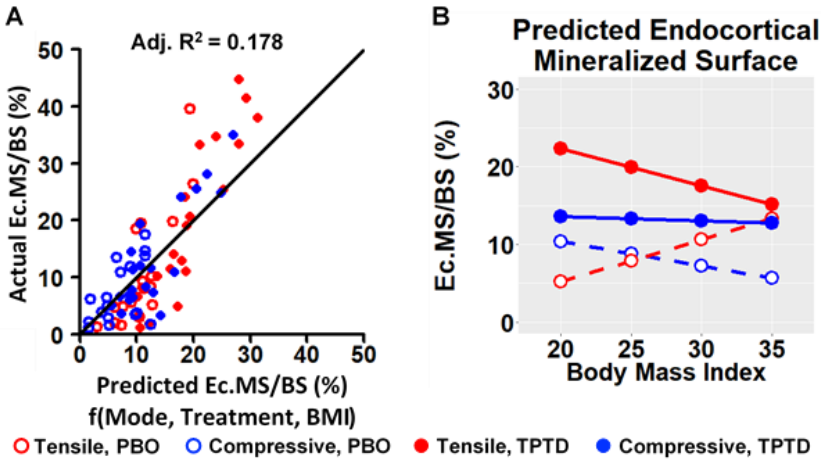

Supplemental Figure 4.1 BMI had a high explanatory power over the variability in endocortical formation indices. (A) Multivariable linear mixed effects model shown as predicted endocortical MS/BS versus measured values. Variations in endocortical MS/BS were well explained by loading modality, treatment, and patient BMI. (B) Model prediction based on varying patient data. The beneficial effect of TPTD on endocortical MS/BS was predicted to be greatest in the tensile region of patients with low BMI.

Chapter 5

PTH TREATMENT INCREASES CORTICAL BONE MASS MORE IN RESPONSE TO COMPRESSION THAN TENSION IN MICE

5.1 Introduction

Parathyroid hormone (PTH) is one of the few FDA-approved anabolic osteoporosis treatments. PTH stimulates bone formation and improves microarchitecture by increasing osteoblast differentiation, proliferation, and activity [1–3], resulting in increased bone mineral density (BMD) and reduced risk of fracture [4,5]. However, the effects of PTH are site-specific, and limited to an anabolic window during which formation is increased more than resorption [3]. Clinically, PTH greatly increases BMD at the spine, provides a modest increase in BMD at the hip, and potentially decreases BMD at the radius [4–6]. After approximately two years, resorption levels are increased such that there is no more net bone formation [3]. Understanding how to maximize the effects during this anabolic window and why these site-specific differences exist may lead to new methods to enhance the effectiveness of PTH.

Mechanical loading has a synergistic anabolic effect when combined with PTH treatment [7], and may help explain these site-specific differences. In cortical bone of mice, PTH treatment increased the anabolic effect of tibial loading more than the additive effects of either treatment alone [8]. In humans, load-bearing sites such as the spine and the hip increase bone mass with PTH but the radius does not. Similarly, the tibia and femur in mice experience daily loading and increase bone mass with PTH,

whereas the minimally-loaded murine spine does not [9]. However, the presence of mechanical loading alone does not explain site-specific differences clinically, as the increase in BMD is greater at the spine compared to the hip even though both locations are load bearing [5,6].

One potential explanation for the variability in efficacy of PTH is the difference in loading modality at each anatomical site. In a study on adult female rats treated with PTH, bending was applied to the tibia, and the anabolic response was analyzed separately for the lateral and medial periosteal surfaces, which were under compression and tension, respectively [10]. Although these two surfaces were not compared directly, PTH enhanced the anabolic response to loading on the tensile surface but not the compressive surface. Similarly, the tensile surface of the femoral neck, which is also under bending, was more responsive to teriparatide, an analog of PTH [11]. Due to the curvature of the mouse tibia, cyclic compression of the entire limb causes bending at the tibial midshaft, placing the anterior surface under tension and the posterior surface under compression with a transitional neutral region between them (Fig. 5.1) [12]. Therefore, cyclic tibial loading can be used to study the differential effects of compression and tension on the response to PTH treatment at a single anatomic location in the mouse *in vivo*.

Most studies involving PTH and mechanical loading focus on healthy, normal bone mass animals, yet estrogen deficient postmenopausal women comprise a large portion of the target population for these therapies. The anabolic effects of mechanical loading and PTH treatment may be influenced by estrogen status. PTH increases bone mass in ovariectomized (OVX) rodents [13,14], but when combined with estrogen

supplementation the effects may be greater [15]. Conversely, loss of estrogen signaling via OVX or bone cell-specific estrogen receptor-alpha deletion may increase the effects of mechanical loading [16–19]. Therefore, it is important to investigate the relationship between PTH and loading in more clinically relevant estrogen signaling-impaired, low bone mass models.

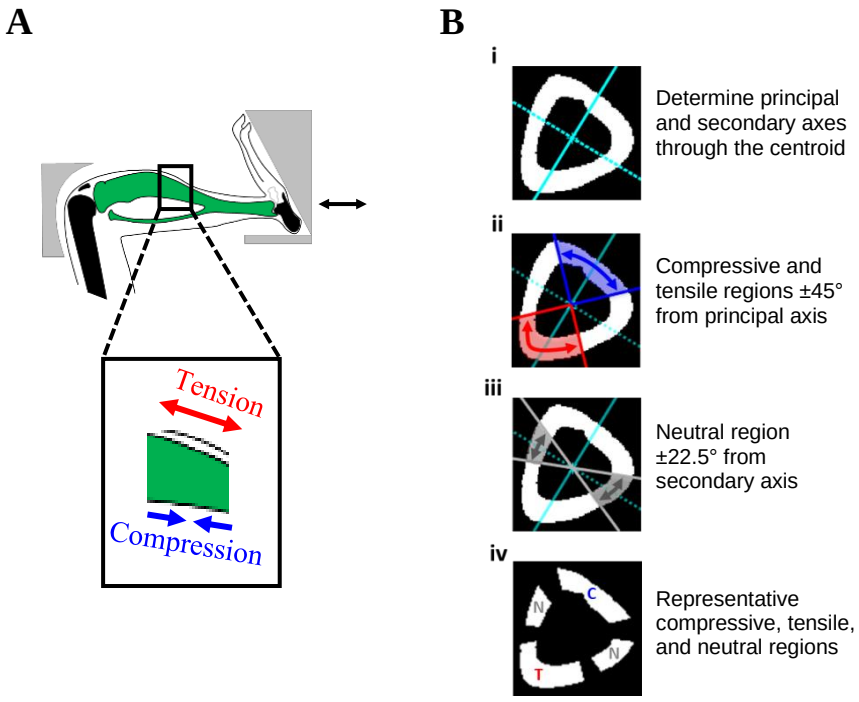

Figure 5.1 Murine hindlimb loading causes tibial bending and produces regions of tension and compression. A) Loading of the mouse hindlimb causes bending at the tibial midshaft due to the curvature of the tibia. B) Representative cross section depicting the identification of the tensile (T), compressive (C), and neutral (N) regions. i) The principal (solid) and secondary (dotted) principal axes through the centroid (*) were determined based on the 3D VOI. ii) The compressive (blue) and tensile (red) regions were defined as ±45° from the primary principal axis on the posterior and anterior segments, respectively. iii) The neutral region (gray) was defined as ±22.5° from the secondary neutral axis on the medial and lateral segments. iv) Representative compressive, tensile, and neutral regions shown together.

In the present study, we sought to elucidate the effect of loading modality on the anabolic skeletal response to PTH and mechanical loading in low bone mass, female osteoblast-specific estrogen receptor-alpha knockout mice via the osteocalcin

promoter (pOC-ERαKO) and their littermate controls (LC) [20]. These mice concurrently received cyclic tibial loading and treatment with either PTH or saline vehicle (VEH) for 2 or 6 weeks. We also examined whether PTH pre-treatment could prime bone cells prior to initiation of mechanical loading to further enhance the anabolic skeletal response during the limited anabolic window. Wild-type 10-week-old female C57Bl/6J mice (WT) were pre-treated with PTH or VEH for 6 weeks prior to starting tibial loading at 16 weeks of age. Changes in bone mass and structure were analyzed in the tensile, compressive, and neutral regions of the mid-diaphysis separately. Loading in the compressive region was the most anabolic and increased the effect PTH treatment more than regions experiencing tension, while the neutral region was unaffected by loading. Low bone mass did not influence the response to PTH with or without mechanical loading. PTH pre-treatment maintained the synergistic anabolic response with loading long term, but concurrent treatment and loading was only effective short term.

5.2 Materials and Methods

5.2.1 Animals

Generation of osteoblast-specific ERαKO mice (pOC-ERαKO): Osteoblast-specific ERα knockout (pOC-ERαKO) and littermate control (LC) mice were generated as previously described [20]. Briefly, mice with loxP sequences flanking exon 3 of the DNA-binding domain of the ERα gene (*Esr1*) ($ERα^{fl/fl}$, provided by Dr. Sohaib Kahn, University of Cincinnati, Cincinnati, OH, USA) [21] were crossed with mice containing a transgene encoding *Cre* recombinase driven by the human

osteocalcin promoter (*OC-Cre*, provided by Dr. Thomas Clemens, The Johns Hopkins University, Baltimore, MD, USA) [22,23]. *ERα*$^{fl/fl}$ mice were inbred to be >99% pure C57Bl/6 by speed congenics (DartMouse Speed Congenic Core Facility, Geisel School of Medicine at Dartmouth, Hanover, NH, USA) prior to crossing with *OC-Cre* mice that had previously been inbred to the C57Bl/6 strain. Mice were genotyped using lysed tail PCR as described [20].

Wild type mice: Wild type, 9-week-old female C57Bl/6J mice (WT) were purchased from Jackson Laboratories and allowed to acclimate to the Cornell animal facility for 1 week prior to the start of the experiment at 10 weeks of age. All mice were housed 3 to 5 per cage and had *ad libitum* access to food and water. All animal procedures were approved by Cornell University's IACUC.

5.2.2 Parathyroid hormone treatment

Human parathyroid hormone (1-34) (Bachem Americas, Inc; Torrance, CA, USA) was injected subcutaneously 5 days per week at a dose of 40μg/kg. Mice receiving vehicle (VEH) treatment were injected subcutaneously with a similar volume of sterile phosphate buffered saline (PBS) 5 days per week.

5.2.3 Tibial strain gauging

The applied load magnitudes were based on the *in vivo* strains in each group. Single-element strain gauges (C2A-06-015LW-120, Micro-Measurements, Wendell, NC, USA) were surgically attached to the medial surface of the tibial midshafts of small subsets of mice. Axial cyclic compressive loads with peak load magnitudes

ranging from -2 to -16N were applied to the tibiae in our custom tibial loading device [24,25]. Mice were immediately euthanized following data collection. Using the load and strain data, we calculated bone stiffness and the peak load required to induce +1000 microstrain (με) on the anteromedial surface of the tibial midshaft as previously described [25].

Concurrent treatment: Strain gauging was performed on the left and right limbs of 10- and 16-week old female pOC-ERαKO and LC mice (n=5 per genotype per age). Bone stiffness was similar between LC and pOC-ERαKO mice and between each age group (0.00803 ± 0.0014N/με 10wk LC, 0.00719 ± 0.0023N/με 10wk pOC-ERαKO, 0.00811 ± 0.0023N/με 16wk LC, 0.00723 ± 0.0015N/με 16wk pOC-ERαKO; mean ± SD). A peak load of -7.9N was applied to female LC and pOC-ERαKO mice of both ages to induce +1000με at the midshaft.

Pre-treatment: 10-week-old female WT mice were treated with PTH or VEH 5 days per week for 6 weeks. At 16 weeks of age, strain gauging was performed on the left tibiae of n=8 mice per treatment group. Right limbs were harvested for pre-treatment baseline analysis. Bone stiffness differed by treatment group (0.00925 ± 0.0022N/με VEH, 0.0106 ± 0.0014N/με PTH; mean ± SD). Therefore, peak loads of -8.7N and -10.6N were applied to induce +1000με at the midshaft in mice pre-treated with VEH and PTH, respectively.

5.2.4 In vivo tibial mechanical loading

Left tibiae were loaded in cyclic compression *in vivo* at a rate of 4Hz for 1200 cycles per day, 5 days per week in a triangular waveform [25]. A dwell of 100ms at -

1N was maintained between successive load cycles, and the dwell-to-peak time was 75ms. Peak load magnitudes were determined by strain gauging as described above. The right limbs served as contralateral controls. Three days after the last session of *in vivo* tibial compression mice were euthanized via isoflurane overdose and cardiac puncture.

Concurrent treatment: The left tibiae of 10- and 16-week-old female LC and pOC-ERαKO mice (n=10-11 per group) were loaded in cyclic compression at a peak load of -7.9N *in vivo* for 2 weeks, with a second group of 16-week-old mice undergoing cyclic compression for 6 weeks (Fig. 5.2).

Pre-treatment: Following 6 weeks of pre-treatment, 16-week-old female WT mice commenced cyclic tibial compression for 2 or 6 weeks. Overall, we examined three treatment groups: 1) VEH pre-treated and VEH treated during loading (VEH/VEH), 2) VEH pre-treated and PTH treated during loading (VEH/PTH), and 3) PTH pre-treated and PTH treated during loading (PTH/PTH) (Fig. 5.2). Based on the strain gauge analysis, groups 1 and 2 received a peak load magnitude of -8.7N and group 3 received a peak load magnitude of -10.6N.

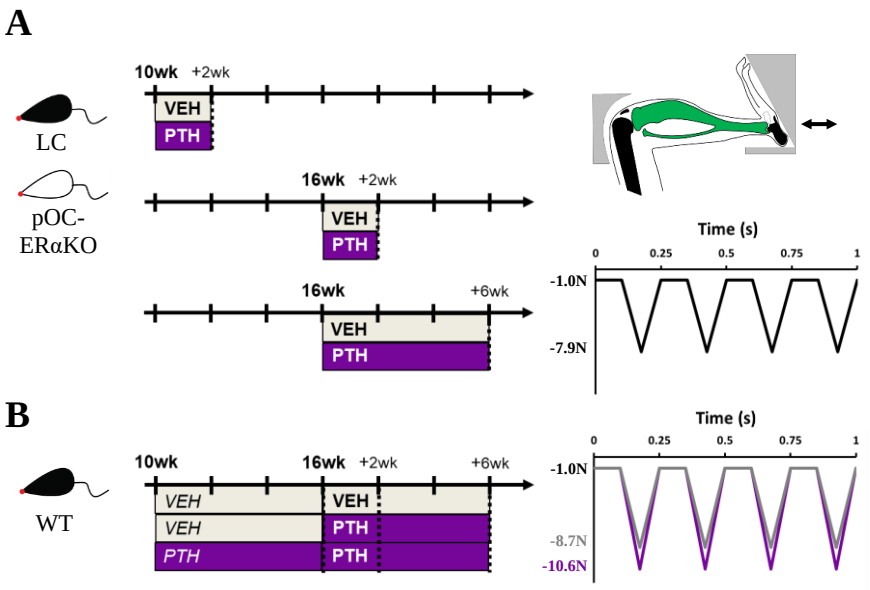

Figure 5.2 Experimental timeline. A) All concurrently loaded pOC-ERαKO and LC mice underwent tibial compression at -7.9N peak load and treatment with VEH or PTH 5 days per week. 10-week-old mice were loaded and treated for 2 weeks. 16-week-old mice were loaded and treated for 2 or 6 weeks. B) Pre-treated WT mice received VEH or PTH pre-treatment from 10 weeks of age to 16 weeks of age with no tibial loading (*Italic*). At 16 weeks of age, loading and treatment (**Bold**) commenced for 2 or 6 weeks. Mice pre-treated with VEH or PTH were loaded at -8.7N or -10.6N peak load, respectively.

5.2.5 Microcomputed tomography

Bone morphology was examined using microcomputed tomography (microCT). At euthanasia, limbs were stored in 4% paraformaldehyde overnight and later scanned in 70% ethanol at 15µm voxel resolution at the tibial mid-diaphysis (µCT35, Scanco Medical AG; 55kVp, 145µA, 600ms integration time). Due to the COVID-19 pandemic shut down, n=4 mice per treatment group of the pre-treated, 2-week loaded mice were scanned on a different microCT system (µCT40, Scanco Medical AG; 55kVp, 145µA, 300ms integration time). The diaphysis volume of interest (VOI) was defined as 2.5% of the total tibial length centered at the midshaft

[20]. Outcome measures for each loading modality region were cortical area (Ct.Ar) and cortical thickness (Ct.Th).

5.2.6 Loading modality regions

Segmentation of the tensile, compressive, and neutral VOIs was performed using custom MATLAB code. The complete 3D diaphyseal VOI obtained from microCT analysis was imported to MATLAB, binarized, and the centroid, primary principal axis, and secondary principal axis were calculated (Fig. 5.1). The tensile and compressive regions were defined as the area from the centroid extending ±45° from the primary principal axis on the anterior and posterior sides, respectively. The neutral region was defined from the centroid to ±22.5° from the secondary principal axis on both the medial and lateral sides.

Cortical area was calculated by multiplying the number of bone voxels by the area per voxel and averaging across all slices of the 3D VOI. Cortical thickness was calculated using the Euclidian distance transform, defined as the shortest distance from each bone voxel to the nearest background voxel, multiplied by the skeletonized original VOI. Thickness values were averaged in each slice across the region of interest, then averaged across all slices of the 3D VOI.

5.2.7 Statistics

The systemic effects of PTH were analyzed using the non-loaded control limbs with an ANOVA for loading modality, treatment group, genotype where applicable, and their interactions. The effects of loading were analyzed using the differences

between the loaded and control limbs [Loaded-Control] with an ANOVA for loading modality, treatment group, genotype where applicable, and their interactions. Limb differences were determined to be different from zero if analysis of the individual limbs revealed differences between the loaded and control limbs within a group using a linear mixed-effects model with loading, treatment group, loading modality, genotype where applicable, and their interactions as fixed effects and a random mouse effect to account for the repeated measure (loaded and control limbs). A Tukey HSD post-hoc test was performed when the interaction terms were significant. Significance was set at $p < 0.05$. All results reported are significant unless stated otherwise.

Concurrent loading: Data were analyzed separately for each age and loading duration. To directly examine the effects of age and load duration on the response to PTH and mechanical loading, we compared the limb differences from the 10-week-old mice to those of the 16-week-old mice that received 2 weeks of loading, and the limb differences from the 16-week-old mice that received 2 weeks of loading to those that received 6 weeks of loading. Comparisons were tested using an ANOVA for genotype, loading modality, treatment, age or duration, and their interactions. A Tukey HSD post-hoc test was performed when the interaction terms were significant.

Pre-treatment: Data for each loading duration were analyzed separately as a function of treatment group: VEH/VEH, VEH/PTH, or PTH/PTH. Additionally, the effect of duration was analyzed between the 2- and 6-week loaded groups using an ANOVA for loading modality, treatment group, duration, and their interactions.

5.3 Results

5.3.1 PTH alone increased cortical bone mass only after 6 weeks

PTH only altered cortical bone mass in non-loaded control limbs following at least 6 weeks of treatment (Fig. 5.3). Two weeks of PTH treatment did not increase Ct.Ar or Ct.Th in 10- and 16-week-old pOC-ERαKO and LC mice, nor in 16-week-old WT mice that had been pre-treated with VEH prior to 2 weeks of PTH treatment (Fig. 5.3). PTH increased Ct.Ar (+4.2%) and Ct.Th (+3.6%) in 16-week-old pOC-ERαKO and LC mice similarly in all regions after 6 weeks of treatment (Fig. 5.3). The response to PTH was not different in low bone mass pOC-ERαKO mice compared to LC mice. Following 6 weeks of pre-treatment in 10-week-old WT mice, PTH increased Ct.Ar (+7.4%) and Ct.Th (+5.5%) regardless of modality region (Fig. 5.3). In the control limbs of pre-treated mice that had been loaded for 2 weeks, Ct.Ar was only increased in the PTH/PTH group (+7.4%), which had received 8 weeks of PTH treatment. Ct.Th was not increased in the PTH/PTH group compared to the VEH/VEH group, but was increased compared to the VEH/PTH group (+7.0%) (Fig. 5.3). Treatment group did not affect Ct.Ar in the control limbs of pre-treated mice that had been loaded for 6 weeks, but Ct.Th was greater in the VEH/PTH and PTH/PTH groups compared to the VEH/VEH group (+5.2%) (Fig. 5.3).

Inherent differences in bone mass existed by region. Ct.Ar and Ct.Th were greater in the tensile region compared to the compressive region of the tibial cortex, and lowest in the neutral region, except at the pre-treatment baseline for which Ct.Ar and Ct.Th were similar in the compressive and tensile regions (Fig. 5.3). Ct.Ar and Ct.Th were lower in pOC-ERαKO mice than LC in all groups; however, the

differences by modality region were not different by genotype. The systemic response to PTH also was not different by modality region.

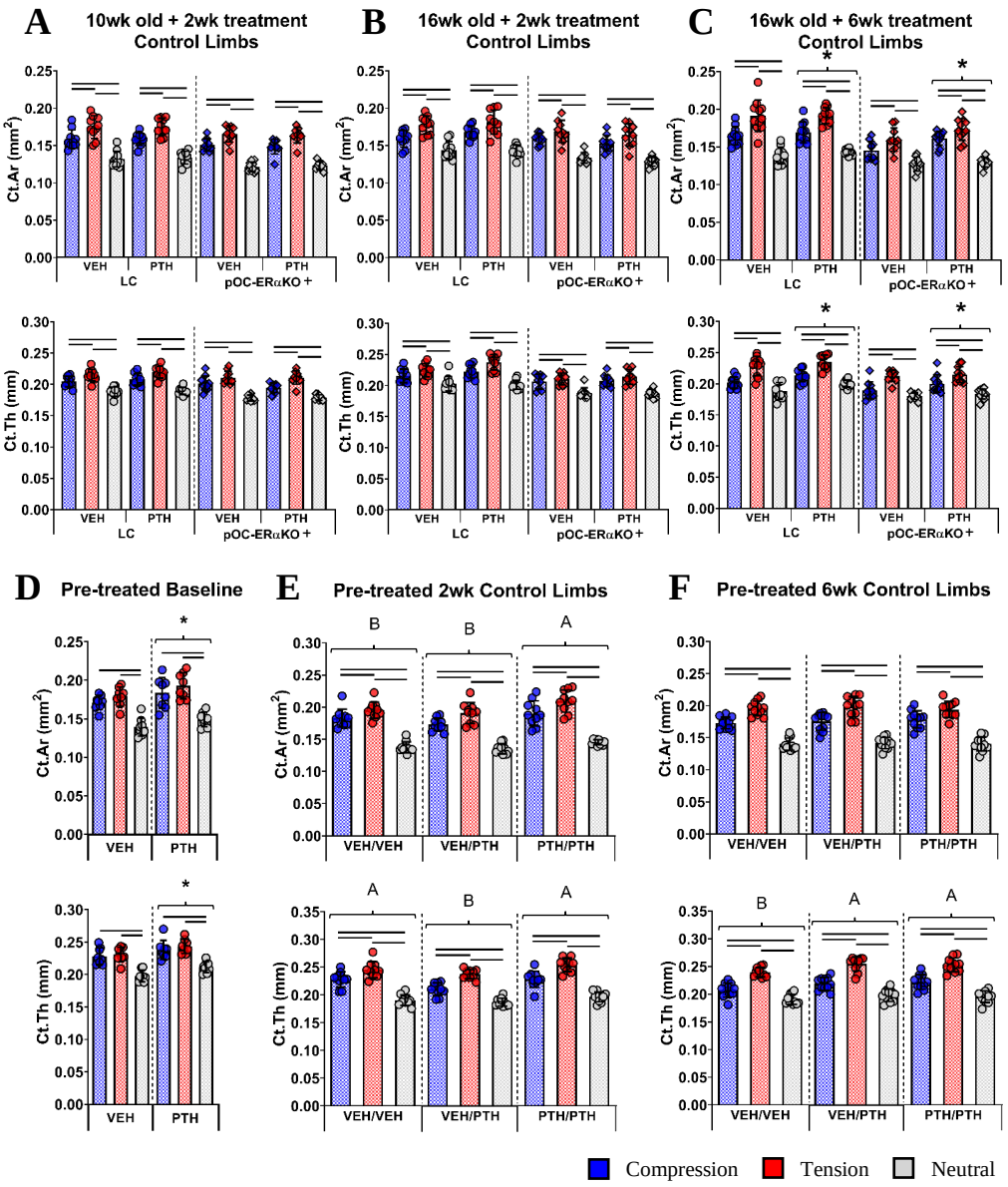

Figure 5.3 PTH increased diaphyseal cortical bone mass in non-loaded control limbs after a minimum of 6 weeks. A,B,C) Ct.Ar and Ct.Th were greatest in the tensile region and least in the neutral region in 10- and 16-week-old mice. PTH increased Ct.Ar and Ct.Th only in 16-week-old mice treated for 6 weeks and the increase was similar in all regions. Ct.Ar and Ct.Th were lower in pOC-ERαKO mice compared to LC mice in all groups. D) Following 6 weeks of pre-treatment, PTH increased Ct.Ar and Ct.Th. The compressive and tensile regions had greater Ct.Ar and Ct.Th than the neutral region. E,F) Only the PTH pre-treated 2 week control limbs had increased Ct.Ar, although the VEH/PTH group had reduced Ct.Th compared to the other groups. Ct.Ar in 6 week control limbs were not different by treatment group. Ct.Th was increased with any PTH treatment, regardless of pre-treatment. The tensile region had greater bone mass than the compressive region, and the neutral region had the lowest bone mass for 2 and 6wk limbs. Data are mean ± SD. — Differences by loading modality region, * PTH different from VEH, + pOC-ERαKO different from LC, A > B treatment groups different, $p<0.05$ by ANOVA with Tukey post-hoc.

5.3.2 Compression increased cortical bone mass more than tension, and the neutral region was unaffected by loading

Overall, applied compression was more anabolic than in the applied tension, and the neutral region was unaffected by mechanical loading. The effect of loading was analyzed by comparing the limb differences [Loaded-Control] within each mouse. Two weeks of loading increased Ct.Ar in the compressive region more than in the tensile region in 10- and 16-week-old pOC-ERαKO and LC mice (Fig. 5.4). Compression also increased Ct.Th more than tension in 10-week-old pOC-ERαKO and LC mice. Compression, but not tension, increased Ct.Th with 2 weeks of loading in 16-week-old pOC-ERαKO, LC, and WT mice (Fig. 5.4). Six weeks of loading increased Ct.Ar in the compressive and tensile regions similarly in 16-week-old pOC-ERαKO, LC, and WT mice (Fig. 5.4). Ct.Th increased more under compression than tension after 6 weeks of loading in all 16-week-old mice, independent of treatment (Fig. 5.4). Bone mass in the neutral region was unaffected by loading regardless of age, genotype, duration, or treatment. Low bone mass in pOC-ERαKO mice did not influence the loading responses by modality region.

To analyze the effect of age on the response to loading modality, we compared the limb differences between 10- and 16-week-old pOC-ERαKO and LC mice treated and loaded for 2 weeks. 10-week-old mice had similar Ct.Ar and Ct.Th loading responses as 16-week-old mice regardless of loading modality (Supp Fig. 5.1). Across age groups, compression was the most anabolic, and tension increased Ct.Ar but not Ct.Th with loading.

Compression reached peak anabolic effects earlier than tension. In concurrently-treated 16-week-old pOC-ERαKO and LC mice, the Ct.Ar loading response under tension was increased from 2 to 6 weeks to the same level as compression. The compressive loading response was unchanged with increased duration (Supp Fig. 5.2). In WT mice, the loading responses under compression and tension increased from 2 to 6 weeks as measured by Ct.Ar and Ct.Th (Supp Fig. 5.3). Compression and tension increased Ct.Ar similarly, but compression maintained a greater Ct.Th loading response at both timepoints. After 6 weeks of loading, tension increased the loading response in Ct.Th to the same level as compression after 2 weeks of loading.

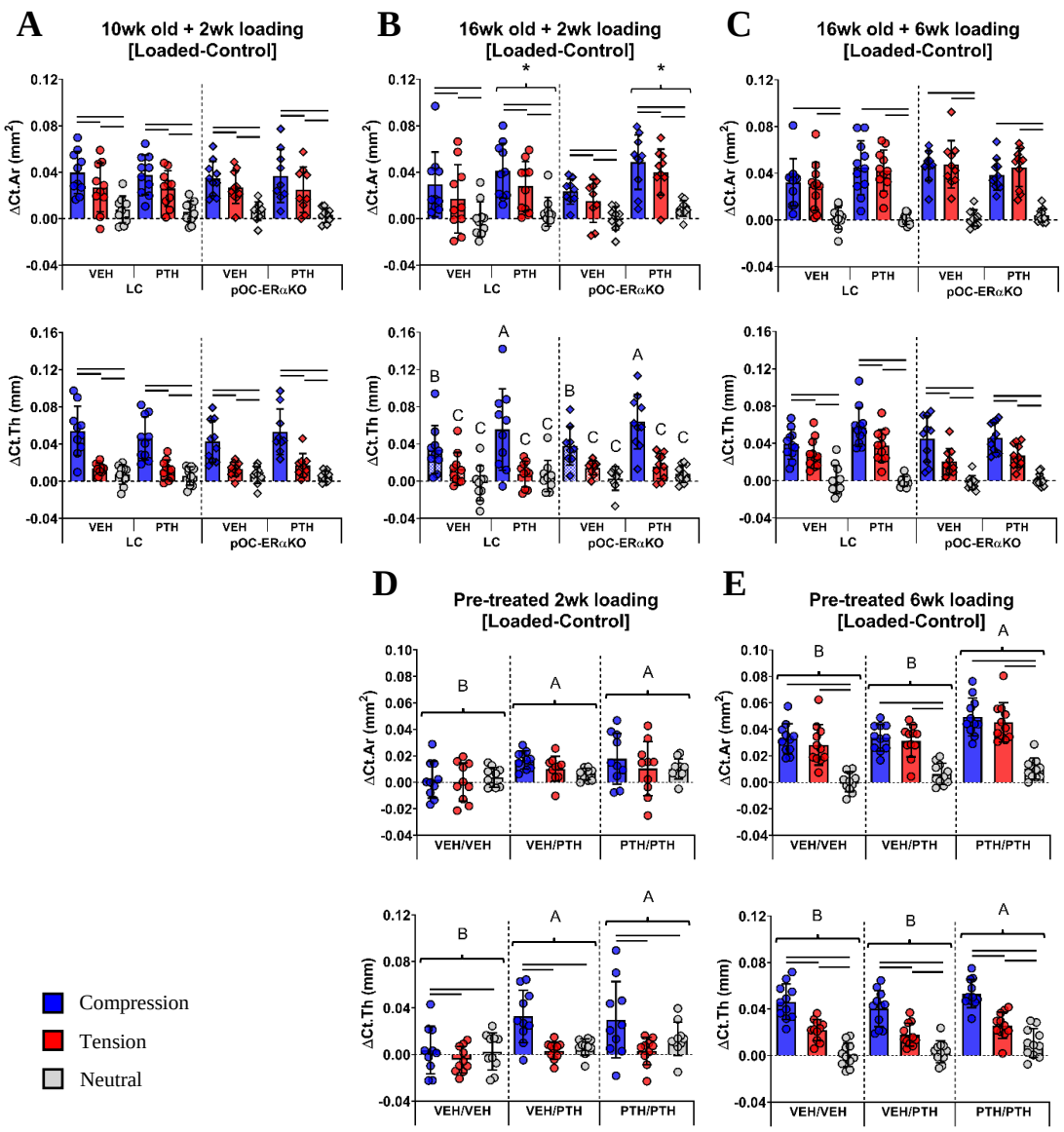

Figure 5.4 Compression was the most anabolic and PTH increased the anabolic response to loading. A) 2 weeks of loading increased Ct.Ar and Ct.Th the most in the compressive region in 10-week-old mice. The neutral region was unchanged by loading. B) 16-week-old mice loaded for 2 weeks increased Ct.Ar and Ct.Th the most under compression. PTH increased the loading response regardless of loading modality in Ct.Ar, but only increased the loading response in Ct.Th under compression. C) Compression and tension increased Ct.Ar similarly in 16-week-old mice loaded for 6 weeks. Compression increased Ct.Th more than tension, and the neutral region was unaffected. D) 2 weeks of tibial loading increased cortical bone mass when PTH was given during loading, regardless of the pre-treatment, while VEH pre-treated mice did not increase bone mass with loading. Compression increased Ct.Th more than in the tensile or neutral regions. E) After 6 weeks of loading, PTH pre-treated mice had a greater anabolic response than either VEH pre-treated group. Compression and tension increased Ct.Ar similarly, and compression increased Ct.Th more than tension. The neutral region was unaffected by loading. Data are mean ± SD. — Differences by loading modality region. *PTH different from VEH. A > B > C, groups not sharing the same letter are different by Tukey post-hoc. $p<0.05$ by ANOVA.

5.3.3 PTH increased the anabolic effect of loading only after 2 weeks in 16-week-old mice

PTH increased the anabolic effects of loading only in 16-week-old mice loaded for 2 weeks. Six weeks of loading in 16-week-old pOC-ERαKO, LC, and VEH pre-treated WT mice increased Ct.Ar and Ct.Th similarly regardless of the treatment administered during loading (Fig. 5.4). PTH also did not affect the response to loading in 10-week-old pOC-ERαKO and LC mice loaded for 2 weeks (Fig. 5.4). However, in response to 2 weeks of loading PTH-treated 16-week-old pOC-ERαKO and LC mice increased Ct.Ar more than VEH treated mice (Fig. 5.4). PTH only increased the Ct.Th anabolic response to applied compression in these mice, not the response to tension (Fig. 5.4). Similarly, WT mice that received PTH during the 2 weeks of loading increased Ct.Ar and Ct.Th with loading while the VEH/VEH group did not (Fig. 5.4). PTH did not influence the response to loading differently in low bone mass pOC-ERαKO mice.

Comparison between the 2- and 6-week loaded groups revealed that the synergistic effect of PTH and mechanical loading peaked after 2 weeks. In concurrently-loaded pOC-ERαKO and LC mice, longer duration only increased the loading response in PTH-treated mice under tension as measured by Ct.Th (Supp Fig. 5.2). Tension did not increase the loading response of VEH-treated mice from 2 weeks to 6 weeks, and the response to compression did not increase from 2 to 6 weeks regardless of the treatment group. However, the PTH group had a greater compressive anabolic response than the VEH group at 2 weeks but not 6 weeks. Ct.Ar trended

toward an increased loading response in VEH-treated pOC-ERαKO and LC mice from 2 to 6 weeks to match the level of PTH treated mice (p=0.0578), but the loading response in the PTH-treated mice was unchanged with longer duration.

Similarly, the loading response of WT mice in the VEH/VEH group increased from 2 to 6 weeks of loading to the same level as the VEH/PTH group as measured by Ct.Th, but the VEH/PTH group retained the same loading response with longer duration (Supp Fig. 5.3). Although Ct.Ar in pre-treated mice trended toward an increased loading response with duration in all groups, the greater loading response in the VEH/PTH group compared to the VEH/VEH group at 2 weeks was no longer present after 6 weeks of loading (p=0.0834).

5.3.4 PTH pre-treatment increased the anabolic effects of loading long term

PTH pre-treatment only increased the anabolic effects of loading compared to concurrent treatment after 6 weeks of loading. After 2 weeks of loading, WT mice that received PTH during loading increased Ct.Ar and Ct.Th similarly, regardless of pre-treatment, and the VEH/VEH group did not increase bone mass with loading (Fig. 5.4). After 6 weeks of loading, however, PTH pre-treated mice had greater anabolic responses in Ct.Ar and Ct.Th than both VEH pre-treated groups. PTH pre-treatment did not alter the response to loading differently by loading modality.

PTH pre-treatment increased the response to loading from 2 to 6 weeks as measured by Ct.Th (Supp Fig. 5.3). PTH pre-treated mice also trended toward increased loading response in Ct.Ar from 2 to 6 weeks, and a greater loading response at 6 weeks compared to the VEH/PTH group that was not present at 2 weeks

(p=0.0834). Together these data indicate that although PTH and mechanical loading may be synergistically anabolic in the short term, longer term treatment may require PTH pre-treatment to sustain the synergistic response.

5.4. Discussion

Overall, combining PTH with mechanical loading had a synergistic anabolic effect on cortical bone mass in the short term; longer term mechanical loading was only synergistically anabolic when mice were pre-treated with PTH. Generally, applied compression was more anabolic than tension, and the neutral region was not affected by loading. The anabolic effect of PTH on mechanical loading was more apparent in the short term under compression and not influenced by low bone mass in pOC-ERαKO mice.

PTH systemically increased cortical bone mass in non-loaded control limbs only after a treatment period of 6 weeks or more, suggesting a minimum treatment duration between 2 and 6 weeks to achieve an anabolic effect in cortical bone in mice. Studies tracking changes in bone morphology and mineral content over time with PTH treatment showed similar results. PTH treatment in 18-week-old female C57Bl/6J mice only caused structural and mineral changes in tibial cortical bone after 3 weeks of treatment [26,27]. Similarly, 4-month-old male C57Bl/6J mice treated with PTH only increased tibial BMD compared to saline-treated mice after 4 weeks of treatment [28]. Notably, the dosage of PTH in these experiments was greater than the dose given in this study. We chose a relatively low dose of 40μg/kg to avoid saturating the anabolic effects in order to investigate whether the PTH response increased further

with different types of mechanical loading. In mice, PTH given at 40μg/kg has been shown to be anabolic [8,9], although many studies use 80μg/kg or more [26–30].

Applied compression increased bone mass more than tension, and the neutral region did not increase bone mass with loading. The lack of anabolic response in the neutral region of the tibial midshaft indicates that bone formation was driven by the local strain magnitude and not the strain gradient as others have previously reported [31,32]. Additionally, these results confirm that our model induces localized anabolic responses and not systemic changes in bone mass following tibial loading, highlighting the non-loaded contralateral limb as an appropriate internal control. Ulnar loading in rats showed similar results; peak bone formation occurred in regions with the highest axial compressive strain [33]. Analyses of animal models with bones that are naturally under both tension and compression suggest that skeletal tissue adapts differently to different loading modalities during normal development, but these studies produced conflicting results. Some models showed thicker cortices and higher levels of mineralization in regions of compression [34] while others showed no difference by loading modality [35,36]. In our mouse model the response to tibial loading was greater under compression even though baseline thicknesses were greater in the tensile region, demonstrating that differences due to daily physiologic loading do not necessarily correspond to the responses to applied loading.

The differences in the response to loading modality may reflect a more rapid response to compressive loading rather than an increase in the magnitude of response. In 16-week-old pOC-ERαKO and LC mice, the response to applied compression did not increase from 2 to 6 weeks of loading, but the response to tension increased to the

level of compression at 6 weeks (Supp Fig. 5.2). Although the response to compression in WT mice increased from 2 to 6 weeks of loading, the magnitude of the response at 2 weeks was less than the 2-week response in pOC-ERαKO and LC mice and the response at 6 weeks was similar to the 2 and 6 week responses in non-pre-treated mice [Mean compressive ΔCt.Ar (mm^2): Pre-treated 2wk = 0.012, Pre-treated 6wk = 0.039, 2wk = 0.036, 6wk = 0.040]. These data suggest that the longer loading duration did not increase the level of response once the peak response was achieved for these physiologically relevant load magnitudes. One explanation could be that the load-induced increases in bone mass over the first few weeks lowered the strain magnitude experienced at these locations such that they were no longer anabolic. Strain gauge analyses performed before and after 6 weeks of loading could determine whether increased bone mass decreased strain magnitudes at the midshaft over this time frame.

PTH and tibial loading were synergistically anabolic, but only in 16-week-old mice. 10-week-old mice are still undergoing rapid skeletal growth, which may have obscured any PTH effects. Without pre-treatment, the synergistic effects of PTH and loading were only apparent through 2 weeks of loading. After 6 weeks the loading effects were not different in VEH- or PTH-treated mice, indicating that PTH treatment may have achieved peak loading response earlier than VEH treatment while not affecting the steady state magnitude of the response. Pre-treatment, on the other hand, increased the anabolic effects of loading and maintained a greater loading response compared to PTH treatment alone from 2 to 6 weeks. Therefore, pre-treating patients with PTH prior to initiating exercise or physical therapy regimens may extend the

synergistic anabolic effects of both treatments and achieve the same results as concurrent treatment with fewer sessions.

PTH was more effective at increasing the anabolic effect of compression than tension. PTH amplified the load-induced increase in Ct.Th only under compression after 2 weeks of loading in 16-week-old pOC-ERαKO and LC mice. PTH also had a slight effect under tension, increasing the loading response from 2 to 6 weeks, although neither timepoint was different from VEH-treated mice. PTH may only amplify the loading effect where one already exists. The VEH group did not increase Ct.Th with applied tension, and PTH did not affect the lack of response. These trends followed the site-specific differences in PTH efficacy seen clinically, for which PTH is most effective in the spine, mildly effective in the hip, and not effective in the radius [4–6]. Hagino and colleagues found that PTH increased bone formation due to applied tibial bending on the tensile but not the compressive surface [10]. The two surfaces were not compared directly and the strains on the tensile surface were much higher compared to the strains on the compressive surface, which may explain the differences in our results. A limitation of our study is that the strain magnitudes within each region and across mice are unknown, and may have influenced the loading responses. Additionally, the modality regions were calculated based on the mid-diaphyseal volume of interest rather than the whole tibia, which may have rotated the regions slightly. However, the modality regions visually corresponded well with regions associated with these loading modes in finite element models from other groups [12], and re-determining the regions based on anatomical alignment of the tibia did not alter the trends in the data (Appendix A).

In conclusion, applied compression was more anabolic and increased the response to PTH more than tension. In addition to explaining the site-specificity of PTH clinically, physical therapy and exercise regimens could be designed to induce more compressive strains to further increase the anabolic effects of PTH. The response to PTH was not influenced by the osteopenic phenotype of the pOC-ERαKO mice, although more severe osteoporotic phenotypes may respond differently and should be investigated further. Priming tissue with PTH prior to initiating mechanical loading was more effective long term than concurrent PTH and loading, suggesting a potential for pre-treating osteoporosis patients prior to physical therapy regimens to maximize the beneficial effects during the limited anabolic window. Exploiting the benefits of applied compressive loading and utilizing a pre-treatment period may increase bone mass to a greater degree during the limited anabolic window of PTH and help to prevent more fractures.

5.5 References

[1] D.W. Dempster, F. Cosman, E.S. Kurland, H. Zhou, J. Nieves, L. Woelfert, E. Shane, K. Plavetić, R. Müller, J. Bilezikian, R. Lindsay, Effects of daily treatment with parathyroid hormone on bone microarchitecture and turnover in patients with osteoporosis: a paired biopsy study., J. Bone Miner. Res. 16 (2001) 1846–53. doi:10.1359/jbmr.2001.16.10.1846.

[2] R. Lindsay, H. Zhou, F. Cosman, J. Nieves, D.W. Dempster, A.B. Hodsman, Effects Of a One-Month Treatment With PTH(1-34) on Bone Formation on Cancellous, Endocortical, and Periosteal Surfaces of the Human Ilium, J. Bone Miner. Res. 22 (2007) 495–502. doi:10.1359/jbmr.070104.

[3] D. Aslan, M.D. Andersen, L.B. Gede, T.K. de Franca, S.R. Jørgensen, P. Schwarz, N.R. Jørgensen, Mechanisms for the bone anabolic effect of parathyroid hormone treatment in humans, Scand. J. Clin. Lab. Investig. 72 (2012) 14–22. doi:10.3109/00365513.2011.624631.

[4] F. Cosman, Anabolic and Antiresorptive Therapy for Osteoporosis : Combination and Sequential Approaches, Curr. Osteoporos. Rep. (2014) 385–395. doi:10.1007/s11914-014-0237-9.

[5] S.L. Greenspan, H.G. Bone, M.P. Ettinger, D.A. Hanley, R. Lindsay, J.R. Zanchetta, C.M. Blosch, A.L. Mathisen, S.A. Morris, T.B. Marriott, Effect of Recombinant Human Parathyroid Hormone (1-84) on Vertebral Fracture and Bone Mineral Density in Postmenopausal Women with Osteoporosis, Ann. Intern. Med. 146 (2013) 326. doi:10.7326/0003-4819-146-5-200703060-00005.

[6] J.W. Mandema, J. Zheng, C. Libanati, J. Jose, P. Ruixo, Time Course of Bone Mineral Density Changes With Denosumab Compared With Other Drugs in Postmenopausal Osteoporosis : A Dose-Response-Based Meta-Analysis, J. Clin. Endocrinol. Metab. 99 (2014) 3746–3755. doi:10.1210/jc.2013-3795.

[7] Y. Ma, W.S. Jee, Z. Yuan, W. Wei, H. Chen, S. Pun, H. Liang, C. Lin, Parathyroid hormone and mechanical usage have a synergistic effect in rat tibial diaphyseal cortical bone., J. Bone Miner. Res. 14 (1999) 439–48. doi:10.1359/jbmr.1999.14.3.439.

[8] T. Sugiyama, L.K. Saxon, G. Zaman, A. Moustafa, A. Sunters, J.S. Price, L.E. Lanyon, Mechanical loading enhances the anabolic effects of intermittent parathyroid hormone (1-34) on trabecular and cortical bone in mice, Bone. 43 (2008) 238–248. doi:10.1016/j.bone.2008.04.012.

[9] A. Iida-Klein, H. Zhou, S.S. Lu, L.R. Levine, M. Ducayen-Knowles, D.W. Dempster, J. Nieves, R. Lindsay, Anabolic action of parathyroid hormone is skeletal site specific at the tissue and cellular levels in mice, J. Bone Miner. Res. 17 (2002) 808–816. doi:10.1359/jbmr.2002.17.5.808.

[10] H. Hagino, T. Okano, M.P. Akhter, M. Enokida, R. Teshima, Effect of parathyroid hormone on cortical bone response to in vivo external loading of the rat tibia, J. Bone Miner. Metab. 19 (2001) 244–250. doi:10.1007/s007740170027.

[11] A.M. Rooney, M.P.G. Bostrom, D.W. Dempster, J.W. Nieves, H. Zhou, F. Cosman, Loading modality and age influence teriparatide-induced bone formation in the human femoral neck, Bone. 136 (2020).

doi:10.1016/j.bone.2020.115373.
[12] T.K. Patel, M.D. Brodt, M.J. Silva, Experimental and finite element analysis of strains induced by axial tibial compression in young-adult and old female C57Bl/6 mice, J. Biomech. 47 (2014). doi:10.1016/j.jbiomech.2013.10.052.
[13] N. Andersson, M.K. Lindberg, C. Ohlsson, K. Andersson, B. Ryberg, Repeated in vivo determinations of bone mineral density during parathyroid hormone treatment in ovariectomized mice, J. Endocrinol. 170 (2001) 529–537. doi:10.1677/joe.0.1700529.
[14] H. Zhou, A. Iida-Klein, S.S. Lu, M. Ducayen-Knowles, L.R. Levine, D.W. Dempster, R. Lindsay, Anabolic action of parathyroid hormone on cortical and cancellous bone differs between axial and appendicular skeletal sites in mice, Bone. 32 (2003) 513–520. doi:10.1016/S8756-3282(03)00057-7.
[15] D. von Stechow, D. Zurakowski, A.R. Pettit, R. Müller, G. Gronowicz, M. Chorev, H. Otu, T. Libermann, J.M. Alexander, Differential transcriptional effects of PTH and estrogen during anabolic bone formation, J. Cell. Biochem. 93 (2004) 476–490. doi:10.1002/jcb.20174.
[16] T.L.N. Järvinen, P. Kannus, I. Pajamäki, T. Vuohelainen, J. Tuukkanen, M. Järvinen, H. Sievänen, Estrogen deposits extra mineral into bones of female rats in puberty, but simultaneously seems to suppress the responsiveness of female skeleton to mechanical loading, Bone. 32 (2003) 642–651. doi:10.1016/S8756-3282(03)00100-5.
[17] J.C. Tou, A. Foley, Y. V Yuan, S. Arnaud, C.E. Wade, M. Brown, The effect of ovariectomy combined with hindlimb unloading and reloading on the long bones of mature Sprague-Dawley rats., Menopause. 15 (2008) 494–502. doi:10.1097/gme.0b013e318148bbad.
[18] K.M. Melville, N.H. Kelly, G. Surita, D.B. Buchalter, J.C. Schimenti, R.P. Main, F.P. Ross, M.C.H. Van Der Meulen, Effects of Deletion of ERα in Osteoblast-Lineage Cells on Bone Mass and Adaptation to Mechanical Loading Differ in Female and Male Mice, J. Bone Miner. Res. 30 (2015) 1468–1480. doi:10.1002/jbmr.2488.
[19] S. Kondoh, K. Inoue, K. Igarashi, H. Sugizaki, Y. Shirode-Fukuda, E. Inoue, T. Yu, J.K. Takeuchi, J. Kanno, L.F. Bonewald, Y. Imai, Estrogen receptor α in osteocytes regulates trabecular bone formation in female mice, Bone. 60 (2014) 68–77. doi:10.1016/j.bone.2013.12.005.
[20] K.M. Melville, N.H. Kelly, S. a Khan, J.C. Schimenti, F.P. Ross, R.P. Main, M.C. van der Meulen, Female mice lacking estrogen receptor-alpha in osteoblasts have compromised bone mass and strength, J Bone Min. Res. 29 (2014) 370–379. doi:10.1002/jbmr.2082.
[21] Y. Feng, D. Manka, K.-U. Wagner, S.A. Khan, Estrogen receptor-alpha expression in the mammary epithelium is required for ductal and alveolar morphogenesis in mice., Proc. Natl. Acad. Sci. U. S. A. 104 (2007) 14718–23. doi:10.1073/pnas.0706933104.
[22] T.L. Clemens, H. Tang, S. Maeda, R. a Kesterson, F. Demayo, J.W. Pike, C.M. Gundberg, Analysis of osteocalcin expression in transgenic mice reveals a species difference in vitamin D regulation of mouse and human osteocalcin genes., J. Bone Miner. Res. 12 (1997) 1570–6.

doi:10.1359/jbmr.1997.12.10.1570.
[23] M. Zhang, S. Xuan, M.L. Bouxsein, D. Von Stechow, N. Akeno, M.C. Faugere, H. Malluche, G. Zhao, C.J. Rosen, A. Efstratiadis, T.L. Clemens, Osteoblast-specific knockout of the insulin-like growth factor (IGF) receptor gene reveals an essential role of IGF signaling in bone matrix mineralization, J. Biol. Chem. 277 (2002) 44005–44012. doi:10.1074/jbc.M208265200.
[24] J.C. Fritton, E.R. Myers, T.M. Wright, M.C.H. Van Der Meulen, Loading induces site-specific increases in mineral content assessed by microcomputed tomography of the mouse tibia, Bone. 36 (2005) 1030–1038. doi:10.1016/j.bone.2005.02.013.
[25] M.E. Lynch, R.P. Main, Q. Xu, D.J. Walsh, M.B. Schaffler, T.M. Wright, M.C.H. van der Meulen, Cancellous bone adaptation to tibial compression is not sex dependent in growing mice., J. Appl. Physiol. 109 (2010) 685–691. doi:10.1152/japplphysiol.00210.2010.
[26] Y. Lu, M. Boudiffa, E. Dall'Ara, Y. Liu, I. Bellantuono, M. Viceconti, Longitudinal effects of Parathyroid Hormone treatment on morphological, densitometric and mechanical properties of mouse tibia, J. Mech. Behav. Biomed. Mater. 75 (2017) 244–251. doi:10.1016/j.jmbbm.2017.07.034.
[27] Y. Lu, J. He, H. Zhu, Y. Wang, Effect of parathyroid hormone on the structural, densitometric and failure behaviors of mouse tibia in the spatiotemporal space, PLoS One. 14 (2019) 1–15. doi:10.1371/journal.pone.0219575.
[28] C. Le Henaff, F. Ricarte, B. Finnie, Z. He, J. Johnson, J. Warshaw, V. Kolupaeva, N.C. Partridge, Abaloparatide at the Same Dose Has the Same Effects on Bone as PTH (1-34) in Mice, J. Bone Miner. Res. 35 (2020) 714–724. doi:10.1002/jbmr.3930.
[29] S. Mohan, S. Kutilek, C. Zhang, H.G. Shen, Y. Kodama, A.K. Srivastava, J.E. Wergedal, W.G. Beamer, D.J. Baylink, Comparison of bone formation responses to parathyroid hormone(1-34), (1-31), and (2-34) in mice, Bone. 27 (2000) 471–478. doi:10.1016/S8756-3282(00)00355-0.
[30] E. Knopp, N. Troiano, M. Bouxsein, B.H. Sun, K. Lostritto, C. Gundberg, J. Dziura, K. Insogna, The effect of aging on the skeletal response to intermittent treatment with parathyroid hormone, Endocrinology. 146 (2005) 1983–1990. doi:10.1210/en.2004-0770.
[31] S. Judex, T.S. Gross, R.F. Zernicke, Strain gradients correlate with sites of exercise-induced bone-forming surfaces in the adult skeleton, J. Bone Miner. Res. 12 (1997) 1737–1745. doi:10.1359/jbmr.1997.12.10.1737.
[32] T.S. Gross, J.L. Edwards, K.J. Mcleod, C.T. Rubin, Strain gradients correlate with sites of periosteal bone formation, J. Bone Miner. Res. 12 (1997) 982–988. doi:10.1359/jbmr.1997.12.6.982.
[33] S.P. Kotha, Y.F. Hsieh, R.M. Strigel, R. Müller, M.J. Silva, Experimental and finite element analysis of the rat ulnar loading model - Correlations between strain and bone formation following fatigue loading, J. Biomech. 37 (2004) 541–548. doi:10.1016/j.jbiomech.2003.08.009.
[34] J.G. Skedros, R.D. Bloebaum, M.W. Mason, D.M. Bramble, Analysis of a Tension/Compression Skeletal System: Possible Strain-Specific Differences in the Hierarchical Organization of Bone, Anat. Rec. 239 (1994) 396–404.

[35] L.E. Lanyon, S. Bourn, The influence of mechanical function on the development and remodeling of the tibia. An experimental study in sheep., J. Bone Jt. Surg. 61 (1979) 263–273.
[36] L.E. Lanyon, D.G. Baggott, Mechanical function as an influence on the structure and form of bone, J. Bone Jt. Surg. 58B (1976) 436–443.

5.6 Chapter 5 Supplemental Information

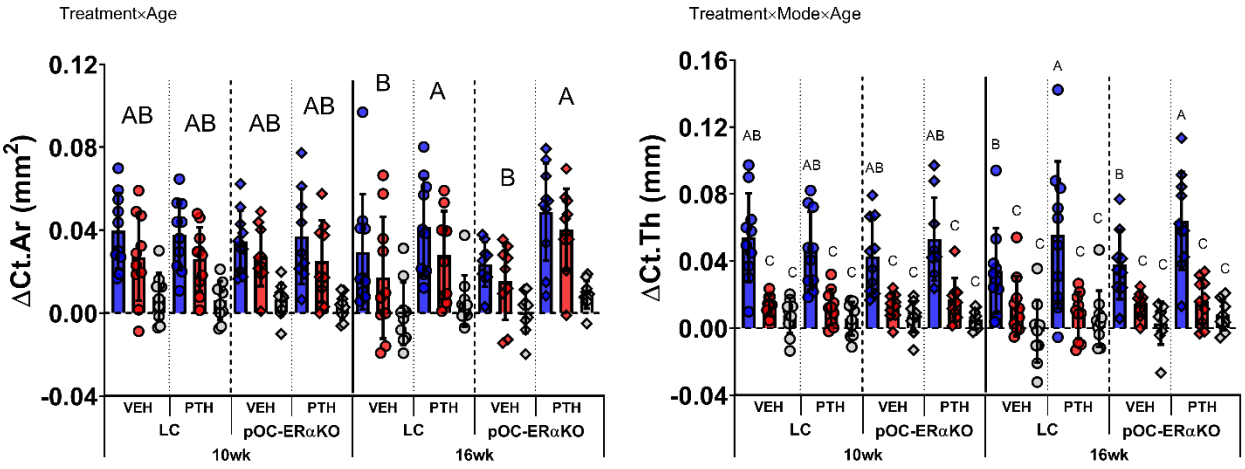

Supplemental Figure 5.1 Loading effects in concurrently-treated 10- and 16-week-old pOC-ERαKO and LC mice [Loaded-Control]. Data are mean ± SD. A > B > C, groups not sharing the same letter are different by Tukey post-hoc. $p<0.05$ by ANOVA.

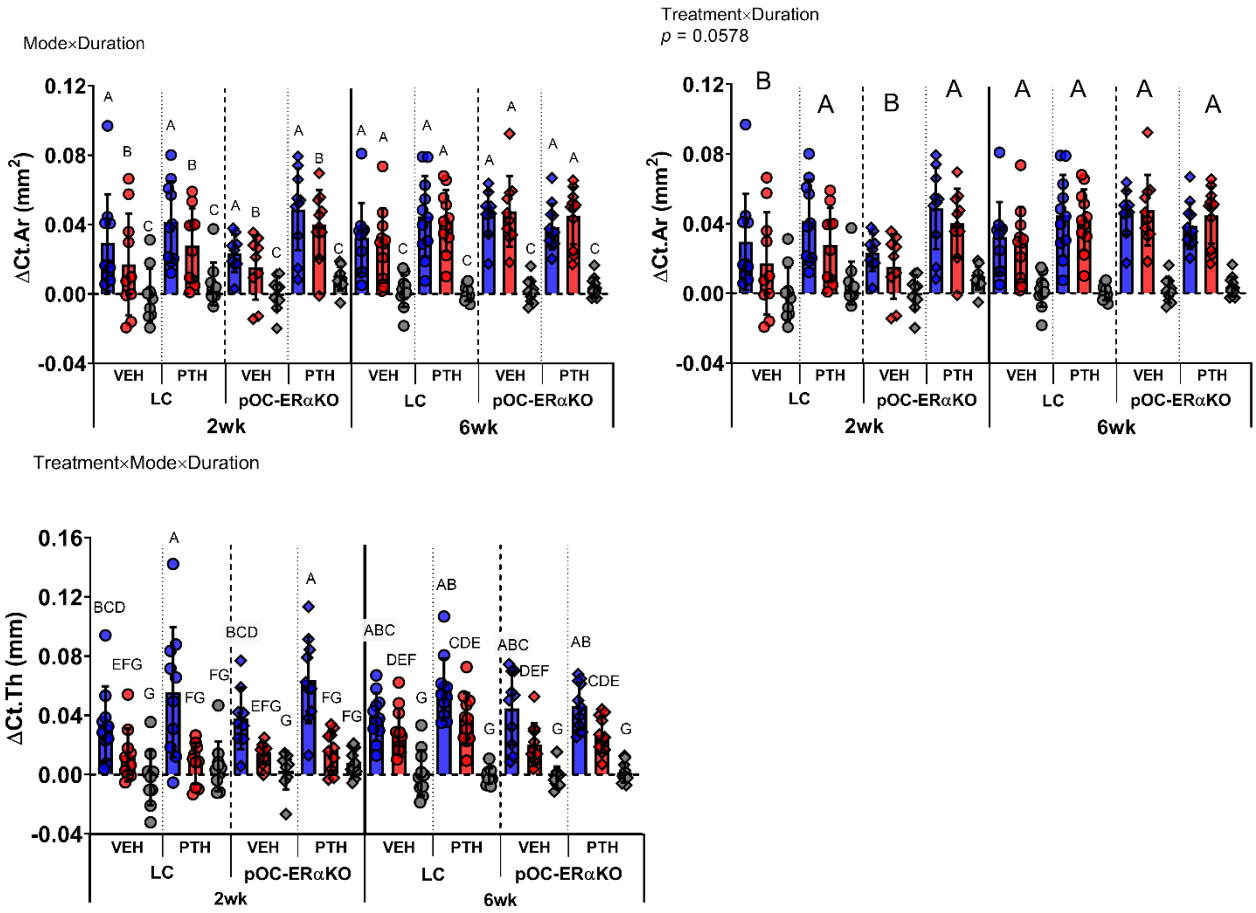

Supplemental Figure 5.2 Loading effects in concurrently-treated 16-week-old pOC-ERαKO and LC mice loaded for 2 or 6 weeks [Loaded-Control]. Data are mean ± SD. A > B > C, groups not sharing the same letter are different by Tukey post-hoc. $p<0.05$ by ANOVA.

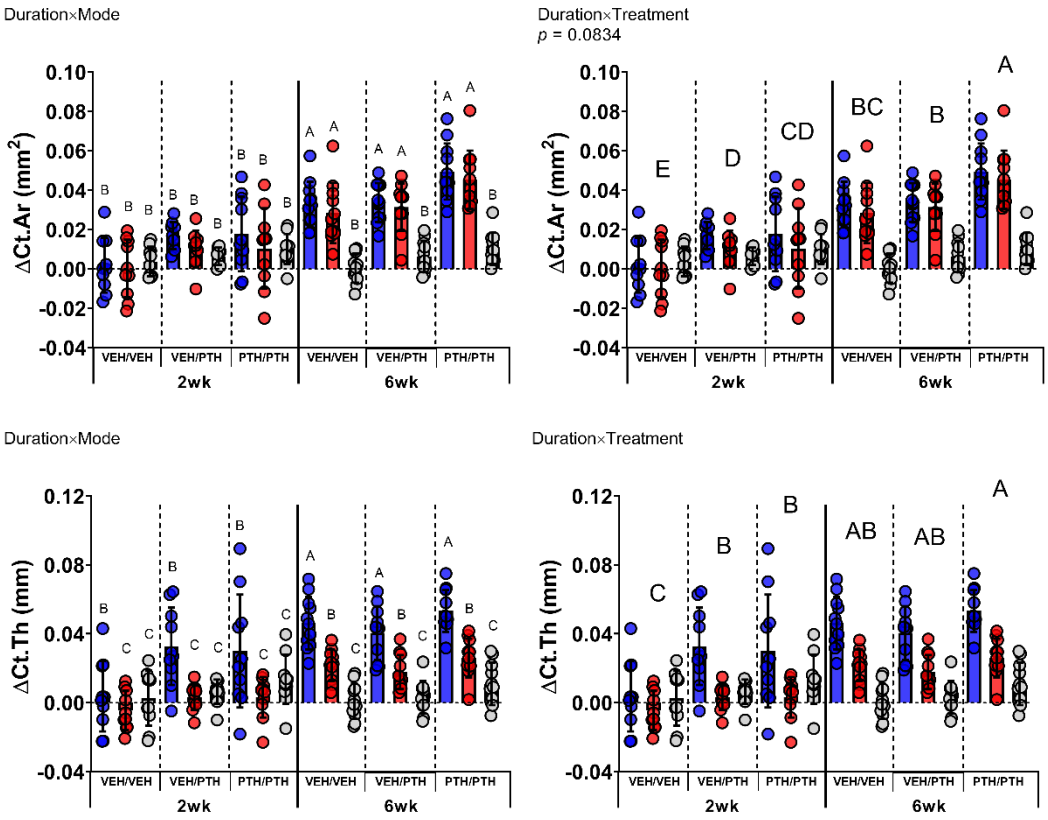

Supplemental Figure 5.3 Loading effects in pre-treated 16-week-old WT mice loaded for 2 or 6 weeks [Loaded-Control]. Data are mean ± SD. A > B > C, groups not sharing the same letter are different by Tukey post-hoc. $p<0.05$ by ANOVA.

Chapter 6

PTH PRE-TREATMENT PRIOR TO TIBIAL MECHANICAL LOADING IMPROVES THEIR SYNERGISTIC ANABOLIC EFFECTS IN MICE

6.1 Introduction

Parathyroid hormone (PTH) is one of the few FDA-approved anabolic osteoporosis treatments available. PTH stimulates bone formation, increases bone mineral density (BMD), and reduces fracture risk [1–5]. A delayed and more gradual increase in bone resorption eventually matches the increases in formation, and these benefits plateau after approximately 2 years [3]. This period is known as the "anabolic window", after which continuing treatment has no added benefit. Therefore, bone growth must be maximized during this time.

In addition to being independently skeletally anabolic, applied mechanical loading has synergistic effects when combined with PTH treatment [6]. The anabolic effects of tibial bending in rats were enhanced by the addition of PTH treatment [7,8]. However, most PTH and mechanical loading studies are performed in animals with normal bone mass. Postmenopausal women respond less to exercise interventions than pre-menopausal women [9], but estrogen treatment can rescue their response [10]. Additionally, ovariectomy (OVX) or deletion of estrogen receptor-alpha (ERα) can alter the response to mechanical loading [11–13]. Therefore, it is important to study the effects of PTH and mechanical loading in estrogen-impaired, low bone mass animals.

Many osteoporosis-related fractures occur at corticocancellous sites. Bone's ability to respond to mechanical loading decreases with age, particularly in cancellous bone [14–17], highlighting the need to increase cancellous bone in at risk patients. Adding PTH treatment to mechanical loading regimens may help overcome the loss of mechanoresponsiveness, but may not be sufficient. Tibial compression and PTH treatment in mice were synergistically anabolic in cortical bone, but the effects were only additive in cancellous bone [18]. Therefore, we hypothesized that pre-treating mice would prime bone tissue prior to the initiation of mechanical loading and further augment the anabolic response to loading.

In this study, we investigated the effects of low bone mass due to impaired estrogen signaling and PTH pre-treatment on the synergistic response to applied mechanical loading. Cyclic tibial compression was applied to female 10- and 16-week-old osteoblast-specific estrogen receptor-alpha knockout mice (pOC-ERαKO) and their littermate controls (LC) along with PTH treatment for 2 or 6 weeks. Additionally, female wild type C57Bl/6J mice (WT) were pre-treated with vehicle or PTH for 6 weeks prior to starting tibial loading at 16 weeks of age for 2 or 6 weeks. Bone mass and morphology were assessed using microcomputed tomography (microCT), and cellular activity was assessed using histology. PTH increased cancellous bone mass but was more effective in cortical bone. With PTH, load-induced increases in bone mass were blunted in cancellous bone and increased in cortical bone. PTH pre-treatment rescued the cancellous loading response and extended the synergistic effects in cortical bone. Analyses for these experiments were

delayed due to the COVID-19 pandemic shut down. Histomorphometry analyses are ongoing.

6.2 Materials and Methods

6.2.1 Animals

Generation of osteoblast-specific ERαKO mice (pOC-ERαKO): Osteoblast-specific ERα knockout (pOC-ERαKO) and littermate control (LC) mice were generated as previously described [19]. Briefly, mice with loxP sequences flanking exon 3 of the DNA-binding domain of the ERα gene (*Esr1*) (*ERα*$^{fl/fl}$, provided by Dr. Sohaib Kahn, University of Cincinnati, Cincinnati, OH, USA) [20] were inbred to be >99% pure C57Bl/6 by speed congenics (DartMouse Speed Congenic Core Facility, Geisel School of Medicine at Dartmouth, Hanover, NH, USA). Mice containing a transgene encoding *Cre* recombinase driven by the human osteocalcin promoter had been previously inbred to the C57Bl/6 strain (*OC-Cre*, provided by Dr. Thomas Clemens, The Johns Hopkins University, Baltimore, MD, USA) [21,22], and were crossed with *ERα*$^{fl/fl}$ mice. Mice were genotyped using lysed tail PCR as described [19].

Wild type mice: 9-week-old female, wild type C57Bl/6J mice (WT) were purchased from Jackson Laboratories and allowed to acclimate to the Cornell animal facility for 1 week prior to the start of the experiment at 10 weeks of age. Mice were housed 3 to 5 per cage and had *ad libitum* access to food and water. All animal procedures were approved by Cornell University's IACUC.

6.2.2 Parathyroid hormone treatment

Human parathyroid hormone (1-34) (Bachem Americas, Inc; Torrance, CA, USA) was administered subcutaneously 5 days per week at a dose of 40μg/kg. Mice receiving vehicle (VEH) treatment were injected subcutaneously with a similar volume of sterile phosphate-buffered saline (PBS) 5 days per week.

6.2.3 Tibial strain gauging

The applied loads were based on the *in vivo* strains in each group. Single-element strain gauges (C2A-06-015LW-120, Micro-Measurements, Wendell, NC, USA) were surgically attached to the anteromedial surface of the tibial midshafts of small subsets of mice. Axial cyclic compressive loads with peak load magnitudes ranging from -2 to -16N were applied to the tibiae in our custom tibial loading device [23,24]. Mice were immediately euthanized following data collection. Bone stiffness and the peak load required to induce +1000 microstrain (με) on the anteromedial surface of the tibial midshaft were calculated using the load and strain data as previously described [24].

Concurrent treatment: Strain gauges were attached to the left and right limbs of 10- and 16-week old female pOC-ERαKO and LC mice (n=5 per genotype per age). Bone stiffness was similar between LC and pOC-ERαKO mice and between each age group (0.00803 ± 0.0014N/με 10wk LC, 0.00719 ± 0.0023N/με 10wk pOC-ERαKO, 0.00811 ± 0.0023N/με 16wk LC, 0.00723 ± 0.0015N/με 16wk pOC-ERαKO; mean ± SD). A peak load of -7.9N was applied to female LC and pOC-ERαKO mice of both ages to induce +1000με at the midshaft.

Pre-treatment: 10-week-old female WT mice were treated with PTH or VEH 5 days per week for 6 weeks. At 16 weeks of age, strain gauges were attached to the left tibiae of n=8 mice per treatment group. Right limbs were harvested for pre-treatment baseline analysis. Bone stiffness differed by treatment group (0.00925 ± 0.0022N/με VEH, 0.0106 ± 0.0014N/με PTH; mean ± SD). Therefore, peak loads of -8.7N and -10.6N were applied to induce +1000με at the midshaft in mice pre-treated with VEH and PTH, respectively.

6.2.4 In vivo tibial mechanical loading

In vivo cyclic compression was applied to the left tibiae at a rate of 4Hz for 1200 cycles per day, 5 days per week in a triangular waveform, and the right limbs served as contralateral controls [24]. A dwell of 100ms at -1N was maintained between successive load cycles, and the dwell-to-peak time was 75ms. Peak load magnitudes were determined by strain gauging as described above. Three days after the last session of *in vivo* tibial compression mice were euthanized via isoflurane overdose and cardiac puncture.

Concurrent treatment: The left tibiae of 10- and 16-week-old female LC and pOC-ERαKO mice (n=10-11 per group) were loaded in cyclic compression at a peak load of -7.9N *in vivo* for 2 weeks, with a second group of 16-week-old mice undergoing cyclic compression for 6 weeks (Fig. 6.1).

Pre-treatment: 10-week-old female WT mice were treated with VEH or PTH for 6 weeks. At 16 weeks of age, cyclic tibial compression commenced alongside treatment for 2 or 6 weeks (n=10-12 per group). Overall, there were three treatment

groups: 1) VEH pre-treated and VEH treated during loading (VEH/VEH), 2) VEH pre-treated and PTH treated during loading (VEH/PTH), and 3) PTH pre-treated and PTH treated during loading (PTH/PTH) (Fig. 6.1). Based on the strain gauge analysis, groups 1 and 2 received a peak load magnitude of -8.7N and group 3 received a peak load magnitude of -10.6N.

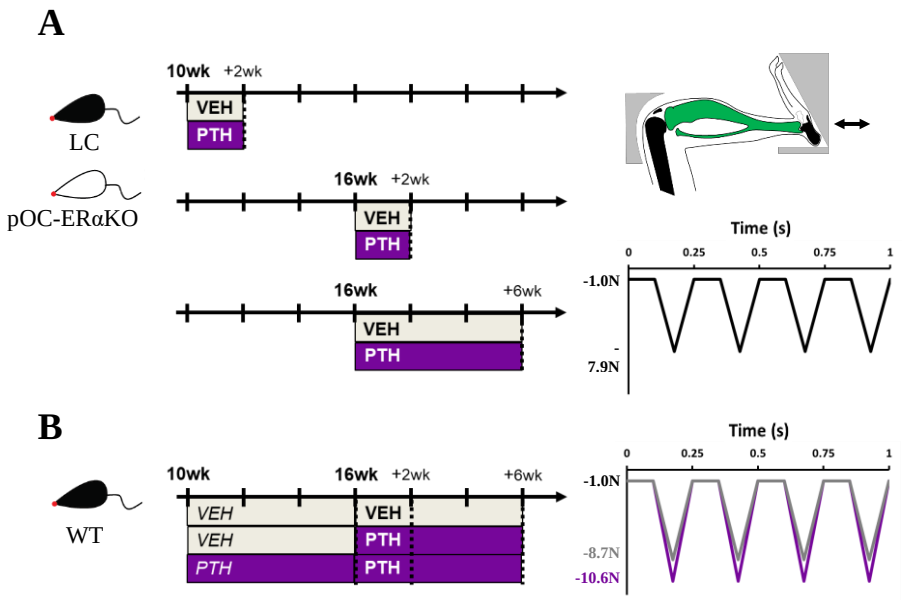

Figure 6.1 Experimental timeline. (A) All concurrently-loaded pOC-ERαKO and LC mice underwent tibial compression at a -7.9N peak load and treatment with VEH or PTH 5 days per week. 10-week-old mice were loaded and treated for 2 weeks. 16-week-old mice were loaded and treated for 2 or 6 weeks. (B) Pre-treated WT mice received VEH or PTH pre-treatment from 10 weeks of age to 16 weeks of age with no tibial loading (*Italic*). At 16 weeks of age, loading and treatment (**Bold**) commenced for 2 or 6 weeks. Mice pre-treated with VEH or PTH were loaded at -8.7N or -10.6N peak loads, respectively.

6.2.5 Microcomputed tomography

Bone morphology was analyzed using microcomputed tomography (microCT). At euthanasia, tibiae were stored in 4% paraformaldehyde overnight and later scanned in 70% ethanol at 10μm and 15μm voxel resolution at the metaphysis and diaphysis,

respectively (μCT35, Scanco Medical AG; 55kVp, 145μA, 600ms integration time). Due to the COVID-19 pandemic shut down, n=4 mice per treatment group of the pre-treated, 2-week mechanically loaded mice were scanned on a different microCT system (μCT40, Scanco Medical AG; 55kVp, 145μA, 300ms integration time). The metaphysis volume of interest (VOI) was defined as 10% of the total tibial length beginning 50μm distal to the growth plate. Cancellous bone and metaphyseal cortical shell were segmented by hand and analyzed separately. The diaphysis VOI was defined as 2.5% of the total tibial length centered at the midshaft [19]. Outcome measures for cancellous bone were bone volume fraction (BV/TV), trabecular thickness (Tb.Th), number (Tb.N), and separation (Tb.Sp), and tissue mineral density (cn.TMD). Outcome measures for cortical bone were cortical area (Ct.Ar) and thickness (Ct.Th), marrow area (Ma.Ar, diaphysis only), maximum (I_{MAX}) and minimum moment of inertia (I_{MIN}), and tissue mineral density (ct.TMD).

6.2.6 Histology

Following microCT scanning, left and right tibiae from mechanically-loaded mice (n=5-6 mice/group) and right limbs from pre-treated baseline mice (n=5 mice/group) were decalcified in 10% EDTA, embedded in paraffin, and sectioned at a 6μm thickness in the sagittal plane using a rotary microtome (Leica RM2255; Germany).

The presence of osteoclasts was analyzed using tartrate-resistant acid phosphatase (TRAP) staining. Sections were deparaffinized and rehydrated, submerged in TRAP buffer for 10 minutes (3.28g Na-acetate, 46.01g Na-tartrate in 1L

deionized water, pH 5.0; Sigma-Aldrich), and incubated in TRAP staining solution at 37°C for 120 minutes (40mg Napthol AS-MX, 4ML N-N dimethylformamide, 240mg Fast Red Violet LB Salt, 2mL Triton X-100; Sigma-Aldrich, in 200mL TRAP buffer). Sections were then counterstained with hematoxylin for 10 minutes, dehydrated, and coverslipped.

Active osteoblasts were identified using procollagen I immunostaining. Sections were deparaffinized and rehydrated prior to antigen retrieval with citrate buffer at 60°C for 60 minutes (0.96g citric acid in 500mL deionized water, pH 6.0, add 0.25mL tween 20; Sigma-Aldrich). Blocking was performed using 3% hydrogen peroxide for 10 minutes, mouse IgG blocking reagent for 1 hour (Vector M.O.M Immunodetection Kit), and protein blocking for 5 minutes (Vector M.O.M Immunodetection Kit). Sections were incubated in primary antibody overnight at 4°C (5µg/mL, SP1.D8; Developmental Studies Hybridoma Bank, Iowa City, IA, USA). Secondary antibody was delivered for 10 minutes (Biotinylated anti-mouse IgG, Vector M.O.M Immunodetection Kit), and staining was visualized using diaminobenzidine. Sections were dehydrated and coverslipped.

6.2.7 Statistics

The systemic effects of PTH were analyzed using the non-loaded control limbs with an ANOVA for treatment group, genotype where applicable, and their interactions. The effects of loading were analyzed using the differences between the loaded and control limbs [Loaded-Control] with an ANOVA for treatment group, genotype where applicable, and their interactions. Loading effects were determined to

be nonzero if analyses of the individual limbs revealed differences between the loaded and control limbs within a group using a linear mixed-effects model with loading, treatment group, genotype where applicable, and their interactions as fixed effects and a random mouse effect to account for the repeated measure (loaded and control limbs). A Tukey HSD post-hoc test was performed when the interaction terms were significant. Significance was set at $p < 0.05$. All results reported are significant unless stated otherwise.

6.3 Results

6.3.1 PTH increased cortical bone mass more than cancellous

PTH treatment increased cortical bone volume at earlier time points than cancellous bone volume. Metaphyseal cancellous BV/TV only increased with PTH in 16-week-old LC and pOC-ERαKO mice after 6 weeks and pre-treated WT mice after 6 additional weeks of treatment (Fig. 6.2). WT mice that were not pre-treated prior to 6 weeks of PTH treatment trended toward increased BV/TV. PTH increased Tb.Th in 16-week-old LC and pOC-ERαKO mice after 2 and 6 weeks of treatment. Pre-treated baseline WT mice and 10-week-old LC and pOC-ERαKO mice trended toward greater Tb.Th with PTH. Cancellous TMD was reduced in pre-treated WT mice after 2 weeks, potentially indicating the presence of less mineralized newly formed bone tissue. Similarly, WT mice that received PTH regardless of pre-treatment had reduced cn.TMD after 6 weeks. The cancellous response to PTH was not different in low bone mass pOC-ERαKO mice.

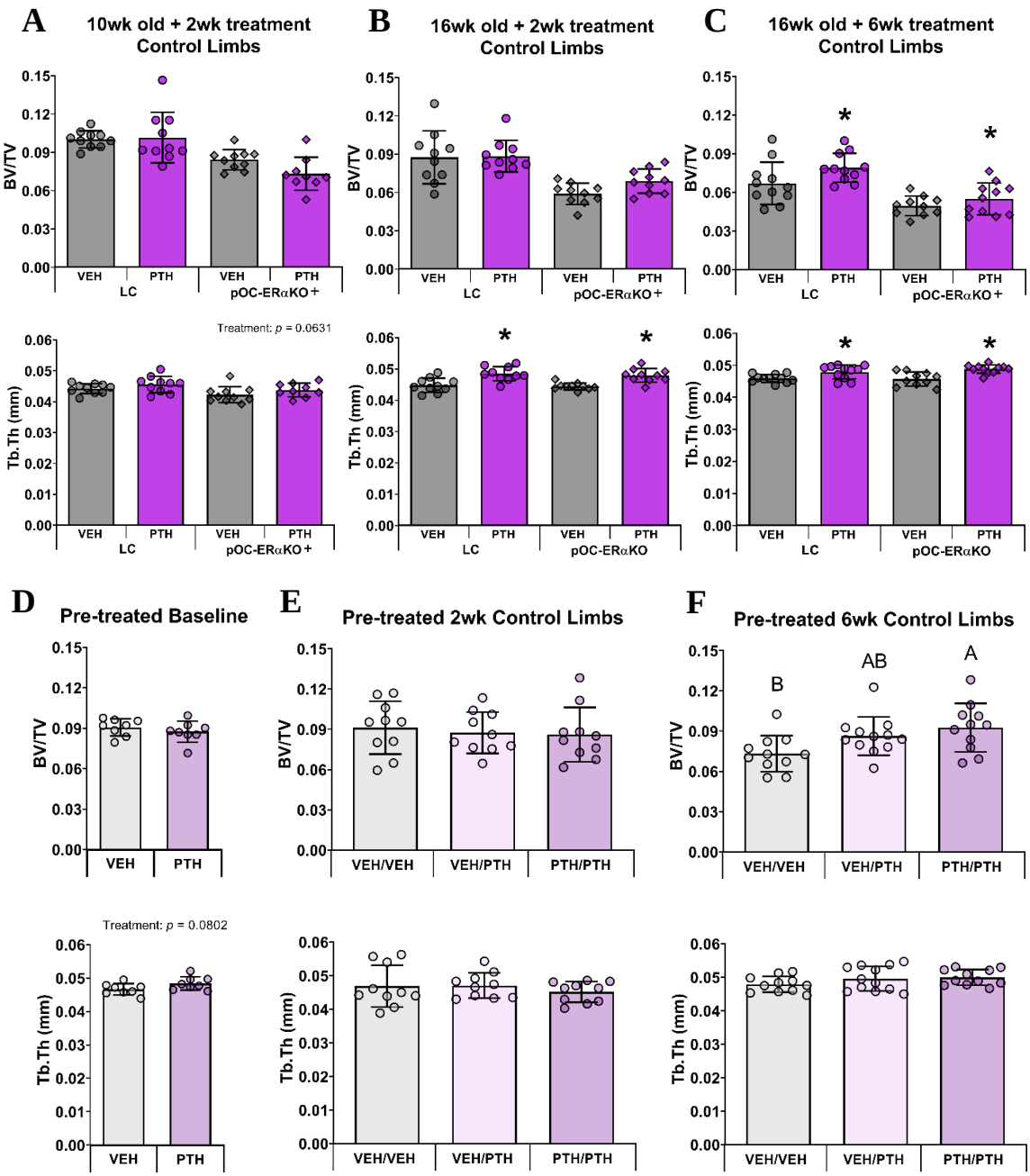

Figure 6.2 Metaphyseal cancellous bone mass in non-loaded control limbs. (A,B,D,E) PTH did not increase BV/TV in 10- or 16-week-old mice treated for 2 weeks or pre-treated baseline mice. (C,F) PTH increased cancellous BV/TV in 16-week-old mice treated for 6 weeks with and without pre-treatment. * PTH different from VEH, + pOC-ERαKO different from LC, A > B treatment groups different, $p<0.05$ by ANOVA with Tukey post-hoc.

The metaphyseal cortical shell was very responsive to PTH. Young, 10-week-old LC and pOC-ERαKO mice increased Ct.Ar, Ct.Th, and I_{MAX} with PTH treatment,

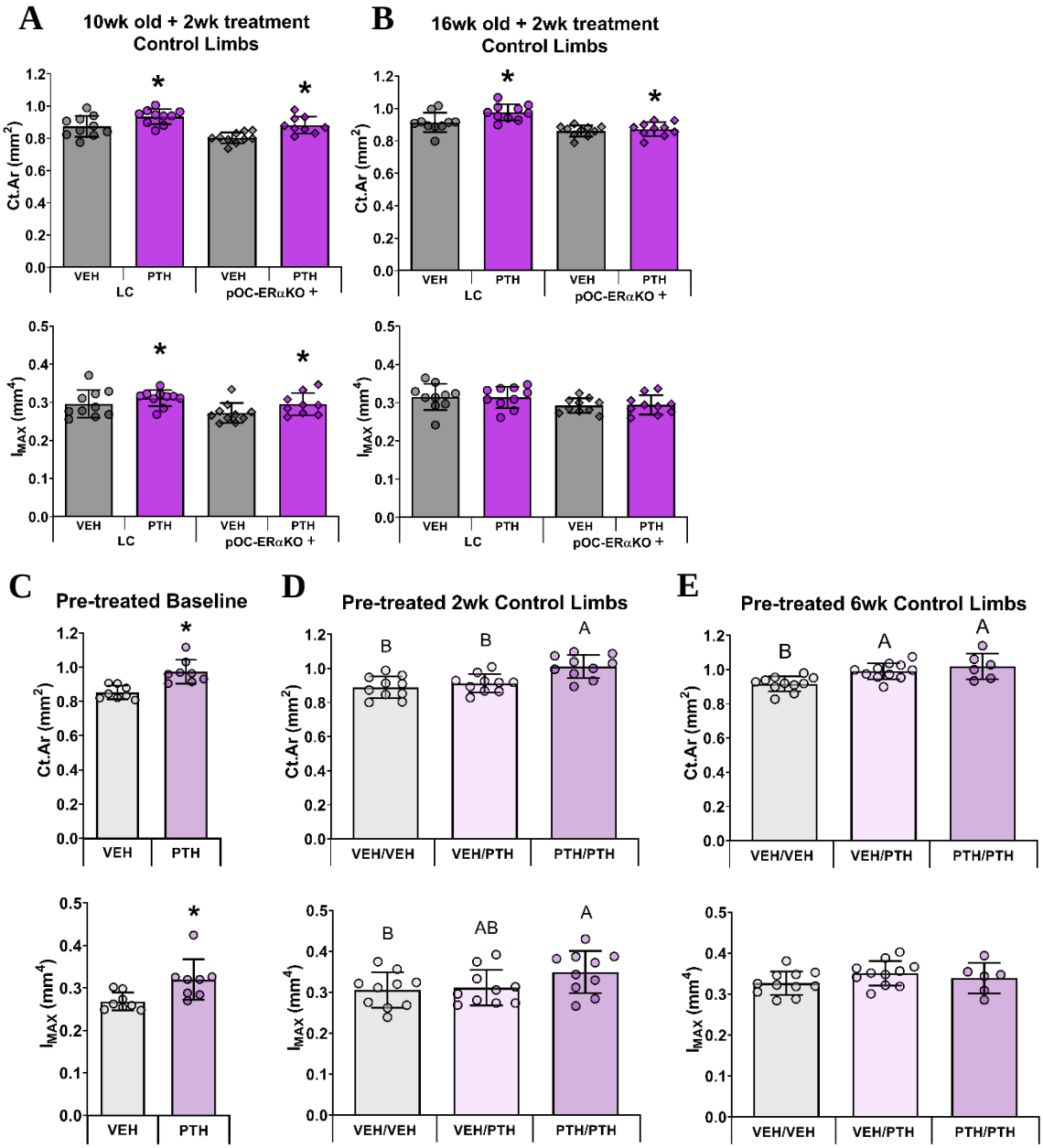

Figure 6.3 Metaphyseal shell cortical bone mass in non-loaded control limbs. (A,B) PTH increased cortical bone mass in 10- and 16-week-old pOC-ERαKO and LC mice treated for 2 weeks. (C,D,E) PTH increased cortical bone mass in 16-week-old WT mice at baseline, after 2 weeks when pre-treated, and after 6 weeks regardless of pre-treatment. * PTH different from VEH, + pOC-ERαKO different from LC, A > B treatment groups different, $p<0.05$ by ANOVA with Tukey post-hoc.

with a trend toward increased I_{MIN} (Fig. 6.3). In 16-week-old LC and pOC-ERαKO mice, Ct.Ar increased with PTH, but Ct.Th only increased in LC mice. Following pre-

treatment, WT mice increased Ct.Ar, Ct.Th, I_{MAX}, and I_{MIN} with PTH at baseline. Only pre-treated WT mice had increased Ct.Ar, Ct.Th, and I_{MAX} after 2 weeks. After 6 weeks, however, the VEH/PTH group also had increased Ct.Ar and Ct.Th, with even greater Ct.Th in pre-treated mice.

The effects of PTH at the diaphysis were not as pronounced as the metaphyseal shell. 16-week-old LC and pOC-ERαKO mice increased Ct.Ar and Ct.Th with PTH after 6 weeks, with a trend in Ct.Th after 2 weeks (Fig. 6.4). After 6 weeks, Ma.Ar was decreased in LC mice with PTH. After 6 weeks of pre-treatment, WT mice had increased Ct.Th and a trend toward increased Ct.Ar at baseline. Pre-treated WT mice had greater Ct.Ar than mice that only received PTH during the 2 week treatment period, and greater Ct.Th than all other mice. TMD was lower in the VEH/PTH group at 2 weeks, indicating newly formed bone, but the pre-treated mice had time to mineralize new tissue and were no different from the VEH/VEH group. After 6 weeks, all mice that received PTH had reduced Ma.Ar, and TMD was greater in pre-treated mice. There was a trend toward greater Ct.Th in WT mice that received PTH.

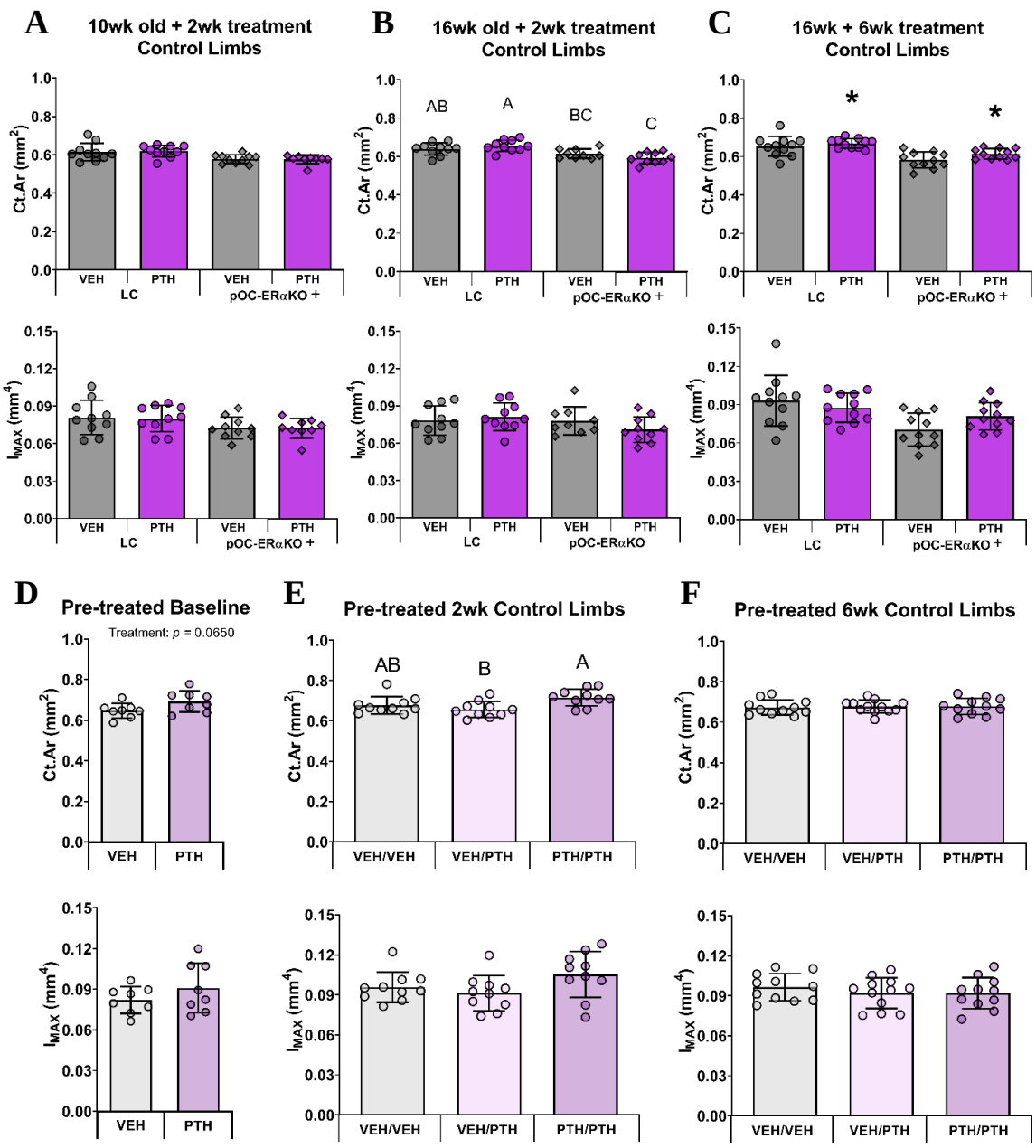

Figure 6.4 Diaphyseal cortical bone mass in non-loaded control limbs. (A,B,C) PTH increased cortical bone mass in 16-week-old pOC-ERαKO and LC mice treated for 6 weeks. (D,E,F) PTH increased cortical bone mass in 16-week-old WT mice after 2 weeks when pre-treated compared to non-pre-treated mice. * PTH different from VEH, + pOC-ERαKO different from LC, A > B treatment groups different, $p<0.05$ by ANOVA with Tukey post-hoc.

6.3.2 PTH synergistically increased loading effects in cortical bone, blunted loading effects in cancellous bone

PTH treatment during loading did not increase the cancellous response to loading unless the mice were pre-treated. Cancellous BV/TV trended toward an increased response to loading with PTH in 10-week-old LC and pOC-ERαKO mice (p=0.0567) but the response to loading was blunted with PTH in 16-week-old LC and pOC-ERαKO mice loaded for 6 weeks (Fig. 6.5). Non-pre-treated WT mice that received PTH during loading had reduced responses to loading in BV/TV compared to VEH-treated mice after 6 weeks. Pre-treatment rescued the loading response to the level of VEH-treated mice after 6 weeks, and was more anabolic than treatment during loading in BV/TV and Tb.Th after 2 weeks (Fig. 6.5). The effect of treatment on loading responses was not different in pOC-ERαKO compared to LC mice.

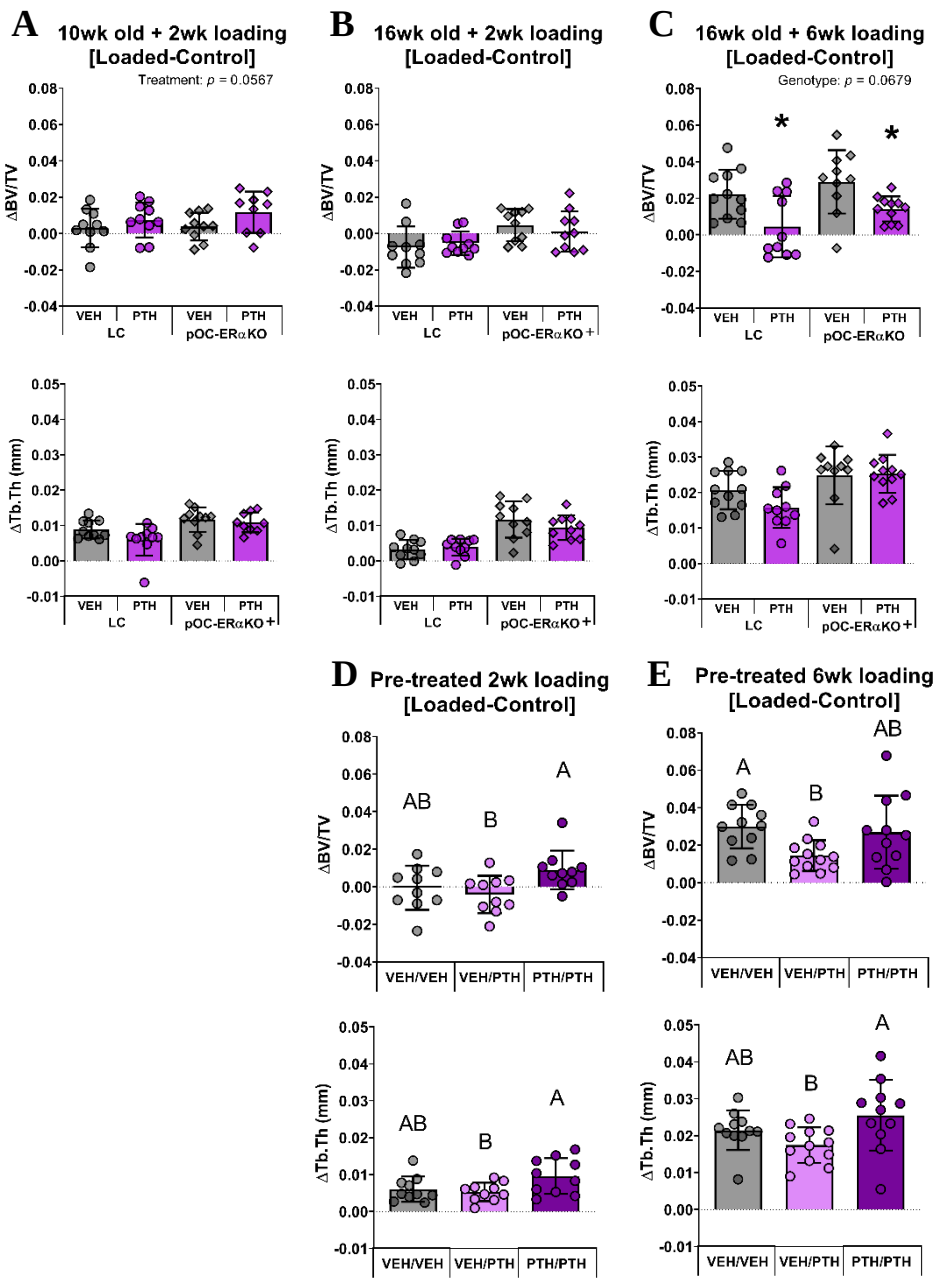

Figure 6.5 Changes in metaphyseal cancellous bone mass with loading [Loaded-Control]. (A) Load-induced increases in BV/TV trended higher with PTH treatment in 10-week-old pOC-ERαKO and LC mice. (B) PTH did not influence the response to loading in 16-week-old pOC-ERαKO and LC mice after 2 weeks, but (C) decreased the loading response after 6 weeks. (D,E) PTH pre-treatment was more effective than concurrent treatment alone and rescued the loading response in 16-week-old WT mice. * PTH different from VEH, + pOC-ERαKO different from LC, A > B treatment groups different, $p<0.05$ by ANOVA with Tukey post-hoc.

PTH was synergistically anabolic with loading in the metaphyseal cortical shell. Load-induced increases in I_{MAX} were greater with PTH in 10-week-old LC and pOC-ERαKO mice (Fig. 6.6). Two weeks of loading increased Ct.Ar and I_{MAX} more with PTH in 16-week-old LC and pOC-ERαKO mice. Similarly, WT mice that received PTH during the 2-week loading period trended toward greater loading responses in Ct.Ar. The effect of treatment on loading responses was not different in low bone mass pOC-ERαKO mice. The cortical shell was unable to be analyzed separately after 6 weeks of loading due to the presence of osteophytes at the medial proximal tibia.

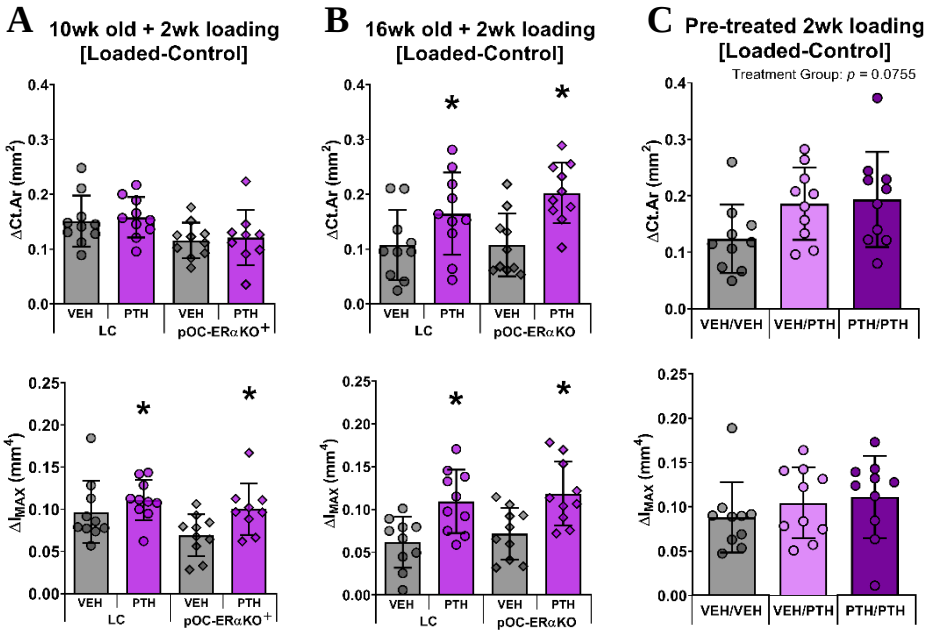

Figure 6.6 Changes in metaphyseal shell cortical bone mass with loading [Loaded-Control]. (A,B) Load-induced increases in Ct.Ar in 10-week-old pOC-ERαKO and LC mice and I_{MAX} in 10- and 16-week-old pOC-ERαKO and LC mice were greater with PTH treatment after 2 weeks. (C) PTH treatment trended toward increased loading responses in 16-week-old WT mice after 2 weeks. * PTH different from VEH, + pOC-ERαKO different from LC, A > B treatment groups different, $p<0.05$ by ANOVA with Tukey post-hoc.

PTH and loading were synergistically anabolic at the diaphysis and pre-treatment extended the period of synergism. PTH increased the loading response in Ct.Ar, I_{MAX}, and I_{MIN}, with a trend in Ct.Th in 16-week-old LC and pOC-ERαKO mice after 2 weeks of loading (Fig. 6.7). Non-pre-treated WT mice that received PTH during 2 weeks of loading trended toward increased loading responses in Ct.Ar and Ct.Th. After 6 weeks, however, PTH did not affect the response to loading in all non-pre-treated mice. Pre-treated WT mice had an increased loading response in Ct.Ar compared to all other WT mice, and a greater loading response than VEH-treated WT mice after 6 weeks of loading (Fig. 6.7). The effect of treatment on loading responses was not different in pOC-ERαKO compared to LC mice.

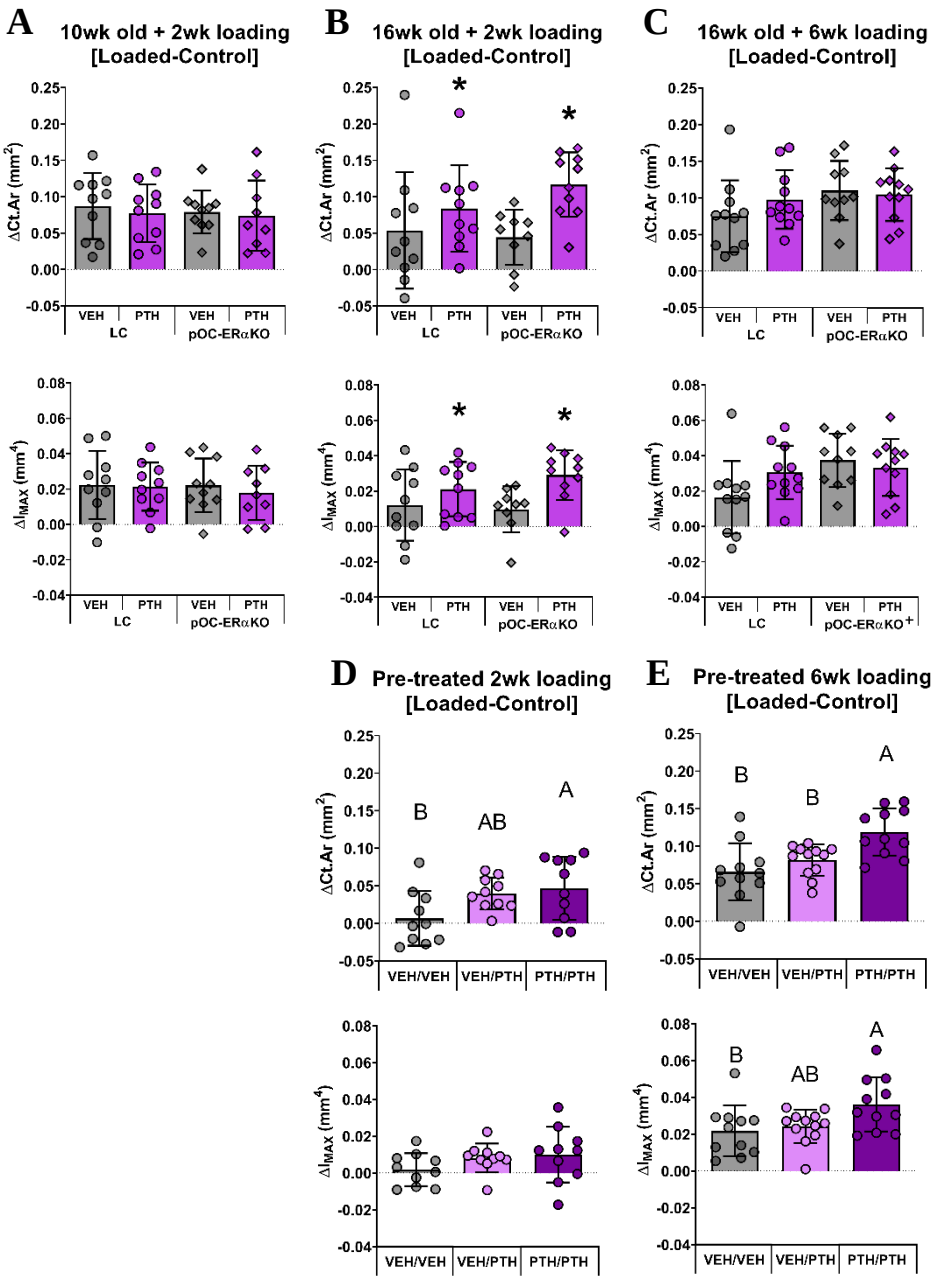

Figure 6.7 Changes in diaphyseal cortical bone mass with loading [Loaded-Control]. (A,B,C) Load-induced increases in Ct.Ar and I_{MAX} were only increased with PTH in 16-week-old pOC-ERαKO and LC mice after 2 weeks. (C) PTH pre-treatment increased the loading response in 16-week-old WT mice after 2 and 6 weeks. * PTH different from VEH, + pOC-ERαKO different from LC, A > B treatment groups different, $p<0.05$ by ANOVA with Tukey post-hoc.

6.4 Discussion

PTH was more effective in cortical bone than cancellous bone. PTH enhanced the anabolic effects of tibial loading in cortical bone but limited the response to loading in cancellous bone. Pre-treatment rescued the cancellous loading response to the level of VEH-treated mice and extended the synergistic period in cortical bone. Lack of ERα did not impair the response to PTH nor the effect of PTH on load-induced bone growth.

Although PTH trended toward increasing the cancellous anabolic response to loading in 10-week-old mice, treatment reduced the loading response in 16-week-old mice. The changes in BV/TV with 6 weeks of loading were lower in treated pOC-ERαKO and LC mice and non-pre-treated WT mice compared to VEH-treated controls. Similar effects were seen in 19-month-old female C57Bl/6 mice. After 2 weeks of treatment and tibial loading with or without a 4 week pre-treatment, loading increased cancellous bone mass in VEH-treated but not PTH-treated mice [25]. Unlike in those aged mice, here, pre-treatment rescued the load-induced increases of BV/TV to the level of VEH-treated 16-week-old mice. Consistent with our findings, a 4 week pre-treatment period prior to 2 weeks of tibial loading in 17-week-old female C57Bl/6 mice created additive anabolic effects in cancellous bone [18]. Pre-treatment prior to loading may overcome loading-induced bone loss in young animals but may not be able to create a synergistic response in cancellous bone.

The 16-week-old mice with blunted loading responses were also the only concurrently-loaded mice that increased cancellous bone mass in the non-loaded control limbs with PTH. This finding may indicate that the anabolic effects of PTH

prevented the response to loading and should be investigated further. Cellular responses in the cancellous bone are being investigated with histology but analyses are still ongoing due to the COVID-19 pandemic shut down. Once completed, differences in osteoblast and osteoclast activity with treatment and loading may reveal more about the mechanisms behind these differences.

PTH augmented the cortical loading response short term, but after 6 weeks of loading the benefit was lost. Mechanical loading and PTH synergistically increased cortical bone mass at the metaphyseal shell and diaphysis after 2 weeks in 16-week-old mice. Similar cortical synergistic effects have been reported elsewhere and are fairly well-established [6,7,18]. After 6 weeks of loading, PTH no longer increased the loading response. Pre-treated mice, however, retained the synergistic response to loading after 6 weeks. Similarly, PTH-treated 19-month-old female C57Bl/6 mice had a trend toward a greater increase in Ct.Ar with loading when pre-treated with PTH that was not evident without pre-treatment [25].

Estrogen status has been shown to alter the skeletal response to loading [11,12,26], but its effect on the influence of combined PTH and mechanical loading has not been well investigated. In postmenopausal osteoporosis patients, whole body vibration and PTH treatment increased BMD at the spine more than PTH alone [27]. However, because no groups received only whole body vibration or neither treatment, it is difficult to determine whether these effects were synergistic or additive. Nonetheless, there was a clear benefit to combining PTH and mechanical stimulation in low bone mass patients that we also saw here. pOC-ERαKO mice increased bone mass similarly to LC mice with PTH treatment. Although the effect of loading differed

by genotype at certain timepoints and locations, PTH increased the anabolic response similarly between genotypes.

We have shown that PTH and its effects on loading differ greatly between cortical and cancellous bone, and the mechanisms behind these differences should be investigated further. Overall, PTH pre-treatment prior to mechanical loading was more anabolic than concurrent treatment and loading. Pre-treating patients prior to starting exercise or physical therapy regimens may be more beneficial during the limited anabolic window of PTH. PTH and its effects on loading were not altered in low bone mass pOC-ERαKO mice, indicating that these therapies still will be effective in osteoporosis patients and adding exercise to PTH treatments will be effective clinically.

6.5 References

[1] D.W. Dempster, F. Cosman, E.S. Kurland, H. Zhou, J. Nieves, L. Woelfert, E. Shane, K. Plavetić, R. Müller, J. Bilezikian, R. Lindsay, Effects of daily treatment with parathyroid hormone on bone microarchitecture and turnover in patients with osteoporosis: a paired biopsy study., J. Bone Miner. Res. 16 (2001) 1846–53. doi:10.1359/jbmr.2001.16.10.1846.

[2] R. Lindsay, H. Zhou, F. Cosman, J. Nieves, D.W. Dempster, A.B. Hodsman, Effects Of a One-Month Treatment With PTH(1-34) on Bone Formation on Cancellous, Endocortical, and Periosteal Surfaces of the Human Ilium, J. Bone Miner. Res. 22 (2007) 495–502. doi:10.1359/jbmr.070104.

[3] D. Aslan, M.D. Andersen, L.B. Gede, T.K. de Franca, S.R. Jørgensen, P. Schwarz, N.R. Jørgensen, Mechanisms for the bone anabolic effect of parathyroid hormone treatment in humans, Scand. J. Clin. Lab. Investig. 72 (2012) 14–22. doi:10.3109/00365513.2011.624631.

[4] F. Cosman, Anabolic and Antiresorptive Therapy for Osteoporosis : Combination and Sequential Approaches, Curr. Osteoporos. Rep. (2014) 385–395. doi:10.1007/s11914-014-0237-9.

[5] S.L. Greenspan, H.G. Bone, M.P. Ettinger, D.A. Hanley, R. Lindsay, J.R. Zanchetta, C.M. Blosch, A.L. Mathisen, S.A. Morris, T.B. Marriott, Effect of Recombinant Human Parathyroid Hormone (1-84) on Vertebral Fracture and Bone Mineral Density in Postmenopausal Women with Osteoporosis, Ann. Intern. Med. 146 (2013) 326. doi:10.7326/0003-4819-146-5-200703060-00005.

[6] Y. Ma, W.S. Jee, Z. Yuan, W. Wei, H. Chen, S. Pun, H. Liang, C. Lin, Parathyroid hormone and mechanical usage have a synergistic effect in rat tibial diaphyseal cortical bone., J. Bone Miner. Res. 14 (1999) 439–48. doi:10.1359/jbmr.1999.14.3.439.

[7] H. Hagino, T. Okano, M.P. Akhter, M. Enokida, R. Teshima, Effect of parathyroid hormone on cortical bone response to in vivo external loading of the rat tibia, J. Bone Miner. Metab. 19 (2001) 244–250. doi:10.1007/s007740170027.

[8] M.D. Roberts, T.J. Santner, R.T. Hart, Local bone formation due to combined mechanical loading and intermittent hPTH-(1-34) treatment and its correlation to mechanical signal distributions, J. Biomech. 42 (2009) 2431–2438. doi:10.1016/j.jbiomech.2009.08.030.

[9] E.J. Bassey, M.C. Rothwell, J.J. Littlewood, D.W. Pye, Pre- and postmenopausal women have different bone mineral density responses to the same high-impact exercise., J. Bone Miner. Res. 13 (1998) 1805–1813. doi:10.1359/jbmr.1998.13.12.1805.

[10] R. Zhao, Z. Xu, M. Zhao, Effects of Oestrogen Treatment on Skeletal Response to Exercise in the Hips and Spine in Postmenopausal Women: A Meta-Analysis, Sport. Med. 45 (2015) 1163–1173. doi:10.1007/s40279-015-0338-3.

[11] J.C. Tou, A. Foley, Y. V Yuan, S. Arnaud, C.E. Wade, M. Brown, The effect of ovariectomy combined with hindlimb unloading and reloading on the long bones of mature Sprague-Dawley rats., Menopause. 15 (2008) 494–502. doi:10.1097/gme.0b013e318148bbad.

[12] K.M. Melville, N.H. Kelly, G. Surita, D.B. Buchalter, J.C. Schimenti, R.P. Main, F.P. Ross, M.C.H. Van Der Meulen, Effects of Deletion of ERα in Osteoblast-Lineage Cells on Bone Mass and Adaptation to Mechanical Loading Differ in Female and Male Mice, J. Bone Miner. Res. 30 (2015) 1468–1480. doi:10.1002/jbmr.2488.
[13] S. Kondoh, K. Inoue, K. Igarashi, H. Sugizaki, Y. Shirode-Fukuda, E. Inoue, T. Yu, J.K. Takeuchi, J. Kanno, L.F. Bonewald, Y. Imai, Estrogen receptor α in osteocytes regulates trabecular bone formation in female mice, Bone. 60 (2014) 68–77. doi:10.1016/j.bone.2013.12.005.
[14] N. Holguin, M.D. Brodt, M.E. Sanchez, M.J. Silva, Aging diminishes lamellar and woven bone formation induced by tibial compression in adult C57BL/6, Bone. 65 (2014) 83–91. doi:10.1016/j.bone.2014.05.006.
[15] B.M. Willie, A.I. Birkhold, H. Razi, T. Thiele, M. Aido, B. Kruck, A. Schill, S. Checa, R.P. Main, G.N. Duda, Diminished response to in vivo mechanical loading in trabecular and not cortical bone in adulthood of female C57Bl/6 mice coincides with a reduction in deformation to load, Bone. (2013). doi:10.1016/j.bone.2013.04.023.
[16] M.E. Lynch, R.P. Main, Q. Xu, T.L. Schmicker, M.B. Schaffler, T.M. Wright, M.C.H. van der Meulen, Tibial compression is anabolic in the adult mouse skeleton despite reduced responsiveness with aging, Bone. 49 (2011) 439–446. doi:10.1016/j.bone.2011.05.017.
[17] R.P. Main, M.E. Lynch, M.C.H. van der Meulen, Load-induced changes in bone stiffness and cancellous and cortical bone mass following tibial compression diminish with age in female mice., J. Exp. Biol. 217 (2014) 1775–83. doi:10.1242/jeb.085522.
[18] T. Sugiyama, L.K. Saxon, G. Zaman, A. Moustafa, A. Sunters, J.S. Price, L.E. Lanyon, Mechanical loading enhances the anabolic effects of intermittent parathyroid hormone (1-34) on trabecular and cortical bone in mice, Bone. 43 (2008) 238–248. doi:10.1016/j.bone.2008.04.012.
[19] K.M. Melville, N.H. Kelly, S. a Khan, J.C. Schimenti, F.P. Ross, R.P. Main, M.C. van der Meulen, Female mice lacking estrogen receptor-alpha in osteoblasts have compromised bone mass and strength, J Bone Min. Res. 29 (2014) 370–379. doi:10.1002/jbmr.2082.
[20] Y. Feng, D. Manka, K.-U. Wagner, S.A. Khan, Estrogen receptor-alpha expression in the mammary epithelium is required for ductal and alveolar morphogenesis in mice., Proc. Natl. Acad. Sci. U. S. A. 104 (2007) 14718–23. doi:10.1073/pnas.0706933104.
[21] T.L. Clemens, H. Tang, S. Maeda, R. a Kesterson, F. Demayo, J.W. Pike, C.M. Gundberg, Analysis of osteocalcin expression in transgenic mice reveals a species difference in vitamin D regulation of mouse and human osteocalcin genes., J. Bone Miner. Res. 12 (1997) 1570–6. doi:10.1359/jbmr.1997.12.10.1570.
[22] M. Zhang, S. Xuan, M.L. Bouxsein, D. Von Stechow, N. Akeno, M.C. Faugere, H. Malluche, G. Zhao, C.J. Rosen, A. Efstratiadis, T.L. Clemens, Osteoblast-specific knockout of the insulin-like growth factor (IGF) receptor gene reveals an essential role of IGF signaling in bone matrix mineralization, J. Biol. Chem.

277 (2002) 44005–44012. doi:10.1074/jbc.M208265200.
[23] J.C. Fritton, E.R. Myers, T.M. Wright, M.C.H. Van Der Meulen, Loading induces site-specific increases in mineral content assessed by microcomputed tomography of the mouse tibia, Bone. 36 (2005) 1030–1038. doi:10.1016/j.bone.2005.02.013.
[24] M.E. Lynch, R.P. Main, Q. Xu, D.J. Walsh, M.B. Schaffler, T.M. Wright, M.C.H. van der Meulen, Cancellous bone adaptation to tibial compression is not sex dependent in growing mice., J. Appl. Physiol. 109 (2010) 685–691. doi:10.1152/japplphysiol.00210.2010.
[25] L.B. Meakin, H. Todd, P.J. Delisser, G.L. Galea, A. Moustafa, L.E. Lanyon, S.H. Windahl, J.S. Price, Parathyroid hormone's enhancement of bones' osteogenic response to loading is affected by ageing in a dose- and time-dependent manner, Bone. 98 (2017) 59–67. doi:10.1016/j.bone.2017.02.009.
[26] T.L.N. Järvinen, P. Kannus, I. Pajamäki, T. Vuohelainen, J. Tuukkanen, M. Järvinen, H. Sievänen, Estrogen deposits extra mineral into bones of female rats in puberty, but simultaneously seems to suppress the responsiveness of female skeleton to mechanical loading, Bone. 32 (2003) 642–651. doi:10.1016/S8756-3282(03)00100-5.
[27] D.B. Jepsen, J. Ryg, S. Hansen, N.R. Jørgensen, J. Gram, T. Masud, The combined effect of Parathyroid hormone (1–34) and whole-body Vibration exercise in the treatment of postmenopausal OSteoporosis (PaVOS study): a randomized controlled trial, Osteoporos. Int. 30 (2019) 1827–1836. doi:10.1007/s00198-019-05029-z.

Chapter 7

CONCLUSIONS AND DISCUSSION

7.1 Summary

The objective of this research was to elucidate the relationships between impaired estrogen signaling, parathyroid hormone (PTH), and mechanical loading in skeletal health and how these relationships change with age. Mechanical loading is a potential anabolic therapy for osteoporosis, but its efficacy is altered by age, estrogen signaling via estrogen receptor alpha (ERα), and PTH treatment. Therefore, understanding how these factors interact is essential for developing effective treatments for patients with low bone mass. However, much of the previous work has been done *in vitro* or focused on cortical bone in young, healthy animals. We generated osteoblast-specific ERα knockout mice (pOC-ERαKO) to investigate how their skeletal phenotype and response to loading change with age, PTH treatment, and different loading modalities. We also examined human femoral neck samples from patients treated with an analog of PTH, teriparatide (TPTD), prior to undergoing a total hip replacement to compare bone formation under two different loading modalities. TPTD increased bone formation on the endocortical but not the periosteal surface, and may have been more effective in older, female, low body mass patients in regions under tension. Adult male pOC-ERαKO mice had similar bone mass and response to loading as controls, and retained their response to loading with age. Adult, female mice had greatly reduced responses to loading compared to young mice, and female pOC-ERαKO mice had reduced bone mass compared to their controls. PTH

treatment synergistically increased the response to loading in the short term, but pre-treatment prior to loading maintained the synergistic effects for longer durations and was more effective in cancellous bone. The effects of PTH alone and with loading were not different in pOC-ERαKO mice. Compression was more anabolic and more repsonsive to PTH than tension.

Aim 1

Global ERαKO mice have confounding systemic effects [1–5], and limited work has been done on the response to loading in cell-specific ERα knockout mice [6–9]. We have previously shown that young, 10-week-old female osteoblast-specific pOC-ERαKO mice have reduced bone mass and increased responses to loading compared to controls, and male pOC-ERαKO mice have increased bone mass and similar responses to loading as controls [6]. We hypothesized that these results would remain true for adult 26-week-old mice, and that adult mice would have reduced adaptation to loading compared to young mice. In 26-week-old females, pOC-ERαKO mice had lower cancellous and cortical bone mass at the tibial metaphysis and diaphysis compared to their controls. Adult female mice increased cortical bone mass similarly between genotypes at a moderate load magnitude, but pOC-ERαKO mice responded more than controls at high-magnitude loading. High-magnitude loading, however, was not sufficient to increase cancellous bone mass in either genotype, nor to rescue the robust anabolic response in young mice. Adult male pOC-ERαKO mice had similar tibial bone mass as their controls. Both genotypes had similar adaptation to loading at the cancellous metaphysis and cortical shell, but no adaptation at the

diaphysis. Adult male mice retained their adaptation to loading with age.

Aim 2

Clinically TPTD is used to treat osteoporosis, but most clinical data comes from dual-energy X-ray absorptiometry (DXA) scans with limited bone dynamic and structural data from iliac crest biopsies [10–14]. Changes in BMD measured by DXA do not fully capture changes in geometry and strength [15]; therefore, understanding structural changes and cellular activity in response to treatment is important for predicting skeletal fracture risk. Additionally, the effects of TPTD are site-specific [16,17], so the changes elicited at the iliac crest may not be representative of more clinically relevant fracture sites. We hypothesized that these site-specific differences are driven by differences in loading environment, specifically by differences in loading modality. Femoral neck samples were obtained from patients receiving total hip replacements. Pateints were treated with TPTD prior to surgery and given fluorescent labels for new bone formation. The samples were analyzed for static and dynamic bone formation indices on the tensile and compressive surfaces of the femoral neck, and regression models were created using patient-specific data. TPTD increased bone formation on the endocortical but not the periosteal surface. Formation was greater on the tensile endocortical surface and compressive periosteal surface, regardless of treatment. Regresssion models indicated that TPTD was more effective in older patients, female patients particularly on the tensile surface, and patients with lower body mass.

Aim 3

The results from Aim 2 suggested that loading modality may influence the response to TPTD, but the low sample size and large patient variability made strong conclusions difficult. To reduce variability and control for treatment duration and loading, we moved to a preclinical mouse model. Due to the curvature of the murine tibia, compression of the hindlimb causes bending at the tibial midshaft, placing the anterior surface under tension and the posterior surface under compression [18]. We assessed the role of loading modality on the response to PTH in a low bone mass environment using cyclic tibial loading in female pOC-ERαKO mice and their littermate controls. We also investigated whether pre-treating mice with PTH prior to mechanical loading could prime the bone tissue and further increase the anabolic effects. We hypothesized that tension would increase the effects of PTH more than compression, the response would be altered in pOC-ERαKO mice, and pre-treating mice with PTH would enhance bone formation. 10- and 16-week-old female pOC-ERαKO and LC mice were concurrently loaded at -7.9N and treated with VEH or PTH for 2 or 6 weeks. Wild-type C57Bl/6J female mice (WT) were pre-treated with VEH or PTH for 6 weeks starting at 10 weeks of age, then loaded for 2 or 6 weeks at -8.7N or -10.6N for VEH and PTH pre-treated mice, respectively. PTH was more anabolic under applied compression than tension in 16-week-old pOC-ERαKO and LC mice loaded for 2 weeks. PTH synergistically increased the anabolic effects of loading after two weeks, but 6 weeks of concurrent loading increased bone mass similarly with or without PTH treatment. PTH pre-treatment prior to loading, however, extended the synergistic effect out to 6 weeks. The response to PTH and loading was not different

between pOC-ERαKO and LC mice.

Aim 4

Bone's ability to adapt to mechanical loading decreases with age, particularly in cancellous bone [19–22]. Because many osteoporosis-related fractures occur at corticocancellous sites [23,24], overcoming this loss of adaptation would allow older patients with osteoporosis to use exercise or physical therapy regimens as a viable treatment option. We hypothesized that combining PTH treatment with tibial mechanical loading would improve the mechanoresponsiveness enough to overcome the loss of adaptation, and pre-treating with PTH prior to loading would further increase cancellous responsiveness. 10- and 16-week-old pOC-ERαKO and LC mice were concurrently treated with PTH or VEH and loaded at -7.9N for 2 or 6 weeks. 10-week-old C57Bl/6J female mice were pre-treated with PTH or VEH for 6 weeks then loaded for 2 or 6 weeks at -8.7N or -10.6N, respectively. PTH decreased the cancellous response to loading after 6 weeks in 16-week-old mice, but pre-treatment increased the loading response. PTH increased the cortical loading response at the metaphysis and diaphysis after 2 weeks, and this effect was augmented by pre-treatment. The response to PTH was not different in pOC-ERαKO mice.

The effects of PTH and tibial loading were remarkably consistent when comparing across studies, further strengthening our results. PTH was more anabolic in cortical than cancellous bone in pOC-ERαKO, LC, and WT mice. Combined PTH and loading was detrimental in cancellous bone but synergistic in cortical bone for all three

genotypes, and pre-treatment rescued the cancellous and prolonged the cortical response. Additionally, applied compression was more anabolic than applied tension acrosss all genotypes, and loading did not increase bone mass in the neutral region. However, our preclinical loading modality data conflict with our clinical femoral neck data, which predicted that the tensile femoral neck surface in females was more responsive to TPTD than the compressive surface. A number of factors could have caused these differences, aside from differences in species. The clinical samples were not subjected to additional external loading and likely experienced reduced daily loading due to the presence of osteoarthritis, which may have obscured the differences between the loading modalities. Additionally, there were no baseline, non-treated controls for these patients. Longitudinal data before and after TPTD treatment from each patient was not feasible in this study design. Comparing TPTD-treated patients to PBO-treated patients introduces more variability than comparing across treatment groups using inbred mouse strains. In our preclinical model, mechanical strains in the region of applied compression may have been higher than those in the region of applied tension, which would have overestimated the compression effect. Further investigation both clinically and in a controlled preclinical setting should be pursued to fully determine the role of loading modality on PTH.

7.2 Strengths

A major strength of this work was the unique clinical data from the high fracture risk femoral neck site. Most clinical data on the effects of PTH at clinically relevant fracture sites such as the spine, hip, and radius come from dual-energy X-ray

absorptiometry (DXA) scans, which only report on the amount of bone present [10–12]. DXA scans do not provide any information about the structure of bone tissue, or about the cellular responses to treatment. For that information, biopsies are taken from the iliac crest [13,14]. However, the iliac crest is not a load-bearing site and may not be representative of other locations. Our data were the first to provide dynamic histomorphometric and structural information on the effects of PTH at a clinically-relevant fracture site in humans, with the added benefit of analyzing the effects of two different loading modalities.

We also had the unique advantage of using these clinical data to inform a preclinical study further investigating the mechanisms behind the results. Our murine tibial loading model applied repeatable, controlled mechanical loading, and allowed the comparison of regions of tension and compression in the same location within the same animal. Combining clinically relevant human data with preclinical data that provided greater experimental control is a key advantage of this work.

The use of a conditional ERα knockout mouse model was an important strength of this work. Other methods of impairing or eliminating estrogen signaling, including global knockout mice and ovariectomy, introduce confounding off-target effects. Global ERα deletion results in increased bone mass, and OVX involves major surgery and confounding body mass changes [1–3,25]. Targeted deletion of ERα in the pOC-ERαKO mice allowed us to isolate the effects of estrogen signaling on mature osteoblasts and osteocytes. Additionally, adult 26-week-old mice are more clinically relevant to patients with osteoporosis than growing 10-week-old mice. At 26 weeks of age, mice were no longer undergoing modeling-based growth, and females exhibited

age-related decreases in bone mass and adaptation that more closely mimic those of postmenopausal women. Furthermore, most work on the role of ERα in response to mechanical loading has been done *in vitro* [26–29]. Limited work has been done *in vivo*, much of which used global ERα knockout mice [3–5]. Few cell-specific ERα knockout loading studies have been performed, and mostly included young animals [6–9]. The use of an adult cell-specific ERα knockout mouse provided a more clinically-relevant low bone mass model with which to study the skeletal response to mechanical loading with aging.

Another advantage of this work was the use of a low bone mass model to study the relationship between PTH and mechanical loading. Although the effects of PTH alone have been studied extensively in OVX animals [30–32], most studies examining the combination of PTH and loading focus on healthy bone mass models [33–36]. PTH treatment is targeted toward individuals with very low bone mass, therefore it is important to understand whether adding mechanical loading would be beneficial for these patients as well. We were able to demonstrate that 10- and 16-week-old female low bone mass pOC-ERαKO mice responded as well as normal bone mass controls to PTH and tibial loading.

7.3 Limitations

Although our unique clinical data provided valuable information about the clinical effects of PTH, the study had some limitations. The treatment duration for most patients was between 4-8 weeks and may have underestimated the PTH effects. In fact, in clinical trials BMD increases in the femoral neck are greater during the last

6 months of a 2-year treatment course [10,37], but in our study the surgeries could not be delayed for ethical reasons. Additionally, these patients presented with severe hip osteoarthritis (OA) and not osteoporosis. The presence of OA at the joint may have altered the periosteal environment and obscured the effects of PTH on the periosteal surface [38]. These patients were also likely in enough pain to limit their daily activity, and the reduced overall mechanical loading may have limited the differential effects of loading modality.

Our pOC-ERαKO mice also have some disadvantages. Unlike in postmenopausal osteoporosis, estrogen signaling in these mice is impaired from birth. Lifelong disruption of estrogen signaling may have altered bone structure and mass during growth and development that influenced their skeletal responses later in life. One way to avoid this is through inducible knockout mice. Tamoxifen-induced knockouts only produce cre recombinase in promoter-specific cells when tamoxifen is administered, allowing gene deletion during specific timeframes [39]. Inducible, osteoblast specific ERα knockout mice would allow for disrupted estrogen signaling in adulthood following normal growth. Tamoxifen-induced osteocalcin-cre [40] and col1a1-cre [41] mice already exist, and may be used to create inducible ERα knockout mice.

Although our conditional knockout mice avoid the confounding systemic effects of global knockouts, ERα deletion was limited to mature osteoblasts and osteocytes. In postmenopausal women, impaired estrogen signaling is systemic. ERα in osteoclast lineages has also been shown to influence bone mass [42–44]. The creation of a mouse model with ERα deleted from multiple bone cells would allow the

investigation of impaired estrogen signaling in bone tissue without confounding effects from OVX surgery. Crossing mice with cre recombinase expressed under an osteoblast-lineage promoter, such as osteocalcin, and an osteoclast-lineage promoter, such as LysM or cathepsin K, would allow ERα to be deleted from both cell types.

Our studies involving PTH treatment and tibial loading investigated the effect of age on the anabolic responses, but the oldest mice from those studies were only 16-weeks old at the start of loading. Even though mice are considered skeletally mature at 16 weeks, they are still relatively young. The response to PTH and loading is greatly altered in aged, 19-month-old mice, with PTH blunting the cancellous loading response and not affecting the cortical loading response [35]. Our findings that PTH and loading are more effective under compression and still effective in low bone mass pOC-ERαKO mice should be evaluated in aged mice to see if they remain true with advanced age.

The tibial loading regimen used in this work has been shown to be anabolic in cancellous and cortical bone at multiple ages [21,22,45,46]. However, in *Chapter 6* cancellous bone mass decreased with loading in 16-week-old female LC mice and loading in *Chapters 5* and *6* resulted in limited cortical bone mass increases. Loading regimens with longer rest insertions and fewer cycles per day have decreased cancellous bone mass in mice [47]. Previously, we have chosen load magnitudes that induce +1200με at the tibial midshaft, but those magnitudes have caused woven bone to form at the mid-diaphysis [6]. Here, we chose magnitudes to induce +1000με at the midshaft to avoid woven bone and allow for the analysis of the modality regions at the mid-diaphysis, which may have reduced the osteogenic capacity of our loading

regimen. Future work focusing on cancellous bone may require applying higher load magnitudes, and lower load magnitudes should only be used for diaphyseal analyses.

7.4 Future Work

The results of this work suggest several future investigations. The mechanisms involved in the tissue-level changes in response to mechanical loading and PTH treatment in this work should be explored further. Age-related changes in mechanoadaptation and the effects of PTH should be investigated to better understand their roles in a clinically-relevant population. Differences in cellular responses under tension and compression would identify new treatment targets for maximizing bone growth. Additionally, translation of this work to a clinical setting would directly benefit patients and increase our knowledge of the effects of loading and PTH in humans.

Retaining adaptation with age

The loss of adaptation to loading with age limits the viability of a simple, low-cost therapy option for older patients with low bone mass. In *Aim 1*, 26-week-old male mice retained their adaptation to loading but females did not. Investigation into the differences in response to loading in adult male and female mice may provide new therapeutic targets to prevent loss of adaptation and increase bone mass in adults. Transcriptional responses to mechanical loading in female mice measured by RNA sequencing vary by tissue envelope and age [48]. Comparing the age-related changes in transcriptional response to loading in males and females may reveal pathways that

change in females with age but not males. These pathways may provide new targets for therapeutics. By restoring expression of these pathways to the level of young females, or augmenting their expression in males, bone mass and adaptation may be increased in adults.

Confirming and expanding loading modality knowledge

Cyclic compressive loading of the mouse hindlimb produces bending at the tibial midshaft, with regions of compression and tension on the posterior and anterior surfaces, respectively [18]. In *Aim 3*, we determined the regions of compression and tension from the principal axes of the 3D volume of interest at the midshaft, but those axes may not correspond to those for the whole tibia. Although re-analyzing the data using modality regions determined from anatomical alignment of the tibia did not significantly change the results (Appendix A), finite element models would allow more accurate determination of these regions based on whole bone mechanics. Additionally, finite element models would provide strain magnitude data for each region. Regional changes in bone mass could be correlated to local strain magnitudes to determine whether the increased loading response on the posterior surface was due to loading modality or strain magnitude differences. Using finite element models, cancellous bone could also be analyzed by loading modality. Comparisons between trabeculae under tension and compression could reveal whether loading modality influences the response to PTH in cancellous bone.

Our tibial loading model applies compression and tension to regions that experience those modalities during daily activity. Ideally, reversing the loading so that

tension was applied to the posterior region and compression was applied to the anterior region would confirm that the differences in response were due to loading modality and not location. Because the modality regions are an effect of the curvature of the tibia, reversing the modalities is not possible with our current loading model. An alternative could be to use tibial bending. Four-point bending in the mouse tibia produces tension on the medial surface and compression on the lateral surface [49]. Four-point bending may be modified to reverse the loading by moving the points of contact. Preliminary studies would need to be done to ensure the posterolateral location of the fibula does not impede loading in the new configuration. However, even if the loading cannot be reversed, applying compression and tension to new locations not acclimated to those modalities would help confirm that the anabolic effects were due to modality and not location.

Cellular mechanisms of loading modality effects on PTH response

Future work on the differential anabolic responses to PTH under compression and tension should investigate the mechanisms behind these responses. Performing RNA sequencing analysis on the tensile and compressive regions of the tibial midshaft separately may uncover pathways that are differentially regulated between the two loading modalities. Consistently isolating the small modality regions for RNA sequencing may be challenging, so an alternative would be *in situ* hybridization (ISH) or immunohistochemistry (IHC) analyses in the separate modality regions. However, unlike the unbiased analysis of the entire transcriptome in RNA sequencing, ISH and IHC require the preselection of a few transcripts or proteins of interest to measure.

Calcium channels have been shown to be important in the skeletal response to both PTH and mechanical loading [50,51]. Genetically modified mice with osteocyte-specific fluorescent calcium indicators have been used to study *in vivo* calcium signaling in response to three-point bending of the metatarsal in mice [52]. Adjusting the loading system to apply four-point bending that could be reversed would allow imaging of calcium signaling under both tension and compression. The use of calcium channel blockers could confirm that calcium signaling is important in the synergistic effect of loading and PTH, and whether compression and tension elicit differences in the magnitude or number of cells responding.

Clinical evaluation of loading modality effects on PTH response

The ultimate goal of this research is to translate our findings into improved osteoporosis treatments in a clinical setting. Our unique clinical data on the effects of PTH in the femoral neck provided new insights into the structural and cellular changes in a clinically relevant fracture site in humans. However, no external loading was applied to these patients, and the amount of daily loading may have varied widely between them. Therefore, future work should focus on the effects of PTH with applied loading. Whole body vibration combined with PTH treatment increased lumbar spine BMD more than PTH alone in postmenopausal women with osteoporosis [53], but it is still unclear whether the response to PTH will be different by loading modality in humans. Musculoskeletal finite element models of various activities show that exercises such as hopping and brisk walking or jogging increase both compressive and tensile strains on the superior and inferior regions of the femoral neck compared to

baseline walking [54,55]. Clinical studies of patients receiving PTH and undergoing different exercises designed to induce more compression or more tension may help determine whether PTH efficacy is influenced by loading modality in humans.

One limitation of PTH is its lack of effectiveness in the radius, which is non-load bearing. Applied loading of the radius may overcome this limitation. Recently, an anabolic *in vivo* cyclic loading model of the human radius was developed that involved patients pressing down on a force plate to achieve target force magnitudes and loading rates [56,57]. This loading model produces dorso-medial bending of the radius, with the dorsal side under compression [56]. Combining this loading regimen with PTH treatment will determine whether applied loading can overcome the deficiency of PTH at the radius and how loading modality affects the response to PTH in a clinically relevant fracture site.

7.5 Conclusions

In conclusion, we identified sex-based differences in mechanoadaptation changes with age that may identify new targets to increasing adaptation in older populations. We provided the first dynamic and structural data on the effects of PTH at a clinically relevant fracture site in humans, and identified regional differences based on experienced loading modality. We identified two methods to augment the effects of PTH and mechanical loading: the use of compression rather than tension, and pre-treating with PTH prior to initiating loading. These methods can be directly applied to clinical settings to benefit patients with osteoporosis.

7.6 References

[1] M.K. Lindberg, S.L. Alatalo, J.M. Halleen, S. Mohan, J.-Å. Gustafsson, C. Ohlsson, Estrogen receptor specificity in the regulation of the skeleton in female mice, J. Endocrinol. 171 (2001) 229–236.

[2] V. Parikka, Z. Peng, T. Hentunen, J. Risteli, T. Elo, H.K. Väänänen, P. Härkönen, Estrogen responsiveness of bone formation in vitro and altered bone phenotype in aged estrogen receptor-α-deficient male and female mice, Eur. J. Endocrinol. 152 (2005) 301–314. doi:10.1530/eje.1.01832.

[3] L.K. Saxon, G. Galea, L. Meakin, J. Price, L.E. Lanyon, Estrogen receptors α and β have different gender-dependent effects on the adaptive responses to load bearing in cancellous and cortical bone, Endocrinology. 153 (2012) 2254–2266. doi:10.1210/en.2011-1977.

[4] K.C.L. Lee, H. Jessop, R. Suswillo, G. Zaman, L.E. Lanyon, The adaptive response of bone to mechanical loading in female transgenic mice is deficient in the absence of oestrogen receptor-alpha and -beta., J. Endocrinol. 182 (2004) 193–201. doi:15283680.

[5] K. Lee, H. Jessop, R. Suswillo, G. Zaman, L. Lanyon, Bone adaptation requires oestrogen receptor-alpha, Nature. 424 (2003) 389.

[6] K.M. Melville, N.H. Kelly, G. Surita, D.B. Buchalter, J.C. Schimenti, R.P. Main, F.P. Ross, M.C.H. Van Der Meulen, Effects of Deletion of ERα in Osteoblast-Lineage Cells on Bone Mass and Adaptation to Mechanical Loading Differ in Female and Male Mice, J. Bone Miner. Res. 30 (2015) 1468–1480. doi:10.1002/jbmr.2488.

[7] N.H. Kelly, J.C. Schimenti, F.P. Ross, M.C.H. van der Meulen, Female mice lacking estrogen receptor alpha in mature osteoblasts have an increased transcriptional response to mechanical loading in cancellous but not cortical bone, Trans Orthop Res Soc. 42 (2017) 776.

[8] S. Kondoh, K. Inoue, K. Igarashi, H. Sugizaki, Y. Shirode-Fukuda, E. Inoue, T. Yu, J.K. Takeuchi, J. Kanno, L.F. Bonewald, Y. Imai, Estrogen receptor α in osteocytes regulates trabecular bone formation in female mice, Bone. 60 (2014) 68–77. doi:10.1016/j.bone.2013.12.005.

[9] S.H. Windahl, A.E. Börjesson, H.H. Farman, C. Engdahl, S. Movérare-Skrtic, K. Sjögren, M.K. Lagerquist, J.M. Kindblom, A. Koskela, J. Tuukkanen, P. Divieti Pajevic, J.Q. Feng, K. Dahlman-Wright, P. Antonson, J.-Å. Gustafsson, C. Ohlsson, Estrogen receptor-α in osteocytes is important for trabecular bone formation in male mice., Proc. Natl. Acad. Sci. U. S. A. 110 (2013) 2294–9. doi:10.1073/pnas.1220811110.

[10] B.Z. Leder, J.N. Tsai, A. V. Uihlein, S.A.M. Burnett-Bowie, Y. Zhu, K. Foley, H. Lee, R.M. Neer, Two years of denosumab and teriparatide administration in postmenopausal women with osteoporosis (The DATA Extension Study): A randomized controlled trial, J. Clin. Endocrinol. Metab. 99 (2014) 1694–1700. doi:10.1210/jc.2013-4440.

[11] H.K. Genant, K. Engelke, M.A. Bolognese, C. Mautalen, J.P. Brown, C. Recknor, S. Goemaere, T. Fuerst, Y.C. Yang, A. Grauer, C. Libanati, Effects of Romosozumab Compared With Teriparatide on Bone Density and Mass at the

Spine and Hip in Postmenopausal Women With Low Bone Mass, J. Bone Miner. Res. 32 (2017) 181–187. doi:10.1002/jbmr.2932.
[12] H. Minne, M. Audran, M.E. Simões, B. Obermayer-Pietsch, G. Sigurdsson, F. Marín, G.P. Dalsky, T. Nickelsen, Bone density after teriparatide in patients with or without prior antiresorptive treatment: One-year results from the EUROFORS study, Curr. Med. Res. Opin. 24 (2008) 3117–3128. doi:10.1185/03007990802466595.
[13] R. Lindsay, H. Zhou, F. Cosman, J. Nieves, D.W. Dempster, A.B. Hodsman, Effects Of a One-Month Treatment With PTH(1-34) on Bone Formation on Cancellous, Endocortical, and Periosteal Surfaces of the Human Ilium, J. Bone Miner. Res. 22 (2007) 495–502. doi:10.1359/jbmr.070104.
[14] D.W. Dempster, H. Zhou, V.A. Ruff, T.E. Melby, J. Alam, K.A. Taylor, Longitudinal Effects of Teriparatide or Zoledronic Acid on Bone Modeling- and Remodeling-Based Formation in the SHOTZ Study, J. Bone Miner. Res. 33 (2018) 627–633. doi:10.1002/jbmr.3350.
[15] S.J. Warden, S.M. Mantila Roosa, M.E. Kersh, A.L. Hurd, G.S. Fleisig, M.G. Pandy, R.K. Fuchs, Physical activity when young provides lifelong benefits to cortical bone size and strength in men, Proc. Natl. Acad. Sci. U. S. A. 111 (2014) 5337–5342. doi:10.1073/pnas.1321605111.
[16] A. Iida-Klein, H. Zhou, S.S. Lu, L.R. Levine, M. Ducayen-Knowles, D.W. Dempster, J. Nieves, R. Lindsay, Anabolic action of parathyroid hormone is skeletal site specific at the tissue and cellular levels in mice, J. Bone Miner. Res. 17 (2002) 808–816. doi:10.1359/jbmr.2002.17.5.808.
[17] F. Cosman, Anabolic and Antiresorptive Therapy for Osteoporosis : Combination and Sequential Approaches, Curr. Osteoporos. Rep. (2014) 385–395. doi:10.1007/s11914-014-0237-9.
[18] T.K. Patel, M.D. Brodt, M.J. Silva, Experimental and finite element analysis of strains induced by axial tibial compression in young-adult and old female C57Bl/6 mice, J. Biomech. 47 (2014). doi:10.1016/j.jbiomech.2013.10.052.
[19] N. Holguin, M.D. Brodt, M.E. Sanchez, M.J. Silva, Aging diminishes lamellar and woven bone formation induced by tibial compression in adult C57BL/6, Bone. 65 (2014) 83–91. doi:10.1016/j.bone.2014.05.006.
[20] B.M. Willie, A.I. Birkhold, H. Razi, T. Thiele, M. Aido, B. Kruck, A. Schill, S. Checa, R.P. Main, G.N. Duda, Diminished response to in vivo mechanical loading in trabecular and not cortical bone in adulthood of female C57Bl/6 mice coincides with a reduction in deformation to load, Bone. (2013). doi:10.1016/j.bone.2013.04.023.
[21] M.E. Lynch, R.P. Main, Q. Xu, T.L. Schmicker, M.B. Schaffler, T.M. Wright, M.C.H. van der Meulen, Tibial compression is anabolic in the adult mouse skeleton despite reduced responsiveness with aging, Bone. 49 (2011) 439–446. doi:10.1016/j.bone.2011.05.017.
[22] R.P. Main, M.E. Lynch, M.C.H. van der Meulen, Load-induced changes in bone stiffness and cancellous and cortical bone mass following tibial compression diminish with age in female mice., J. Exp. Biol. 217 (2014) 1775–83. doi:10.1242/jeb.085522.
[23] B.L. Riggs, Endocrine causes of age-related bone loss and osteoporosis,

Novartis Found. Symp. 242 (2002) 247–264.
[24] O. of the S.G. U.S. Department of Health and Human Services, ed., Bone Health and Osteoporosis A Report of the Surgeon General, Rockville, MD, 2004.
[25] C.C. Danielsen, L. Mosekilde, B. Svenstrup, Cortical bone mass, composition, and mechanical properties in female rats in relation to age, long-term ovariectomy, and estrogen substitution, Calcif. Tissue Int. 52 (1993) 26–33. doi:10.1007/BF00675623.
[26] E. Damien, J.S. Price, L.E. Lanyon, Mechanical strain stimulates osteoblast proliferation through the estrogen receptor in males as well as females., J. Bone Miner. Res. 15 (2000) 2169–2177. doi:10.1359/jbmr.2000.15.11.2169.
[27] E. Damien, J.S. Price, L.E. Lanyon, The estrogen receptor's involvement in osteoblasts' adaptive response to mechanical strain., J. Bone Miner. Res. 13 (1998) 1275–1282. doi:10.1359/jbmr.1998.13.8.1275.
[28] V.J. Armstrong, M. Muzylak, A. Sunters, G. Zaman, L.K. Saxon, J.S. Price, L.E. Lanyon, Wnt/β-catenin signaling is a component of osteoblastic bone cell early responses to load-bearing and requires estrogen receptor α, J. Biol. Chem. 282 (2007) 20715–20727. doi:10.1074/jbc.M703224200.
[29] G.L. Galea, L.B. Meakin, T. Sugiyama, N. Zebda, A. Sunters, H. Taipaleenmaki, G.S. Stein, A.J. Van Wijnen, L.E. Lanyon, J.S. Price, Estrogen receptor α mediates proliferation of osteoblastic cells stimulated by estrogen and mechanical strain, but their acute down-regulation of the Wnt antagonist Sost is mediated by estrogen receptor β, J. Biol. Chem. 288 (2013) 9035–9048. doi:10.1074/jbc.M112.405456.
[30] N. Andersson, M.K. Lindberg, C. Ohlsson, K. Andersson, B. Ryberg, Repeated in vivo determinations of bone mineral density during parathyroid hormone treatment in ovariectomized mice, J. Endocrinol. 170 (2001) 529–537. doi:10.1677/joe.0.1700529.
[31] A. Takakura, J.W. Lee, K. Hirano, Y. Isogai, T. Ishizuya, R. Takao-Kawabata, T. Iimura, Administration frequency as well as dosage of PTH are associated with development of cortical porosity in ovariectomized rats, Bone Res. 5 (2017). doi:10.1038/boneres.2017.2.
[32] C. Vrahnas, P.R. Buenzli, T.A. Pearson, B.L. Pennypacker, M.J. Tobin, K.R. Bambery, L.T. Duong, N.A. Sims, Differing Effects of Parathyroid Hormone , Alendronate , and Odanacatib on Bone Formation and on the Mineralization Process in Intracortical and Endocortical Bone of Ovariectomized Rabbits, Calcif. Tissue Int. 103 (2018) 625–637. doi:10.1007/s00223-018-0455-8.
[33] H. Hagino, T. Okano, M.P. Akhter, M. Enokida, R. Teshima, Effect of parathyroid hormone on cortical bone response to in vivo external loading of the rat tibia, J. Bone Miner. Metab. 19 (2001) 244–250. doi:10.1007/s007740170027.
[34] T. Sugiyama, L.K. Saxon, G. Zaman, A. Moustafa, A. Sunters, J.S. Price, L.E. Lanyon, Mechanical loading enhances the anabolic effects of intermittent parathyroid hormone (1-34) on trabecular and cortical bone in mice, Bone. 43 (2008) 238–248. doi:10.1016/j.bone.2008.04.012.
[35] L.B. Meakin, H. Todd, P.J. Delisser, G.L. Galea, A. Moustafa, L.E. Lanyon,

S.H. Windahl, J.S. Price, Parathyroid hormone's enhancement of bones' osteogenic response to loading is affected by ageing in a dose- and time-dependent manner, Bone. 98 (2017) 59–67. doi:10.1016/j.bone.2017.02.009.
[36] C.H. Kim, E. Takai, H. Zhou, D. von Stechow, R. Müller, D.W. Dempster, X.E. Guo, Trabecular bone response to mechanical and parathyroid hormone stimulation: the role of mechanical microenvironment, J. Bone Miner. Res. 18 (2003) 2116–2125. doi:10.1359/jbmr.2003.18.12.2116.
[37] B.M. Obermayer-Pietsch, F. Marin, E. V. McCloskey, P. Hadji, J. Farrerons, S. Boonen, M. Audran, C. Barker, A.D. Anastasilakis, W.D. Fraser, T. Nickelsen, Effects of two years of daily teriparatide treatment on BMD in postmenopausal women with severe osteoporosis with and without prior antiresorptive treatment, J. Bone Miner. Res. 23 (2008) 1591–1600. doi:10.1359/jbmr.080506.
[38] G.R. Jordan, N. Loveridge, J. Power, M.T. Clarke, J. Reeve, Increased cancellous bone in the femoral neck of patients with coxarthrosis (hip osteoarthritis): a positive remodeling imbalance favoring bone formation, Osteoporos. Int. 14 (2003) 160–165. doi:10.1007/s00198-002-1351-6.
[39] S. Feil, N. Valtcheva, R. Feil, Inducible Cre Mice, in: W. Wurst, R. Kühn (Eds.), Gene Knockout Protoc. Second Ed., Humana Press, Totowa, NJ, 2009: pp. 343–363. doi:10.1007/978-1-59745-471-1_18.
[40] Y. Yoshikawa, A. Kode, L. Xu, I. Mosialou, B.C. Silva, M. Ferron, T.L. Clemens, A.N. Economides, S. Kousteni, Genetic evidence points to an osteocalcin-independent influence of osteoblasts on energy metabolism, J. Bone Miner. Res. 26 (2011) 2012–2025. doi:10.1002/jbmr.417.
[41] J.E. Kim, K. Nakashima, B. De Crombrugghe, Transgenic mice expressing a ligand-inducible cre recombinase in osteoblasts and odontoblasts: A new tool to examine physiology and disease of postnatal bone and tooth, Am. J. Pathol. 165 (2004) 1875–1882. doi:10.1016/S0002-9440(10)63240-3.
[42] M. Martin-Millan, M. Almeida, E. Ambrogini, L. Han, H. Zhao, R.S. Weinstein, R.L. Jilka, C. a O'Brien, S.C. Manolagas, The estrogen receptor-alpha in osteoclasts mediates the protective effects of estrogens on cancellous but not cortical bone., Mol. Endocrinol. 24 (2010) 323–34. doi:10.1210/me.2009-0354.
[43] T. Nakamura, Y. Imai, T. Matsumoto, S. Sato, K. Takeuchi, K. Igarashi, Y. Harada, Y. Azuma, A. Krust, Y. Yamamoto, H. Nishina, S. Takeda, H. Takayanagi, D. Metzger, J. Kanno, K. Takaoka, T.J. Martin, P. Chambon, S. Kato, Estrogen Prevents Bone Loss via Estrogen Receptor α and Induction of Fas Ligand in Osteoclasts, Cell. 130 (2007) 811–823. doi:10.1016/j.cell.2007.07.025.
[44] A.M. Rooney, M.C.H. van der Meulen, Mouse models to evaluate the role of estrogen receptor α in skeletal maintenance and adaptation, Ann. N. Y. Acad. Sci. 1410 (2017) 85–92. doi:10.1111/nyas.13523.
[45] J.C. Fritton, E.R. Myers, T.M. Wright, M.C. van der Meulen, Bone Mass Is Preserved and Cancellous Architecture Altered Due to Cyclic Loading of the Mouse Tibia After Orchidectomy, J. Bone Miner. Res. 23 (2008) 663–671. doi:10.1359/jbmr.080104.
[46] M.E. Lynch, R.P. Main, Q. Xu, D.J. Walsh, M.B. Schaffler, T.M. Wright,

M.C.H. van der Meulen, Cancellous bone adaptation to tibial compression is not sex dependent in growing mice., J. Appl. Physiol. 109 (2010) 685–691. doi:10.1152/japplphysiol.00210.2010.
[47] N. Holguin, M.D. Brodt, M.E. Sanchez, A.A. Kotiya, M.J. Silva, Adaptation of tibial structure and strength to axial compression depends on loading history in Both C57BL/6 and BALB/c mice, Calcif. Tissue Int. 93 (2013) 211–221. doi:10.1007/s00223-013-9744-4.
[48] N.H. Kelly, J.C. Schimenti, F.P. Ross, M.C.H. van der Meulen, Transcriptional profiling of cortical versus cancellous bone from mechanically-loaded murine tibiae reveals differential gene expression, Bone. 86 (2016) 22–29. doi:10.1016/j.bone.2016.02.007.
[49] S.J. Kuruvilla, S.D. Fox, D.M. Cullen, M.P. Akhter, Site specific bone adaptation response to mechanical loading, J. Musculoskelet. Neuronal Interact. 8 (2008) 71–78.
[50] A. Miyauchi, K. Notoya, Y. Mikuni-Takagaki, Y. Takagi, M. Goto, Y. Miki, T. Takano-Yamamoto, K. Jinnai, K. Takahashi, M. Kumegawa, K. Chihara, T. Fujita, Parathyroid hormone-activated volume-sensitive calcium influx pathways in mechanically loaded osteocytes, J. Biol. Chem. 275 (2000) 3335–3342. doi:10.1074/jbc.275.5.3335.
[51] J. Li, R.L. Duncan, D.B. Burr, V.H. Gattone, C.H. Turner, Parathyroid hormone enhances mechanically induced bone formation, possibly involving L-type voltage-sensitive calcium channels, Endocrinology. 144 (2003) 1226–1233. doi:10.1210/en.2002-220821.
[52] K.J. Lewis, D. Frikha-Benayed, J. Louie, S. Stephen, D.C. Spray, M.M. Thi, Z. Seref-Ferlengez, R.J. Majeska, S. Weinbaum, M.B. Schaffler, Osteocyte calcium signals encode strain magnitude and loading frequency in vivo, Proc. Natl. Acad. Sci. 114 (2017). doi:10.1073/pnas.1707863114.
[53] D.B. Jepsen, J. Ryg, S. Hansen, N.R. Jørgensen, J. Gram, T. Masud, The combined effect of Parathyroid hormone (1–34) and whole-body Vibration exercise in the treatment of postmenopausal OSteoporosis (PaVOS study): a randomized controlled trial, Osteoporos. Int. 30 (2019) 1827–1836. doi:10.1007/s00198-019-05029-z.
[54] P. Pellikaan, G. Giarmatzis, J. Vander Sloten, S. Verschueren, I. Jonkers, Ranking of osteogenic potential of physical exercises in postmenopausal women based on femoral neck strains, PLoS One. 13 (2018) 1–18. doi:10.1371/journal.pone.0195463.
[55] S. Martelli, M.E. Kersh, A.G. Schache, M.G. Pandy, Strain energy in the femoral neck during exercise, J. Biomech. 47 (2014) 1784–1791. doi:10.1016/j.jbiomech.2014.03.036.
[56] K.L. Troy, W.B. Edwards, V.A. Bhatia, M. Lou Bareither, In vivo loading model to examine bone adaptation in humans: A pilot study, J. Orthop. Res. 31 (2013) 1406–1413. doi:10.1002/jor.22388.
[57] K.L. Troy, M.E. Mancuso, J.E. Johnson, Z. Wu, T.J. Schnitzer, T.A. Butler, Bone adaptation in adult women is related to loading dose: A 12-month randomized controlled trial., J. Bone Miner. Res. 00 (2020) 1–13. doi:10.1002/jbmr.3999.

Appendix A

MODALITY REGIONS BASED ON ANATOMIC ALIGNMENT

To reduce inconsistencies or biases introduced by determining the modality regions from the principal axes of the 3D volume of interest, we also analyzed the data by determining the regions based on anatomic alignment of the tibia. Scanco microCT analyses for the mouse tibial midshaft include code that aligns the tibia based on the locations of the tibiofibular junction (TFJ), fibular blood vessel, and center of the marrow cavity. The alignment places the anterior portion of the tibia in the bottom right of the image for left limbs, and the bottom left for right limbs (Fig A.1). Therefore, we assigned the tensile region to be the corresponding 90° from the centroid, the compressive region to be the opposite 90°, and the neutral region to be 45° in the two adjacent corners (Fig A.1). We recalculated cortical area (Ct.Ar) and

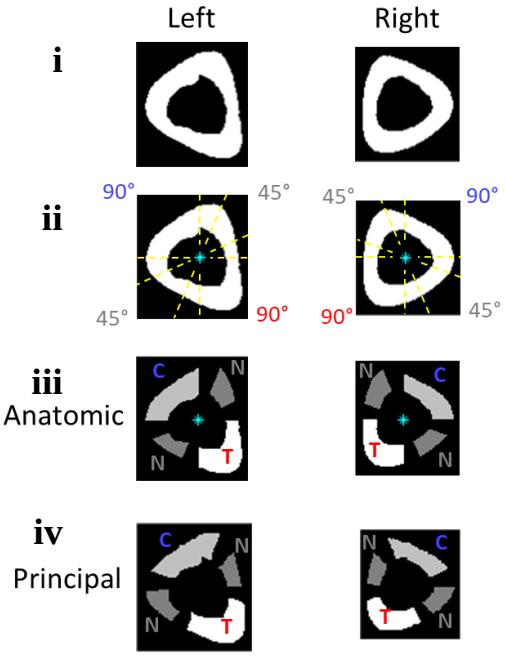

Figure A.1 Comparison of the anatomic alignment and principal axis analyses. i) Representative left and right limb midshaft cross sections. ii) For the anatomic alignment analysis, the tensile and compressive regions were defined as the bottom right and top left 90° corners (left limbs), respectively, and the bottom left and top right 90° corners (right limbs). The neutral regions were defined as the adjacent 45° corners. iii) The resulting modality regions based on the anatomic alignment. iv) The resulting modality regions based on the principal axes.

thickness (Ct.Th) for these regions for the concurrently-loaded mice and compared the results to the original analysis.

Overall, the trends by region were consistent with those from the principal axis analysis. In general, the anatomic alignment analysis reported greater values for the neutral region and lower values for the compressive and tensile regions than the principal axis analysis (Table A.1). The effect of loading was still greatest under compression, but there were some slight alterations under tension. In 10-week-old mice, tension increased Ct.Ar similarly to compression (Fig A.2). In 10- and 16-week-old mice loaded for 2 weeks, the loading effect on Ct.Th was similar in the tensile and neutral regions (Fig A.2). In the control limbs, the tensile region still had the greatest bone mass, but there were some alterations in the compressive region. For all mice, Ct.Ar in the compressive region was not different from the neutral region, and the same was true for Ct.Th in 16-week-old mice treated for 6 weeks (Fig A.3). Additionally, the PTH trends in 16-week-old mice were slightly shifted. PTH increased Ct.Th after 2 weeks, and only increased Ct.Th in the compressive and neutral regions after 6 weeks (Fig A.3). Ct.Ar trended toward an increase with PTH after 6 weeks (p=0.0713).

Analyzing the data using the anatomic alignment to determine the modality regions did not change the main conclusions of the study. Compression was still the most anabolic and increased the response to PTH the most. The neutral region still had little to no adaptation to loading, and tension produced intermediate anabolic effects. Low bone mass in the pOC-ERαKO mice did not influence the response to PTH and

loading. The consistency between these two analysis methods demonstrates the robust nature of our results and supports our conclusions.

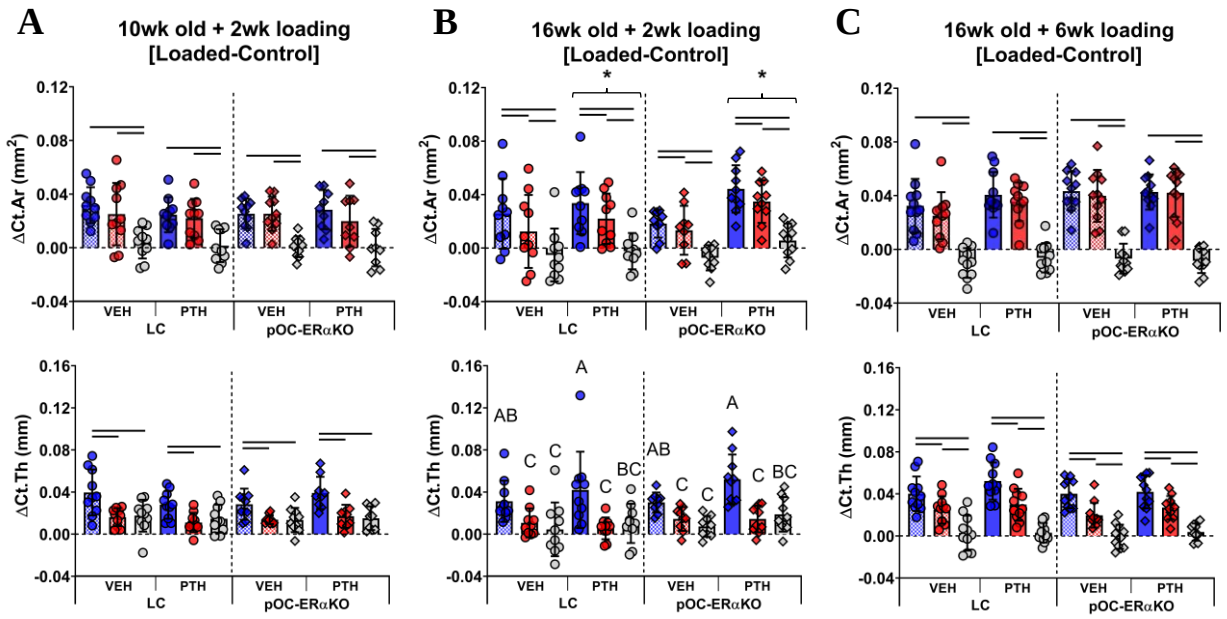

Figure A.2 Anatomic alignment analysis, loading effects [Loaded – Control]. Data are mean ± SD. — Differences by loading modality region, * PTH different from VEH, A > B > C groups not sharing the same letter are different, p<0.05 by ANOVA with Tukey post-hoc.

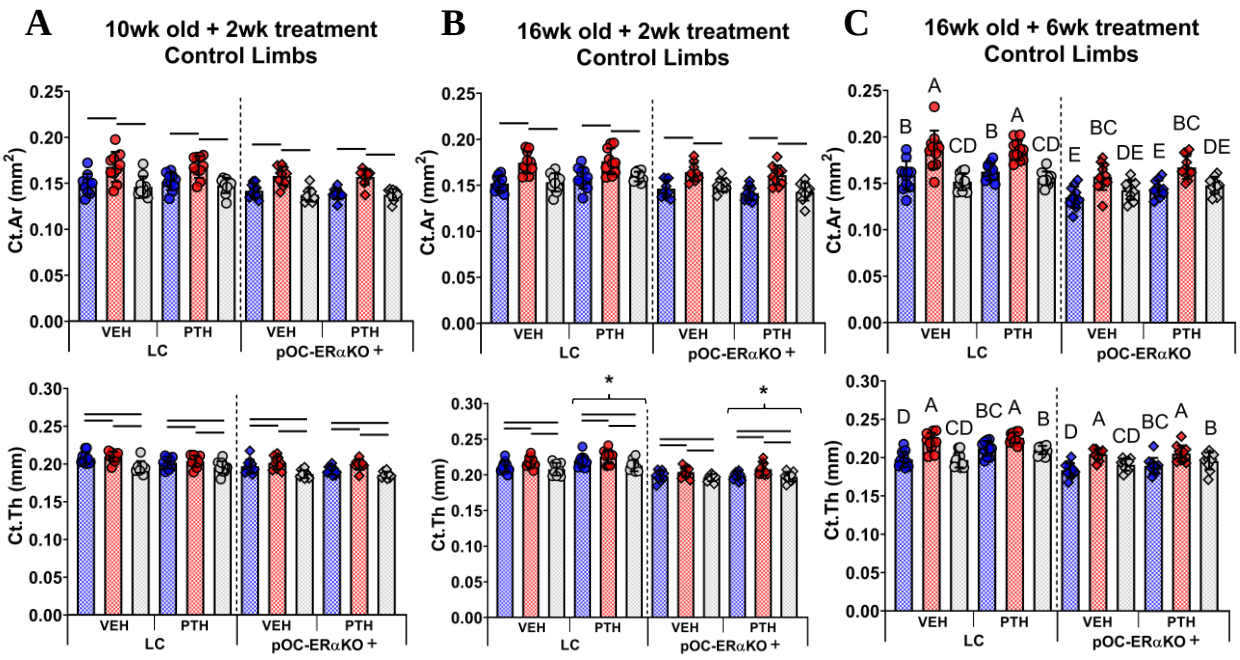

Figure A.3 Anatomic alignment analysis, control limbs. Data are mean ± SD. — Differences by loading modality region, * PTH different from VEH, + pOC-ERαKO different from LC, A > B > C > D > E groups not sharing the same letter are different, p<0.05 by ANOVA with Tukey post-hoc.

Table A.1 Differences between the anatomic alignment and principal axis analyses [Anatomic – Principal].

	Ct.Ar		Ct.Th	
	VEH	PTH	VEH	PTH
10wk+2wk				
LC				
Tension				
Control	-0.00695 ± 0.0040	-0.00730 ± 0.0024	-0.0112 ± 0.0060	-0.00980 ± 0.0046
Loaded	-0.00882 ± 0.0040	-0.0112 ± 0.0040	-0.00927 ± 0.0051	-0.0112 ± 0.0040
Compression				
Control	-0.00909 ± 0.0068	-0.00658 ± 0.0095	-0.00297 ± 0.0049	-0.000130 ± 0.0050
Loaded	-0.0170 ± 0.011	-0.0197 ± 0.0092	-0.0175 ± 0.011	-0.0185 ± 0.014
Neutral				
Control	0.0142 ± 0.0063	0.0139 ± 0.0044	0.00706 ± 0.0042	0.00660 ± 0.0051
Loaded	0.00988 ± 0.0065	0.00947 ± 0.0076	0.0171 ± 0.0072	0.0157 ± 0.0070
pOC-ERαKO				
Tension				
Control	-0.00757 ± 0.0034	-0.00692 ± 0.0043	-0.00959 ± 0.0046	-0.0116 ± 0.0046
Loaded	-0.00928 ± 0.0032	-0.0121 ± 0.0032	-0.00882 ± 0.0040	-0.0111 ± 0.0051
Compression				
Control	-0.00879 ± 0.0052	-0.0103 ± 0.0077	-0.00428 ± 0.0063	-0.00306 ± 0.0045
Loaded	-0.0180 ± 0.0088	-0.0195 ± 0.010	-0.0187 ± 0.0091	-0.0189 ± 0.012
Neutral				
Control	0.0158 ± 0.0042	0.0145 ± 0.0071	0.00839 ± 0.0025	0.00687 ± 0.0030
Loaded	0.0101 ± 0.0051	0.0111 ± 0.0073	0.0151 ± 0.0053	0.0167 ± 0.0056
16wk+2wk				
LC				
Tension				
Control	-0.00270 ± 0.0047	-0.00522 ± 0.0063	-0.00624 ± 0.0063	-0.0121 ± 0.0070
Loaded	-0.00731 ± 0.0048	-0.0112 ± 0.0042	-0.00871 ± 0.0059	-0.0142 ± 0.0055
Compression				
Control	-0.00706 ± 0.0064	-0.0101 ± 0.012	-0.00427 ± 0.0069	-0.00222 ± 0.010
Loaded	-0.0108 ± 0.0078	-0.0180 ± 0.0075	-0.00713 ± 0.0066	-0.0158 ± 0.016
Neutral				
Control	0.00947 ± 0.0098	0.0164 ± 0.0056	0.00500 ± 0.0093	0.0116 ± 0.0077
Loaded	0.00468 ± 0.0083	0.00821 ± 0.0072	0.0115 ± 0.015	0.0162 ± 0.0076
pOC-ERαKO				
Tension				
Control	-0.00462 ± 0.0065	-0.00329 ± 0.0065	-0.00658 ± 0.0064	-0.00577 ± 0.0039
Loaded	-0.00764 ± 0.0049	-0.00872 ± 0.0041	-0.00875 ± 0.0087	-0.00750 ± 0.0046
Compression				
Control	-0.0129 ± 0.0083	-0.0114 ± 0.0091	-0.00808 ± 0.0080	-0.00858 ± 0.0066
Loaded	-0.0199 ± 0.010	-0.0160 ± 0.010	-0.0151 ± 0.012	-0.0204 ± 0.013
Neutral				
Control	0.0167 ± 0.0081	0.0147 ± 0.0072	0.00836 ± 0.0082	0.00986 ± 0.0030
Loaded	0.0116 ± 0.0094	0.0116 ± 0.0086	0.0155 ± 0.010	0.0206 ± 0.012

16wk+6wk				
LC				
Tension				
Control	-0.00506 ± 0.0047	-0.00594 ± 0.0043	-0.00782 ± 0.0059	-0.00916 ± 0.0050
Loaded	-0.00880 ± 0.0037	-0.0128 ± 0.0049	-0.0120 ± 0.0050	-0.0168 ± 0.0067
Compression				
Control	-0.00631 ± 0.0045	-0.00656 ± 0.012	-0.00439 ± 0.0042	-0.00124 ± 0.0063
Loaded	-0.00609 ± 0.0058	-0.0108 ± 0.0061	-0.00336 ± 0.0054	-0.00657 ± 0.0083
Neutral				
Control	0.0131 ± 0.0092	0.0120 ± 0.0077	0.00855 ± 0.0098	0.00946 ± 0.0040
Loaded	0.00155 ± 0.0043	0.00537 ± 0.0055	0.0101 ± 0.0054	0.0132 ± 0.0058
pOC-ERαKO				
Tension				
Control	-0.00361 ± 0.0064	-0.00605 ± 0.0054	-0.00880 ± 0.0075	-0.00951 ± 0.0050
Loaded	-0.00876 ± 0.0055	-0.00882 ± 0.0029	-0.00906 ± 0.0073	-0.00942 ± 0.0030
Compression				
Control	-0.0115 ± 0.0096	-0.0173 ± 0.0099	-0.00664 ± 0.0091	-0.0108 ± 0.0071
Loaded	-0.0117 ± 0.0078	-0.0133 ± 0.0057	-0.00987 ± 0.012	-0.0151 ± 0.0042
Neutral				
Control	0.0145 ± 0.0063	0.0183 ± 0.0086	0.00969 ± 0.0047	0.0121 ± 0.0066
Loaded	0.00634 ± 0.0091	0.00593 ± 0.0035	0.0120 ± 0.012	0.0146 ± 0.0024

Positive values indicate the anatomic alignment analysis reported higher values, negative values indicate the principal axis analysis reported higher values. Data are mean±SD.

Appendix B

PTH PRE-TREATMENT AND TIBIAL COMPRESSION IN FEMALE pOC-ERαKO MICE

B.1 Motivation

Parathyroid hormone (PTH) is one of the few FDA-approved anabolic osteoporosis treatments. PTH stimulates bone formation, improves microarchitecture, and reduces fracture risk [1,2]. However, following the initial increase in bone formation PTH also causes a slower increase in bone resorption, leading to what is known as the "anabolic window". After approximately two years, continuing PTH treatment provided no added benefit. Therefore, the anabolic effect must be maximized during this time period.

One method to increase the anabolic effect of PTH is to combine treatment with mechanical loading. Mechanical loading is synergistically anabolic with PTH, particularly in cortical bone of healthy rodents [3,4], but the effects in cancellous bone are less clear [3,5]. We hypothesized that pre-treating mice with PTH would prime osteoblasts prior to the application of mechanical loading, resulting in a greater anabolic response. Additionally, we wanted to study these responses in a more clinically relevant low bone mass model. We pre-treated 12-week-old female osteoblast-specific estrogen receptor alpha knockout mice (pOC-ERαKO) and their littermate controls (LC) with PTH or saline vehicle (VEH) for 4 weeks. After the pre-treatment period, treatment was continued and cyclic tibial compression was applied for 2 weeks.

B.2 Materials and methods

B.2.1 Generation of pOC-ERαKO mice

Osteoblast-specific ERα knockout and littermate control (LC) mice were generated as previously described [6]. Mice with loxP sequences flanking exon 3 of the DNA-binding domain of the ERα gene (*Esr1*) ($ERα^{fl/fl}$, provided by Dr. Sohaib Kahn, University of Cincinnati, Cincinnati, OH, USA) [7] were inbred to be >99% pure C57Bl/6 by speed congenics (DartMouse Speed Congenic Core Facility, Geisel School of Medicine at Dartmouth, Hanover, NH, USA). $ERα^{fl/fl}$ mice were then crossed with mice containing a transgene encoding *Cre* recombinase driven by the human osteocalcin promoter (*OC-Cre*, provided by Dr. Thomas Clemens, The Johns Hopkins University, Baltimore, MD, USA) that had previously been inbred to the C57Bl/6 strain [8,9]. Mice were genotyped using lysed tail PCR as previously described [6]. Mice were housed 5 per cage and had ad libitum access to food and water. All animal procedures were approved by Cornell University's IACUC.

B.2.2 Parathyroid hormone treatment

Human parathyroid hormone (1-34) (Bachem Americas, Inc; Torrance, CA, USA) was administered subcutaneously 5 days per week at a dose of 40µg/kg. Mice receiving vehicle (VEH) treatment were injected subcutaneously with a similar volume of sterile phosphate buffered saline (PBS) 5 days per week.

B.2.3 In vivo tibial mechanical loading

Loaded mice received axial cyclic compressive tibial loading on their left

limbs while their right limbs served as contralateral controls. Peak load magnitudes were based on *in vivo* strains at the mid-diaphysis. Prior to the start of the experiment, single-element strain gauges (C2A-06-015LW-120, Micro-Measurements, Wendell, NC, USA) were surgically attached to the anteromedial surface of the tibial midshafts of a small subset of mice. Strain gauging was performed on 16-week-old female LC and pOC-ERαKO mice, as well as 16-week-old female LC and pOC-ERαKO mice that had received 4 weeks of PTH treatment (n=5/group). Axial cyclic compressive loads with peak load magnitudes ranging from -2 to -18N were applied to the left and right tibiae in our custom tibial loading device [10,11]. Using the load and strain data, bone stiffness and the peak load required to induce +1000 microstrain (με) on the anteromedial surface of the tibial midshaft were calculated as previously described [11]. Bone stiffness was similar between LC and pOC-ERαKO mice and increased with PTH treatment (0.00811 ± 0.0023N/με LC, 0.00723 ± 0.0015N/με pOC-ERαKO, 0.0107 ± 0.0030N/με LC+PTH, 0.0113 ± 0.0055N/με pOC-ERαKO+PTH; mean ± SD). Peak load magnitudes of -7.9N and -9.8N were applied to LC and pOC-ERαKO mice treated with VEH and PTH, respectively, to induce +1000με at the midshaft.

The left tibiae of 16-week-old female LC and pOC-ERαKO mice and 16-week-old female LC and pOC-ERαKO mice that had been pretreated with PTH or VEH for 4 weeks (n=10 per group) were loaded in cyclic compression *in vivo* for 2 weeks (Fig. B.1), as previously described [11]. Compressive loading was applied at a rate of 4Hz for 1200 cycles per day, 5 days per week, in a triangular waveform with a peak load of -7.9N or -9.8N as described above. A dwell of 100ms at -1N was maintained between successive load cycles, and the dwell-to-peak time was 75ms. The

right limb served as a contralateral control. Three days after the last session of *in vivo* tibial compression, mice were euthanized via isoflurane overdose and cardiac puncture. A separate baseline set of mice was euthanized following the 4 weeks of pre-treatment (n=5/group). The baseline mice received no tibial loading.

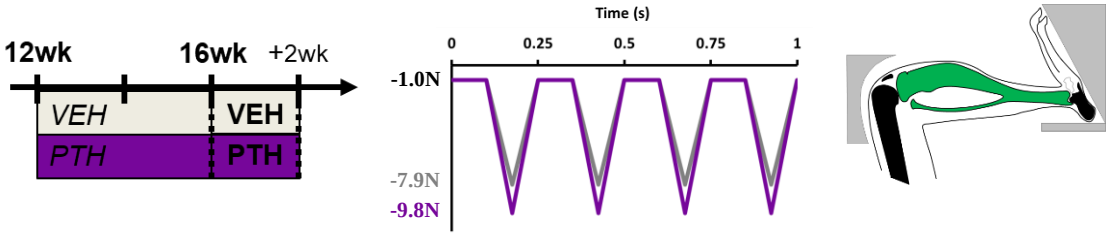

Figure B.1 Experimental design and timeline. 12-week-old female pOC-ERαKO and LC mice were treated with VEH or PTH 5 days per week for 4 weeks (Italic). A baseline group was euthanized at 16 weeks of age. A second group continued treatment and received daily tibial compression 5 days per week for 2 weeks starting at 16 weeks of age (Bold). The VEH and PTH groups were loaded at peak loads of -7.9N and -9.8N, respectively.

B.2.4 Microcomputed tomography

Bone morphology was examined using microCT. At euthanasia, right tibiae were stored in 4% paraformaldehyde and later scanned in 70% ethanol at 10μm voxel resolution at the metaphysis and 15μm voxel resolution at the diaphysis (μCT35, Scanco Medical AG; 55kVp, 145μA, 600ms integration time). The metaphyseal volume of interest (VOI) was defined as 10% of the total tibial length beginning 50μm distal to the growth plate, and the diaphyseal VOI was defined as 2.5% of the total tibial length centered at the midshaft [6]. Within the metaphysis, the cancellous core was segmented manually. Outcome measures for cancellous bone were bone volume fraction (BV/TV), trabecular thickness (Tb.Th), separation (Tb.Sp), and number (Tb.N), and cancellous tissue mineral density (cn.TMD). Outcome measures for cortical bone were cortical area (Ct.Ar), marrow area (Ma.Ar, diaphysis only), cortical

thickness (Ct.Th), maximum and minimum moment of inertia (I_{MAX} and I_{MIN}), and cortical tissue mineral density (ct.TMD).

B.2.5 Statistics

The results were analyzed using an ANOVA for genotype, treatment, and their interaction. Systemic PTH effects were analyzed using the non-loaded control limbs, and the effects of loading were analyzed using the limb differences withing each mouse [Loaded-Control]. These results were also compared to those from the concurrently-loaded mice from *Chapters 5 and 6* to investigate the effects of pre-treatment. A Tukey HSD post-hoc was performed when the interactions terms were significant. Significance was set at $p<0.05$. All results are significant unless stated otherwise.

B.3 Results

B.3.1 PTH increased cortical but not cancellous bone

PTH did not increase cancellous bone mass at the metaphysis at baseline or after 2 weeks of continued treatment (Figs. B.2&B.3, Tables B.1&B.2). After the full 6 weeks, PTH increased Tb.Th in pOC-ERαKO mice, but only trended toward increased BV/TV in both genotypes. PTH decreased cn.TMD at both timepoints which may indicate the presence of less mineralized, newly formed bone. There was a trend toward reduced BV/TV at baseline in pOC-ERαKO mice compared to LC ($p=0.055$) due to reduced Tb.N and increased Tb.Sp, and this was significant in control limbs after 2 weeks of loading. pOC-ERαKO mice also had reduced cn.TMD at baseline.

Table B.1 Baseline microCT data following 4 weeks of treatment.

	LC		pOC-ERαKO	
	VEH	**PTH**	**VEH**	**PTH**
Metaphysis				
BV/TV	0.109±0.0099	0.111±0.013	0.102±0.016	0.0870±0.025
Tb.Th (mm)	0.0507±0.0023	0.0487±0.0018	0.0473±0.0037	0.0483±0.0036
Tb.N (1/mm)	3.51±0.20	3.46±0.26	$3.28±0.35^{\#}$	$3.00±0.43^{\#}$
Tb.Sp (mm)	0.288±0.021	0.291±0.024	$0.310±0.037^{\#}$	$0.341±0.048^{\#}$
cn.TMD (mg HA/cc)	925±27	$913±25^{*}$	$908±21^{\#}$	$863±37^{*,\#}$
Metaphyseal Shell				
Ct.Ar (mm^2)	$0.942±0.0096^{A}$	$0.977±0.051^{A}$	$0.822±0.039^{B}$	$0.945±0.056^{A}$
Ct.Th (mm)	0.153±0.0045	$0.167±0.0077^{*}$	$0.138±0.0092^{\#}$	$0.157±0.0048^{*,\#}$
I_{MAX} (mm^4)	$0.329±0.014^{A}$	$0.325±0.029^{A}$	$0.276±0.014^{B}$	$0.323±0.036^{A}$
I_{MIN} (mm^4)	$0.272±0.020^{A}$	$0.256±0.019^{AB}$	$0.225±0.014^{B}$	$0.260±0.030^{AB}$
ct.TMD (mg HA/cc)	1004±6.7	1005±23	$966±17^{\#}$	$968±11^{\#}$
Diaphysis				
Ct.Ar (mm^2)	0.745±0.037	0.811±0.049	0.764±0.097	0.725±0.029
Ma.Ar (mm^2)	0.368±0.015	$0.388±0.030^{*}$	0.340±0.042	$0.381±0.021^{*}$
Ct.Th (mm)	0.245±0.0099	0.251±0.016	0.255±0.034	0.239±0.0087
I_{MAX} (mm^4)	$0.104±0.0095^{B}$	$0.132±0.012^{A}$	$0.109±0.019^{AB}$	$0.105±0.0088^{B}$
I_{MIN} (mm^4)	0.0783±0.0054	0.0866±0.0083	$0.0744±0.011^{\#}$	$0.0726±0.0037^{\#}$
ct.TMD (mg HA/cc)	1062±8.2	1051±22	1054±8.3	1056±13

Data are mean±SD. # pOC-ERαKO different from LC. * PTH different from VEH. A > B Groups sharing a letter are not different.

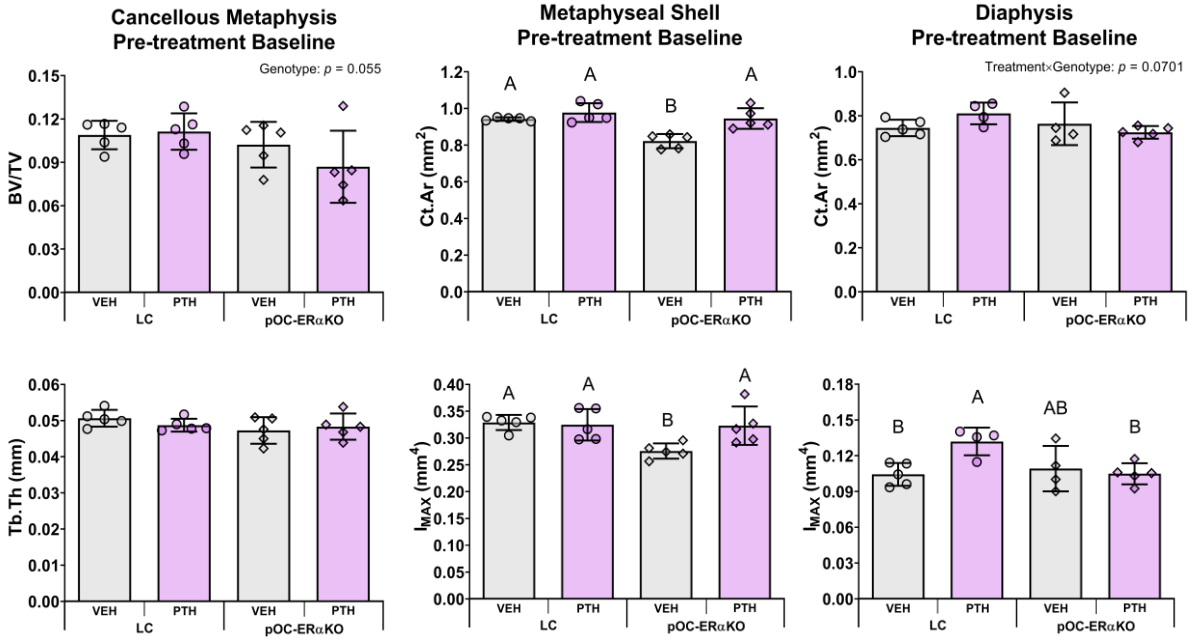

Figure B.2 After 4 weeks of pre-treatment, PTH did not affect cancellous bone mass and increased cortical bone mass differently by genotype. A > B.

PTH pre-treatment increased metaphyseal cortical shell bone mass only in pOC-ERαKO mice at baseline but increased bone mass in both genotypes at the 2-week timepoint (Figs. B.2&B.3, Tables B.1&B.2). PTH increased metaphyseal Ct.Ar and I_{MAX} in pOC-ERαKO mice to the level of LC mice at baseline, but increased both genotypes similarly after an additional 2 weeks. I_{MIN} was lower in pOC-ERαKO mice treated with VEH compared to LC mice treated with VEH at baseline, but PTH increased I_{MIN} in both genotypes at the 2-week timepoint. Ct.Th was lower in pOC-ERαKO mice and was increased with PTH similarly in both genotypes. pOC-ERαKO mice also had lower ct.TMD compared to LC mice.

PTH increased diaphyseal cortical bone mass only in LC mice at baseline (Figs. B.2&B.3, Tables B.1&B.2). PTH only increased I_{MAX} in LC mice and trended toward an increase in Ct.Ar in LC mice (p=0.07), but after an additional 2 weeks PTH increased Ct.Ar, Ct.Th, I_{MAX}, and I_{MIN} similarly in both genotypes. PTH increased Ma.Ar similarly in both genotypes at baseline and only in pOC-ERαKO mice at 2 weeks, suggesting that PTH increased bone mass via periosteal expansion. I_{MIN} was lower in pOC-ERαKO mice compared to LC mice at baseline, and Ct.Ar and Ct.Th were lower in pOC-ERαKO mice at 2 weeks.

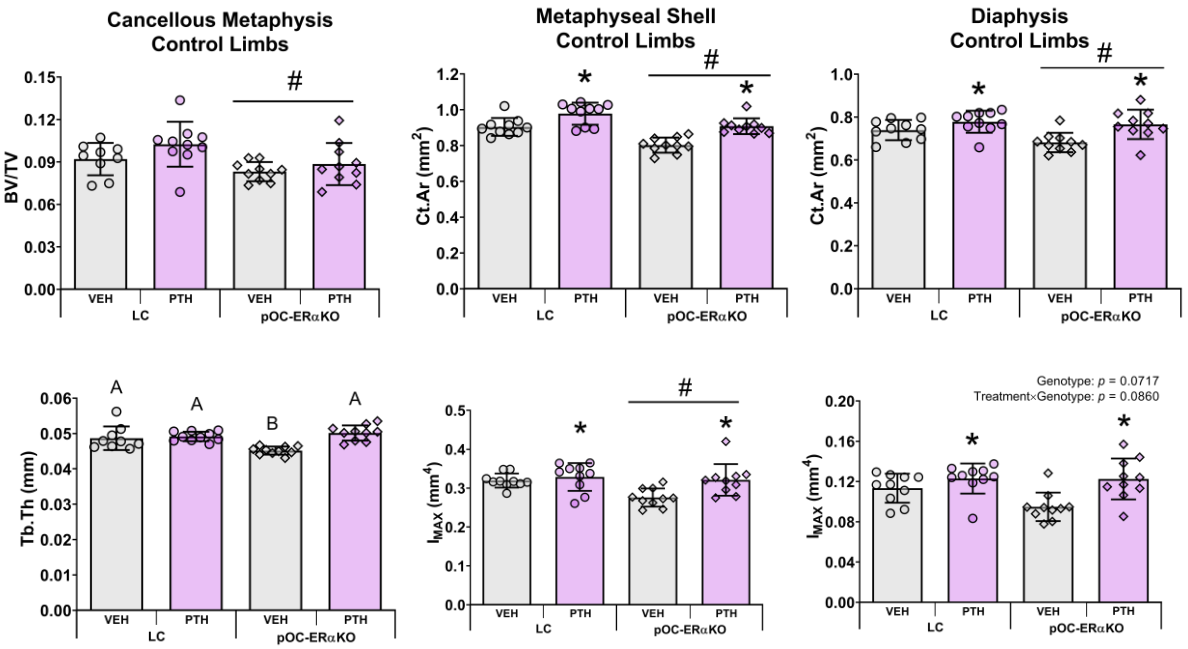

Figure B.3 PTH increased cortical bone mass in non-loaded control limbs, and pOC-ERαKO mice had lower bone mass compared to LC. * PTH different from VEH, # pOC-ERαKO different from LC, A > B.

B.3.2 PTH increased the loading effect in cortical but not cancellous bone

Tibial loading did not increase cancellous bone mass, and PTH pre-treatment did not influence this response. Cancellous BV/TV did not change with loading in any group (Fig. B.4, Table B.2). Loading increased Tb.Th more in pOC-ERαKO mice compared to LC mice, and there was a trend toward a greater increase with PTH (p=0.077). Tb.Sp increased and cn.TMD decreased with loading similarly in all groups.

Unlike cancellous bone, loading and PTH were synergistically anabolic in cortical bone at the metaphyseal shell. Load-induced increases in Ct.Ar, Ct.Th, and I_{MAX} were greater with PTH treatment (Fig. B.4, Table B.2). I_{MIN} increased and ct.TMD decreased with loading, but the changes were similar in all groups. PTH

similarly altered the response to loading in cortical bone at the diaphysis. Loading only increased Ct.Ar only when combined with PTH, with a similar trend in I_{MAX} (p=0.0753) (Fig. B.4, Table B.2). PTH increased the loading response in Ct.Th in all groups, and prevented the increase in Ma.Ar with loading in the VEH group.

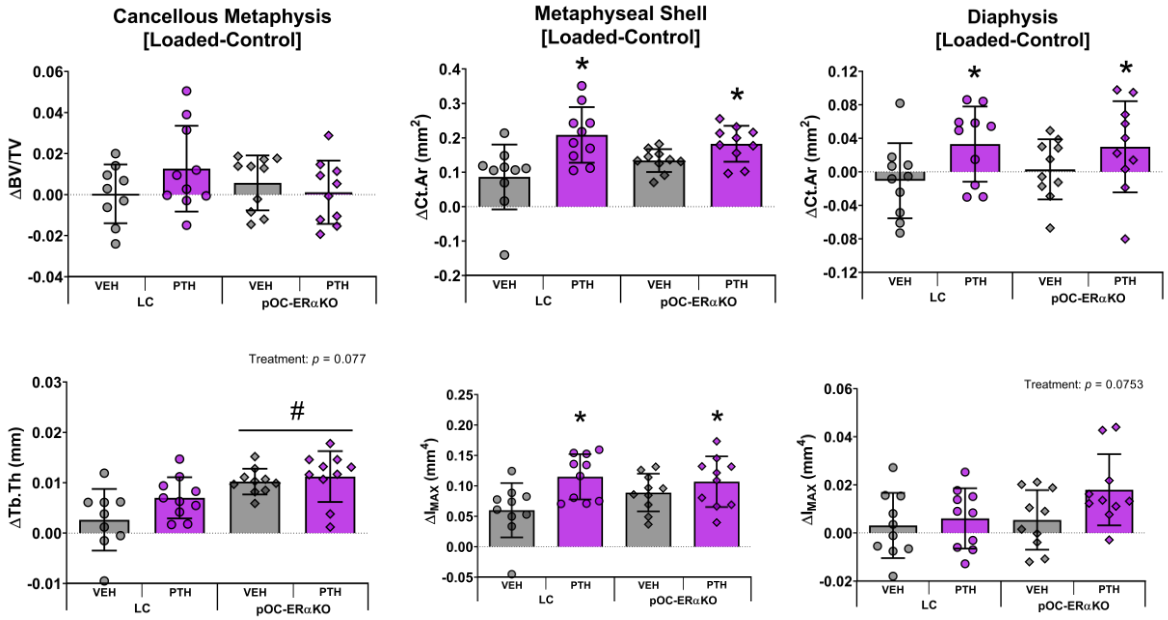

Figure B.4 PTH increased the loading effects in cortical but not cancellous bone. * PTH different from VEH, # pOC-ERαKO different from LC.

Table B.2 MicroCT data following 4 weeks of pre-treatment and 2 weeks of tibial loading.

		LC		pOC-ERαKO	
		VEH	**PTH**	**VEH**	**PTH**
Metaphysis					
BV/TV	Control	0.0920±0.011	0.103±0.016*	0.0832±0.0068$^{\#}$	0.0885±0.015$^{*,\#}$
	Loaded	0.0925±0.014	0.115±0.018*	0.0889±0.010$^{\#}$	0.0897±0.014$^{*,\#}$
Tb.Th (mm)	Control	0.0487±0.0033^{C,b}	0.0492±0.0013^{C,b}	0.0452±0.0011^{C,b}	0.0502±0.0021^{C,a}
	Loaded	0.0518±0.0040^{B,b}	0.0562±0.0038^{B,b}	0.0554±0.0028^{A,b}	0.0614±0.0055^{A,a}
Tb.N (1/mm)	Control	3.36±0.41	3.27±0.29	2.92±0.35$^{\#}$	2.74±0.34$^{\#}$
	Loaded	3.31±0.32	3.23±0.34	2.68±0.25$^{\#}$	2.61±0.49$^{\#}$
Tb.Sp (mm)	Control	0.303±0.042	0.307±0.034	0.349±0.048$^{\#}$	0.373±0.051$^{\#}$
	Loaded	0.303±0.031†	0.313±0.037†	0.378±0.037$^{\dagger,\#}$	0.398±0.070$^{\dagger,\#}$
cn.TMD (mg HA/cc)	Control	903±25	875±17*	884±26$^{\#}$	871±26$^{*,\#}$
	Loaded	895±26†	870±27†,*	862±22$^{\dagger,\#}$	863±25$^{\dagger,*,\#}$
Metaphyseal Shell					
Ct.Ar (mm^2)	Control	0.904±0.050^{C}	0.978±0.062^{B}	0.802±0.042$^{C,\#}$	0.908±0.044$^{B,\#}$
	Loaded	0.991±0.062^{B}	1.19±0.042^{A}	0.936±0.029$^{B,\#}$	1.09±0.038$^{A,\#}$
Ct.Th (mm)	Control	0.154±0.0083^{D}	0.167±0.0062^{B}	0.135±0.0063$^{D,\#}$	0.150±0.0069$^{B,\#}$
	Loaded	0.156±0.0060^{C}	0.181±0.0058^{A}	0.144±0.0089$^{C,\#}$	0.162±0.010$^{A,\#}$
I_{MAX} (mm^4)	Control	0.319±0.018^{C}	0.329±0.036^{C}	0.276±0.023$^{C,\#}$	0.321±0.041$^{C,\#}$
	Loaded	0.379±0.035^{B}	0.444±0.034^{A}	0.365±0.028$^{B,\#}$	0.428±0.036$^{A,\#}$
I_{MIN} (mm^4)	Control	0.239±0.021	0.256±0.037*	0.216±0.028$^{\#}$	0.250±0.037$^{*,\#}$
	Loaded	0.276±0.034†	0.327±0.026†,*	0.256±0.014$^{\dagger,\#}$	0.301±0.025$^{\dagger,*,\#}$
ct.TMD (mg HA/cc)	Control	990±44^{ABCDEF}	1004±48^{AB}	970±41^{ABCE}	974±38^{ACD}
	Loaded	981±40^{ABCDEF}	980±41^{CDEF}	945±35^{DF}	952±36^{BEF}
Diaphysis					
Ct.Ar (mm^2)	Control	0.739±0.047^{C}	0.778±0.051^{B}	0.681±0.045$^{C,\#}$	0.766±0.068$^{B,\#}$
	Loaded	0.729±0.046^{C}	0.811±0.034^{A}	0.685±0.039$^{C,\#}$	0.796±0.060$^{A,\#}$
Ma.Ar (mm^2)	Control	0.413±0.034^{B}	0.404±0.041^{AB}	0.381±0.030^{B}	0.426±0.036^{AB}
	Loaded	0.434±0.038^{A,†}	0.395±0.046^{AB,†}	0.405±0.036^{A,†}	0.430±0.039^{AB,†}
Ct.Th (mm)	Control	0.234±0.011^{B}	0.246±0.010^{A}	0.227±0.0092$^{B,\#}$	0.239±0.013$^{A,\#}$
	Loaded	0.227±0.011^{B}	0.256±0.0088^{A}	0.223±0.0086$^{B,\#}$	0.241±0.015$^{A,\#}$
I_{MAX} (mm^4)	Control	0.113±0.014^{A}	0.123±0.015^{A}	0.0948±0.014^{B}	0.123±0.020^{A}
	Loaded	0.116±0.014^{A,†}	0.129±0.012^{A,†}	0.100±0.014^{B,†}	0.141±0.020^{A,†}
I_{MIN} (mm^4)	Control	0.0796±0.010	0.0828±0.011*	0.0671±0.0085	0.0831±0.013*
	Loaded	0.0797±0.011†	0.0875±0.011†,*	0.0701±0.0086†	0.0846±0.011†,*
ct.TMD (mg HA/cc)	Control	1029±41^{A}	1064±32^{A}	1054±36^{A}	1032±40^{A}
	Loaded	1035±39^{A}	1062±38^{A}	1054±31^{A}	1039±34^{A}

Data are mean±SD. † Loaded limb different from Control. # pOC-ERαKO different from LC. * PTH different from VEH. A > B Groups sharing a capitalized letter are not different. a > b Groups sharing a lower-cased letter are not different.

B.3.3 VEH pre-treatment altered bone mass

When the pre-treated mice from this study were compared to the concurrently-loaded mice from *Chapters 5 and 6*, some discrepancies became apparent. Bone mass in VEH-treated, non-loaded control limbs from 16-week-old mice loaded for 2 weeks was different depending on whether the mice received VEH pre-treatment or no pre-treatment. Cancellous BV/TV and diaphyseal Ct.Ar and I_{MAX} were greater in mice that received 4 weeks of VEH pre-treatment (Fig. B.5). VEH pre-treated mice also started loading with lower body mass than non-pre-treated mice (Fig. B.5). Together, these data suggest that pre-treating the mice, even with saline, altered their skeletal phenotype.

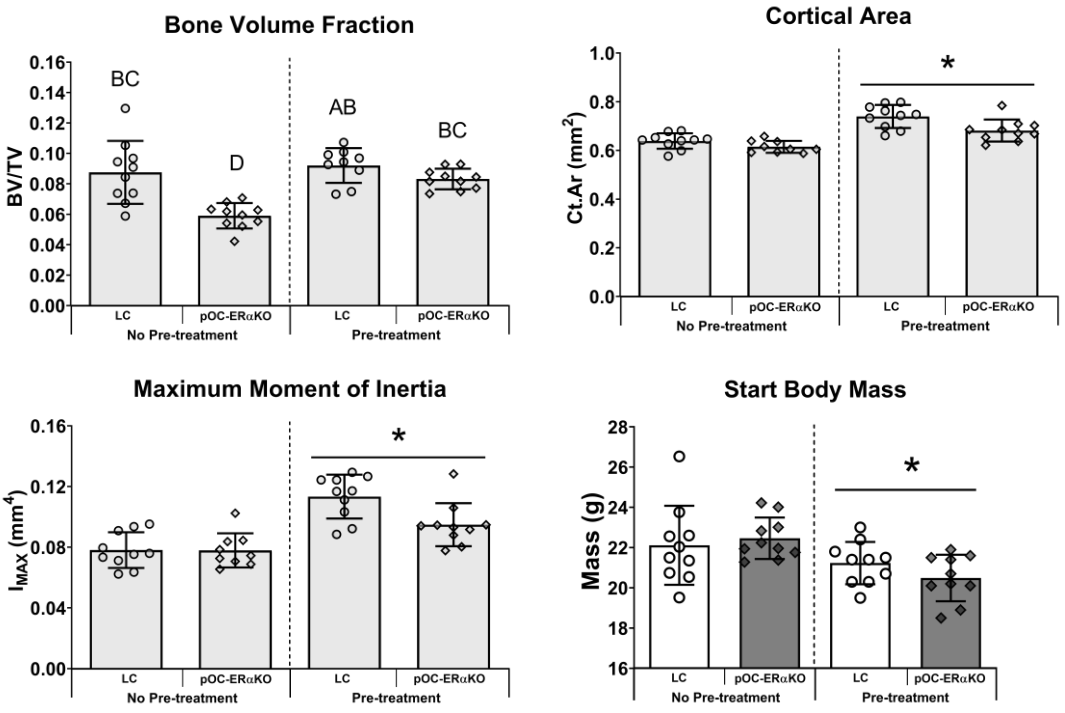

Figure B.5 Phenotype comparisons between VEH pre-treated and non-pre-treated mice. Metaphyseal cancellous BV/TV and diaphyseal Ct.Ar and I_{MAX} were greater in VEH pre-treated control limbs. VEH pre-treated mice started loading with lower body mass. A > B > C > D, groups not sharing a letter are statistically different. * Pre-treatment different from No Pre-treatment.

B.4 Discussion & Conclusions

PTH increased the response to loading in cortical bone, but cancellous bone did not respond to loading regardless of PTH treatment. Non-loaded control limbs from VEH-treated mice had greater bone mass when the mice also received VEH pre-treatment. During the pre-treatment period, mice were awake when the injections were administered, while mice that only received treatment concurrently with loading were injected while under anesthesia for tibial loading. The stress of daily handling and injections may have altered hormone levels or cage activity and resulted in increased bone mass. Stressors, including restraint and foot shocks, have been shown to increase serum osteocalcin levels to approximately double their baseline levels in mice and rats [12]. Another study divided female C57Bl/6NHsd mice to receive no handling, daily handling and no injection, or daily handling and saline IP injections from 9 to 17 weeks of age [13]. Although there were no significant differences in bone mass between the groups, tibial diaphyseal Ct.Ar and Ct.Th trended higher in the injected mice (p=0.077, p=0.069, respectively). The longer timeline of 8 weeks may have allowed the mice to become accustomed to the handling, reducing stress levels compared to our 4-week treatment period. Nonetheless, daily handling and injections of mice appears to increase tibial bone mass.

The anabolic effect of daily handling and injections may have reduced the effect of loading. We performed strain gauge experiments on 16-week-old mice that had been pre-treated with PTH and 16-week-old mice that had received no pre-treatment, but not on 16-week-old mice that had received VEH pre-treatment. The increased bone mass in VEH pre-treated mice, particularly at the diaphysis, would

alter the stiffness and the load required to induce +1000με at the midshaft. Overall, daily handling and injections may influence skeletal phenotypes in mice and should be considered in future studies.

B.5 References

[1] D. Aslan, M.D. Andersen, L.B. Gede, T.K. de Franca, S.R. Jørgensen, P. Schwarz, N.R. Jørgensen, Mechanisms for the bone anabolic effect of parathyroid hormone treatment in humans, Scand. J. Clin. Lab. Investig. 72 (2012) 14–22. doi:10.3109/00365513.2011.624631.

[2] D.W. Dempster, F. Cosman, E.S. Kurland, H. Zhou, J. Nieves, L. Woelfert, E. Shane, K. Plavetić, R. Müller, J. Bilezikian, R. Lindsay, Effects of daily treatment with parathyroid hormone on bone microarchitecture and turnover in patients with osteoporosis: a paired biopsy study., J. Bone Miner. Res. 16 (2001) 1846–53. doi:10.1359/jbmr.2001.16.10.1846.

[3] T. Sugiyama, L.K. Saxon, G. Zaman, A. Moustafa, A. Sunters, J.S. Price, L.E. Lanyon, Mechanical loading enhances the anabolic effects of intermittent parathyroid hormone (1-34) on trabecular and cortical bone in mice, Bone. 43 (2008) 238–248. doi:10.1016/j.bone.2008.04.012.

[4] H. Hagino, T. Okano, M.P. Akhter, M. Enokida, R. Teshima, Effect of parathyroid hormone on cortical bone response to in vivo external loading of the rat tibia, J. Bone Miner. Metab. 19 (2001) 244–250. doi:10.1007/s007740170027.

[5] C.H. Kim, E. Takai, H. Zhou, D. von Stechow, R. Müller, D.W. Dempster, X.E. Guo, Trabecular bone response to mechanical and parathyroid hormone stimulation: the role of mechanical microenvironment, J. Bone Miner. Res. 18 (2003) 2116–2125. doi:10.1359/jbmr.2003.18.12.2116.

[6] K.M. Melville, N.H. Kelly, S. a Khan, J.C. Schimenti, F.P. Ross, R.P. Main, M.C. van der Meulen, Female mice lacking estrogen receptor-alpha in osteoblasts have compromised bone mass and strength, J Bone Min. Res. 29 (2014) 370–379. doi:10.1002/jbmr.2082.

[7] Y. Feng, D. Manka, K.-U. Wagner, S.A. Khan, Estrogen receptor-alpha expression in the mammary epithelium is required for ductal and alveolar morphogenesis in mice., Proc. Natl. Acad. Sci. U. S. A. 104 (2007) 14718–23. doi:10.1073/pnas.0706933104.

[8] T.L. Clemens, H. Tang, S. Maeda, R. a Kesterson, F. Demayo, J.W. Pike, C.M. Gundberg, Analysis of osteocalcin expression in transgenic mice reveals a species difference in vitamin D regulation of mouse and human osteocalcin genes., J. Bone Miner. Res. 12 (1997) 1570–6. doi:10.1359/jbmr.1997.12.10.1570.

[9] M. Zhang, S. Xuan, M.L. Bouxsein, D. Von Stechow, N. Akeno, M.C. Faugere, H. Malluche, G. Zhao, C.J. Rosen, A. Efstratiadis, T.L. Clemens, Osteoblast-specific knockout of the insulin-like growth factor (IGF) receptor gene reveals an essential role of IGF signaling in bone matrix mineralization, J. Biol. Chem. 277 (2002) 44005–44012. doi:10.1074/jbc.M208265200.

[10] J.C. Fritton, E.R. Myers, T.M. Wright, M.C.H. Van Der Meulen, Loading induces site-specific increases in mineral content assessed by microcomputed tomography of the mouse tibia, Bone. 36 (2005) 1030–1038. doi:10.1016/j.bone.2005.02.013.

[11] M.E. Lynch, R.P. Main, Q. Xu, D.J. Walsh, M.B. Schaffler, T.M. Wright,

M.C.H. van der Meulen, Cancellous bone adaptation to tibial compression is not sex dependent in growing mice., J. Appl. Physiol. 109 (2010) 685–691. doi:10.1152/japplphysiol.00210.2010.

[12] J.M. Berger, P. Singh, L. Khrimian, K. Rahmouni, X. Gao, G. Karsenty, J.M. Berger, P. Singh, L. Khrimian, D.A. Morgan, S. Chowdhury, Mediation of the Acute Stress Response by the Skeleton, Cell Metab. (2019) 1–13. doi:10.1016/j.cmet.2019.08.012.

[13] R.A. Larsen, J.L. Peveler, J.B. Klutzke, D.L. Hickman, M.W. Aref, J.M. Wallace, D.M. Brown, M.R. Allen, Effects of daily restraint with and without injections on skeletal properties in C57BL/6NHsd mice, Lab Anim. (NY). 46 (2017) 299–301. doi:10.1038/laban.1295.

Appendix C

DAILY HANDLING AND INJECTIONS ALTER BONE MASS IN MICE

C.1 Motivation

We previously discovered that mice injected with saline vehicle daily for four weeks had greater bone mass than non-injected mice of the same age (Appendix B) and hypothesized that this increase was due to the stress of daily handling and injections. Physical restraint and acute stressors have been shown to increase serum osteocalcin levels in mice [1], which can influence bone remodeling. Although Larsen and colleagues did not observe significant changes in bone mass following 8 weeks of saline injections in 9-week-old mice, there were strong trends toward increased cortical bone mass [2]. Therefore, we sought to determine whether 4 weeks of daily handling and saline injections increases bone mass in 12-week-old mice.

C.2 Materials and methods

C.2.1 Animals

Twenty-four 12-week-old female C57Bl/6J mice (Jackson Laboratories) were randomized to receive no injections, daily subcutaneous injections of sterile saline 5 days/week, or daily intraperitoneal injections of sterile saline 5 days/week for 4 weeks (n=8/group). Mice were euthanized at 16 weeks of age, 3 days after the last injection. All mice were weighed twice a week for the duration of the experiment.

C.2.2 Microcomputed tomography

Bone morphology was examined using microCT. At euthanasia, right tibiae were stored in 4% paraformaldehyde and later scanned in 70% ethanol at 10μm voxel resolution at the metaphysis and 15μm voxel resolution at the diaphysis (μCT35, Scanco Medical AG; 55kVp, 145μA, 600ms integration time). The metaphyseal volume of interest (VOI) was defined as 10% of the total tibial length beginning 50μm distal to the growth plate, and the diaphyseal VOI was defined as 2.5% of the total tibial length centered at the midshaft [3]. Within the metaphysis, the cancellous core was segmented manually. Outcome measures for cancellous bone were bone volume fraction (BV/TV), trabecular thickness (Tb.Th), separation (Tb.Sp), and number (Tb.N), and cancellous tissue mineral density (cn.TMD). Outcome measures for cortical bone were cortical area (Ct.Ar), marrow area (Ma.Ar), cortical thickness (Ct.Th), maximum and minimum moment of inertia (I_{MAX} and I_{MIN}), and cortical tissue mineral density (ct.TMD).

C.2.3 Statistics

The results were analyzed using an ANOVA for treatment method. A Tukey post hoc was performed to identify differences between the three groups. Significance was set at $p<0.05$.

C.3 Results

In the cancellous metaphysis, BV/TV was increased in the IP group compared to the control group (+13%), with a trend towards increased BV/TV in the SQ group

(+3.1%) (Fig C.1, Table C.1). Tb.Th was greater in the IP group compared to the SQ group (+5.9%), although there was no difference between either injection group and the control group. There was a slight trend towards increased Tb.N in the injection groups (+4.5%, *p*=0.1205) compared to the control group, with a corresponding decrease in Tb.Sp (-4.5%, *p*=0.1492). Injections did not affect cn.TMD.

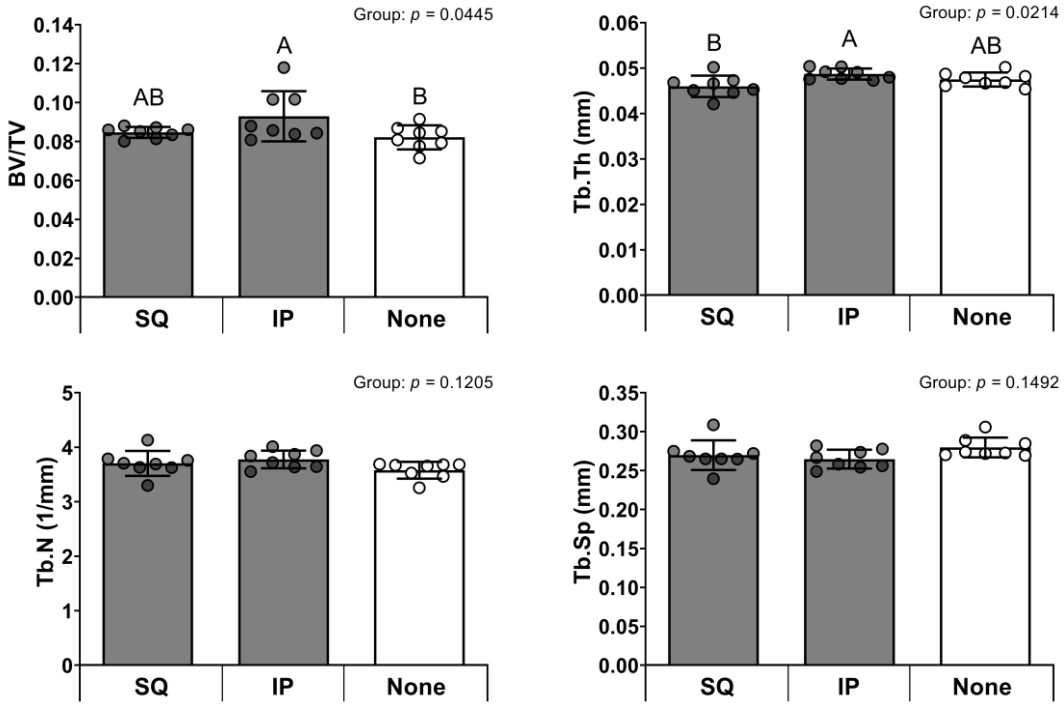

Figure C.1 IP injections increased cancellous bone mass.

At the diaphysis, there was a trend towards increased Ct.Ar and Ma.Ar in the injection groups, particularly the IP group (Ct.Ar: +5.6%; Ma.Ar: +8.1%). These changes resulted in increased I_{MAX} in the IP group (+17%) with a trend in the SQ group (+8.2%) (Fig C.2, Table C.1). I_{MIN} also trended toward an increase in the IP group compared to the control group (+11%, *p*=0.1182). Together with no alterations in Ct.Th, these results suggest that the diaphyses of the injected mice underwent periosteal expansion in response to daily handling and injections. Injections did not

affect ct.TMD.

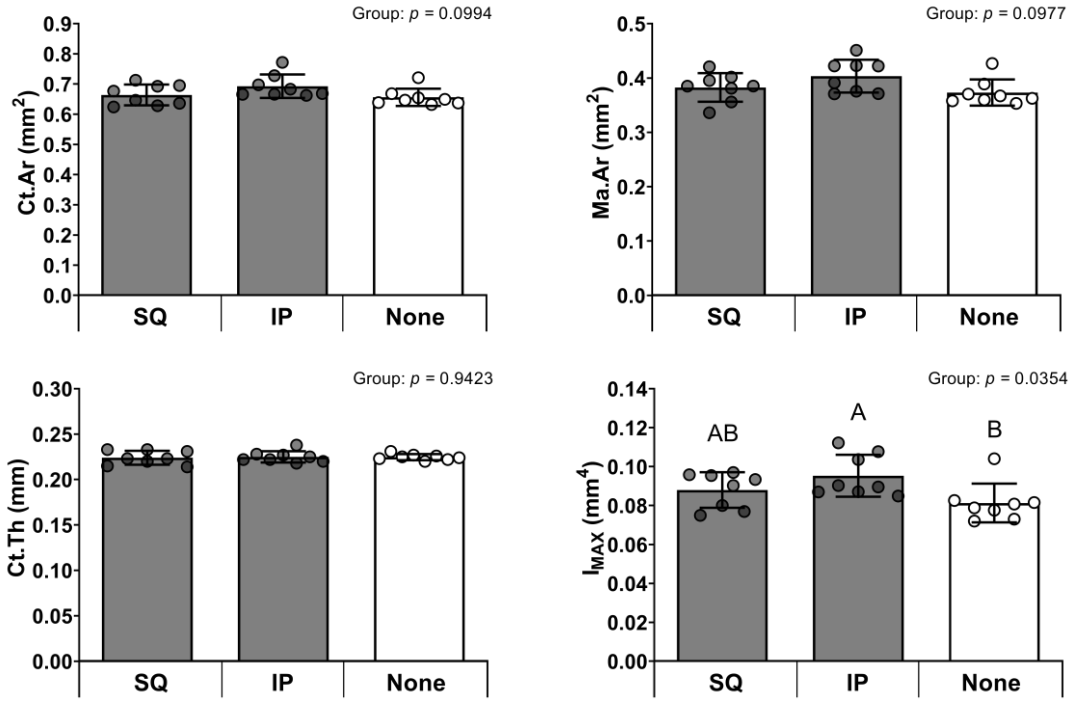

Figure C.2 IP injections increased cortical bone mass at the diaphysis.

Injections did not influence body mass. Body masses in all groups were similar at the start of the experiment. Although not significant, non-injected mice gained slightly more body mass than injected mice over the course of the experiment (p=0.1991, Fig C.3).

C.4 Conclusions

Daily injections increased cortical and cancellous bone mass, particularly IP injections. Therefore, inclusion of VEH-treated groups is an important control for all experiments. Increased diaphyseal I_{MAX} with injections also highlights the need to

include VEH-treated mice in strain gauging experiments when determining appropriate load magnitudes to apply.

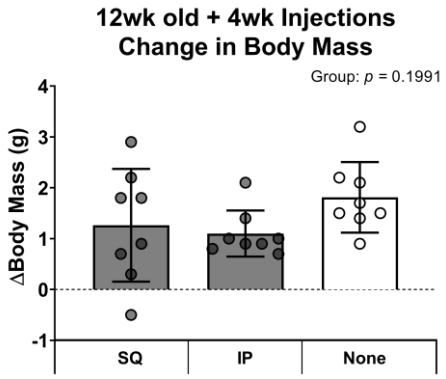

Figure C.3 Change in body mass over the course of treatment.

Table C.1 MicroCT results for the cancellous metaphysis and cortical diaphysis.

	Subcutaneous (SQ)	**Intraperitoneal (IP)**	**None**
Metaphysis			
BV/TV	0.0847 ± 0.0028^{AB}	0.0930 ± 0.013^{A}	0.0822 ± 0.0062^{B}
Tb.Th (mm)	0.0460 ± 0.0024^{B}	0.0487 ± 0.0012^{A}	0.0475 ± 0.0016^{AB}
Tb.N (1/mm)	3.70±0.23	3.78±0.16	3.58±0.15
Tb.Sp (mm)	0.270±0.019	0.265±0.012	0.280±0.013
cn.TMD (mg HA/cc)	911±22	913±8.2	915±11
Diaphysis			
Ct.Ar (mm^2)	0.664±0.034	0.693±0.039	0.656±0.029
Ma.Ar (mm^2)	0.383±0.026	0.403±0.030	0.373±0.024
Ct.Th (mm)	0.224±0.0077	0.225±0.0063	0.225±0.0034
I_{MAX} (mm^4)	0.0880 ± 0.0092^{AB}	0.0953 ± 0.011^{A}	0.0813 ± 0.010^{B}
I_{MIN} (mm^4)	0.0669±0.0078	0.0749±0.0097	0.0675±0.0066
ct.TMD (mg HA/cc)	1062 ± 7.5^{A}	1052 ± 9.1^{A}	1062 ± 6.4^{A}

Data are mean±SD. Analyzed using an ANOVA for treatment group. Tukey post hoc performed when significant, groups sharing letters are not statistically different, A > B.

C.5 References

[1] J.M. Berger, P. Singh, L. Khrimian, K. Rahmouni, X. Gao, G. Karsenty, J.M. Berger, P. Singh, L. Khrimian, D.A. Morgan, S. Chowdhury, Mediation of the Acute Stress Response by the Skeleton, Cell Metab. (2019) 1–13. doi:10.1016/j.cmet.2019.08.012.

[2] R.A. Larsen, J.L. Peveler, J.B. Klutzke, D.L. Hickman, M.W. Aref, J.M. Wallace, D.M. Brown, M.R. Allen, Effects of daily restraint with and without injections on skeletal properties in C57BL/6NHsd mice, Lab Anim. (NY). 46 (2017) 299–301. doi:10.1038/laban.1295.

[3] K.M. Melville, N.H. Kelly, S. a Khan, J.C. Schimenti, F.P. Ross, R.P. Main, M.C. van der Meulen, Female mice lacking estrogen receptor-alpha in osteoblasts have compromised bone mass and strength, J Bone Min. Res. 29 (2014) 370–379. doi:10.1002/jbmr.2082.

Appendix D

CHAPTER 3 DATA

Table D.1 Moderate load magnitude (6.5N) adult 26-week-old pOC-ERαKO (cKO) and LC female phenotype measures.

Animal ID	Genotype	Body Mass (g)	Crown/ Rump Length (mm)	Ovary Mass (g)	Uterine Mass (g)	Left Tibia Length (mm)	Right Tibia Length (mm)
A8501	cKO	20.9	85.91	0.0251	0.0619	17.763	18.101
A8509	cKO	25.58	86.1	0.022	0.0824	18.194	17.807
A8510	cKO	20.36	85.05	0.0217	0.0865	17.742	17.742
A8513	cKO	21.43	85.93	0.0241	0.0535	17.947	17.712
B8607	cKO	21.66	86.32	0.0312	0.0748	18.506	18.265
B9404	cKO	24.02	90.99	0.0339	0.1484	18.417	18.476
B9405	cKO	21.94	87.49	0.0297	0.0497	18.039	17.793
B9407	cKO	22.12	84.2	0.0338	0.0555	18.015	18.348
C8403	LC	21.43	85.85	0.0358	0.091	18.167	18.043
C8406	LC	25.59	91.04	0.0325	0.0562	17.757	17.59
C8410	LC	21.01	86.71	0.0393	0.0968	17.26	17.599
C8905	LC	23.6	88.77	0.0325	0.0804	18.117	18.39
D8912	LC	23.06	90.95	0.0206	0.0796	18.045	18.155
D8913	LC	23.85	90.68	0.029	0.0525	17.833	18.401
D8914	LC	22.38	89.07	0.0297	0.0866	18.016	18.025
D9403	LC	22.37	87.78	0.0321	0.1191	17.968	18.028

Table D.2 Adult 26-week-old pOC-ERαKO (cKO) and LC male phenotype measures.

Animal ID	Genotype	Body Mass (g)	Crown/ Rump Length (mm)	Left Tibia Length (mm)	Right Tibia Length (mm)
E8409	cKO	27.52	89.2	17.633	18.061
E8413	cKO	28.93	93.21	17.827	18.022
E8603	cKO	27.23	93.72	17.477	17.166
F8904	cKO	29.58	94.16	17.983	17.788
F9301	cKO	28.82	91.17	17.71	17.282
F9305	cKO	31.01	93.75	17.672	17.944
G9112	cKO	31.14	97.35	18.006	18.049
G9406	cKO	30.7	95.54	17.715	17.785
G9409	cKO	32.56	99.54	18.171	17.954
H8803	LC	31.61	98.47	18.102	17.068
H8805	LC	30.92	93.55	17.412	17.686
H8807	LC	28.42	94.83	17.453	17.285
H9304	LC	30.16	95.59	17.714	17.437
I9111	LC	29.23	95.03	17.18	17.184
I9113	LC	26.62	94.16	17.241	17.086
I9114	LC	29.2	93.64	17.586	17.444
I9408	LC	30.9	93.09	17.868	18.105

Table D.3 High load magnitude (9N) adult 26-week-old pOC-ERαKO (cKO) and LC female phenotype measures.

Animal ID	Genotype	Body Mass (g)	Crown/ Rump Length (mm)	Ovary Mass (g)	Uterine Mass (g)	Left Tibia Length (mm)	Right Tibia Length (mm)
C8112	LC	19.59	85.17	0.0192	0.1214	16.96	16.14
C8206	LC	22.45	86.37	0.0789*	0.0708	16.90	16.84
C8207	LC	20.75	85.36	0.0276	0.0840	16.74	16.84
D8208	LC	21.05	84.32	0.0147	0.0573	16.63	16.48
D8210	LC	20.14	82.60	0.0151	0.0792	17.00	17.11
D8306	LC	21.30	89.72	0.0200	0.0473	17.72	17.20
G7809	cKO	20.92	83.28	0.0185	0.0689	16.99	16.74
G7901	cKO	20.06	85.66	0.0227	0.1375	16.98	16.97
G7906	cKO	21.08	85.67	0.0210	0.0680	16.74	17.36
H8001	cKO	21.26	84.88	0.0270	0.0754	16.99	17.18
H8101	cKO	21.04	87.46	0.0195	0.0527	17.51	17.15
H8105	cKO	20.62	85.16	0.0303	0.0681	17.07	16.85

* Bloody growth on ovary

Table D.4 Moderate load magnitude (6.5N) adult 26-week-old pOC-ERαKO (cKO) and LC female tibial metaphyseal cancellous bone measures from loaded left (L) and control right (R) limbs.

Animal Limb	Genotype	BV/TV	Tb.Th (mm)	Tb.N (1/mm)	Tb.Sp (mm)	cn.TMD (mg HA/cc)
A8501L	cKO	0.0455	0.0612	1.8787	0.5347	890.5996
A8501R	cKO	0.0496	0.0525	1.744	0.563	905.069
A8509L	cKO	0.0492	0.0637	1.4563	0.6985	904.0426
A8509R	cKO	0.0387	0.0507	1.6965	0.5957	847.633
A8510L	cKO	0.0446	0.0673	1.3941	0.7214	907.4701
A8510R	cKO	0.0521	0.0569	1.5457	0.6528	850.666
A8513L	cKO	0.0348	0.064	1.608	0.6235	893.6957
A8513R	cKO	0.0417	0.0567	1.4272	0.713	893
B8607L	cKO	0.0308	0.0596	1.8281	0.5469	903.11
B8607R	cKO	0.0457	0.0502	1.6036	0.6217	862.671
B9404L	cKO	0.0782	0.0571	2.5279	0.3995	851.235
B9404R	cKO	0.0601	0.0489	2.3996	0.4218	880.805
B9405L	cKO	0.0558	0.0639	1.5579	0.6519	896.9813
B9405R	cKO	0.0468	0.0531	1.5558	0.6569	877.52
B9407L	cKO	0.0443	0.0596	1.5696	0.6511	852.435
B9407R	cKO	0.0509	0.0525	2.0512	0.4883	892.179
C8403L	LC	0.0412	0.0486	2.2826	0.4456	859.765
C8403R	LC	0.0618	0.0499	2.9198	0.3433	860.902
C8406L	LC	0.0479	0.0568	2.0493	0.4927	904.058
C8406R	LC	0.043	0.0495	2.1709	0.4578	930.216
C8410L	LC	0.0488	0.0518	2.2205	0.4501	905.637
C8410R	LC	0.0817	0.0499	2.5642	0.3838	883.08
C8905L	LC	0.0623	0.0504	1.9382	0.5176	893.885
C8905R	LC	0.0662	0.0491	2.1726	0.4673	905.384
D8912L	LC	0.0695	0.0529	2.6728	0.3725	905.953
D8912R	LC	0.0665	0.0479	2.9377	0.3406	830.257
D8913L	LC	0.0689	0.0547	2.4623	0.4076	888.704
D8913R	LC	0.0665	0.054	2.6571	0.3771	931.733
D8914L	LC	0.0675	0.06	2.3303	0.431	901.783
D8914R	LC	0.0761	0.0516	2.7362	0.3698	892.558
D9403L	LC	0.061	0.0504	2.899	0.3388	888.135
D9403R	LC	0.0544	0.0477	2.718	0.3654	890.22

Table D.5 Adult 26-week-old pOC-ERαKO (cKO) and LC male tibial metaphyseal cancellous bone measures from loaded left (L) and control right (R) limbs.

Animal Limb	Genotype	BV/TV	Tb.Th (mm)	Tb.N (1/mm)	Tb.Sp (mm)	cn.TMD (mg HA/cc)
E8409L	cKO	0.1739	0.0493	4.4166	0.2131	887.314
E8409R	cKO	0.1531	0.0431	4.4598	0.2184	895.148
E8413L	cKO	0.1519	0.0499	4.1963	0.226	879.226
E8413R	cKO	0.1343	0.0428	4.3004	0.2245	879.542
E8603L	cKO	0.1466	0.0505	4.2778	0.2207	880.047
E8603R	cKO	0.1363	0.0517	4.3866	0.2194	899.887
F8904L	cKO	0.1624	0.0491	4.4745	0.2136	889.462
F8904R	cKO	0.142	0.0399	4.4974	0.216	871.075
F9301L	cKO	0.1522	0.0522	3.8943	0.2492	873.35
F9301R	cKO	0.1408	0.0425	3.6721	0.2687	863.493
F9305L	cKO	0.1457	0.0517	3.8726	0.2479	893.442
F9305R	cKO	0.1413	0.0441	4.0734	0.2357	857.49
G9112L	cKO	0.1639	0.0527	4.1981	0.2266	900.709
G9112R	cKO	0.1384	0.0406	4.3116	0.2269	863.745
G9406L	cKO	0.131	0.0544	3.8308	0.2492	883.838
G9406R	cKO	0.151	0.0582	4.1046	0.2309	920.865
G9409L	cKO	0.1242	0.0543	3.7804	0.2502	905.195
G9409R	cKO	0.12	0.049	3.9901	0.239	924.34
H8803L	LC	0.1123	0.0504	3.3043	0.2968	888.64
H8803R	LC	0.1112	0.0401	3.6795	0.2669	877.393
H8805L	LC	0.202	0.0561	4.7013	0.1925	886.303
H8805R	LC	0.1546	0.0413	4.6248	0.2056	879.415
H8807L	LC	0.127	0.0491	3.9156	0.2474	900.709
H8807R	LC	0.1075	0.0392	4.0965	0.2362	884.723
H9304L	LC	0.1371	0.0488	4.0592	0.2342	909.302
H9304R	LC	0.1161	0.0402	3.9891	0.2434	873.097
I9111L	LC	0.1516	0.0489	4.1434	0.2327	878.468
I9111R	LC	0.1296	0.042	4.2429	0.2301	842.768
I9113L	LC	0.157	0.0532	4.414	0.2086	880.11
I9113R	LC	0.1451	0.0459	4.5018	0.209	904.689
I9114L	LC	0.1445	0.0491	4.2547	0.2242	923.519
I9114R	LC	0.1397	0.0413	4.3698	0.2194	904.816
I9408L	LC	0.1232	0.0604	3.837	0.2486	890.9155
I9408R	LC	0.1017	0.0535	3.8352	0.2549	901.909

Table D.6 High load magnitude (9N) adult 26-week-old pOC-ERαKO (cKO) and LC female tibial metaphyseal cancellous bone measures from loaded left (L) and control right (R) limbs.

Animal Limb	Genotype	BV/TV	Tb.Th (mm)	Tb.N (1/mm)	Tb.Sp (mm)	cn.TMD (mg HA/cc)
C8112L	LC	0.0772	0.0558	2.6148	0.3834	815.203
C8112R	LC	0.0717	0.0495	2.9727	0.3367	784.471
C8206L	LC	0.0862	0.0629	2.6497	0.3831	813.0544
C8206R	LC	0.0607	0.0462	2.7087	0.3813	790.331
C8207L	LC	0.0706	0.0591	2.6504	0.3813	806.348
C8207R	LC	0.0534	0.0502	2.5354	0.401	815.203
D8208L	LC	0.07	0.0602	2.8285	0.3524	806.2179
D8208R	LC	0.0703	0.05	2.8639	0.3511	813.184
D8210L	LC	0.0568	0.0583	2.3533	0.4277	820.542
D8210R	LC	0.0655	0.0519	3.1142	0.3185	830.178
D8306L	LC	0.0462	0.0603	2.0382	0.4964	809.7338
D8306R	LC	0.0502	0.0552	2.0573	0.5031	821.714
G7809L	cKO	0.0686	0.0781	1.3393	0.7844	800.2278
G7809R	cKO	0.032	0.0469	1.6228	0.6241	790.982
G7901L	cKO	0.0478	0.0731	1.5864	0.6412	802.3113
G7901R	cKO	0.0275	0.0505	1.7729	0.5718	801.985
G7906L	cKO	0.0536	0.0685	1.3966	0.7259	809.0827
G7906R	cKO	0.0371	0.0581	1.9096	0.5409	800.032
H8001L	cKO	0.0626	0.0731	1.7585	0.5761	815.0078
H8001R	cKO	0.0523	0.0541	1.7587	0.5815	813.9
H8101L	cKO	0.0397	0.0714	1.6739	0.6025	818.1981
H8101R	cKO	0.0389	0.0521	1.6546	0.6184	811.947
H8105L	cKO	0.035	0.0726	1.7203	0.5975	840.8564
H8105R	cKO	0.0296	0.0507	1.5756	0.6435	800.032

Table D.7 Moderate load magnitude (6.5N) adult 26-week-old pOC-ERαKO (cKO) and LC female tibial metaphyseal cortical shell bone measures from loaded left (L) and control right (R) limbs.

Animal Limb	Genotype	Ct.Ar (mm^2)	Ct.Th (mm)	I_{MAX} (mm^4)	I_{MIN} (mm^4)	ct.TMD (mg HA/cc)
A8501L	cKO	0.92677	0.141	0.39965	0.23418	983.3556
A8501R	cKO	0.82354	0.14	0.28662	0.22292	1030.3655
A8509L	cKO	0.91603	0.152	0.33999	0.25688	1030.9973
A8509R	cKO	0.83071	0.134	0.32724	0.23374	1012.2313
A8510L	cKO	0.98585	0.157	0.38216	0.24642	1000.7316
A8510R	cKO	0.78778	0.142	0.2557	0.18199	1000.4788
A8513L	cKO	0.99969	0.156	0.38668	0.25223	1000.4788
A8513R	cKO	0.80547	0.143	0.27464	0.19333	1027.5221
B8607L	cKO	0.91859	0.137	0.36512	0.26555	1002.1216
B8607R	cKO	0.84756	0.14	0.28635	0.23598	1025.8162
B9404L	cKO	0.817	0.141	0.29248	0.21696	971.2872
B9404R	cKO	0.80712	0.123	0.33469	0.22941	986.6412
B9405L	cKO	0.92573	0.163	0.33412	0.22026	1032.0714
B9405R	cKO	0.81482	0.143	0.28035	0.19064	1019.4344
B9407L	cKO	0.98237	0.144	0.39964	0.25419	963.7682
B9407R	cKO	0.82787	0.144	0.29112	0.20906	1027.7749
C8403L	LC	0.97575	0.151	0.35879	0.25496	1028.0908
C8403R	LC	0.88846	0.156	0.2898	0.22361	1040.2224
C8406L	LC	1.03441	0.167	0.39364	0.30406	1057.3456
C8406R	LC	0.95739	0.165	0.3389	0.25097	1087.6113
C8410L	LC	1.00848	0.161	0.34904	0.25632	1037.7582
C8410R	LC	0.86629	0.15	0.28624	0.22826	1037.5686
C8905L	LC	0.96019	0.148	0.37702	0.29037	1013.8109
C8905R	LC	0.92274	0.154	0.33852	0.2566	1042.1179
D8912L	LC	0.97827	0.158	0.37115	0.27292	1061.1367
D8912R	LC	0.9484	0.16	0.34402	0.23949	1046.1617
D8913L	LC	1.03289	0.177	0.37644	0.28532	1060.5049
D8913R	LC	0.94627	0.159	0.34533	0.25311	1068.7821
D8914L	LC	1.00731	0.147	0.40964	0.3254	1028.0908
D8914R	LC	1.00453	0.141	0.42834	0.3271	1027.0166
D9403L	LC	0.99512	0.164	0.36514	0.26541	1039.2745
D9403R	LC	0.90077	0.162	0.29632	0.21452	1060.4417

Table D.8 Adult 26-week-old pOC-ERαKO (cKO) and LC male tibial metaphyseal cortical shell bone measures from loaded left (L) and control right (R) limbs.

Animal Limb	Genotype	Ct.Ar (mm^2)	Ct.Th (mm)	I_{MAX} (mm^4)	I_{MIN} (mm^4)	ct.TMD (mg HA/cc)
E8409L	cKO	1.07943	0.147	0.51208	0.36565	967.3698
E8409R	cKO	0.96805	0.134	0.43688	0.32858	990.3691
E8413L	cKO	1.11461	0.153	0.52677	0.34613	970.9081
E8413R	cKO	0.95757	0.142	0.45027	0.3021	991.1906
E8603L	cKO	1.11819	0.148	0.52729	0.35827	954.4167
E8603R	cKO	0.9723	0.138	0.4395	0.29866	972.2982
F8904L	cKO	1.09376	0.141	0.57405	0.36877	970.1499
F8904R	cKO	0.95258	0.135	0.4749	0.33775	1000.6052
F9301L	cKO	1.23067	0.16	0.60097	0.42164	970.7817
F9301R	cKO	0.99064	0.144	0.42762	0.32183	998.141
F9305L	cKO	1.1625	0.148	0.58902	0.40748	982.7238
F9305R	cKO	1.03642	0.153	0.48625	0.30976	998.0146
G9112L	cKO	1.15338	0.148	0.5383	0.41005	977.353
G9112R	cKO	1.01718	0.146	0.46668	0.33899	1002.3744
G9406L	cKO	1.27116	0.163	0.60425	0.45118	957.576
G9406R	cKO	1.01542	0.146	0.47668	0.34211	1002.248
G9409L	cKO	1.31244	0.164	0.63308	0.47484	964.7792
G9409R	cKO	0.97619	0.136	0.472	0.3364	1005.8496
H8803L	LC	1.1579	0.142	0.65993	0.39513	971.0344
H8803R	LC	0.95281	0.135	0.50062	0.3093	1005.0913
H8805L	LC	1.20176	0.162	0.57367	0.40553	966.8643
H8805R	LC	0.98248	0.136	0.49166	0.3398	979.1222
H8807L	LC	1.03934	0.127	0.53177	0.33582	966.3588
H8807R	LC	0.90547	0.13	0.43724	0.29208	995.3608
H9304L	LC	1.21536	0.149	0.66018	0.43238	980.2595
H9304R	LC	0.96846	0.141	0.47291	0.31771	998.3937
I9111L	LC	1.17344	0.155	0.58016	0.36661	984.7457
I9111R	LC	1.03464	0.146	0.49212	0.33582	982.155
I9113L	LC	1.19293	0.155	0.52241	0.40244	959.9138
I9113R	LC	0.98367	0.135	0.42068	0.35898	989.8005
I9114L	LC	1.12173	0.149	0.5235	0.43393	996.4982
I9114R	LC	0.99298	0.138	0.45483	0.34026	1004.4595
I9408L	LC	1.18639	0.169	0.54323	0.35903	980.1332
I9408R	LC	0.98999	0.154	0.44276	0.28263	1001.9321

Table D.9 High load magnitude (9N) adult 26-week-old pOC-ERαKO (cKO) and LC female tibial metaphyseal cortical shell bone measures from loaded left (L) and control right (R) limbs.

Animal Limb	Genotype	Ct.Ar (mm^2)	Ct.Th (mm)	I_{MAX} (mm^4)	I_{MIN} (mm^4)	ct.TMD (mg HA/cc)
C8112L	LC	1.10168	0.167	0.46476	0.30564	979.4108
C8112R	LC	0.93393	0.155	0.32987	0.25927	998.6182
C8206L	LC	1.17788	0.18	0.47343	0.32144	954.3434
C8206R	LC	0.918	0.157	0.3244	0.22686	1000.0507
C8207L	LC	1.20387	0.176	0.49035	0.35978	961.5706
C8207R	LC	0.94637	0.154	0.32865	0.27829	1006.8221
D8208L	LC	1.10328	0.166	0.46156	0.30469	950.4368
D8208R	LC	0.96478	0.164	0.33474	0.25717	1012.3565
D8210L	LC	1.16011	0.18	0.43839	0.31441	976.2855
D8210R	LC	1.04989	0.164	0.3944	0.30386	1007.2779
D8306L	LC	1.06395	0.184	0.36761	0.25767	974.3322
D8306R	LC	0.92499	0.161	0.33326	0.21981	1016.2631
G7809L	cKO	1.12664	0.178	0.46449	0.29632	931.0991
G7809R	cKO	0.84735	0.137	0.29643	0.25006	971.1418
G7901L	cKO	1.10458	0.172	0.42234	0.30073	933.7034
G7901R	cKO	0.81394	0.136	0.28191	0.21601	968.4072
G7906L	cKO	1.13785	0.175	0.46745	0.30266	918.0119
G7906R	cKO	0.8154	0.139	0.2991	0.21234	950.6972
H8001L	cKO	1.20354	0.184	0.4838	0.33767	935.1359
H8001R	cKO	0.90437	0.146	0.3348	0.25337	979.0201
H8101L	cKO	1.08257	0.173	0.40584	0.28453	933.7034
H8101R	cKO	0.86871	0.136	0.31781	0.25039	959.9428
H8105L	cKO	1.17634	0.174	0.47046	0.32937	946.3349
H8105R	cKO	0.87896	0.139	0.32544	0.26048	971.5976

Table D.10 Moderate load magnitude (6.5N) adult 26-week-old pOC-ERαKO (cKO) and LC female tibial diaphyseal cortical bone measures from loaded left (L) and control right (R) limbs.

Animal Limb	Genotype	Ct.Ar (mm^2)	Ma.Ar (mm^2)	Ct.Th (mm)	I_{MAX} (mm^4)	I_{MIN} (mm^4)	ct.TMD (mg HA/cc)
A8501L	cKO	0.66736	0.4164	0.21	0.09771	0.07305	1055.8291
A8501R	cKO	0.57078	0.38945	0.197	0.07375	0.05185	1074.3424
A8509L	cKO	0.66627	0.40257	0.221	0.0894	0.06978	1079.2709
A8509R	cKO	0.63063	0.41395	0.209	0.08201	0.06727	1061.5159
A8510L	cKO	0.65754	0.4038	0.212	0.09758	0.06637	1057.7878
A8510R	cKO	0.58073	0.35008	0.206	0.06581	0.05504	1060.1257
A8513L	cKO	0.62452	0.40742	0.205	0.08623	0.06154	1064.8015
A8513R	cKO	0.61612	0.42628	0.2	0.08216	0.06666	1044.7085
B8607L	cKO	0.60647	0.42179	0.2	0.07891	0.06423	1062.7163
B8607R	cKO	0.56028	0.35642	0.201	0.06199	0.05204	1049.8265
B9404L	cKO	0.66002	0.40592	0.217	0.08952	0.06852	1036.6208
B9404R	cKO	0.57214	0.41176	0.192	0.07063	0.05792	1050.0792
B9405L	cKO	0.68302	0.37893	0.226	0.08848	0.07313	1065.6229
B9405R	cKO	0.60776	0.37918	0.207	0.07581	0.06059	1048.7524
B9407L	cKO	0.57175	0.38539	0.198	0.06789	0.05592	1050.5216
B9407R	cKO	0.62417	0.40942	0.204	0.08643	0.06265	1052.2908
C8403L	LC	0.59762	0.35456	0.21	0.07167	0.05399	1076.9962
C8403R	LC	0.65016	0.36457	0.221	0.08061	0.06547	1063.7905
C8406L	LC	0.69557	0.40021	0.226	0.09933	0.0725	1079.2078
C8406R	LC	0.6743	0.41078	0.219	0.0957	0.06998	1080.661
C8410L	LC	0.62252	0.32106	0.222	0.07416	0.05473	1090.9602
C8410R	LC	0.66408	0.35328	0.226	0.08036	0.06918	1072.2573
C8905L	LC	0.70298	0.45374	0.215	0.10638	0.08329	1053.6177
C8905R	LC	0.66349	0.39674	0.218	0.08733	0.07052	1083.5043
D8912L	LC	0.76163	0.42195	0.239	0.11552	0.08669	1083.062
D8912R	LC	0.68706	0.38252	0.231	0.08203	0.07837	1078.7023
D8913L	LC	0.7736	0.39299	0.241	0.10579	0.09278	1081.6088
D8913R	LC	0.71057	0.32282	0.246	0.08956	0.06469	1109.9158
D8914L	LC	0.73143	0.47534	0.219	0.11736	0.09108	1051.9116
D8914R	LC	0.63832	0.40571	0.209	0.08301	0.06876	1064.296
D9403L	LC	0.67237	0.36828	0.23	0.08542	0.06613	1082.7461
D9403R	LC	0.61929	0.40044	0.209	0.07174	0.06856	1068.719

Table D.11 Adult 26-week-old pOC-ERαKO (cKO) and LC male tibial diaphyseal cortical bone measures from loaded left (L) and control right (R) limbs.

Animal Limb	Genotype	Ct.Ar (mm^2)	Ma.Ar (mm^2)	Ct.Th (mm)	I_{MAX} (mm^4)	I_{MIN} (mm^4)	ct.TMD (mg HA/cc)
E8409L	cKO	0.83246	0.60627	0.226	0.18236	0.10799	1059.6202
E8409R	cKO	0.78019	0.64052	0.204	0.17157	0.10704	1039.2745
E8413L	cKO	0.83012	0.58285	0.224	0.17797	0.10835	1042.6866
E8413R	cKO	0.79022	0.64652	0.212	0.15994	0.11644	1043.5081
E8603L	cKO	0.77623	0.45939	0.235	0.12903	0.08767	1050.0792
E8603R	cKO	0.79148	0.54493	0.218	0.16658	0.09688	1020.5085
F8904L	cKO	0.80541	0.62625	0.22	0.16008	0.1112	1087.1058
F8904R	cKO	0.83276	0.76322	0.201	0.21068	0.12876	1037.9478
F9301L	cKO	0.84128	0.55755	0.235	0.17836	0.1009	1061.7053
F9301R	cKO	0.83356	0.62334	0.222	0.192	0.10326	1051.8485
F9305L	cKO	0.96257	0.60013	0.241	0.25484	0.13061	1033.272
F9305R	cKO	0.88812	0.66202	0.221	0.22789	0.1242	1014.7587
G9112L	cKO	0.83483	0.60199	0.229	0.17276	0.10913	1070.8041
G9112R	cKO	0.86244	0.61518	0.23	0.19088	0.11405	1062.9691
G9406L	cKO	0.84931	0.51632	0.237	0.18937	0.0926	1050.2057
G9406R	cKO	0.8846	0.48963	0.257	0.18349	0.09643	1074.7216
G9409L	cKO	0.82615	0.55216	0.232	0.16336	0.10193	1031.8187
G9409R	cKO	0.90822	0.5096	0.248	0.21249	0.10019	1047.6151
H8803L	LC	0.83043	0.68513	0.219	0.18216	0.12189	1076.0485
H8803R	LC	0.87157	0.85876	0.204	0.22359	0.15897	1031.6292
H8805L	LC	0.97765	0.62464	0.248	0.22885	0.15255	1061.3263
H8805R	LC	0.9054	0.73785	0.213	0.24062	0.14726	1024.426
H8807L	LC	0.78157	0.6276	0.213	0.15	0.11452	1068.5925
H8807R	LC	0.76813	0.68918	0.201	0.16235	0.11364	1049.9529
H9304L	LC	0.84384	0.6396	0.229	0.17332	0.11976	1078.3231
H9304R	LC	0.77721	0.6518	0.209	0.15942	0.10771	1052.8594
I9111L	LC	0.84678	0.64503	0.225	0.1897	0.1158	1057.6615
I9111R	LC	0.87673	0.62134	0.233	0.189	0.11894	1045.5299
I9113L	LC	0.82159	0.40825	0.256	0.14202	0.08327	1065.686
I9113R	LC	0.76045	0.43494	0.234	0.13383	0.07618	1073.3314
I9114L	LC	0.87379	0.63317	0.232	0.18835	0.12459	1074.8479
I9114R	LC	0.82288	0.62304	0.218	0.17874	0.11165	1049.3843
I9408L	LC	0.86606	0.46652	0.253	0.15908	0.10075	1058.6093
I9408R	LC	0.80614	0.50796	0.233	0.15158	0.09625	1051.0271

Table D.12 High load magnitude (9N) adult 26-week-old pOC-ERαKO (cKO) and LC female tibial diaphyseal cortical bone measures from loaded left (L) and control right (R) limbs.

Animal Limb	Genotype	Ct.Ar (mm^2)	Ma.Ar (mm^2)	Ct.Th (mm)	I_{MAX} (mm^4)	I_{MIN} (mm^4)	ct.TMD (mg HA/cc)
C8112L	LC	0.6962	0.36445	0.233	0.09423	0.06933	1079.0292
C8112R	LC	0.64936	0.39426	0.213	0.08715	0.06693	1052.9851
C8206L	LC	0.74872	0.34813	0.254	0.09805	0.07505	1076.3596
C8206R	LC	0.65268	0.38657	0.217	0.07959	0.07234	1069.1975
C8207L	LC	0.7959	0.3473	0.26	0.11813	0.07827	1061.5145
C8207R	LC						
D8208L	LC	0.71378	0.32307	0.249	0.09108	0.06645	1065.3561
D8208R	LC	0.66026	0.33141	0.234	0.07601	0.0646	1088.8608
D8210L	LC	0.76503	0.34014	0.258	0.10492	0.07565	1083.652
D8210R	LC	0.70285	0.32575	0.244	0.08449	0.06909	1088.0144
D8306L	LC	0.69408	0.32472	0.241	0.08612	0.06661	1076.0341
D8306R	LC	0.67305	0.3545	0.23	0.08116	0.07004	1082.7405
G7809L	cKO	0.76997	0.40396	0.242	0.11791	0.08168	1029.6757
G7809R	cKO	0.62044	0.40192	0.201	0.08908	0.06054	1034.8845
G7901L	cKO	0.72615	0.33772	0.244	0.09387	0.0706	1011.0543
G7901R	cKO	0.54671	0.41911	0.184	0.06763	0.05618	1038.4656
G7906L	cKO	0.71931	0.37583	0.239	0.10163	0.07129	1036.8379
G7906R	cKO	0.56783	0.3605	0.2	0.06123	0.0573	1035.9915
H8001L	cKO	0.7434	0.34694	0.248	0.10486	0.07121	1040.8096
H8001R	cKO	0.56833	0.39715	0.196	0.06489	0.05978	1056.5662
H8101L	cKO	0.65874	0.37415	0.223	0.09008	0.06141	1044.1953
H8101R	cKO	0.5396	0.29428	0.207	0.05936	0.03911	1077.2061
H8105L	cKO	0.75412	0.40406	0.24	0.11803	0.07676	1044.651
H8105R	cKO	0.64706	0.39834	0.204	0.09807	0.0633	1030.2617

Appendix E

CHAPTER 4 DATA

Table E.1 Demographic and anatomical data from the femoral neck (FN)for patients treated with teriparatide (TPTD) or placebo (PBO).

ID #	Treatment	Sex	Age (y)	BMI	Body Weight (lbs)	FN Angle (°)	FN Offset (mm)
3	PBO	F	64	35.96	203	142	36
8	PBO	F	69	27.25	149	133	43
9	TPTD	F	72	33.48	189	137	34
11	TPTD	F	63	23.24	119	153	20
14	TPTD	F	64	24.33	160	124	56
15	TPTD	M	69	23.73	175	128	58
16	PBO	F	71	23.57	155	131	50
24	TPTD	M	83	23.57	155	136	45
25	TPTD	F	84	24.98	141		
28	TPTD	F	75	19.75	108	136	42
30	PBO	F	80	19.85	123	131	40
32	PBO	M	76	38.77	255	140	44
37	PBO	F	68	32.81	168	138	33
39	TPTD	F	84	27.25	149	135	44
40	PBO	F	62	33.81	197	141	32
41	PBO	M	63	38.74	270	135	38
42	PBO	M	64	34.11	231	134	32
43	PBO	M	63	30.85	215	134	39
44	PBO	M	70	27.50	220	137	43
45	TPTD	F	79	33.07	175	137	35
47	TPTD	F	89	23.21	131	142	34
51	TPTD	M	60	35.57	300	144	45
53	PBO	M	80	25.85	170	135	41
54	PBO	F	63	32.03	164	137	32
55	TPTD	M	70	33.15	218	135	42
56	PBO	F	68	25.50	158	132	47
59	TPTD	M	62	28.66	183	129	49
61	TPTD	F	57	30.27	155	136	35
63	PBO	F	69	39.33	222	124	44
64	TPTD	M	64	23.10	161	138	35
67	PBO	F	68	32.56	178	138	39
68	TPTD	F	74	18.89	100	135	33
69	TPTD	F	79	35.14	174	142	31
70	PBO	F	64	24.53	152	134	32
72	TPTD	F	69	22.45	161	137	35
73	TPTD	F	66	23.34	136	142	32
76	TPTD	M	60	33.73	209	139	34
77	TPTD	M	80	25.84	165	131	41

Table E.2 Anatomical data in the tensile (T) and compressive (C) regions of the femoral neck for patients treated with teriparatide (TPTD) or placebo (PBO).

ID #	Treatment	Ct.Wi.T (mm)	Ct.Wi.C (mm)	Ct.Po.Ar.T (%)	Ct.Po.Ar.C (%)
3	PBO	0.624	1.789	7.73	19.59
8	PBO	0.473	1.286	8.59	5.08
9	TPTD	0.606	1.801	12.36	15.88
11	TPTD	0.400	1.294	8.90	13.15
14	TPTD	0.903	1.103	10.10	6.20
15	TPTD	0.515	1.382	11.31	8.53
16	PBO	0.781	1.682	13.03	4.76
24	TPTD	0.413	1.398	8.32	6.86
25	TPTD	0.338	1.422	7.52	7.90
28	TPTD	0.904	0.590	12.72	11.15
30	PBO	0.441	1.702	13.16	9.68
32	PBO	0.562	1.669	12.95	12.45
37	PBO	0.585	2.059	12.72	10.63
39	TPTD	1.152	0.535	7.05	7.43
40	PBO	0.766	0.634	3.37	4.16
41	PBO	0.313	1.254	4.55	7.96
42	PBO	0.232	1.107	5.84	4.88
43	PBO	1.254	0.802	7.98	9.45
44	PBO	0.569	1.445	13.40	13.02
45	TPTD	0.560	0.631	11.89	12.32
47	TPTD	1.109	2.823	18.84	16.54
51	TPTD	0.586	1.652	6.77	10.19
53	PBO	0.804	1.746	10.99	10.50
54	PBO	0.586	2.145	9.06	11.26
55	TPTD	1.356	1.447	7.63	5.64
56	PBO	0.731	0.785	9.15	9.17
59	TPTD	0.439	1.238	7.49	9.23
61	TPTD	0.460	0.935	14.43	12.39
63	PBO	0.525	0.861	8.48	6.17
64	TPTD	0.751	1.223	6.82	4.89
67	PBO	0.794	1.899	11.15	14.95
68	TPTD	1.282	1.233	15.44	7.69
69	TPTD	0.899	0.671	13.50	10.77
70	PBO	0.307	0.417	8.38	5.77
72	TPTD	0.389	0.537	13.61	8.81
73	TPTD	0.322	0.894	7.30	9.46
76	TPTD	0.224	0.678	11.53	18.06
77	TPTD	0.744	2.273	8.92	13.59

Table E.3 Endocortical bone formation data in the tensile and compressive regions of the femoral neck for patients treated with teriparatide (TPTD) or placebo (PBO).

		Tensile			Compressive		
ID #	Treatment	MS/BS (%)	MAR (μm/d)	BFR/BS ($mm^3/mm^2/y$)	MS/BS (%)	MAR (μm/d)	BFR/BS ($mm^3/mm^2/y$)
3	PBO	26.4103	0.5789	0.0557	13.6912	0.6751	0.0444
8	PBO	19.4663	0.8026	0.0552	3.4234	0.6150	0.0077
9	TPTD	1.8291	1.0077	0.0082	14.4451	0.6120	0.0555
11	TPTD	25.3709	0.7753	0.0729	24.0199	0.8990	0.0741
14	TPTD	33.2595	0.8103	0.0968	3.3068	0.7960	0.0095
15	TPTD	13.9411	0.6147	0.0480	6.4609	0.6844	0.0166
16	PBO	1.2108		0.0000	1.4773		
24	TPTD	34.6041	0.6449	0.0846	10.8665	0.7153	0.0537
25	TPTD	4.7928	0.5299	0.0113	19.3276	0.6414	0.0473
28	TPTD	38.0012	0.7957	0.1109	28.1283	0.9609	0.0987
30	PBO	4.6203	0.5824	0.0105	14.6196	0.6760	0.0612
32	PBO	8.2913	0.8642	0.0496	2.0454		
37	PBO	1.5263	0.5594	0.0031	1.0322		0.0000
39	TPTD	24.0982	0.6088	0.0534	7.1916	0.8174	0.0215
40	PBO	8.0416	0.6019	0.0203	6.3925	0.5563	0.0118
41	PBO	5.1440	0.4374	0.0082	6.0884	0.4933	0.0189
42	PBO	39.6077	0.7688	0.1112	1.7067	0.7782	0.0071
43	PBO	2.9741	0.3936	0.0043	13.4883	0.5622	0.0136
44	PBO	1.9889			5.0059	0.8241	0.0203
45	TPTD	44.6959	0.7951	0.1282	24.8392	0.7704	0.0708
47	TPTD	33.3291	0.6177	0.0742	25.4558	0.6276	0.0566
51	TPTD	8.1506	0.8384	0.0216	6.0227	0.5653	0.0128
53	PBO	18.4881	0.6425	0.0433	3.6826		
54	PBO	5.5819	0.6217	0.0179	3.8469	0.7226	0.0151
55	TPTD	2.9147			6.5162	0.5135	0.0166
56	PBO	9.3291	0.6995	0.0239	17.4052	0.7982	0.0520
59	TPTD	1.1371	0.3734	0.0016	4.8967	0.5425	0.0095
61	TPTD	10.0630	0.6002	0.0402	7.7356	0.4839	0.0130
63	PBO	19.7125	0.5288	0.0474	2.7781	0.4791	0.0070
64	TPTD	12.8193	0.5827	0.0417	12.0645	0.5557	0.0254
67	PBO	10.1351	0.6348	0.0231	10.7840	0.6019	0.0242
68	TPTD	11.0235	0.4811	0.0211	11.2653	0.7283	0.0303
69	TPTD	41.4320	0.7285	0.1095	34.8994	0.5958	0.0760
70	PBO	4.8680	0.5332	0.0095	11.8673	0.7987	0.0349
72	TPTD	20.6697	0.5182	0.0391	8.2013	0.5770	0.0179
73	TPTD	11.3677	0.7014	0.0484	6.8198	0.5715	0.0157
76	TPTD	6.4949	0.6247	0.0275	3.4891	0.4673	0.0057
77	TPTD	18.9904	0.6022	0.0451	11.5519	0.5652	0.0238

Table E.4 Endocortical bone resorption data in the tensile and compressive regions of the femoral neck for patients treated with teriparatide (TPTD) or placebo (PBO).

		Tensile		Compressive	
ID #	Treatment	ES/BS (%)	Oc.N/BS (#/mm)	ES/BS (%)	Oc.N/BS (#/mm)
3	PBO	4.010	0.2278	4.918	0.1197
8	PBO	6.625	0.1002	6.378	0.3780
9	TPTD	4.514	0.2772	4.562	0.1691
11	TPTD	7.064	0.5111	11.927	0.3769
14	TPTD	10.346	0.3664	5.382	0.1639
15	TPTD	2.913	0.1283	3.273	0.1029
16	PBO	2.481	0	7.301	0
24	TPTD	6.119	0	6.833	0
25	TPTD	2.408	0	6.724	0.1186
28	TPTD	6.723	0.4077	4.588	0.1043
30	PBO	5.255	0.1952	20.172	0.1208
32	PBO	1.519	0	3.010	0
37	PBO	2.320	0	1.520	0
39	TPTD	5.180	0.1884	12.073	0.1575
40	PBO	3.180	0.0844	13.923	0.1828
41	PBO	4.527	0	25.145	0
42	PBO	10.883	0.3270	1.010	0.0417
43	PBO	1.351	0	2.846	0
44	PBO	3.413	0.0182	1.524	0.0204
45	TPTD	15.125	0.2342	5.271	0.0911
47	TPTD	2.071	0.0359	5.131	0.1579
51	TPTD	1.246	0.0785	2.873	0.0472
53	PBO	3.490	0.1684	2.951	0
54	PBO	1.206	0.0596	7.308	0.1526
55	TPTD	2.456	0	4.349	0
56	PBO	7.312	0.1523	4.200	0.0937
59	TPTD	0.513	0	1.056	0
61	TPTD	2.709	0.1218	4.798	0.0720
63	PBO	3.643	0.0206	2.602	0.0550
64	TPTD	0.714	0.0630	4.097	0.0548
67	PBO	2.402	0.1060	6.471	0.2706
68	TPTD	10.392	0.1871	3.217	0.1953
69	TPTD	1.275	0.0277	0.290	0
70	PBO	0.761	0.0236	7.765	0.0935
72	TPTD	7.346	0.1893	3.479	0.0420
73	TPTD	3.968	0.0239	1.463	0.0494
76	TPTD	4.112	0	3.292	0
77	TPTD	3.136	0	4.865	0

Table E.5 Periosteal bone formation data in the tensile and compressive regions of the femoral neck for patients treated with teriparatide (TPTD) or placebo (PBO).

		Tensile			Compressive		
ID #	Treatment	MS/BS (%)	MAR (μm/d)	BFR/BS ($mm^3/mm^2/y$)	MS/BS (%)	MAR (μm/d)	BFR/BS ($mm^3/mm^2/y$)
3	PBO	16.2500	0.5232	0.0411	41.3214	0.8969	0.1612
8	PBO	21.3579	1.2459	0.1054	58.7002	0.9784	0.2098
9	TPTD	4.6645			51.1321	1.4189	0.2798
11	TPTD	13.9540	0.9805	0.0530	31.9598	1.2628	0.1469
14	TPTD	51.5371	0.8816	0.1720	34.5984	0.6144	0.0757
15	TPTD	5.6053	0.6727	0.0074	5.0012	0.7659	0.0150
16	PBO	5.3571	1.3219	0.0259	53.0925	1.0512	0.2105
24	TPTD	40.5455	0.6768	0.1023	49.4577	1.1573	0.2074
25	TPTD	15.5703	0.6532	0.0381	40.7875	0.8975	0.1373
28	TPTD	25.3897	0.9201	0.0863	47.3270	1.1826	0.2044
30	PBO	6.0472			21.9198	0.7775	0.0633
32	PBO	18.0438	0.5878	0.0737	22.5865	0.7112	0.0593
37	PBO	4.5050			10.8751	0.6455	0.0446
39	TPTD	11.1086	0.7454	0.0238	2.2854		
40	PBO	18.4417	0.7422	0.0589	11.3404	0.8339	0.0354
41	PBO	33.3840	1.5805	0.1927	20.9974	0.8191	0.0642
42	PBO	13.8620	0.5138	0.0260	1.3931		0
43	PBO	10.2034	0.6273	0.0235	5.2982		
44	PBO	3.0758			9.7837	0.4172	0.0115
45	TPTD	28.0390	0.9947	0.0948	33.2565	0.6363	0.0860
47	TPTD	43.1435	1.0559	0.1707	21.6180	1.3902	0.0636
51	TPTD	20.5023	1.2222	0.0915	22.2195	1.0165	0.0816
53	PBO	15.9195			40.0564	0.9230	0.1375
54	PBO	13.6582	0.5226	0.0401	61.2980	1.2005	0.2701
55	TPTD	5.3342	0.2562	0.0033	25.6854	1.0053	0.0953
56	PBO	17.5747	0.8588	0.0596	10.3904	1.0361	0.0741
59	TPTD	12.7648	0.8368	0.0142	35.0923	0.9482	0.1215
61	TPTD	38.9533	0.8316	0.1198	51.8758	1.0854	0.2200
63	PBO	12.4186	0.8911	0.0694	4.4537	0.4241	0.0087
64	TPTD	2.9214			19.3533	0.5024	0.0357
67	PBO	0.6054		0	6.1996	1.2104	0.0307
68	TPTD	0.9736		0	1.0204	0.5721	0.0021
69	TPTD	22.8599	1.2551	0.1114	11.3506	0.5081	0.0277
70	PBO	7.1562	0.7410	0.0219	45.6291	1.0845	0.2346
72	TPTD	27.1367	0.3818	0.0356	12.9613		
73	TPTD	26.3424	0.7582	0.0733	8.7127	0.8087	0.0157
76	TPTD	3.0342			5.1057	0.7066	0.0133
77	TPTD	0		0	1.5608		0

Appendix F

CHAPTER 5 DATA

Table F.1 Phenotype data for 10-week-old pOC-ERαKO (cKO) and LC female mice concurrently loaded and treated with PTH or VEH for 2 weeks.

Animal ID	Genotype	Treatment	Body Mass (g)	Left Tibia Length (mm)	Right Tibia Length (mm)
U23008	cKO	PTH	19.9	17.38	17.51
U23009	cKO	PTH	20.0	17.51	17.16
U23010	cKO	PTH	18.1	17.01	17.04
U23015	cKO	PTH	19.7	17.47	17.46
U23112	cKO	PTH	20.2	17.70	17.29
V27101	cKO	PTH	19.3	17.29	
V27208	cKO	PTH	20.4	17.40	17.60
V27607	cKO	PTH	20.1	17.36	17.18
V27915	cKO	PTH	18.7	16.96	16.61
V28202	cKO	PTH	19.9	17.39	17.53
W23105	LC	PTH	20.3	17.25	17.09
W23107	LC	PTH	20.5	17.30	17.14
W23114	LC	PTH	18.8	17.63	17.33
W23901	LC	PTH	19.0	17.38	17.48
W24204	LC	PTH	20.3	17.25	17.18
X27105	LC	PTH	19.2	17.23	17.44
X27106	LC	PTH	18.5	17.06	16.98
X27202	LC	PTH	20.4	17.34	17.32
X27204	LC	PTH	19.6	17.45	17.13
X27407	LC	PTH	18.4	17.21	16.98
Y23312	cKO	VEH	19.3	17.39	17.26
Y23402	cKO	VEH	18.2	16.73	16.87
Y23406	cKO	VEH	19.7	17.35	17.27
Y23408	cKO	VEH	20.0	17.29	17.16
Y23510	cKO	VEH	19.1	16.59	16.41
Z28001	cKO	VEH	19.7	16.96	16.78
Z28004	cKO	VEH	20.1	17.50	17.22
Z28102	cKO	VEH	19.8	17.52	17.53
Z28106	cKO	VEH	18.7	17.20	17.05
Z28305	cKO	VEH	19.7	17.53	17.39
AB23004	LC	VEH	19.7	16.77	16.86
AB23311	LC	VEH	19.5	16.95	17.17
AB23313	LC	VEH	20.9	17.22	17.21
AB23314	LC	VEH	17.8	17.43	17.30
AB23315	LC	VEH	18.7	16.70	16.60
CD27903	LC	VEH	19.1	17.72	17.50
CD27904	LC	VEH		17.23	16.87
CD28016	LC	VEH	20.1	17.10	17.01
CD28017	LC	VEH	18.6	16.84	16.87
CD28107	LC	VEH	18.0	16.67	16.73

Table F.2 Phenotype data for 16-week-old pOC-ERαKO (cKO) and LC female mice concurrently loaded and treated with PTH or VEH for 2 weeks.

Animal ID	Genotype	Treatment	Body Mass (g)	Left Tibia Length (mm)	Right Tibia Length (mm)
A26404	cKO	PTH	20.19	18.05	17.65
A26407	cKO	PTH	20.22	17.60	17.56
A26614	cKO	PTH	19.85	17.45	17.12
A26618	cKO	PTH	20.06	17.12	17.59
A26904	cKO	PTH	22.37	17.38	17.64
B25804	cKO	PTH	22.07	17.75	18.08
B25816	cKO	PTH	20.80	17.49	17.42
B26308	cKO	PTH	22.15	17.98	18.19
B26506	cKO	PTH	21.99	17.44	17.63
B26804	cKO	PTH	20.06	17.29	17.46
C26303	LC	PTH	21.26	17.80	18.10
C26608	LC	PTH	21.72	17.67	17.98
C26611	LC	PTH	18.91	17.32	17.35
C26702	LC	PTH	20.05	17.95	17.98
C26705	LC	PTH	20.48	17.96	17.86
D26805	LC	PTH	20.25	17.50	17.17
D26807	LC	PTH	20.92	17.99	17.77
D26815	LC	PTH	21.35	17.58	17.91
D26908	LC	PTH	21.33	17.73	17.63
D26909	LC	PTH	21.77	17.62	17.82
E25202	cKO	VEH	22.18	17.86	17.91
E25204	cKO	VEH	21.26	17.88	17.70
E25205	cKO	VEH	20.30	17.64	17.40
E25207	cKO	VEH	21.76	17.59	17.72
E25308	cKO	VEH	21.00	18.03	17.84
F25505	cKO	VEH	21.15	17.09	17.55
F25604	cKO	VEH	20.74	17.56	17.45
F25610	cKO	VEH	20.52	17.90	17.83
F25904	cKO	VEH	21.35	17.61	17.51
F25906	cKO	VEH	19.87	17.74	17.17
G25304	LC	VEH	20.42	17.78	16.96
G25803	LC	VEH	20.61	17.71	17.91
G25902	LC	VEH	18.93	17.37	16.96
G25911	LC	VEH	19.67	17.18	17.48
G26101	LC	VEH	22.52	17.69	17.91
H25010	LC	VEH	22.12	18.06	17.83
H25104	LC	VEH	21.8	17.90	17.93
H25109	LC	VEH	24.48	18.28	18.28
H25408	LC	VEH	20.79	17.64	17.57
H25502	LC	VEH	19.41	17.35	17.22

Table F.3 Phenotype data for 16-week-old pOC-ERαKO (cKO) and LC female mice concurrently loaded and treated with PTH or VEH for 6 weeks.

Animal ID	Genotype	Treatment	Body Mass (g)	Left Tibia Length (mm)	Right Tibia Length (mm)
I23806	cKO	PTH	20.7	17.84	17.63
I24607	cKO	PTH	22.0	17.80	17.35
I24609	cKO	PTH	24.6	18.31	17.47
I24701	cKO	PTH	20.9	17.99	18.14
I24702	cKO	PTH	21.2	18.18	17.93
J22006	cKO	PTH	21.7	17.93	17.88
J22102	cKO	PTH	20.6	18.22	18.28
J22801	cKO	PTH	21.1	18.47	17.95
K22510	cKO	PTH	22.7	18.22	17.92
K22513	cKO	PTH	22.3	18.37	17.46
K22514	cKO	PTH	20.9	18.01	17.68
L21504	LC	PTH	22.2	18.20	18.04
L21911	LC	PTH	22.3	18.15	17.67
L21913	LC	PTH	21.8	18.03	17.78
L22105	LC	PTH	21.9	17.62	17.80
L22501	LC	PTH	21.0	17.60	17.60
M23007	LC	PTH	21.0	17.78	17.47
M23405	LC	PTH	21.1	17.92	17.40
M23801	LC	PTH	21.9	17.55	17.54
N24004	LC	PTH	21.2	17.80	17.64
N24011	LC	VEH	22.8	18.02	17.69
N24014	LC	VEH	22.1	17.87	17.84
O23903	cKO	VEH	23.3	18.10	18.01
O24805*	cKO	VEH		18.21	17.82
O24807	cKO	VEH	22.2	17.42	17.61
O24810	cKO	VEH	21.1	18.12	17.52
O24812	cKO	VEH	21.1	17.87	17.70
P22403	cKO	VEH	24.8	18.40	18.24
P22405	cKO	VEH	20.6	18.20	17.38
P22406	cKO	VEH	20.9	18.01	17.71
Q21101	cKO	VEH	24.2	18.38	18.04
Q22314	cKO	VEH	20.6	17.46	17.56
Q22701	cKO	VEH	23.4	18.85	18.17
R21003	LC	VEH	21.9	17.86	17.67
R22004	LC	VEH	22.4	18.06	17.76
R22205	LC	VEH	22.1	18.42	17.74
R22407	LC	VEH	21.9	18.16	18.06
R22711	LC	VEH	22.5	18.00	17.90
S24803	LC	VEH	22.4	18.04	17.82
S24811	LC	VEH	24.8	18.17	18.13
S24813	LC	VEH	23.1	17.98	18.16
T24108	LC	VEH	25.8	17.81	17.45
T24109	LC	VEH	22.1	17.85	17.40
T24305	LC	VEH	19.6	17.77	17.57

* Mouse died on loading day 25 of 30 (5wks)

Table F.4 Phenotype data for baseline 16-week-old wild type (WT) C57Bl/6J female mice pre-treated with PTH or VEH for 6 weeks

Animal ID	PTH or VEH	Body Mass (g)	Left Tibia Length (mm)	Right Tibia Length (mm)
A01	VEH	20.4	17.16	17.28
A02	VEH	20.4	17.44	17.54
A03	VEH	21.7	17.82	17.74
A04	VEH	19.4	16.83	17.18
A05	VEH	20.2	17.21	17.27
A06	VEH	19.5	16.87	17.00
A07	VEH	18.0	16.87	17.10
A08	VEH	17.4	16.73	16.90
B01	PTH	20.8	17.47	17.71
B02	PTH	18.8	17.10	17.14
B03	PTH	20.9	17.48	17.65
B04	PTH	20.4	17.46	17.60
B05	PTH	18.6	17.54	17.61
B06	PTH	21.3	16.80	16.79
B07	PTH	23.5	17.82	17.97
B08	PTH	18.6	17.07	17.08

Table F.5 Phenotype data for 16-week-old wild type (WT) C57Bl/6J female mice pre-treated with PTH or VEH for 6 weeks prior to 2 weeks of tibial loading

Animal ID	Treatment Group	Body Mass (g)	Left Tibia Length (mm)	Right Tibia Length (mm)
C01	VEH/VEH	21.4	17.87	17.77
C02	VEH/VEH	19.3	17.44	17.37
C03	VEH/VEH	20.7	17.99	17.95
C04	VEH/VEH	20.6	17.48	17.60
C05	VEH/VEH	20.2	17.54	17.52
C06	VEH/VEH	19.6	17.73	17.54
C07	VEH/VEH	20.7	17.92	17.54
C08	VEH/VEH	19.5	17.24	17.27
C09	VEH/VEH	19.7	17.77	17.66
C10	VEH/VEH	19.4	17.39	17.32
D01	VEH/PTH	18.6	17.19	17.19
D02	VEH/PTH	22.7	17.92	17.68
D03	VEH/PTH	20.3	17.80	17.36
D04	VEH/PTH	20.4	17.37	17.49
D05	VEH/PTH	18.5	17.45	17.21
D06	VEH/PTH	20.7	17.07	16.75
D07	VEH/PTH	20.1	17.70	17.30
D08	VEH/PTH	19.2	17.56	17.39
D09	VEH/PTH	19.6	17.54	17.35
D10	VEH/PTH	21.3	18.34	17.77
E01	PTH/PTH	19.8	17.49	17.34
E02	PTH/PTH	19.7	17.50	17.56
E03	PTH/PTH	21.8	17.74	17.62
E-H12	PTH/PTH	20.3	17.59	17.53
E05	PTH/PTH	21.2	17.88	18.15
E06	PTH/PTH	19.6	16.70	16.59
E07	PTH/PTH	19.2	17.42	17.45
E08	PTH/PTH	22.7	18.29	17.57
E09	PTH/PTH	22.4	17.66	17.73
E10	PTH/PTH	20.2	17.76	17.75

Table F.6 Phenotype data for 16-week-old wild type (WT) C57Bl/6J female mice pre-treated with PTH or VEH for 6 weeks prior to 6 weeks of tibial loading

Animal ID	Treatment Group	Body Mass (g)	Left Tibia Length (mm)	Right Tibia Length (mm)
F01	VEH/VEH	21.2	18.01	17.57
F02	VEH/VEH	20.9	17.59	17.75
F03	VEH/VEH	22.4	17.64	17.35
F04	VEH/VEH	21.5	17.26	17.24
F05	VEH/VEH	19.7	17.41	17.03
F06	VEH/VEH	21.3	17.42	17.23
F07	VEH/VEH	20.8	17.61	17.59
F08	VEH/VEH	22.4	17.57	17.33
F09	VEH/VEH	20.0	17.37	17.13
F10	VEH/VEH	20.3	17.49	17.56
F11	VEH/VEH	20.5	17.38	17.09
G01	VEH/PTH	21.8	17.79	17.58
G02	VEH/PTH	21.3	17.75	17.60
G03	VEH/PTH	20.9	17.46	17.56
G04	VEH/PTH	21.2	17.77	17.70
G05	VEH/PTH	22.4	18.15	17.64
G06	VEH/PTH	23.0	17.87	17.74
G07	VEH/PTH	21.8	17.26	17.38
G08	VEH/PTH	19.7	17.31	17.30
G09	VEH/PTH	20.6	17.54	17.45
G10	VEH/PTH	23.4	17.74	17.58
G11	VEH/PTH	22.2	18.06	17.81
G12	VEH/PTH	20.6	17.42	17.19
H01	PTH/PTH	20.9	17.37	17.14
H02	PTH/PTH	20.8	17.06	17.13
H03	PTH/PTH	21.1	17.81	17.75
H04	PTH/PTH	20.1	17.48	17.42
H05	PTH/PTH	17.4	17.05	16.83
H06	PTH/PTH	21.8	17.29	17.22
H07	PTH/PTH	19.4	17.20	17.11
H08	PTH/PTH	21.5	17.78	17.97
H09	PTH/PTH	21.2	17.32	17.39
H10	PTH/PTH	21.3	17.24	17.44
H11	PTH/PTH	19.5	16.88	16.88

Table F.7 Tibial diaphyseal cortical bone measures from loaded left (L) and control right (R) limbs for the tensile (T), compressive (C), and neutral (N) regions from 10-week-old pOC-ERαKO (cKO) and LC female mice concurrently loaded and treated with PTH or VEH for 2 weeks.

Animal Limb	cKO or LC	PTH or VEH	Ct.Ar.T (mm^2)	Ct.Ar.C (mm^2)	Ct.Ar.N (mm^2)	Ct.Th.T (mm)	Ct.Th.C (mm)	Ct.Th.N (mm)
U23008L	cKO	PTH	0.1976	0.2075	0.1437	0.2264	0.2877	0.1972
U23008R	cKO	PTH	0.159	0.1464	0.1328	0.2069	0.1999	0.1846
U23009L	cKO	PTH	0.1902	0.1738	0.1202	0.2271	0.2301	0.1731
U23009R	cKO	PTH	0.1727	0.1524	0.1264	0.2118	0.1863	0.1742
U23010L	cKO	PTH	0.1976	0.2021	0.1299	0.2342	0.2781	0.1887
U23010R	cKO	PTH	0.1401	0.1248	0.1186	0.1883	0.181	0.1754
U23015L	cKO	PTH	0.1626	0.1666	0.1279	0.2184	0.2411	0.1912
U23015R	cKO	PTH	0.1627	0.1478	0.1251	0.212	0.1985	0.1851
U23112L	cKO	PTH	0.183	0.1809	0.1269	0.2282	0.247	0.1853
U23112R	cKO	PTH	0.1659	0.1568	0.1201	0.2167	0.2001	0.1781
V27101L	cKO	PTH	0.1965	0.2024	0.1415	0.2328	0.2845	0.2046
V27101R	cKO	PTH						
V27208L	cKO	PTH	0.1816	0.1915	0.1276	0.2283	0.2405	0.1836
V27208R	cKO	PTH	0.1699	0.1478	0.1236	0.2067	0.1984	0.1742
V27607L	cKO	PTH	0.1805	0.165	0.1185	0.2277	0.2221	0.1773
V27607R	cKO	PTH	0.1775	0.1586	0.1137	0.2263	0.1899	0.1757
V27915L	cKO	PTH	0.2066	0.1986	0.121	0.2303	0.2556	0.178
V27915R	cKO	PTH	0.1647	0.1474	0.1262	0.209	0.1934	0.1805
V28202L	cKO	PTH	0.2001	0.1854	0.1216	0.2299	0.2282	0.1819
V28202R	cKO	PTH	0.1626	0.1564	0.1225	0.2201	0.2044	0.182
W23105L	LC	PTH	0.1991	0.1804	0.1329	0.2251	0.2174	0.1846
W23105R	LC	PTH	0.1693	0.1508	0.1405	0.2018	0.1957	0.1896
W23107L	LC	PTH	0.1849	0.1811	0.1374	0.2374	0.2481	0.1985
W23107R	LC	PTH	0.1772	0.1584	0.1276	0.2253	0.2196	0.1883
W23114L	LC	PTH	0.1891	0.1829	0.1416	0.2279	0.2555	0.2019
W23114R	LC	PTH	0.1878	0.1722	0.1296	0.2189	0.2149	0.1854
W23901L	LC	PTH	0.2304	0.2282	0.1462	0.2482	0.2928	0.2065
W23901R	LC	PTH	0.1844	0.1636	0.1454	0.2162	0.2107	0.1926
W24204L	LC	PTH	0.1857	0.1773	0.1334	0.2112	0.2214	0.1805
W24204R	LC	PTH	0.1706	0.1574	0.1399	0.2132	0.203	0.1917
X27105L	LC	PTH	0.218	0.202	0.1361	0.2344	0.2299	0.1862
X27105R	LC	PTH	0.1884	0.1581	0.1361	0.2193	0.2017	0.1847
X27106L	LC	PTH	0.1871	0.1946	0.1292	0.2246	0.2734	0.1941
X27106R	LC	PTH	0.1592	0.1415	0.1178	0.2121	0.1987	0.1807
X27202L	LC	PTH	0.2047	0.2146	0.1508	0.247	0.2754	0.2039
X27202R	LC	PTH	0.1865	0.1619	0.1359	0.2276	0.2031	0.1879
X27204L	LC	PTH	0.2057	0.1936	0.1442	0.2278	0.2562	0.1994
X27204R	LC	PTH	0.1697	0.1576	0.1399	0.2244	0.2083	0.1944
X27407L	LC	PTH	0.2056	0.2083	0.146	0.236	0.2722	0.1965
X27407R	LC	PTH	0.1577	0.1643	0.1249	0.2357	0.2244	0.2008
Y23312L	cKO	VEH	0.2111	0.1879	0.121	0.215	0.2228	0.1726
Y23312R	cKO	VEH	0.1673	0.145	0.1311	0.2072	0.2023	0.1857

Y23402L	cKO	VEH	0.1658	0.1758	0.1247	0.2252	0.2429	0.1906
Y23402R	cKO	VEH	0.1426	0.1411	0.125	0.2012	0.197	0.1819
Y23406L	cKO	VEH	0.1934	0.2003	0.1362	0.2229	0.2713	0.1933
Y23406R	cKO	VEH	0.1749	0.1492	0.1265	0.2075	0.1921	0.174
Y23408L	cKO	VEH	0.2247	0.2212	0.126	0.2445	0.2922	0.1854
Y23408R	cKO	VEH	0.1758	0.1589	0.1133	0.2247	0.2256	0.1739
Y23510L	cKO	VEH	0.1746	0.1837	0.1326	0.2236	0.2511	0.1965
Y23510R	cKO	VEH	0.1737	0.1673	0.1306	0.2045	0.1837	0.1803
Z28001L	cKO	VEH	0.1731	0.1668	0.125	0.2073	0.2293	0.1814
Z28001R	cKO	VEH	0.1537	0.1464	0.1164	0.1998	0.2018	0.1746
Z28004L	cKO	VEH	0.2176	0.1885	0.1233	0.2273	0.2309	0.174
Z28004R	cKO	VEH	0.1774	0.1576	0.1158	0.2166	0.2142	0.1766
Z28102L	cKO	VEH	0.1828	0.1728	0.1229	0.2183	0.2274	0.1769
Z28102R	cKO	VEH	0.1613	0.142	0.1158	0.2052	0.192	0.1726
Z28106L	cKO	VEH	0.1936	0.1863	0.1314	0.2293	0.2447	0.189
Z28106R	cKO	VEH	0.1659	0.1476	0.1232	0.2146	0.1972	0.18
Z28305L	cKO	VEH	0.1908	0.1702	0.1387	0.2272	0.2288	0.1901
Z28305R	cKO	VEH	0.164	0.1527	0.1189	0.2296	0.2067	0.1829
AB23004L	LC	VEH	0.2358	0.2211	0.1334	0.2278	0.2478	0.1829
AB23004R	LC	VEH	0.1869	0.1513	0.1208	0.2093	0.1899	0.1727
AB23311L	LC	VEH	0.1686	0.1978	0.1375	0.2113	0.2903	0.2006
AB23311R	LC	VEH	0.15	0.143	0.1307	0.1968	0.2002	0.1882
AB23313L	LC	VEH	0.2037	0.1887	0.1572	0.2312	0.2419	0.2038
AB23313R	LC	VEH	0.1714	0.1587	0.1271	0.2124	0.2119	0.1836
AB23314L	LC	VEH	0.2201	0.2034	0.1477	0.2331	0.2605	0.2009
AB23314R	LC	VEH	0.1971	0.1752	0.1548	0.2096	0.2005	0.1982
AB23315L	LC	VEH	0.1742	0.1776	0.1364	0.2244	0.2749	0.2035
AB23315R	LC	VEH	0.183	0.161	0.1232	0.2199	0.2101	0.1865
CD27903L	LC	VEH	0.1918	0.213	0.1477	0.2317	0.3045	0.2056
CD27903R	LC	VEH	0.1723	0.1538	0.1315	0.2178	0.2072	0.1927
CD27904L	LC	VEH	0.1972	0.2006	0.1412	0.2254	0.2486	0.2018
CD27904R	LC	VEH	0.1684	0.1516	0.1285	0.2156	0.1992	0.189
CD28016L	LC	VEH	0.2362	0.2112	0.1375	0.2467	0.253	0.1914
CD28016R	LC	VEH	0.1892	0.1842	0.1439	0.2323	0.2161	0.1979
CD28017L	LC	VEH	0.1784	0.1736	0.1347	0.2348	0.2425	0.1924
CD28017R	LC	VEH	0.1768	0.1549	0.1364	0.2214	0.1976	0.1853
CD28107L	LC	VEH	0.2123	0.1936	0.1267	0.2244	0.2239	0.1776
CD28107R	LC	VEH	0.1533	0.15	0.1236	0.2137	0.2141	0.1912

Table F.8 Tibial diaphyseal cortical bone measures from loaded left (L) and control right (R) limbs for the tensile (T), compressive (C), and neutral (N) regions from 16-week-old pOC-ERαKO (cKO) and LC female mice concurrently loaded and treated with PTH or VEH for 2 weeks.

Animal Limb	cKO or LC	PTH or VEH	Ct.Ar.T (mm^2)	Ct.Ar.C (mm^2)	Ct.Ar.N (mm^2)	Ct.Th.T (mm)	Ct.Th.C (mm)	Ct.Th.N (mm)
A26404L	cKO	PTH	0.2183	0.1988	0.1232	0.2403	0.2585	0.1933
A26404R	cKO	PTH	0.1707	0.1485	0.1283	0.2137	0.201	0.1898
A26407L	cKO	PTH	0.2082	0.2027	0.1369	0.2341	0.2789	0.2025
A26407R	cKO	PTH	0.1524	0.1486	0.1278	0.216	0.1999	0.1841
A26614L	cKO	PTH	0.2201	0.2345	0.1482	0.212	0.259	0.195
A26614R	cKO	PTH	0.1815	0.1552	0.1381	0.2007	0.2008	0.1928
A26618L	cKO	PTH	0.2091	0.2166	0.1298	0.2394	0.3094	0.1988
A26618R	cKO	PTH	0.1636	0.1426	0.1221	0.2078	0.196	0.1793
A26904L	cKO	PTH	0.2051	0.2079	0.1496	0.2137	0.258	0.1909
A26904R	cKO	PTH	0.1355	0.1557	0.1308	0.1979	0.2154	0.187
B25804L	cKO	PTH	0.2104	0.1893	0.1374	0.2335	0.2402	0.1862
B25804R	cKO	PTH	0.1748	0.1745	0.1322	0.2298	0.2272	0.1891
B25816L	cKO	PTH	0.2041	0.2039	0.1352	0.2312	0.3021	0.1984
B25816R	cKO	PTH	0.15	0.1379	0.1178	0.2052	0.2107	0.1775
B26308L	cKO	PTH	0.1921	0.1876	0.1395	0.2274	0.2663	0.193
B26308R	cKO	PTH	0.1717	0.154	0.1319	0.2307	0.204	0.1987
B26506L	cKO	PTH	0.1959	0.203	0.1372	0.2445	0.293	0.1994
B26506R	cKO	PTH	0.1603	0.1479	0.1316	0.2107	0.2086	0.1865
B26804L	cKO	PTH	0.1816	0.1731	0.1347	0.2234	0.2509	0.1975
B26804R	cKO	PTH	0.1827	0.1648	0.1229	0.2256	0.2126	0.1895
C26303L	LC	PTH	0.2097	0.2117	0.1581	0.2485	0.2975	0.2162
C26303R	LC	PTH	0.2014	0.1714	0.154	0.2397	0.214	0.202
C26608L	LC	PTH	0.2184	0.2301	0.1537	0.2337	0.3117	0.2161
C26608R	LC	PTH	0.1789	0.1731	0.1502	0.2435	0.2238	0.2155
C26611L	LC	PTH	0.2135	0.2204	0.143	0.2328	0.2779	0.1958
C26611R	LC	PTH	0.174	0.154	0.144	0.2192	0.2123	0.1996
C26702L	LC	PTH	0.2238	0.2428	0.1644	0.2777	0.3799	0.2402
C26702R	LC	PTH	0.1647	0.1627	0.1269	0.2512	0.2377	0.1935
C26705L	LC	PTH	0.2081	0.2065	0.1535	0.2386	0.2787	0.2092
C26705R	LC	PTH	0.1548	0.1682	0.1469	0.2202	0.2071	0.2009
D26805L	LC	PTH	0.2242	0.2249	0.1467	0.2551	0.2679	0.2048
D26805R	LC	PTH	0.1995	0.1641	0.1466	0.2445	0.2184	0.2003
D26807L	LC	PTH	0.1909	0.1821	0.1317	0.2453	0.248	0.187
D26807R	LC	PTH	0.186	0.1618	0.1389	0.2237	0.2172	0.1989
D26815L	LC	PTH	0.2033	0.2	0.1454	0.2321	0.2278	0.1957
D26815R	LC	PTH	0.2024	0.1814	0.1415	0.2453	0.2332	0.1924
D26908L	LC	PTH	0.2097	0.1914	0.1429	0.2427	0.2529	0.1996
D26908R	LC	PTH	0.1697	0.1793	0.1443	0.2515	0.2345	0.2118
D26909L	LC	PTH	0.1913	0.1856	0.1508	0.2447	0.2351	0.2045
D26909R	LC	PTH	0.1819	0.1643	0.138	0.2363	0.2229	0.1982
E25202L	cKO	VEH	0.1638	0.1781	0.1251	0.2264	0.2344	0.1859
E25202R	cKO	VEH						

E25204L	cKO	VEH	0.2035	0.1938	0.1408	0.2364	0.2597	0.195
E25204R	cKO	VEH	0.1713	0.1581	0.1295	0.2181	0.2176	0.1848
E25205L	cKO	VEH	0.1913	0.1973	0.1332	0.2359	0.2675	0.1972
E25205R	cKO	VEH	0.1647	0.1687	0.1292	0.2212	0.2086	0.1878
E25207L	cKO	VEH	0.1926	0.1886	0.1394	0.2391	0.2437	0.1931
E25207R	cKO	VEH	0.1832	0.1633	0.1343	0.2223	0.2192	0.1803
E25308L	cKO	VEH	0.213	0.1988	0.136	0.2354	0.2656	0.1954
E25308R	cKO	VEH	0.1775	0.161	0.1381	0.2105	0.1887	0.1886
F25505L	cKO	VEH	0.1546	0.166	0.1276	0.2135	0.2112	0.1943
F25505R	cKO	VEH	0.1674	0.1471	0.1357	0.2136	0.2055	0.1894
F25604L	cKO	VEH	0.1678	0.1886	0.139	0.2179	0.2498	0.2005
F25604R	cKO	VEH	0.1559	0.1607	0.1272	0.2109	0.2151	0.1861
F25610L	cKO	VEH	0.1713	0.1657	0.129	0.2094	0.2366	0.1824
F25610R	cKO	VEH	0.1432	0.149	0.1488	0.1985	0.1951	0.2091
F25904L	cKO	VEH	0.1854	0.1749	0.1293	0.2182	0.2401	0.1786
F25904R	cKO	VEH	0.1642	0.1575	0.1255	0.2005	0.216	0.1803
F25906L	cKO	VEH	0.179	0.1706	0.1309	0.2195	0.2238	0.1793
F25906R	cKO	VEH	0.1935	0.1676	0.1344	0.1993	0.1907	0.1836
G25304L	LC	VEH	0.2002	0.1868	0.132	0.2371	0.243	0.1879
G25304R	LC	VEH	0.1643	0.1423	0.1348	0.2253	0.2072	0.1982
G25803L	LC	VEH	0.2267	0.2361	0.1607	0.2613	0.3027	0.2281
G25803R	LC	VEH	0.1603	0.1392	0.1295	0.2072	0.2086	0.1926
G25902L	LC	VEH	0.1801	0.1681	0.1181	0.23	0.2347	0.1717
G25902R	LC	VEH	0.1961	0.1625	0.1375	0.2155	0.2063	0.1927
G25911L	LC	VEH	0.2206	0.2034	0.152	0.2571	0.2701	0.1994
G25911R	LC	VEH	0.1631	0.1627	0.1639	0.2268	0.2168	0.2316
G26101L	LC	VEH	0.2036	0.1745	0.1405	0.2288	0.227	0.1926
G26101R	LC	VEH	0.1738	0.1576	0.1487	0.2295	0.2038	0.203
H25010L	LC	VEH	0.1967	0.1892	0.1479	0.232	0.2583	0.1976
H25010R	LC	VEH	0.1893	0.1728	0.1472	0.2256	0.2197	0.1953
H25104L	LC	VEH	0.1892	0.1964	0.1591	0.2232	0.2386	0.2088
H25104R	LC	VEH	0.1794	0.1555	0.1412	0.2206	0.2061	0.1948
H25109L	LC	VEH	0.1668	0.1812	0.1491	0.2327	0.2319	0.213
H25109R	LC	VEH	0.1861	0.1709	0.1621	0.2148	0.2245	0.2109
H25408L	LC	VEH	0.1779	0.1749	0.1366	0.2369	0.25	0.2052
H25408R	LC	VEH	0.1787	0.1596	0.1351	0.2371	0.2257	0.2034
H25502L	LC	VEH	0.1836	0.1747	0.1382	0.2366	0.2399	0.2041
H25502R	LC	VEH	0.1837	0.1669	0.1379	0.2418	0.2361	0.2057

Table F.9 Tibial diaphyseal cortical bone measures from loaded left (L) and control right (R) limbs for the tensile (T), compressive (C), and neutral (N) regions from 16-week-old pOC-ERαKO (cKO) and LC female mice concurrently loaded and treated with PTH or VEH for 6 weeks.

Animal Limb	cKO or LC	PTH or VEH	Ct.Ar.T (mm^2)	Ct.Ar.C (mm^2)	Ct.Ar.N (mm^2)	Ct.Th.T (mm)	Ct.Th.C (mm)	Ct.Th.N (mm)
I23806L	cKO	PTH	0.227	0.2177	0.1402	0.2674	0.259	0.1913
I23806R	cKO	PTH	0.171	0.1725	0.131	0.2271	0.2335	0.1923
I24607L	cKO	PTH	0.2021	0.1925	0.1327	0.2346	0.2594	0.1898
I24607R	cKO	PTH	0.1519	0.1634	0.1294	0.2178	0.2137	0.1889
I24609L	cKO	PTH	0.2109	0.1953	0.1398	0.2446	0.2572	0.196
I24609R	cKO	PTH	0.149	0.1672	0.1323	0.2006	0.1894	0.1834
I24701L	cKO	PTH	0.2299	0.2092	0.1313	0.2309	0.2588	0.1854
I24701R	cKO	PTH	0.1644	0.1423	0.1252	0.216	0.1974	0.1827
I24702L	cKO	PTH	0.2026	0.1976	0.1333	0.2443	0.2555	0.1884
I24702R	cKO	PTH	0.1856	0.1638	0.1358	0.202	0.1907	0.1907
J22006L	cKO	PTH	0.2285	0.208	0.1375	0.241	0.2421	0.1867
J22006R	cKO	PTH	0.1851	0.1622	0.14	0.2341	0.203	0.1938
J22102L	cKO	PTH	0.2209	0.1993	0.1292	0.2263	0.2193	0.1725
J22102R	cKO	PTH	0.1685	0.1465	0.1307	0.2037	0.1903	0.1784
J22801L	cKO	PTH	0.2289	0.2003	0.1285	0.2536	0.2405	0.1802
J22801R	cKO	PTH	0.1792	0.1647	0.125	0.2347	0.2071	0.1812
K22510L	cKO	PTH	0.2186	0.2037	0.1333	0.2501	0.2648	0.1842
K22510R	cKO	PTH	0.1966	0.166	0.1324	0.2136	0.2016	0.1864
K22513L	cKO	PTH	0.2225	0.1892	0.1321	0.2348	0.2193	0.173
K22513R	cKO	PTH	0.1713	0.1585	0.1156	0.2096	0.1906	0.1664
K22514L	cKO	PTH	0.207	0.1898	0.1295	0.2304	0.235	0.1865
K22514R	cKO	PTH	0.1822	0.1696	0.1279	0.2035	0.185	0.1751
L21504L	LC	PTH	0.2296	0.211	0.1427	0.2673	0.2563	0.1984
L21504R	LC	PTH	0.1904	0.1822	0.1424	0.2446	0.197	0.1964
L21911L	LC	PTH	0.243	0.2054	0.1534	0.283	0.2542	0.2108
L21911R	LC	PTH	0.1916	0.1979	0.1466	0.2441	0.2139	0.2001
L21913L	LC	PTH	0.2372	0.2108	0.1327	0.2725	0.2611	0.1872
L21913R	LC	PTH	0.2046	0.1711	0.1387	0.2481	0.2089	0.1902
L22105L	LC	PTH	0.2334	0.2128	0.1395	0.2755	0.2602	0.1968
L22105R	LC	PTH	0.1779	0.1581	0.1416	0.2284	0.2118	0.1961
L22501L	LC	PTH	0.2195	0.2078	0.1342	0.2832	0.2739	0.1921
L22501R	LC	PTH	0.1847	0.1594	0.1368	0.2453	0.2149	0.1992
M23007L	LC	PTH	0.2041	0.1813	0.145	0.2537	0.2467	0.1981
M23007R	LC	PTH	0.1941	0.1626	0.1416	0.2288	0.2111	0.1995
M23405L	LC	PTH	0.2189	0.2162	0.1435	0.2625	0.3015	0.2073
M23405R	LC	PTH	0.1751	0.1535	0.1441	0.2317	0.2209	0.206
M23801L	LC	PTH	0.217	0.201	0.1479	0.2563	0.2625	0.1996
M23801R	LC	PTH	0.1948	0.1705	0.1456	0.2469	0.2275	0.202
N24004L	LC	PTH	0.248	0.233	0.1468	0.2739	0.2728	0.1986
N24004R	LC	PTH	0.1824	0.1539	0.1483	0.224	0.2113	0.2065
N24011L	LC	PTH	0.2494	0.2242	0.1451	0.2803	0.2808	0.207
N24011R	LC	PTH	0.2075	0.1801	0.149	0.2274	0.2266	0.21

N24014L	LC	PTH	0.2704	0.2502	0.1503	0.2885	0.3075	0.2014
N24014R	LC	PTH	0.2024	0.1713	0.1427	0.2159	0.2007	0.1986
O23903L	cKO	VEH	0.238	0.1995	0.148	0.2451	0.2335	0.182
O23903R	cKO	VEH	0.1456	0.1531	0.1408	0.1924	0.1798	0.18
O24805L*	cKO	VEH	0.1932	0.1877	0.1383	0.2379	0.2313	0.1832
O24805R*	cKO	VEH	0.1801	0.1552	0.1326	0.2124	0.1973	0.1884
O24807L	cKO	VEH	0.2007	0.1797	0.1234	0.222	0.2307	0.1698
O24807R	cKO	VEH	0.1584	0.1307	0.1276	0.2131	0.1804	0.1813
O24810L	cKO	VEH	0.1882	0.1834	0.1346	0.2508	0.2526	0.199
O24810R	cKO	VEH	0.1556	0.1363	0.1276	0.2214	0.197	0.1837
O24812L	cKO	VEH	0.1882	0.183	0.1241	0.2336	0.2297	0.1801
O24812R	cKO	VEH	0.17	0.1656	0.1294	0.2196	0.2211	0.1876
P22403L	cKO	VEH	0.1955	0.1843	0.1317	0.2287	0.2012	0.18
P22403R	cKO	VEH	0.1579	0.1498	0.1288	0.2182	0.1889	0.1859
P22405L	cKO	VEH	0.1928	0.1845	0.1141	0.2289	0.2522	0.1691
P22405R	cKO	VEH	0.1587	0.134	0.122	0.2068	0.1819	0.1692
P22406L	cKO	VEH	0.1939	0.1943	0.1258	0.2322	0.2581	0.1744
P22406R	cKO	VEH	0.1346	0.1356	0.1097	0.2156	0.1882	0.1755
Q21101L	cKO	VEH	0.2299	0.202	0.1365	0.2196	0.2044	0.1718
Q21101R	cKO	VEH	0.1833	0.1514	0.1379	0.2157	0.1721	0.1788
Q22314L	cKO	VEH	0.2035	0.1973	0.1181	0.2363	0.2619	0.1768
Q22314R	cKO	VEH	0.1486	0.1336	0.1166	0.2052	0.1874	0.1766
Q22701L	cKO	VEH	0.241	0.206	0.1335	0.2353	0.2201	0.1784
Q22701R	cKO	VEH	0.1827	0.1601	0.1328	0.2213	0.1997	0.1819
R21003L	LC	VEH	0.2329	0.2093	0.144	0.2736	0.2317	0.1942
R21003R	LC	VEH	0.2007	0.1723	0.1425	0.2491	0.2188	0.203
R22004L	LC	VEH	0.2224	0.1897	0.1348	0.2634	0.2257	0.1765
R22004R	LC	VEH	0.2015	0.1651	0.1425	0.2447	0.206	0.191
R22205L	LC	VEH	0.2051	0.1894	0.1264	0.2636	0.243	0.1777
R22205R	LC	VEH	0.1761	0.1539	0.1276	0.2376	0.2052	0.1795
R22407L	LC	VEH	0.2091	0.1923	0.1455	0.2472	0.2555	0.1984
R22407R	LC	VEH	0.2074	0.1799	0.1323	0.2322	0.2069	0.1799
R22711L	LC	VEH	0.2059	0.1886	0.1314	0.2532	0.2376	0.1789
R22711R	LC	VEH	0.1762	0.1522	0.1252	0.2367	0.1911	0.1789
S24803L	LC	VEH	0.2576	0.2377	0.1455	0.2602	0.2279	0.1849
S24803R	LC	VEH	0.1841	0.1568	0.1428	0.212	0.1982	0.2036
S24811L	LC	VEH	0.2396	0.2014	0.1526	0.2628	0.2482	0.2047
S24811R	LC	VEH	0.2357	0.1886	0.153	0.2341	0.2125	0.2049
S24813L	LC	VEH	0.2295	0.2002	0.1403	0.2613	0.2404	0.1969
S24813R	LC	VEH	0.1826	0.1633	0.1586	0.1991	0.1976	0.2049
T24108L	LC	VEH	0.2293	0.2063	0.1507	0.2723	0.2648	0.2006
T24108R	LC	VEH	0.1983	0.167	0.1358	0.2307	0.1978	0.1673
T24109L	LC	VEH	0.1964	0.1688	0.1435	0.2372	0.222	0.1893
T24109R	LC	VEH	0.1874	0.1638	0.1386	0.2087	0.1911	0.1769
T24305L	LC	VEH	0.1938	0.182	0.1253	0.2395	0.2547	0.1842
T24305R	LC	VEH	0.1546	0.1482	0.1245	0.2293	0.1966	0.1826

* Mouse died on loading day 25 of 30 (5wks)

Table F.10 Tibial diaphyseal cortical bone measures from baseline control right (R) limbs for the tensile (T), compressive (C), and neutral (N) regions from 16-week-old wild type (WT) C57Bl/6J female mice pre-treated with PTH or VEH for 6 weeks.

Animal Limb	PTH or VEH	Ct.Ar.T (mm^2)	Ct.Ar.C (mm^2)	Ct.Ar.N (mm^2)	Ct.Th.T (mm)	Ct.Th.C (mm)	Ct.Th.N (mm)
A01R	VEH	0.1558	0.1533	0.1343	0.2088	0.2147	0.1937
A02R	VEH	0.1833	0.165	0.1395	0.2271	0.2153	0.1954
A03R	VEH	0.1949	0.1726	0.1628	0.2326	0.2234	0.2106
A04R	VEH	0.1691	0.1669	0.129	0.2264	0.2257	0.1884
A05R	VEH	0.1761	0.1741	0.148	0.2255	0.2186	0.1969
A06R	VEH	0.1831	0.1729	0.1411	0.2419	0.241	0.2113
A07R	VEH	0.1778	0.1806	0.1336	0.2434	0.2491	0.197
A08R	VEH	0.1911	0.1832	0.1253	0.2391	0.2381	0.188
B01R	PTH	0.181	0.1684	0.1582	0.231	0.2337	0.2167
B02R	PTH	0.1741	0.1548	0.1452	0.2386	0.2207	0.2127
B03R	PTH	0.2098	0.1963	0.1484	0.2487	0.2394	0.2081
B04R	PTH	0.2058	0.1977	0.1504	0.2442	0.2397	0.2101
B05R	PTH	0.1978	0.1939	0.1531	0.2538	0.2699	0.2256
B06R	PTH	0.1732	0.1648	0.1363	0.2309	0.2302	0.2
B07R	PTH	0.2158	0.2135	0.1639	0.2618	0.2423	0.2166
B08R	PTH	0.184	0.1784	0.1377	0.2385	0.2277	0.2014

Table F.11 Tibial diaphyseal cortical bone measures for the tensile (T), compressive (C), and neutral (N) regions from 16-week-old wild type (WT) C57Bl/6J female mice pre-treated with PTH or VEH for 6 weeks prior to 2 weeks of tibial loading.

Animal Limb	Treatment Group	Ct.Ar.T (mm^2)	Ct.Ar.C (mm^2)	Ct.Ar.N (mm^2)	Ct.Th.T (mm)	Ct.Th.C (mm)	Ct.Th.N (mm)
C01L	VEH/VEH	0.214	0.1986	0.1571	0.2555	0.2543	0.2111
C01R	VEH/VEH	0.2028	0.1843	0.1479	0.243	0.233	0.1866
C02L	VEH/VEH	0.1873	0.1777	0.1356	0.2393	0.2288	0.1908
C02R	VEH/VEH	0.1907	0.1774	0.1339	0.254	0.2255	0.194
C03L	VEH/VEH	0.223	0.2095	0.1533	0.2566	0.2406	0.2017
C03R	VEH/VEH	0.2226	0.2174	0.1569	0.2774	0.2504	0.209
C04L	VEH/VEH	0.2169	0.2018	0.152	0.2564	0.2489	0.2066
C04R	VEH/VEH	0.1975	0.173	0.1371	0.2548	0.2058	0.19
C05L	VEH/VEH	0.175	0.1691	0.1415	0.235	0.2097	0.2
C05R	VEH/VEH	0.1929	0.1859	0.1333	0.2449	0.2319	0.1868
C06L	VEH/VEH	0.1894	0.1722	0.1334	0.2335	0.2265	0.1819
C06R	VEH/VEH	0.1753	0.1723	0.1366	0.2243	0.2286	0.2019
C07L	VEH/VEH	0.1902	0.17	0.131	0.2273	0.2088	0.1691
C07R	VEH/VEH	0.2029	0.1834	0.1353	0.2415	0.2312	0.1912
C08L	VEH/VEH	0.1845	0.1786	0.1295	0.2284	0.2311	0.1842
C08R	VEH/VEH	0.1877	0.1815	0.134	0.2342	0.2277	0.187
C09L	VEH/VEH	0.2118	0.2028	0.1407	0.2521	0.2629	0.196
C09R	VEH/VEH	0.196	0.1886	0.1341	0.245	0.2409	0.1826
C10L	VEH/VEH	0.1632	0.1685	0.1388	0.2242	0.2074	0.1895
C10R	VEH/VEH	0.1846	0.1662	0.126	0.2337	0.2061	0.1755
D01L	VEH/PTH	0.2023	0.1808	0.1329	0.2302	0.2272	0.1868
D01R	VEH/PTH	0.1929	0.17	0.1317	0.2344	0.2072	0.1808
D02L	VEH/PTH	0.2109	0.1945	0.1574	0.2529	0.2344	0.2147
D02R	VEH/PTH	0.1991	0.1883	0.1486	0.2446	0.2244	0.202
D03L	VEH/PTH	0.1916	0.1835	0.139	0.2422	0.234	0.1935
D03R	VEH/PTH	0.2018	0.174	0.1356	0.2423	0.207	0.1853
D04L	VEH/PTH	0.1992	0.1997	0.1414	0.2422	0.2556	0.1941
D04R	VEH/PTH	0.1951	0.1783	0.1315	0.2433	0.1928	0.1817
D05L	VEH/PTH	0.1957	0.1854	0.1265	0.2307	0.2459	0.1816
D05R	VEH/PTH	0.192	0.1679	0.1267	0.2424	0.2167	0.1916
D06L	VEH/PTH	0.189	0.1778	0.1344	0.237	0.2174	0.1847
D06R	VEH/PTH	0.1742	0.161	0.126	0.232	0.2222	0.179
D07L	VEH/PTH	0.2026	0.198	0.1486	0.2398	0.2562	0.1912
D07R	VEH/PTH	0.1907	0.1769	0.1373	0.2314	0.1918	0.1835
D08L	VEH/PTH	0.1974	0.1815	0.1374	0.2387	0.2354	0.1883
D08R	VEH/PTH	0.1718	0.1582	0.13	0.2315	0.2105	0.1817
D09L	VEH/PTH	0.1847	0.184	0.1387	0.2295	0.2543	0.1915
D09R	VEH/PTH	0.1684	0.1694	0.1373	0.2228	0.2103	0.1909
D10L	VEH/PTH	0.2358	0.2144	0.1593	0.2649	0.2725	0.2081
D10R	VEH/PTH	0.2225	0.1863	0.1476	0.25	0.2222	0.1941
E01L	PTH/PTH	0.2019	0.1891	0.1591	0.239	0.2615	0.2179
E01R	PTH/PTH	0.227	0.1968	0.1473	0.262	0.236	0.2085
E02L	PTH/PTH	0.2238	0.1922	0.156	0.2597	0.2426	0.2032
E02R	PTH/PTH	0.2085	0.1875	0.1445	0.2575	0.2375	0.1967

E03L	PTH/PTH	0.2198	0.2079	0.1592	0.2617	0.2467	0.2128
E03R	PTH/PTH	0.2314	0.2145	0.1502	0.2704	0.2334	0.1992
E-H12L	PTH/PTH	0.2289	0.2495	0.1648	0.2601	0.2935	0.2207
E-H12R	PTH/PTH	0.2142	0.2028	0.1428	0.2503	0.2232	0.1811
E05L	PTH/PTH	0.2625	0.2331	0.1624	0.278	0.2367	0.2123
E05R	PTH/PTH	0.2295	0.2238	0.1506	0.2702	0.2549	0.2018
E06L	PTH/PTH	0.2289	0.2048	0.1339	0.2731	0.2717	0.1942
E06R	PTH/PTH	0.1862	0.1665	0.1389	0.2585	0.2279	0.2092
E07L	PTH/PTH	0.202	0.1933	0.1611	0.241	0.2667	0.2283
E07R	PTH/PTH	0.1812	0.1631	0.1406	0.2336	0.2204	0.198
E08L	PTH/PTH	0.2096	0.1906	0.1478	0.2561	0.2294	0.1975
E08R	PTH/PTH	0.2074	0.1782	0.1423	0.2571	0.2265	0.1861
E09L	PTH/PTH	0.1948	0.2024	0.1526	0.2503	0.248	0.2053
E09R	PTH/PTH	0.1984	0.1876	0.1461	0.2441	0.2272	0.1893
E10L	PTH/PTH	0.2258	0.2185	0.1562	0.2568	0.2864	0.2108
E10R	PTH/PTH	0.2105	0.1826	0.1493	0.2405	0.1969	0.1969

Table F.12 Tibial diaphyseal cortical bone measures for the tensile (T), compressive (C), and neutral (N) regions from 16-week-old wild type (WT) C57Bl/6J female mice pre-treated with PTH or VEH for 6 weeks prior to 6 weeks of tibial loading.

Animal Limb	Treatment Group	Ct.Ar.T (mm^2)	Ct.Ar.C (mm^2)	Ct.Ar.N (mm^2)	Ct.Th.T (mm)	Ct.Th.C (mm)	Ct.Th.N (mm)
F01L	VEH/VEH	0.2332	0.2075	0.1448	0.2565	0.256	0.1875
F01R	VEH/VEH	0.1986	0.1752	0.153	0.2346	0.2196	0.2013
F02L	VEH/VEH	0.2225	0.2037	0.142	0.2716	0.2598	0.1901
F02R	VEH/VEH	0.1804	0.164	0.1333	0.2405	0.2049	0.1884
F03L	VEH/VEH	0.2404	0.2124	0.1484	0.2658	0.2492	0.1963
F03R	VEH/VEH	0.2151	0.1877	0.151	0.2526	0.2264	0.2034
F04L	VEH/VEH	0.2135	0.2105	0.1403	0.2741	0.2682	0.1983
F04R	VEH/VEH	0.1966	0.1749	0.1299	0.2516	0.2192	0.1813
F05L	VEH/VEH	0.21	0.2031	0.1357	0.2551	0.2683	0.1907
F05R	VEH/VEH	0.191	0.1724	0.1376	0.2286	0.1965	0.1838
F06L	VEH/VEH	0.2431	0.2205	0.1411	0.2632	0.2574	0.1836
F06R	VEH/VEH	0.1807	0.1631	0.1381	0.2349	0.1998	0.1856
F07L	VEH/VEH	0.2161	0.1991	0.147	0.26	0.2472	0.1993
F07R	VEH/VEH	0.1981	0.1741	0.1372	0.2366	0.2014	0.1839
F08L	VEH/VEH	0.2184	0.2032	0.1452	0.258	0.2457	0.2018
F08R	VEH/VEH	0.211	0.1845	0.158	0.2475	0.2124	0.2065
F09L	VEH/VEH	0.2242	0.205	0.1355	0.2683	0.2495	0.1938
F09R	VEH/VEH	0.1858	0.1612	0.1334	0.232	0.2098	0.1858
F10L	VEH/VEH	0.2201	0.1998	0.1298	0.2486	0.2417	0.1803
F10R	VEH/VEH	0.1921	0.1649	0.1348	0.2427	0.21	0.1925
F11L	VEH/VEH	0.2239	0.2011	0.1354	0.252	0.2469	0.1815
F11R	VEH/VEH	0.2049	0.1829	0.1347	0.2313	0.181	0.1824
G01L	VEH/PTH	0.2218	0.2062	0.1574	0.27	0.2684	0.1988
G01R	VEH/PTH	0.2174	0.1895	0.1549	0.2641	0.2253	0.2077
G02L	VEH/PTH	0.2263	0.2107	0.1416	0.2732	0.2579	0.2021
G02R	VEH/PTH	0.1882	0.1848	0.1444	0.2592	0.237	0.2037
G03L	VEH/PTH	0.2294	0.199	0.1503	0.2657	0.2477	0.2032
G03R	VEH/PTH	0.2013	0.1662	0.1334	0.2364	0.2049	0.1795
G04L	VEH/PTH	0.2357	0.2068	0.1412	0.2757	0.2484	0.1961
G04R	VEH/PTH	0.207	0.1807	0.1409	0.2624	0.2175	0.1919
G05L	VEH/PTH	0.2508	0.2306	0.1378	0.2778	0.2476	0.1861
G05R	VEH/PTH	0.2143	0.188	0.1421	0.2652	0.2287	0.1969
G06L	VEH/PTH	0.2393	0.208	0.1519	0.2746	0.2497	0.2038
G06R	VEH/PTH	0.2023	0.1846	0.1388	0.2642	0.2282	0.1995
G07L	VEH/PTH	0.2434	0.2266	0.155	0.2765	0.2736	0.2071
G07R	VEH/PTH	0.2007	0.1842	0.1469	0.2608	0.2268	0.2048
G08L	VEH/PTH	0.2347	0.2162	0.1439	0.2749	0.277	0.1941
G08R	VEH/PTH	0.2173	0.1825	0.1244	0.2536	0.2124	0.1867
G09L	VEH/PTH	0.2109	0.1986	0.1385	0.2554	0.2585	0.1929
G09R	VEH/PTH	0.1744	0.1498	0.1344	0.2272	0.1997	0.1845
G10L	VEH/PTH	0.2146	0.2041	0.1439	0.2638	0.2567	0.1951
G10R	VEH/PTH						
G11L	VEH/PTH	0.2213	0.1979	0.1541	0.2836	0.2553	0.2119
G11R	VEH/PTH	0.1741	0.163	0.1532	0.2467	0.2114	0.203

G12L	VEH/PTH	0.2151	0.2014	0.157	0.2683	0.2649	0.2153
G12R	VEH/PTH	0.1871	0.1586	0.1459	0.2601	0.2122	0.2167
H01L	PTH/PTH	0.2372	0.2265	0.1462	0.2739	0.2704	0.2009
H01R	PTH/PTH	0.2024	0.1827	0.1352	0.2721	0.222	0.1927
H02L	PTH/PTH	0.2576	0.2298	0.1471	0.2699	0.2471	0.1891
H02R	PTH/PTH	0.2166	0.1815	0.1428	0.2495	0.2153	0.1966
H03L	PTH/PTH	0.2785	0.2386	0.1597	0.3006	0.2822	0.2112
H03R	PTH/PTH	0.1981	0.1945	0.156	0.271	0.235	0.2108
H04L	PTH/PTH	0.2058	0.2153	0.1447	0.2603	0.2515	0.1979
H04R	PTH/PTH	0.1715	0.1558	0.1375	0.2418	0.2011	0.187
H05L	PTH/PTH	0.233	0.2332	0.1359	0.2935	0.2819	0.2018
H05R	PTH/PTH	0.1875	0.1652	0.1202	0.2544	0.2154	0.1845
H06L	PTH/PTH	0.2411	0.225	0.1593	0.2777	0.2701	0.2102
H06R	PTH/PTH	0.1856	0.1809	0.1457	0.2559	0.2232	0.2012
H07L	PTH/PTH	0.2362	0.2209	0.1456	0.2836	0.2835	0.2034
H07R	PTH/PTH	0.2055	0.1814	0.1456	0.2541	0.2255	0.2008
H08L	PTH/PTH	0.2373	0.2308	0.1668	0.2977	0.2803	0.2336
H08R	PTH/PTH	0.2002	0.2018	0.1573	0.2612	0.2345	0.2051
H09L	PTH/PTH	0.2376	0.2283	0.1579	0.2599	0.2798	0.203
H09R	PTH/PTH	0.186	0.172	0.129	0.239	0.214	0.173
H10L	PTH/PTH	0.254	0.241	0.144	0.275	0.282	0.199
H10R	PTH/PTH	0.198	0.165	0.139	0.233	0.207	0.201
H11L	PTH/PTH	0.218	0.219	0.151	0.273	0.296	0.217
H11R	PTH/PTH	0.186	0.185	0.135	0.247	0.246	0.196

Appendix G

CHAPTER 6 SUPPLEMENTARY DATA

Note: Phenotype data for mice used in Chapter 6 are listed in Appendix F

Table G.1 Tibial metaphyseal cancellous bone measures from loaded left (L) and control right (R) limbs from 10-week-old pOC-ERαKO (cKO) and LC female mice concurrently loaded and treated with PTH or VEH for 2 weeks.

Animal Limb	cKO or LC	PTH or VEH	BV/TV	Tb.Th (mm)	Tb.N (1/mm)	Tb.Sp (mm)	cn.TMD (mg HA/cc)
U23008L	cKO	PTH	0.0953	0.0563	3.5421	0.2814	876.843
U23008R	cKO	PTH	0.0704	0.043	3.1183	0.3208	872.803
U23009L	cKO	PTH	0.076	0.0532	3.1374	0.315	858.535
U23009R	cKO	PTH	0.053	0.0434	2.4796	0.4057	855.568
U23010L	cKO	PTH	0.0851	0.0555	2.3642	0.4239	878.485
U23010R	cKO	PTH	0.0666	0.0413	3.2593	0.3062	872.992
U23015L	cKO	PTH	0.0841	0.0549	2.8498	0.3537	895.025
U23015R	cKO	PTH	0.0839	0.046	3.1399	0.3196	914.975
U23112L	cKO	PTH	0.1134	0.0521	3.6338	0.2698	883.662
U23112R	cKO	PTH	0.1	0.0455	3.2626	0.3067	881.01
V27101L	cKO	PTH	0.1015	0.0537	3.1056	0.3189	893.258
V27101R	cKO	PTH					
V27208L	cKO	PTH	0.0594	0.0555	2.9009	0.3492	894.394
V27208R	cKO	PTH	0.0671	0.047	2.6014	0.3856	893.7
V27607L	cKO	PTH	0.0715	0.055	2.8005	0.3557	836.439
V27607R	cKO	PTH	0.071	0.0402	2.8797	0.3495	822.297
V27915L	cKO	PTH	0.0913	0.0555	2.6824	0.3786	881.894
V27915R	cKO	PTH	0.0752	0.0446	3.1797	0.3225	882.525
V28202L	cKO	PTH	0.0891	0.0537	3.3464	0.2971	857.525
V28202R	cKO	PTH	0.0723	0.043	3.3106	0.3037	861.123
W23105L	LC	PTH	0.0998	0.0501	3.7881	0.2621	891.553
W23105R	LC	PTH	0.0919	0.0434	4.0295	0.2466	877.79
W23107L	LC	PTH	0.1529	0.0534	4.5777	0.2111	905.316
W23107R	LC	PTH	0.1466	0.0466	4.6293	0.2114	921.793
W23114L	LC	PTH	0.1331	0.0551	4.0046	0.248	904.053
W23114R	LC	PTH	0.1153	0.0482	4.069	0.2416	891.048
W23901L	LC	PTH	0.0854	0.0444	3.3634	0.297	892.753
W23901R	LC	PTH	0.0791	0.0505	3.5337	0.2829	897.109
W24204L	LC	PTH	0.0832	0.0493	3.4838	0.2882	847.55
W24204R	LC	PTH	0.0911	0.0416	3.8435	0.2576	879.811
X27105L	LC	PTH	0.1096	0.053	3.8644	0.2533	917.437
X27105R	LC	PTH	0.1052	0.0463	3.868	0.2571	875.265
X27106L	LC	PTH	0.0996	0.0516	3.7552	0.2652	887.26
X27106R	LC	PTH	0.0869	0.0424	3.86	0.2571	887.765
X27202L	LC	PTH	0.108	0.0523	3.8541	0.2537	917.942

X27202R	LC	PTH	0.0932	0.046	3.7111	0.2692	905
X27204L	LC	PTH	0.1077	0.0507	4.2083	0.2305	899.445
X27204R	LC	PTH	0.1153	0.046	4.2201	0.2334	880.379
X27407L	LC	PTH	0.1117	0.0554	3.8585	0.2533	916.743
X27407R	LC	PTH	0.0913	0.0447	3.6456	0.2705	911.882
Y23312L	cKO	VEH	0.0798	0.0515	3.118	0.3158	886.881
Y23312R	cKO	VEH	0.0886	0.0404	3.5069	0.2868	898.75
Y23402L	cKO	VEH	0.0893	0.0512	3.1685	0.3101	884.545
Y23402R	cKO	VEH	0.0836	0.0392	3.7926	0.2675	899.192
Y23406L	cKO	VEH	0.0919	0.054	3.0398	0.3294	869.204
Y23406R	cKO	VEH	0.0877	0.0408	3.5091	0.2855	886.124
Y23408L	cKO	VEH	0.099	0.0528	3.178	0.3115	897.677
Y23408R	cKO	VEH	0.0998	0.0483	3.2805	0.3057	932.21
Y23510L	cKO	VEH	0.077	0.0575	2.901	0.3556	909.672
Y23510R	cKO	VEH	0.073	0.0414	2.8426	0.3578	867.058
Z28001L	cKO	VEH	0.0872	0.053	3.3351	0.2974	897.677
Z28001R	cKO	VEH	0.0746	0.0404	3.4674	0.2938	836.123
Z28004L	cKO	VEH	0.0724	0.0511	3.0249	0.3305	874.886
Z28004R	cKO	VEH	0.0788	0.0438	3.0742	0.3287	876.149
Z28102L	cKO	VEH	0.0894	0.0559	3.1397	0.3129	903.801
Z28102R	cKO	VEH	0.087	0.0433	3.2088	0.3257	905.821
Z28106L	cKO	VEH	0.0999	0.0568	3.453	0.2852	902.475
Z28106R	cKO	VEH	0.0885	0.0416	3.0946	0.3253	891.616
Z28305L	cKO	VEH	0.0946	0.0554	2.885	0.3432	902.917
Z28305R	cKO	VEH	0.0808	0.0432	2.8963	0.3628	845.088
AB23004L	LC	VEH	0.1084	0.0545	3.6271	0.2745	889.659
AB23004R	LC	VEH	0.1035	0.0411	3.954	0.251	871.351
AB23311L	LC	VEH	0.1099	0.0542	3.6935	0.2693	881.831
AB23311R	LC	VEH	0.099	0.043	4.0079	0.2507	832.777
AB23313L	LC	VEH	0.0963	0.0543	3.4964	0.2865	871.288
AB23313R	LC	VEH	0.0945	0.0429	3.8562	0.2584	900.202
AB23314L	LC	VEH	0.1047	0.0538	3.5644	0.2772	918.258
AB23314R	LC	VEH	0.1034	0.0455	3.965	0.2501	903.864
AB23315L	LC	VEH	0.1074	0.0544	3.6547	0.273	902.096
AB23315R	LC	VEH	0.0889	0.0436	3.6976	0.2757	901.339
CD27903L	LC	VEH	0.1145	0.0515	4.0391	0.2411	914.723
CD27903R	LC	VEH	0.1012	0.0445	3.9665	0.2507	907.399
CD27904L	LC	VEH	0.0877	0.0527	3.7354	0.2629	890.101
CD27904R	LC	VEH	0.1062	0.0464	3.8158	0.2606	915.291
CD28016L	LC	VEH	0.0994	0.0512	3.672	0.2684	917.564
CD28016R	LC	VEH	0.0946	0.0451	3.7357	0.267	908.536
CD28017L	LC	VEH	0.1046	0.052	4.0339	0.2407	918.069
CD28017R	LC	VEH	0.1124	0.0447	3.7705	0.2646	889.659
CD28107L	LC	VEH	0.0999	0.0531	3.8819	0.2499	926.528
CD28107R	LC	VEH	0.099	0.0458	3.8837	0.2549	941.428

Table G.2 Tibial metaphyseal cancellous bone measures from loaded left (L) and control right (R) limbs from 16-week-old pOC-ERαKO (cKO) and LC female mice concurrently loaded and treated with PTH or VEH for 2 weeks.

Animal Limb	cKO or LC	PTH or VEH	BV/TV	Tb.Th (mm)	Tb.N (1/mm)	Tb.Sp (mm)	cn.TMD (mg HA/cc)
A26404L	cKO	PTH	0.0684	0.0628	2.5613	0.3858	878.4221
A26404R	cKO	PTH	0.0695	0.0468	2.5955	0.3888	902.538
A26407L	cKO	PTH	0.0554	0.0579	2.4288	0.4153	891.806
A26407R	cKO	PTH	0.0657	0.0492	2.6638	0.3802	882.652
A26614L	cKO	PTH	0.0593	0.06	2.1536	0.4779	903.9906
A26614R	cKO	PTH	0.059	0.0482	2.2952	0.4419	904.306
A26618L	cKO	PTH	0.0619	0.059	2.1758	0.4726	931.326
A26618R	cKO	PTH	0.055	0.0479	2.4145	0.4175	899.129
A26904L	cKO	PTH	0.0902	0.0541	3.2338	0.3079	822.487
A26904R	cKO	PTH	0.068	0.044	3.3333	0.301	853.548
B25804L	cKO	PTH	0.0687	0.056	2.8492	0.3503	900.265
B25804R	cKO	PTH	0.0763	0.0499	2.5292	0.3988	921.162
B25816L	cKO	PTH	0.0976	0.0586	2.6854	0.3777	886.755
B25816R	cKO	PTH	0.0838	0.0467	2.9925	0.335	885.556
B26308L	cKO	PTH	0.0629	0.0563	2.5816	0.3837	913.397
B26308R	cKO	PTH	0.072	0.0519	2.748	0.3672	941.428
B26506L	cKO	PTH	0.0661	0.0542	2.5894	0.3866	926.339
B26506R	cKO	PTH	0.0592	0.0483	2.8431	0.3534	929.622
B26804L	cKO	PTH	0.0701	0.0544	3.0141	0.3373	914.912
B26804R	cKO	PTH	0.0804	0.0465	2.9356	0.3391	917.311
C26303L	LC	PTH	0.0687	0.0518	2.8217	0.3611	923.561
C26303R	LC	PTH	0.0793	0.0471	3.2121	0.3078	905.821
C26608L	LC	PTH	0.0914	0.0522	3.4714	0.282	923.182
C26608R	LC	PTH	0.086	0.0483	3.3205	0.2994	922.425
C26611L	LC	PTH	0.0944	0.0549	3.1256	0.3239	925.834
C26611R	LC	PTH	0.097	0.0512	3.291	0.3045	915.354
C26702L	LC	PTH	0.0683	0.0523	3.0179	0.3345	921.92
C26702R	LC	PTH	0.0741	0.0466	3.6071	0.272	906.137
C26705L	LC	PTH	0.0874	0.0538	3.2953	0.3023	909.861
C26705R	LC	PTH	0.0813	0.0478	3.4605	0.2872	886.25
D26805L	LC	PTH	0.082	0.052	3.0869	0.3196	940.796
D26805R	LC	PTH	0.0896	0.0489	3.4	0.2924	938.587
D26807L	LC	PTH	0.0755	0.0468	3.0113	0.3316	906.389
D26807R	LC	PTH	0.0837	0.0479	3.5262	0.2812	918.132
D26815L	LC	PTH	0.106	0.053	3.7555	0.2608	931.074
D26815R	LC	PTH	0.1181	0.0518	3.5675	0.2826	949.698
D26908L	LC	PTH	0.0738	0.0505	2.9325	0.3404	919.899
D26908R	LC	PTH	0.0821	0.0444	3.3616	0.2972	899.823
D26909L	LC	PTH	0.0842	0.0566	2.8054	0.3529	942.816
D26909R	LC	PTH	0.0942	0.0506	3.6806	0.2731	949.761
E25202L	cKO	VEH	0.0714	0.0618	2.673	0.3713	894.0789
E25202R	cKO	VEH	0.0595	0.0441	2.6824	0.3673	900.96
E25204L	cKO	VEH	0.0745	0.0593	2.7198	0.3685	912.766

E25204R	cKO	VEH	0.0628	0.0438	2.8575	0.35	894.899
E25205L	cKO	VEH	0.0606	0.0535	2.6256	0.3829	868.636
E25205R	cKO	VEH	0.0681	0.0454	2.572	0.4004	902.475
E25207L	cKO	VEH	0.0678	0.0541	2.6375	0.3772	904.243
E25207R	cKO	VEH	0.0541	0.0437	2.301	0.4486	871.667
E25308L	cKO	VEH	0.0598	0.0615	2.0127	0.5071	903.9906
E25308R	cKO	VEH	0.0618	0.0467	2.5608	0.3936	943.195
F25505L	cKO	VEH	0.0561	0.0467	2.9016	0.3455	902.159
F25505R	cKO	VEH	0.0422	0.0444	2.5987	0.3857	920.973
F25604L	cKO	VEH	0.0449	0.0608	2.3551	0.4266	914.9756
F25604R	cKO	VEH	0.0521	0.0425	2.6691	0.3764	931.895
F25610L	cKO	VEH	0.069	0.0556	2.3975	0.4285	913.523
F25610R	cKO	VEH	0.0633	0.0445	2.7925	0.3629	922.93
F25904L	cKO	VEH	0.0668	0.0509	3.1592	0.3156	887.955
F25904R	cKO	VEH	0.0708	0.0446	2.9014	0.35	912.008
F25906L	cKO	VEH	0.0649	0.0572	2.809	0.3514	936.377
F25906R	cKO	VEH	0.0553	0.0446	2.842	0.3553	922.109
G25304L	LC	VEH	0.084	0.0498	3.5153	0.2803	923.561
G25304R	LC	VEH	0.0909	0.0459	3.7126	0.2666	932.021
G25803L	LC	VEH	0.1177	0.0496	4.273	0.2288	897.109
G25803R	LC	VEH	0.1296	0.0442	4.6194	0.2122	867.374
G25902L	LC	VEH	0.0611	0.0465	3.0609	0.3309	883.725
G25902R	LC	VEH	0.0672	0.0473	3.2063	0.3124	924.698
G25911L	LC	VEH	0.0753	0.0506	3.2013	0.3179	925.897
G25911R	LC	VEH	0.0588	0.0445	2.9775	0.3358	945.026
G26101L	LC	VEH	0.0571	0.0419	3.1477	0.3144	903.801
G26101R	LC	VEH	0.0738	0.042	3.4108	0.2914	919.394
H25010L	LC	VEH	0.0857	0.052	2.9744	0.3327	920.973
H25010R	LC	VEH	0.0968	0.0488	3.3958	0.2951	943.826
H25104L	LC	VEH	0.0909	0.0514	2.6866	0.3768	912.008
H25104R	LC	VEH	0.0844	0.0439	2.9367	0.3464	907.21
H25109L	LC	VEH	0.0893	0.0456	3.6523	0.2732	903.864
H25109R	LC	VEH	0.1053	0.0437	3.8608	0.2569	896.477
H25408L	LC	VEH	0.0728	0.0478	2.8613	0.3519	899.382
H25408R	LC	VEH	0.0945	0.0461	3.5121	0.2881	914.028
H25502L	LC	VEH	0.0664	0.045	2.846	0.3553	886.061
H25502R	LC	VEH	0.0739	0.0415	3.2469	0.3057	927.475

Table G.3 Tibial metaphyseal cancellous bone measures from loaded left (L) and control right (R) limbs from 16-week-old pOC-ERαKO (cKO) and LC female mice concurrently loaded and treated with PTH or VEH for 6 weeks.

Animal Limb	cKO or LC	PTH or VEH	BV/TV	Tb.Th (mm)	Tb.N (1/mm)	Tb.Sp (mm)	cn.TMD (mg HA/cc)
I23806L	cKO	PTH	0.0675	0.0658	2.392	0.4214	879.2428
I23806R	cKO	PTH	0.0557	0.0478	2.3769	0.4265	860.682
I24607L	cKO	PTH	0.0814	0.0762	2.1482	0.4694	864.8488
I24607R	cKO	PTH	0.0764	0.051	2.7558	0.3699	904.116
I24609L	cKO	PTH	0.08	0.0733	2.7252	0.367	867.6897
I24609R	cKO	PTH	0.063	0.0487	2.6115	0.3812	894.773
I24701L	cKO	PTH	0.0831	0.0666	2.0212	0.5033	885.7455
I24701R	cKO	PTH	0.0689	0.0496	2.324	0.4356	913.207
I24702L	cKO	PTH	0.0837	0.0778	2.302	0.4369	894.5208
I24702R	cKO	PTH	0.0629	0.0495	2.8251	0.3574	891.995
J22006L	cKO	PTH	0.0462	0.0792	2.0302	0.4526	910.8088
J22006R	cKO	PTH	0.0408	0.0498	2.0877	0.482	903.233
J22102L	cKO	PTH	0.0671	0.0826	2.1491	0.4669	894.3945
J22102R	cKO	PTH	0.0412	0.046	2.1561	0.4655	910.682
J22801L	cKO	PTH	0.0621	0.0727	1.8558	0.5468	903.9275
J22801R	cKO	PTH	0.0471	0.0489	1.8688	0.541	916.617
K22510L	cKO	PTH	0.0608	0.0742	2.3395	0.4293	911.5033
K22510R	cKO	PTH	0.0426	0.0478	2.2832	0.4392	923.119
K22513L	cKO	PTH	0.0647	0.0719	2.4106	0.4167	899.382
K22513R	cKO	PTH	0.0603	0.0488	2.7299	0.3633	921.667
K22514L	cKO	PTH	0.0626	0.0755	2.4107	0.4025	927.16
K22514R	cKO	PTH	0.0453	0.0493	2.1391	0.4707	917.185
L21504L	LC	PTH	0.0709	0.0621	2.5873	0.3884	919.3317
L21504R	LC	PTH	0.0783	0.05	2.9809	0.3363	924.129
L21911L	LC	PTH	0.055	0.0594	2.588	0.3901	871.098
L21911R	LC	PTH	0.0658	0.0444	2.5943	0.3724	893.132
L21913L	LC	PTH	0.0632	0.0616	2.2865	0.4322	933.4733
L21913R	LC	PTH	0.0643	0.0461	2.6562	0.3811	922.425
L22105L	LC	PTH	0.0581	0.0603	2.6145	0.3865	923.6879
L22105R	LC	PTH	0.0704	0.0443	2.9764	0.3327	936.819
L22501L	LC	PTH					
L22501R	LC	PTH	0.0903	0.0487	3.4892	0.2858	938.713
M23007L	LC	PTH	0.0918	0.0752	2.6122	0.3839	882.0837
M23007R	LC	PTH	0.0737	0.049	2.9638	0.3413	922.425
M23405L	LC	PTH	0.0933	0.0633	3.2958	0.304	908.978
M23405R	LC	PTH	0.1	0.0496	3.5396	0.2818	892.753
M23801L	LC	PTH	0.0672	0.0542	2.8768	0.3474	914.281
M23801R	LC	PTH	0.0781	0.0485	3.1301	0.3252	926.655
N24004L	LC	PTH	0.1031	0.0669	2.7111	0.3732	943.7638
N24004R	LC	PTH	0.0796	0.0471	3.231	0.315	919.268
N24011L	LC	PTH	0.1052	0.0712	2.8691	0.3546	947.4255
N24011R	LC	PTH	0.0767	0.0493	2.9617	0.3322	960.493
N24014L	LC	PTH	0.1169	0.0621	3.0406	0.3267	952.0973

N24014R	LC	PTH	0.093	0.0501	3.2894	0.3044	922.488
O23903L	cKO	VEH	0.0655	0.0694	2.2178	0.4481	898.2456
O23903R	cKO	VEH	0.0372	0.043	2.2656	0.4454	898.624
O24805L*	cKO	VEH	0.0843	0.0703	2.4259	0.4177	930.6954
O24805R*	cKO	VEH	0.0606	0.0448	2.7794	0.3583	922.362
O24807L	cKO	VEH	0.1085	0.0778	2.2162	0.451	891.0486
O24807R	cKO	VEH	0.0538	0.0485	2.3779	0.4252	929.559
O24810L	cKO	VEH	0.0832	0.0765	2.3736	0.4325	928.6122
O24810R	cKO	VEH	0.0425	0.0467	2.154	0.4663	921.415
O24812L	cKO	VEH	0.0878	0.0709	2.4445	0.4108	925.708
O24812R	cKO	VEH	0.0573	0.0448	2.0026	0.5095	914.218
P22403L	cKO	VEH	0.0817	0.0671	2.3442	0.4178	871.3513
P22403R	cKO	VEH	0.0504	0.0486	2.2037	0.4539	936.188
P22405L	cKO	VEH	0.0751	0.0698	2.1905	0.4672	878.5483
P22405R	cKO	VEH	0.0631	0.0424	2.4638	0.4121	874.129
P22406L	cKO	VEH	0.088	0.073	2.1187	0.4697	920.9731
P22406R	cKO	VEH	0.0446	0.0465	2.1833	0.5102	913.207
Q21101L	cKO	VEH	0.0453	0.0493	2.1391	0.4707	917.185
Q21101R	cKO	VEH	0.0526	0.0451	2.4422	0.4125	933.41
Q22314L	cKO	VEH	0.0839	0.0749	2.3125	0.4256	929.3698
Q22314R	cKO	VEH	0.0491	0.0475	2.3901	0.4299	923.877
Q22701L	cKO	VEH	0.0654	0.0774	2.0936	0.4914	886.5662
Q22701R	cKO	VEH	0.0441	0.0441	2.2163	0.4524	899.697
R21003L	LC	VEH	0.1117	0.0586	3.5927	0.2682	929.748
R21003R	LC	VEH	0.0894	0.045	3.5495	0.2806	947.614
R22004L	LC	VEH	0.0533	0.0648	2.0889	0.4837	927.6021
R22004R	LC	VEH	0.0466	0.0476	2.6233	0.3841	948.625
R22205L	LC	VEH	0.064	0.0668	2.7743	0.3633	918.1322
R22205R	LC	VEH	0.0576	0.0459	2.8881	0.3493	932.4
R22407L	LC	VEH	0.0801	0.0733	2.6239	0.3814	915.4175
R22407R	LC	VEH	0.0603	0.0472	2.6736	0.3781	948.498
R22711L	LC	VEH	0.0764	0.0643	2.9048	0.3452	978.2971
R22711R	LC	VEH	0.0674	0.0453	3.2287	0.3086	972.047
S24803L	LC	VEH	0.1205	0.0611	3.7832	0.2584	856.4521
S24803R	LC	VEH	0.1012	0.0446	4.0071	0.245	901.654
S24811L	LC	VEH	0.0775	0.0608	2.4511	0.4072	896.2253
S24811R	LC	VEH	0.0639	0.0477	3.1356	0.3229	899.697
S24813L	LC	VEH	0.1097	0.0743	2.8666	0.345	900.9603
S24813R	LC	VEH	0.0735	0.0457	2.974	0.3349	932.273
T24108L	LC	VEH	0.1056	0.067	2.6464	0.3856	929.9379
T24108R	LC	VEH	0.058	0.046	2.7564	0.3635	949.698
T24109L	LC	VEH	0.0812	0.0722	2.5448	0.3913	950.2032
T24109R	LC	VEH	0.0488	0.0461	2.5692	0.3946	979.18
T24305L	LC	VEH	0.102	0.0695	2.8405	0.3548	881.705
T24305R	LC	VEH	0.0706	0.0437	2.5818	0.3896	864.785

* Mouse died on loading day 25 of 30 (5wks)

Table G.4 Tibial metaphyseal cortical shell bone measures from loaded left (L) and control right (R) limbs from 10-week-old pOC-ERαKO (cKO) and LC female mice concurrently loaded and treated with PTH or VEH for 2 weeks.

Animal Limb	cKO or LC	PTH or VEH	Ct.Ar (mm^2)	Ct.Th (mm)	I_{MAX} (mm^4)	I_{MIN} (mm^4)	ct.TMD (mg HA/cc)
U23008L	cKO	PTH	1.01302	0.162	0.39497	0.27007	950.1401
U23008R	cKO	PTH	0.86756	0.15	0.28408	0.23988	944.1426
U23009L	cKO	PTH	0.96157	0.158	0.35526	0.26484	925.8344
U23009R	cKO	PTH	0.83144	0.149	0.26684	0.21194	938.7133
U23010L	cKO	PTH	0.90282	0.149	0.334	0.24316	949.3195
U23010R	cKO	PTH	0.81172	0.133	0.27218	0.23057	943.9532
U23015L	cKO	PTH	1.01266	0.152	0.41289	0.29303	959.7362
U23015R	cKO	PTH	0.97733	0.15	0.34643	0.29937	965.2288
U23112L	cKO	PTH	1.03121	0.151	0.44467	0.29875	962.1984
U23112R	cKO	PTH	0.93266	0.15	0.33233	0.27355	951.7185
V27101L	cKO	PTH	0.99162	0.159	0.35989	0.2604	962.9559
V27101R	cKO	PTH					
V27208L	cKO	PTH	1.04774	0.161	0.40976	0.31077	950.077
V27208R	cKO	PTH	0.92166	0.159	0.30778	0.24053	942.1224
V27607L	cKO	PTH	1.00463	0.153	0.39014	0.31487	893.7001
V27607R	cKO	PTH	0.87804	0.145	0.29329	0.25886	870.0887
V27915L	cKO	PTH	0.9676	0.151	0.35767	0.25713	934.1046
V27915R	cKO	PTH	0.85568	0.151	0.26127	0.21453	928.2333
V28202L	cKO	PTH	1.08475	0.156	0.45977	0.28704	930.6323
V28202R	cKO	PTH	0.86122	0.149	0.2929	0.22668	922.9934
W23105L	LC	PTH	1.01877	0.164	0.37929	0.28857	950.077
W23105R	LC	PTH	0.89813	0.147	0.31712	0.26109	954.4331
W23107L	LC	PTH	1.08492	0.158	0.43818	0.3106	988.2089
W23107R	LC	PTH	0.93945	0.156	0.30969	0.26502	995.4059
W23114L	LC	PTH	1.10171	0.162	0.45672	0.30766	975.0142
W23114R	LC	PTH	1.0059	0.165	0.34398	0.28255	969.5848
W23901L	LC	PTH	1.13911	0.18	0.43009	0.33578	950.9609
W23901R	LC	PTH	0.9389	0.158	0.32123	0.27284	964.2186
W24204L	LC	PTH	1.04551	0.157	0.39619	0.32537	936.2511
W24204R	LC	PTH	0.88008	0.148	0.28474	0.25397	955.6327
X27105L	LC	PTH	1.12437	0.178	0.42359	0.31605	971.0369
X27105R	LC	PTH	0.97133	0.165	0.31603	0.26537	956.0746
X27106L	LC	PTH	1.00515	0.162	0.3682	0.2578	941.1123
X27106R	LC	PTH	0.84841	0.151	0.26815	0.20247	940.481
X27202L	LC	PTH	1.15372	0.173	0.45727	0.31024	993.5118
X27202R	LC	PTH	0.96466	0.169	0.31542	0.23682	978.2971
X27204L	LC	PTH	1.08289	0.174	0.41766	0.28702	969.7111
X27204R	LC	PTH	0.94659	0.159	0.32283	0.25417	961.3146
X27407L	LC	PTH	1.16868	0.172	0.45461	0.34216	978.6127
X27407R	LC	PTH	0.95165	0.157	0.3111	0.26656	978.2339
Y23312L	cKO	VEH	0.92224	0.148	0.33908	0.25549	963.8398
Y23312R	cKO	VEH	0.77085	0.133	0.24604	0.20987	961.2515
Y23402L	cKO	VEH	0.8598	0.141	0.31235	0.23475	943.7007

Y23402R	cKO	VEH	0.73715	0.128	0.24454	0.1889	934.9885
Y23406L	cKO	VEH	0.90969	0.144	0.3384	0.26083	933.5364
Y23406R	cKO	VEH	0.79832	0.135	0.25889	0.23164	930.0642
Y23408L	cKO	VEH	0.97047	0.157	0.36715	0.26632	945.5946
Y23408R	cKO	VEH	0.84525	0.142	0.3342	0.20313	957.4004
Y23510L	cKO	VEH	0.92942	0.152	0.33271	0.25639	963.0823
Y23510R	cKO	VEH	0.80168	0.135	0.27674	0.22102	937.8926
Z28001L	cKO	VEH	0.85873	0.137	0.28685	0.24812	941.8068
Z28001R	cKO	VEH	0.79287	0.134	0.25851	0.22262	915.2913
Z28004L	cKO	VEH	0.9142	0.148	0.34578	0.27569	931.8319
Z28004R	cKO	VEH	0.83046	0.141	0.26749	0.22219	939.9127
Z28102L	cKO	VEH	0.9073	0.144	0.34968	0.25224	954.9382
Z28102R	cKO	VEH	0.80519	0.131	0.26533	0.23643	945.8472
Z28106L	cKO	VEH	0.97135	0.147	0.38099	0.29901	935.0516
Z28106R	cKO	VEH	0.79525	0.13	0.27463	0.24389	929.8748
Z28305L	cKO	VEH	0.94168	0.147	0.35824	0.25727	947.1099
Z28305R	cKO	VEH	0.84927	0.139	0.29379	0.23578	935.7461
AB23004L	LC	VEH	0.9853	0.156	0.38386	0.27171	960.557
AB23004R	LC	VEH	0.77467	0.138	0.25551	0.19484	920.6575
AB23311L	LC	VEH	0.96911	0.152	0.35009	0.27949	939.092
AB23311R	LC	VEH	0.84138	0.144	0.27644	0.22256	907.5891
AB23313L	LC	VEH	1.04777	0.157	0.43511	0.31701	949.2563
AB23313R	LC	VEH	0.90667	0.152	0.32222	0.27369	952.0973
AB23314L	LC	VEH	1.0888	0.172	0.40191	0.33211	979.244
AB23314R	LC	VEH	0.94072	0.155	0.31042	0.27994	983.2845
AB23315L	LC	VEH	1.06674	0.16	0.44692	0.29812	942.5643
AB23315R	LC	VEH	0.8188	0.138	0.26251	0.22946	964.0292
CD27903L	LC	VEH	0.98914	0.154	0.36654	0.27294	972.2365
CD27903R	LC	VEH	0.87695	0.145	0.28768	0.24882	971.7944
CD27904L	LC	VEH	0.95375	0.151	0.34517	0.28232	955.5063
CD27904R	LC	VEH	0.82306	0.142	0.268	0.216	968.7642
CD28016L	LC	VEH	1.14812	0.167	0.44833	0.40412	963.0192
CD28016R	LC	VEH	0.98894	0.149	0.37053	0.32866	971.1631
CD28017L	LC	VEH	1.06474	0.161	0.38565	0.34798	975.3298
CD28017R	LC	VEH	0.9195	0.151	0.32883	0.23894	966.1125
CD28107L	LC	VEH	0.93842	0.145	0.36342	0.28458	960.9358
CD28107R	LC	VEH	0.8494	0.14	0.27763	0.24261	972.552

Table G.5 Tibial metaphyseal cortical shell bone measures from loaded left (L) and control right (R) limbs from 16-week-old pOC-ERαKO (cKO) and LC female mice concurrently loaded and treated with PTH or VEH for 2 weeks.

Animal Limb	cKO or LC	PTH or VEH	Ct.Ar (mm^2)	Ct.Th (mm)	I_{MAX} (mm^4)	I_{MIN} (mm^4)	ct.TMD (mg HA/cc)
A26404L	cKO	PTH	1.03737	0.172	0.36023	0.2513	964.5343
A26404R	cKO	PTH	0.88318	0.156	0.28464	0.21804	1007.212
A26407L	cKO	PTH	1.04474	0.164	0.38941	0.27495	968.8904
A26407R	cKO	PTH	0.85567	0.151	0.27594	0.21811	988.0194
A26614L	cKO	PTH	1.08231	0.167	0.39651	0.28997	988.3982
A26614R	cKO	PTH	0.84991	0.139	0.28996	0.24046	1000.078
A26618L	cKO	PTH	1.13342	0.173	0.42005	0.27303	988.1456
A26618R	cKO	PTH	0.87833	0.158	0.26672	0.21296	1007.275
A26904L	cKO	PTH	1.08074	0.147	0.4722	0.28349	901.2128
A26904R	cKO	PTH	0.83156	0.138	0.29382	0.23004	954.1807
B25804L	cKO	PTH	1.10375	0.165	0.42766	0.28522	986.6305
B25804R	cKO	PTH	0.92672	0.156	0.337	0.23487	1003.108
B25816L	cKO	PTH	1.07773	0.158	0.42984	0.25046	932.7788
B25816R	cKO	PTH	0.78889	0.142	0.26002	0.17831	958.0316
B26308L	cKO	PTH	1.03084	0.159	0.40315	0.28262	999.3832
B26308R	cKO	PTH	0.92795	0.156	0.33123	0.24517	1032.654
B26506L	cKO	PTH	1.0719	0.169	0.40958	0.28007	1015.166
B26506R	cKO	PTH	0.90108	0.151	0.30561	0.25935	1017.313
B26804L	cKO	PTH	1.0874	0.165	0.41854	0.28325	1006.138
B26804R	cKO	PTH	0.88229	0.153	0.29684	0.23064	1021.858
C26303L	LC	PTH	1.21387	0.197	0.43646	0.30722	1009.8
C26303R	LC	PTH	1.02132	0.171	0.33888	0.27918	1023.31
C26608L	LC	PTH	1.22642	0.18	0.45431	0.37337	1003.487
C26608R	LC	PTH	1.00814	0.17	0.30891	0.26981	1026.53
C26611L	LC	PTH	1.09414	0.179	0.3741	0.26781	1011.631
C26611R	LC	PTH	0.94094	0.167	0.2991	0.22147	1018.702
C26702L	LC	PTH	1.17759	0.202	0.39942	0.26168	1009.863
C26702R	LC	PTH	0.9282	0.174	0.26108	0.21504	1045.785
C26705L	LC	PTH	1.04978	0.174	0.39428	0.23887	1010.179
C26705R	LC	PTH	0.89925	0.166	0.27913	0.20503	1010.242
D26805L	LC	PTH	1.25251	0.187	0.47928	0.35697	1021.858
D26805R	LC	PTH	0.97123	0.167	0.30878	0.26198	1039.409
D26807L	LC	PTH	1.04196	0.173	0.39553	0.25723	1007.212
D26807R	LC	PTH	0.99812	0.171	0.33691	0.26125	1021.543
D26815L	LC	PTH	1.13169	0.18	0.41603	0.31235	1031.075
D26815R	LC	PTH	1.06781	0.184	0.34717	0.27271	1059.232
D26908L	LC	PTH	1.08217	0.177	0.42432	0.2813	1026.783
D26908R	LC	PTH	0.95351	0.166	0.33225	0.24037	1039.535
D26909L	LC	PTH	1.13984	0.168	0.4589	0.2957	1009.295
D26909R	LC	PTH	0.97583	0.166	0.32606	0.25927	1045.343
E25202L	cKO	VEH	0.96728	0.158	0.36574	0.26055	982.1481
E25202R	cKO	VEH	0.8293	0.145	0.27267	0.22264	1019.08
E25204L	cKO	VEH	0.99087	0.159	0.37629	0.25051	982.6532

E25204R	cKO	VEH	0.8595	0.148	0.28424	0.22667	998.373
E25205L	cKO	VEH	0.97267	0.154	0.35716	0.26962	975.2667
E25205R	cKO	VEH	0.87367	0.152	0.27773	0.23388	1012.199
E25207L	cKO	VEH	1.08365	0.166	0.40548	0.28901	991.7443
E25207R	cKO	VEH	0.86515	0.15	0.29997	0.21824	993.8275
E25308L	cKO	VEH	0.96651	0.159	0.35958	0.24065	997.7417
E25308R	cKO	VEH	0.90551	0.155	0.30008	0.24288	1008.79
F25505L	cKO	VEH	0.93998	0.153	0.35329	0.25291	987.4512
F25505R	cKO	VEH	0.88627	0.153	0.31246	0.2397	1008.601
F25604L	cKO	VEH	0.95172	0.156	0.35639	0.25165	994.7114
F25604R	cKO	VEH	0.88583	0.146	0.32443	0.225	1014.535
F25610L	cKO	VEH	0.90056	0.156	0.31416	0.21684	1018.512
F25610R	cKO	VEH	0.8386	0.142	0.2809	0.22448	1004.244
F25904L	cKO	VEH	0.96682	0.157	0.37879	0.26622	969.2692
F25904R	cKO	VEH	0.7881	0.143	0.26416	0.18679	994.7114
F25906L	cKO	VEH	0.95038	0.153	0.37133	0.25684	1018.575
F25906R	cKO	VEH	0.88213	0.144	0.30579	0.25577	1023.184
G25304L	LC	VEH	1.00469	0.167	0.34585	0.25996	1018.26
G25304R	LC	VEH	0.8932	0.158	0.29644	0.2178	1016.366
G25803L	LC	VEH	1.00914	0.167	0.33085	0.26625	971.8575
G25803R	LC	VEH	0.79896	0.143	0.24176	0.18804	987.2618
G25902L	LC	VEH	0.95958	0.156	0.33891	0.27252	985.6835
G25902R	LC	VEH	0.91869	0.158	0.31357	0.22769	1010.242
G25911L	LC	VEH	1.1281	0.181	0.42488	0.29619	1009.989
G25911R	LC	VEH	0.91724	0.15	0.32375	0.24569	1024.573
G26101L	LC	VEH	0.98827	0.153	0.3926	0.27163	1005.065
G26101R	LC	VEH	0.89209	0.159	0.31316	0.21447	1035.621
H25010L	LC	VEH	1.09134	0.177	0.40842	0.29641	1018.891
H25010R	LC	VEH	0.99619	0.17	0.32922	0.27012	1047.742
H25104L	LC	VEH	1.02309	0.161	0.39458	0.28096	1015.798
H25104R	LC	VEH	0.88762	0.147	0.31973	0.23595	1017.25
H25109L	LC	VEH	1.00898	0.156	0.39803	0.29496	990.9866
H25109R	LC	VEH	0.91408	0.149	0.3533	0.23928	982.7163
H25408L	LC	VEH	1.0408	0.171	0.3703	0.27783	1002.729
H25408R	LC	VEH	1.01641	0.161	0.36443	0.27682	1009.674
H25502L	LC	VEH	0.96114	0.17	0.35897	0.2171	1015.419
H25502R	LC	VEH	0.90859	0.164	0.29278	0.21326	1039.914

Table G.6 Tibial diaphyseal cortical bone measures from loaded left (L) and control right (R) limbs from 10-week-old pOC-ERαKO (cKO) and LC female mice concurrently loaded and treated with PTH or VEH for 2 weeks.

Animal Limb	cKO or LC	PTH or VEH	Ct.Ar (mm^2)	Ma.Ar (mm^2)	Ct.Th (mm)	I_{MAX} (mm^4)	I_{MIN} (mm^4)	ct.TMD (mg HA/cc)
U23008L	cKO	PTH	0.71122	0.39165	0.234	0.10166	0.07314	1043.8914
U23008R	cKO	PTH	0.5807	0.4004	0.198	0.07005	0.06018	1033.9164
U23009L	cKO	PTH	0.63113	0.39022	0.213	0.08978	0.05851	1024.0679
U23009R	cKO	PTH	0.5956	0.418	0.196	0.07856	0.06131	1022.6158
U23010L	cKO	PTH	0.67872	0.36833	0.229	0.09693	0.06265	1033.0326
U23010R	cKO	PTH	0.5173	0.35547	0.189	0.05468	0.04743	1023.8153
U23015L	cKO	PTH	0.60069	0.34338	0.216	0.06889	0.05459	1059.2955
U23015R	cKO	PTH	0.57802	0.38408	0.2	0.07095	0.05516	1049.4469
U23112L	cKO	PTH	0.63366	0.37258	0.222	0.08432	0.05879	1053.4874
U23112R	cKO	PTH	0.57897	0.39408	0.199	0.0745	0.05451	1034.9265
V27101L	cKO	PTH	0.69216	0.3474	0.235	0.09402	0.06559	1027.9188
V27101R	cKO	PTH						
V27208L	cKO	PTH	0.65119	0.40851	0.217	0.09345	0.06283	1060.4319
V27208R	cKO	PTH	0.59065	0.40168	0.199	0.0768	0.05843	1022.4264
V27607L	cKO	PTH	0.60684	0.38041	0.21	0.07996	0.05531	941.5542
V27607R	cKO	PTH	0.58445	0.41334	0.197	0.08265	0.05246	932.0844
V27915L	cKO	PTH	0.67797	0.37865	0.222	0.10253	0.06229	1023.184
V27915R	cKO	PTH	0.57971	0.39804	0.198	0.07283	0.05695	1029.5603
V28202L	cKO	PTH	0.65533	0.35172	0.22	0.09398	0.05829	1027.6664
V28202R	cKO	PTH	0.57697	0.36857	0.203	0.07079	0.05244	1033.4114
W23105L	LC	PTH	0.66683	0.41316	0.213	0.09964	0.06772	1035.0529
W23105R	LC	PTH	0.61602	0.4263	0.202	0.07995	0.06703	1038.7776
W23107L	LC	PTH	0.65424	0.35947	0.226	0.08321	0.06204	1069.0811
W23107R	LC	PTH	0.61101	0.36173	0.214	0.07644	0.05692	1065.2931
W23114L	LC	PTH	0.67257	0.36081	0.228	0.0884	0.06688	1060.1162
W23114R	LC	PTH	0.64512	0.39608	0.213	0.0906	0.0631	1034.8634
W23901L	LC	PTH	0.779	0.4009	0.246	0.12713	0.08094	1046.101
W23901R	LC	PTH	0.65361	0.44559	0.21	0.09237	0.07321	1054.0555
W24204L	LC	PTH	0.64633	0.45146	0.206	0.09591	0.06869	1034.6741
W24204R	LC	PTH	0.62545	0.43394	0.207	0.08143	0.06922	1035.4316
X27105L	LC	PTH	0.72477	0.41338	0.226	0.11556	0.07654	1037.6412
X27105R	LC	PTH	0.64385	0.40137	0.21	0.08832	0.06783	1029.876
X27106L	LC	PTH	0.65718	0.33984	0.229	0.08717	0.05839	1036.8837
X27106R	LC	PTH	0.55465	0.33737	0.201	0.06358	0.04795	1025.583
X27202L	LC	PTH	0.73521	0.38433	0.24	0.10365	0.07806	1054.9395
X27202R	LC	PTH	0.64491	0.41692	0.212	0.08888	0.06692	1044.8383
X27204L	LC	PTH	0.71081	0.40512	0.229	0.10597	0.07427	1043.5125
X27204R	LC	PTH	0.61508	0.39232	0.21	0.07525	0.06465	1035.116
X27407L	LC	PTH	0.72184	0.41736	0.231	0.10712	0.07818	1047.4899
X27407R	LC	PTH	0.58775	0.28821	0.224	0.0634	0.04596	1073.8159
Y23312L	cKO	VEH	0.67167	0.41103	0.21	0.11302	0.0632	1022.9314
Y23312R	cKO	VEH	0.58982	0.38008	0.204	0.07216	0.05775	1044.2069
Y23402L	cKO	VEH	0.60573	0.33686	0.218	0.07319	0.0527	1045.3434

Y23402R	cKO	VEH	0.54454	0.36434	0.197	0.05871	0.05196	1036.0629
Y23406L	cKO	VEH	0.68943	0.36556	0.231	0.09456	0.06624	1033.3483
Y23406R	cKO	VEH	0.5956	0.43751	0.195	0.08316	0.06126	1028.6133
Y23408L	cKO	VEH	0.72909	0.36853	0.237	0.1172	0.0668	1025.7723
Y23408R	cKO	VEH	0.59124	0.34208	0.212	0.0737	0.0499	1052.6035
Y23510L	cKO	VEH	0.63958	0.36493	0.221	0.08294	0.05955	1051.4041
Y23510R	cKO	VEH	0.61625	0.44759	0.197	0.08835	0.0654	1019.9011
Z28001L	cKO	VEH	0.61232	0.37331	0.208	0.08011	0.05756	1036.2523
Z28001R	cKO	VEH	0.55113	0.37711	0.193	0.06617	0.05089	1015.2925
Z28004L	cKO	VEH	0.67824	0.41337	0.213	0.11543	0.06415	1007.8429
Z28004R	cKO	VEH	0.58929	0.3613	0.204	0.07719	0.05213	1020.343
Z28102L	cKO	VEH	0.62565	0.40066	0.208	0.0875	0.06092	1041.1766
Z28102R	cKO	VEH	0.55727	0.38843	0.193	0.06957	0.05198	1023.3103
Z28106L	cKO	VEH	0.66329	0.38125	0.222	0.09408	0.06275	1038.2726
Z28106R	cKO	VEH	0.57313	0.38142	0.199	0.07133	0.05433	1026.4037
Z28305L	cKO	VEH	0.65619	0.38721	0.217	0.08915	0.06793	1041.1135
Z28305R	cKO	VEH	0.5715	0.33729	0.208	0.06595	0.04973	1041.6816
AB23004L	LC	VEH	0.76078	0.4154	0.231	0.13764	0.07591	1022.4264
AB23004R	LC	VEH	0.60392	0.41352	0.196	0.0889	0.05744	1012.7672
AB23311L	LC	VEH	0.657	0.35119	0.23	0.08212	0.06141	1038.3357
AB23311R	LC	VEH	0.55975	0.37507	0.198	0.06379	0.05466	1030.823
AB23313L	LC	VEH	0.7216	0.44317	0.227	0.10678	0.08522	1043.5125
AB23313R	LC	VEH	0.60513	0.39701	0.206	0.07891	0.05937	1041.8711
AB23314L	LC	VEH	0.74238	0.40641	0.234	0.1179	0.07642	1042.7549
AB23314R	LC	VEH	0.70563	0.44519	0.219	0.10574	0.08174	1030.2548
AB23315L	LC	VEH	0.64244	0.30577	0.234	0.07272	0.05691	1057.4647
AB23315R	LC	VEH	0.60903	0.36314	0.209	0.08286	0.05255	1037.8306
CD27903L	LC	VEH	0.71965	0.36025	0.243	0.09555	0.07243	1044.712
CD27903R	LC	VEH	0.60377	0.37595	0.208	0.07567	0.05807	1045.0908
CD27904L	LC	VEH	0.69026	0.36993	0.226	0.09847	0.06788	1029.8129
CD27904R	LC	VEH	0.58661	0.36827	0.202	0.073	0.05566	1039.8508
CD28016L	LC	VEH	0.75084	0.41566	0.233	0.1299	0.07485	1021.1637
CD28016R	LC	VEH	0.67732	0.42888	0.216	0.09763	0.07416	1040.6715
CD28017L	LC	VEH	0.64177	0.3665	0.225	0.07862	0.06275	1049.005
CD28017R	LC	VEH	0.62455	0.41415	0.206	0.08027	0.06744	1032.0225
CD28107L	LC	VEH	0.6878	0.41016	0.218	0.11254	0.06528	1044.8383
CD28107R	LC	VEH	0.56629	0.34221	0.207	0.06248	0.05052	1057.149

Table G.7 Tibial diaphyseal cortical bone measures from loaded left (L) and control right (R) limbs from 16-week-old pOC-ERαKO (cKO) and LC female mice concurrently loaded and treated with PTH or VEH for 2 weeks.

Animal Limb	cKO or LC	PTH or VEH	Ct.Ar (mm^2)	Ma.Ar (mm^2)	Ct.Th (mm)	I_{MAX} (mm^4)	I_{MIN} (mm^4)	ct.TMD (mg HA/cc)
A26404L	cKO	PTH	0.69392	0.33591	0.232	0.10511	0.05887	1049.258
A26404R	cKO	PTH	0.59624	0.34934	0.209	0.07186	0.05445	1072.111
A26407L	cKO	PTH	0.71209	0.34917	0.238	0.10023	0.06789	1044.333
A26407R	cKO	PTH	0.57358	0.37307	0.202	0.06362	0.05728	1051.467
A26614L	cKO	PTH	0.78287	0.42034	0.235	0.13008	0.08253	1017.376
A26614R	cKO	PTH	0.63131	0.39761	0.206	0.08867	0.06243	1054.119
A26618L	cKO	PTH	0.71644	0.31855	0.249	0.10046	0.05986	1050.899
A26618R	cKO	PTH	0.56964	0.36943	0.2	0.06875	0.05284	1049.51
A26904L	cKO	PTH	0.73842	0.38817	0.233	0.10419	0.08035	999.6989
A26904R	cKO	PTH	0.57179	0.33709	0.207	0.05963	0.05546	1048.563
B25804L	cKO	PTH	0.70532	0.40631	0.223	0.10617	0.07392	1058.538
B25804R	cKO	PTH	0.62462	0.35931	0.216	0.07845	0.05959	1058.285
B25816L	cKO	PTH	0.70148	0.3077	0.246	0.09449	0.05979	1018.323
B25816R	cKO	PTH	0.54014	0.32223	0.201	0.05617	0.04688	1048.374
B26308L	cKO	PTH	0.68614	0.37065	0.23	0.08921	0.07075	1063.147
B26308R	cKO	PTH	0.60657	0.35256	0.213	0.07164	0.05688	1080.192
B26506L	cKO	PTH	0.69894	0.33844	0.243	0.09037	0.06503	1071.922
B26506R	cKO	PTH	0.58632	0.3687	0.206	0.0673	0.05786	1056.455
B26804L	cKO	PTH	0.64745	0.34473	0.227	0.0805	0.05985	1073.942
B26804R	cKO	PTH	0.61695	0.37864	0.211	0.08367	0.0555	1065.23
C26303L	LC	PTH	0.75522	0.3565	0.251	0.10204	0.07842	1068.071
C26303R	LC	PTH	0.69899	0.40961	0.225	0.09668	0.07687	1059.674
C26608L	LC	PTH	0.77919	0.35643	0.251	0.11545	0.07889	1051.53
C26608R	LC	PTH	0.6647	0.34654	0.228	0.07952	0.06726	1068.323
C26611L	LC	PTH	0.7484	0.36218	0.244	0.10987	0.0738	1045.785
C26611R	LC	PTH	0.63609	0.37115	0.217	0.0762	0.06664	1065.167
C26702L	LC	PTH	0.81697	0.27097	0.291	0.10303	0.07397	1065.672
C26702R	LC	PTH	0.60217	0.2772	0.229	0.06129	0.05068	1095.596
C26705L	LC	PTH	0.74226	0.37713	0.242	0.10598	0.07952	1067.629
C26705R	LC	PTH	0.6337	0.36833	0.216	0.07425	0.06755	1048.247
D26805L	LC	PTH	0.77312	0.35176	0.251	0.11067	0.07784	1072.617
D26805R	LC	PTH	0.68283	0.36637	0.229	0.08907	0.07017	1071.417
D26807L	LC	PTH	0.65043	0.37203	0.223	0.0852	0.06258	1070.344
D26807R	LC	PTH	0.64855	0.37534	0.22	0.08482	0.06342	1055.066
D26815L	LC	PTH	0.72088	0.41531	0.23	0.10456	0.07825	1081.202
D26815R	LC	PTH	0.68912	0.40719	0.225	0.09758	0.07231	1073.374
D26908L	LC	PTH	0.71614	0.38371	0.237	0.10311	0.07161	1068.892
D26908R	LC	PTH	0.65384	0.31834	0.237	0.07394	0.0596	1085.243
D26909L	LC	PTH	0.69192	0.35682	0.233	0.08446	0.07386	1081.266
D26909R	LC	PTH	0.64623	0.36175	0.219	0.0795	0.06267	1085.306
E25202L	cKO	VEH	0.62386	0.34613	0.221	0.07518	0.05641	1066.745
E25202R	cKO	VEH						
E25204L	cKO	VEH	0.69725	0.36267	0.23	0.09601	0.06938	1061.126

E25204R	cKO	VEH	0.60455	0.38662	0.208	0.07449	0.05987	1049.258
E25205L	cKO	VEH	0.68055	0.35756	0.233	0.091	0.06509	1057.465
E25205R	cKO	VEH	0.61602	0.39275	0.209	0.07848	0.0612	1058.664
E25207L	cKO	VEH	0.68234	0.40546	0.224	0.09249	0.07256	1066.619
E25207R	cKO	VEH	0.63651	0.40327	0.211	0.08452	0.06624	1031.833
E25308L	cKO	VEH	0.71206	0.37113	0.233	0.10697	0.0677	1045.28
E25308R	cKO	VEH	0.63866	0.4062	0.208	0.0837	0.06716	1064.409
F25505L	cKO	VEH	0.59793	0.35779	0.21	0.07278	0.05433	1069.207
F25505R	cKO	VEH	0.6049	0.38174	0.207	0.0707	0.06338	1058.601
F25604L	cKO	VEH	0.65678	0.36094	0.224	0.08203	0.06462	1062.2
F25604R	cKO	VEH	0.5915	0.36934	0.206	0.06883	0.05807	1058.412
F25610L	cKO	VEH	0.62144	0.37624	0.213	0.07731	0.06115	1065.861
F25610R	cKO	VEH	0.58764	0.38029	0.203	0.06551	0.06102	1063.904
F25904L	cKO	VEH	0.64821	0.40616	0.215	0.08843	0.06601	1049.194
F25904R	cKO	VEH	0.59299	0.37955	0.201	0.0726	0.05978	1045.28
F25906L	cKO	VEH	0.63442	0.39825	0.21	0.08189	0.06719	1065.041
F25906R	cKO	VEH	0.65785	0.45195	0.2	0.10242	0.07176	1049.384
G25304L	LC	VEH	0.68309	0.35091	0.23	0.09223	0.06526	1071.417
G25304R	LC	VEH	0.59869	0.32399	0.218	0.06357	0.05686	1069.334
G25803L	LC	VEH	0.81619	0.27759	0.282	0.10561	0.07623	1039.093
G25803R	LC	VEH	0.5764	0.30365	0.211	0.06234	0.04999	1059.864
G25902L	LC	VEH	0.61353	0.35433	0.214	0.07648	0.05583	1062.515
G25902R	LC	VEH	0.65279	0.38778	0.212	0.09526	0.06276	1065.167
G25911L	LC	VEH	0.75558	0.35947	0.247	0.10468	0.07934	1075.015
G25911R	LC	VEH	0.6467	0.33238	0.227	0.07121	0.06684	1084.548
G26101L	LC	VEH	0.68139	0.39713	0.22	0.09987	0.06982	1066.871
G26101R	LC	VEH	0.64262	0.37829	0.217	0.07531	0.06931	1071.669
H25010L	LC	VEH	0.70522	0.39114	0.232	0.09387	0.0758	1073.879
H25010R	LC	VEH	0.6807	0.43925	0.216	0.0936	0.07956	1071.48
H25104L	LC	VEH	0.71727	0.40265	0.229	0.09473	0.08267	1076.404
H25104R	LC	VEH	0.6396	0.37428	0.213	0.07962	0.06717	1063.715
H25109L	LC	VEH	0.66349	0.35379	0.231	0.08002	0.06588	1069.207
H25109R	LC	VEH	0.67758	0.39679	0.218	0.09094	0.07432	1044.901
H25408L	LC	VEH	0.6415	0.31171	0.231	0.07399	0.05812	1082.718
H25408R	LC	VEH	0.62655	0.32657	0.224	0.07338	0.05665	1064.914
H25502L	LC	VEH	0.64566	0.34438	0.224	0.08134	0.05985	1082.907
H25502R	LC	VEH	0.64295	0.32044	0.23	0.07598	0.05788	1087.579

Table G.8 Tibial diaphyseal cortical bone measures from loaded left (L) and control right (R) limbs from 16-week-old pOC-ERαKO (cKO) and LC female mice concurrently loaded and treated with PTH or VEH for 6 weeks.

Animal Limb	cKO or LC	PTH or VEH	Ct.Ar (mm^2)	Ma.Ar (mm^2)	Ct.Th (mm)	I_{MAX} (mm^4)	I_{MIN} (mm^4)	ct.TMD (mg HA/cc)
I23806L	cKO	PTH	0.76372	0.37000	0.25	0.11225	0.07669	1073.3108
I23806R	cKO	PTH	0.62349	0.34578	0.219	0.07496	0.05831	1070.1543
I24607L	cKO	PTH	0.68811	0.37334	0.231	0.09665	0.06591	1062.1365
I24607R	cKO	PTH	0.58762	0.34619	0.21	0.06664	0.05455	1082.6544
I24609L	cKO	PTH	0.71834	0.39572	0.234	0.10584	0.07318	1069.5229
I24609R	cKO	PTH	0.59732	0.40531	0.202	0.07271	0.06192	1062.6415
I24701L	cKO	PTH	0.74296	0.40986	0.233	0.12956	0.07181	1065.4824
I24701R	cKO	PTH	0.57969	0.36847	0.203	0.06776	0.05582	1072.5532
I24702L	cKO	PTH	0.68997	0.39543	0.227	0.09972	0.06824	1069.5861
I24702R	cKO	PTH	0.64635	0.4114	0.206	0.09284	0.0644	1046.6691
J22006L	cKO	PTH	0.74665	0.42762	0.231	0.1261	0.07659	1074.2578
J22006R	cKO	PTH	0.64502	0.41241	0.211	0.08521	0.06921	1071.7957
J22102L	cKO	PTH	0.71391	0.44436	0.216	0.12243	0.07445	1042.7549
J22102R	cKO	PTH	0.59567	0.42053	0.196	0.07751	0.06252	1059.5481
J22801L	cKO	PTH	0.72422	0.41731	0.229	0.1198	0.07208	1067.2501
J22801R	cKO	PTH	0.61276	0.37913	0.208	0.07856	0.05925	1073.3108
K22510L	cKO	PTH	0.72568	0.39648	0.235	0.11106	0.07168	1085.1797
K22510R	cKO	PTH	0.65294	0.43094	0.207	0.10057	0.06528	1067.8184
K22513L	cKO	PTH	0.7076	0.48363	0.214	0.12455	0.0767	1057.9066
K22513R	cKO	PTH	0.58411	0.44219	0.189	0.08239	0.05863	1059.9269
K22514L	cKO	PTH	0.68488	0.42307	0.221	0.10884	0.0654	1087.2
K22514R	cKO	PTH	0.63272	0.42868	0.202	0.09068	0.06578	1060.8738
L21504L	LC	PTH	0.7516	0.3866	0.244	0.11611	0.07401	1095.7228
L21504R	LC	PTH	0.67807	0.34807	0.23	0.08258	0.06727	1081.2655
L21911L	LC	PTH	0.78318	0.38638	0.252	0.12293	0.0803	1067.3765
L21911R	LC	PTH	0.69496	0.39378	0.224	0.0984	0.07196	1065.4193
L21913L	LC	PTH	0.75481	0.39497	0.243	0.12197	0.07325	1084.5483
L21913R	LC	PTH	0.67928	0.42502	0.219	0.09834	0.07171	1076.1517
L22105L	LC	PTH	0.75101	0.40183	0.24	0.12064	0.07588	1095.0283
L22105R	LC	PTH	0.64281	0.35137	0.222	0.07523	0.06374	1093.8918
L22501L	LC	PTH	0.72636	0.33603	0.247	0.09902	0.06701	1116.3669
L22501R	LC	PTH	0.64605	0.35269	0.225	0.07747	0.06337	1095.344
M23007L	LC	PTH	0.70297	0.37745	0.236	0.09378	0.07322	1083.2858
M23007R	LC	PTH	0.66131	0.36846	0.221	0.09075	0.06358	1076.5306
M23405L	LC	PTH	0.75456	0.32528	0.26	0.10365	0.06957	1104.3718
M23405R	LC	PTH	0.63026	0.3265	0.224	0.07026	0.06086	1067.2501
M23801L	LC	PTH	0.74554	0.39178	0.244	0.10711	0.07929	1106.0764
M23801R	LC	PTH	0.68115	0.37093	0.231	0.08774	0.06924	1084.9902
N24004L	LC	PTH	0.80999	0.40044	0.254	0.1351	0.08424	1078.172
N24004R	LC	PTH	0.64669	0.35397	0.221	0.079	0.06458	1070.6593
N24011L	LC	PTH	0.79438	0.35505	0.259	0.12952	0.07294	1087.2
N24011R	LC	PTH	0.70904	0.36361	0.232	0.10223	0.069	1075.9624
N24014L	LC	PTH	0.85372	0.39881	0.264	0.15045	0.08844	1065.9244

N24014R	LC	PTH	0.68515	0.38384	0.217	0.10175	0.06786	1055.0026
O23903L	cKO	VEH	0.76797	0.46893	0.227	0.13409	0.08973	1045.9115
O23903R	cKO	VEH	0.59651	0.49703	0.189	0.0781	0.07449	1061.5051
O24805L*	cKO	VEH	0.66803	0.43076	0.213	0.09461	0.07344	1084.4852
O24805R*	cKO	VEH	0.61764	0.4062	0.205	0.08457	0.06085	1074.6366
O24807L	cKO	VEH	0.66355	0.42433	0.212	0.10166	0.06687	1055.7601
O24807R	cKO	VEH	0.56218	0.37428	0.198	0.0637	0.05502	1072.1744
O24810L	cKO	VEH	0.65742	0.33889	0.231	0.08204	0.06005	1096.6697
O24810R	cKO	VEH	0.56042	0.34546	0.204	0.0584	0.0534	1066.5557
O24812L	cKO	VEH	0.64626	0.38281	0.211	0.08708	0.06165	1093.7656
O24812R	cKO	VEH	0.60915	0.36716	0.21	0.07543	0.05819	1076.7831
P22403L	cKO	VEH	0.67313	0.3983	0.218	0.09262	0.06986	1066.4926
P22403R	cKO	VEH	0.57934	0.37001	0.201	0.06594	0.0575	1084.2958
P22405L	cKO	VEH	0.63218	0.38437	0.215	0.09185	0.05581	1071.8588
P22405R	cKO	VEH	0.55925	0.39213	0.192	0.06577	0.05617	1059.043
P22406L	cKO	VEH	0.66886	0.39698	0.222	0.09254	0.06728	1080.8867
P22406R	cKO	VEH	0.50833	0.30551	0.198	0.0501	0.03953	1078.0458
Q21101L	cKO	VEH	0.74354	0.48274	0.216	0.13947	0.08229	1059.1061
Q21101R	cKO	VEH	0.64541	0.43687	0.204	0.08776	0.07374	1077.667
Q22314L	cKO	VEH	0.66678	0.38406	0.223	0.10049	0.0588	1086.6317
Q22314R	cKO	VEH	0.53464	0.35182	0.194	0.0582	0.04819	1074.384
Q22701L	cKO	VEH	0.76373	0.46555	0.224	0.1426	0.082	1068.2603
Q22701R	cKO	VEH	0.62895	0.4243	0.204	0.08674	0.06794	1050.962
R21003L	LC	VEH	0.75918	0.36731	0.247	0.11361	0.07575	1089.7883
R21003R	LC	VEH	0.68185	0.37618	0.228	0.09213	0.06782	1100.7733
R22004L	LC	VEH	0.71517	0.44125	0.225	0.11065	0.0769	1082.7806
R22004R	LC	VEH	0.68015	0.42523	0.219	0.09536	0.075	1085.1797
R22205L	LC	VEH	0.68385	0.35518	0.225	0.09007	0.06443	1091.1772
R22205R	LC	VEH	0.61142	0.36565	0.212	0.07329	0.0588	1077.0356
R22407L	LC	VEH	0.71721	0.38937	0.237	0.10149	0.07312	1082.465
R22407R	LC	VEH	0.68124	0.43807	0.215	0.10734	0.06959	1078.8033
R22711L	LC	VEH	0.68162	0.42304	0.221	0.09986	0.07124	1097.6798
R22711R	LC	VEH	0.60225	0.3935	0.205	0.07651	0.0587	1075.7098
S24803L	LC	VEH	0.83135	0.4373	0.245	0.15073	0.09292	1023.184
S24803R	LC	VEH	0.63817	0.37691	0.21	0.08696	0.06285	1045.9115
S24811L	LC	VEH	0.78161	0.39856	0.245	0.1253	0.08262	1083.4751
S24811R	LC	VEH	0.76171	0.46189	0.225	0.13778	0.08388	1065.0405
S24813L	LC	VEH	0.73814	0.40645	0.234	0.11904	0.07466	1077.6039
S24813R	LC	VEH	0.662	0.44302	0.204	0.09584	0.07506	1062.1996
T24108L	LC	VEH	0.76888	0.40846	0.245	0.11551	0.08509	1099.1318
T24108R	LC	VEH	0.65737	0.46782	0.202	0.1	0.07238	1055.1288
T24109L	LC	VEH	0.67589	0.41846	0.221	0.09333	0.07314	1075.5205
T24109R	LC	VEH	0.64827	0.46818	0.2	0.09689	0.07164	1066.9344
T24305L	LC	VEH	0.65556	0.35213	0.228	0.08632	0.05851	992.6281
T24305R	LC	VEH	0.56131	0.35414	0.202	0.06196	0.05167	968.0697

* Mouse died on loading day 25 of 30 (5wks)

Table G.9 Tibial metaphyseal cancellous bone measures from baseline control right (R) limbs from 16-week-old wild type (WT) C57Bl/6J female mice pre-treated with PTH or VEH for 6 weeks.

Animal Limb	PTH or VEH	BV/TV	Tb.Th (mm)	Tb.N (1/mm)	Tb.Sp (mm)	cn.TMD (mg HA/cc)
A01R	VEH	0.0795	0.0474	3.2946	0.3057	887.51
A02R	VEH	0.0976	0.0458	4.0163	0.2458	877.35
A03R	VEH	0.0954	0.0479	3.5028	0.2825	910.3
A04R	VEH	0.092	0.0455	3.7482	0.2678	878.36
A05R	VEH	0.0837	0.046	3.8126	0.2617	916.49
A06R	VEH	0.0962	0.0495	3.7898	0.2634	917.31
A07R	VEH	0.0922	0.0472	3.7229	0.2676	934.17
A08R	VEH	0.0884	0.0439	3.8201	0.2602	904.62
B01R	PTH	0.087	0.0461	3.4904	0.2857	881.45
B02R	PTH	0.0852	0.0482	3.5486	0.2766	892.31
B03R	PTH	0.0881	0.0521	3.5814	0.2783	874.38
B04R	PTH	0.0716	0.0477	3.6467	0.2763	868.26
B05R	PTH	0.0923	0.0465	3.9081	0.2513	910.49
B06R	PTH	0.0994	0.0496	3.7292	0.2648	913.21
B07R	PTH	0.0902	0.0473	3.7048	0.27	905.38
B08R	PTH	0.0852	0.0497	3.4544	0.2855	913.97

Table G.10 Tibial metaphyseal cortical shell bone measures from baseline control right (R) limbs from 16-week-old wild type (WT) C57Bl/6J female mice pre-treated with PTH or VEH for 6 weeks.

Animal Limb	PTH or VEH	Ct.Ar (mm^2)	Ct.Th (mm)	I_{MAX} (mm^4)	I_{MIN} (mm^4)	ct.TMD (mg HA/cc)
A01R	VEH	0.80777	0.143	0.24728	0.20006	992.123
A02R	VEH	0.8783	0.163	0.27349	0.20223	997.4893
A03R	VEH	0.90452	0.158	0.29803	0.23986	1017.439
A04R	VEH	0.82026	0.151	0.2587	0.19862	996.921
A05R	VEH	0.90694	0.159	0.30176	0.23307	1004.6863
A06R	VEH	0.84464	0.155	0.26239	0.20359	1009.5475
A07R	VEH	0.83334	0.15	0.25461	0.20084	1022.4264
A08R	VEH	0.81944	0.147	0.24905	0.20046	991.1129
B01R	PTH	0.96795	0.172	0.32023	0.24098	1004.2444
B02R	PTH	0.91425	0.166	0.28799	0.22074	1012.9565
B03R	PTH	0.96406	0.176	0.32624	0.2209	993.0068
B04R	PTH	0.95934	0.175	0.32533	0.21718	1005.1282
B05R	PTH	1.03015	0.186	0.31986	0.24904	1029.8129
B06R	PTH	0.90454	0.166	0.26977	0.21211	1013.7141
B07R	PTH	1.11616	0.18	0.42447	0.29739	999.3201
B08R	PTH	0.93052	0.17	0.28398	0.22554	1026.4037

Table G.11 Tibial diaphyseal cortical bone measures from baseline control right (R) limbs from 16-week-old wild type (WT) C57Bl/6J female mice pre-treated with PTH or VEH for 6 weeks.

Animal Limb	PTH or VEH	Ct.Ar (mm^2)	Ma.Ar (mm^2)	Ct.Th (mm)	I_{MAX} (mm^4)	I_{MIN} (mm^4)	ct.TMD (mg HA/cc)
A01R	VEH	0.5869	0.36486	0.208	0.06641	0.05784	1035.4
A02R	VEH	0.645	0.40765	0.216	0.08651	0.06677	1051.7
A03R	VEH	0.71106	0.42997	0.23	0.09648	0.08367	1064.9
A04R	VEH	0.61461	0.34898	0.217	0.0724	0.05772	1046.1
A05R	VEH	0.65999	0.43247	0.215	0.08788	0.07402	1049.5
A06R	VEH	0.66249	0.33458	0.234	0.07964	0.0626	1071.7
A07R	VEH	0.64358	0.33068	0.229	0.07709	0.05826	1069.8
A08R	VEH	0.64863	0.36467	0.224	0.0897	0.05711	1065.2
B01R	PTH	0.67769	0.377	0.228	0.08227	0.07351	1061.6
B02R	PTH	0.63622	0.32904	0.227	0.07042	0.06146	1056.6
B03R	PTH	0.72219	0.39747	0.233	0.10703	0.0747	1052
B04R	PTH	0.72329	0.41729	0.232	0.10736	0.0772	1053.4
B05R	PTH	0.71627	0.3204	0.251	0.08935	0.068	1085.2
B06R	PTH	0.62054	0.34443	0.221	0.07315	0.05762	1059
B07R	PTH	0.77758	0.4435	0.241	0.11982	0.09115	1062.5
B08R	PTH	0.66233	0.32096	0.233	0.07876	0.06074	1060.4

Table G.12 Tibial metaphyseal cancellous bone measures from 16-week-old wild type (WT) C57Bl/6J female mice pre-treated with PTH or VEH for 6 weeks prior to 2 weeks of tibial loading.

Animal Limb	Treatment Group	BV/TV	Tb.Th (mm)	Tb.N (1/mm)	Tb.Sp (mm)	cn.TMD (mg HA/cc)
C01L	VEH/VEH	0.0934	0.0486	3.6509	0.2706	897.803
C01R	VEH/VEH	0.0966	0.0442	3.7486	0.2676	916.806
C02L	VEH/VEH	0.0885	0.0528	3.5076	0.2803	933.725
C02R	VEH/VEH	0.0956	0.044	4.0554	0.2442	922.74
C03L	VEH/VEH	0.0898	0.0497	3.7873	0.2624	905.569
C03R	VEH/VEH	0.0802	0.045	3.915	0.2518	925.897
C04L	VEH/VEH	0.0769	0.0527	2.981	0.338	914.723
C04R	VEH/VEH	0.0595	0.0389	3.4877	0.2858	914.849
C05L	VEH/VEH	0.0698	0.0484	3.5375	0.2794	912.513
C05R	VEH/VEH	0.0649	0.0406	3.6994	0.2677	918.258
C06L	VEH/VEH	0.0852	0.051	3.4076	0.2909	900.329
C06R	VEH/VEH	0.081	0.0439	3.2986	0.3016	916.554
C07L	VEH/VEH	0.097	0.0584	3.3116	0.2918	839.87
C07R	VEH/VEH	0.106	0.0557	3.1426	0.3155	848.007
C08L	VEH/VEH	0.0935	0.0587	3.3842	0.2896	831.133
C08R	VEH/VEH	0.117	0.0563	3.5252	0.2792	839.203
C09L	VEH/VEH	0.1033	0.058	3.293	0.3015	833.067
C09R	VEH/VEH	0.0954	0.054	3.2906	0.3012	842.738
C10L	VEH/VEH	0.1089	0.0509	3.8219	0.2555	802.053
C10R	VEH/VEH	0.116	0.0461	3.7926	0.255	796.584
D01L	VEH/PTH	0.0822	0.0466	3.5217	0.2806	919.268
D01R	VEH/PTH	0.0805	0.0435	3.5719	0.2782	897.993
D02L	VEH/PTH	0.067	0.0483	3.2359	0.3082	916.427
D02R	VEH/PTH	0.0765	0.0474	3.6769	0.272	936.188
D03L	VEH/PTH	0.0755	0.0479	3.5505	0.2772	910.177
D03R	VEH/PTH	0.0861	0.0433	3.8587	0.2561	925.834
D04L	VEH/PTH	0.0623	0.0522	2.91	0.3384	921.162
D04R	VEH/PTH	0.0754	0.043	3.4935	0.2852	913.397
D05L	VEH/PTH	0.067	0.0549	3.1285	0.3151	935.241
D05R	VEH/PTH	0.0646	0.0483	3.4675	0.2841	952.476
D06L	VEH/PTH	0.0905	0.0475	3.6274	0.2738	905.316
D06R	VEH/PTH	0.0777	0.0441	3.6426	0.2766	880.063
D07L	VEH/PTH	0.1022	0.0574	3.6581	0.2667	827.264
D07R	VEH/PTH	0.1012	0.0511	3.4849	0.282	820.128
D08L	VEH/PTH	0.0924	0.0604	2.9355	0.3376	843.939
D08R	VEH/PTH	0.1135	0.0543	3.5828	0.2722	831.533
D09L	VEH/PTH	0.0872	0.0513	3.4342	0.2823	825.13
D09R	VEH/PTH	0.0953	0.0466	3.4307	0.2884	795.917
D10L	VEH/PTH	0.1075	0.0575	3.9441	0.2445	832.267
D10R	VEH/PTH	0.1041	0.0492	3.82	0.2503	813.725
E01L	PTH/PTH	0.0833	0.0592	3.3667	0.2933	916.238
E01R	PTH/PTH	0.0761	0.0424	3.6171	0.2746	894.268
E02L	PTH/PTH	0.0789	0.0496	3.389	0.2899	902.412
E02R	PTH/PTH	0.0728	0.0463	3.3001	0.3012	927.475

E03L	PTH/PTH	0.0699	0.0463	3.6947	0.269	888.838
E03R	PTH/PTH	0.0675	0.0403	3.2271	0.3079	871.414
E-H12L	PTH/PTH	0.0832	0.0567	3.4112	0.2987	866.363
E-H12R	PTH/PTH	0.0818	0.0463	3.5686	0.2799	913.902
E05L	PTH/PTH	0.093	0.0556	3.5557	0.2732	935.935
E05R	PTH/PTH	0.0851	0.0429	3.7429	0.2637	893.447
E06L	PTH/PTH	0.0721	0.0553	3.2887	0.2917	909.609
E06R	PTH/PTH	0.0617	0.0416	3.3959	0.2898	910.177
E07L	PTH/PTH	0.122	0.0622	3.416	0.2864	810.7908
E07R	PTH/PTH	0.0879	0.047	3.3669	0.2884	784.779
E08L	PTH/PTH	0.0988	0.0534	3.1482	0.3102	798.852
E08R	PTH/PTH	0.0882	0.0481	3.2797	0.2926	784.378
E09L	PTH/PTH	0.1066	0.0528	3.5624	0.2654	795.45
E09R	PTH/PTH	0.1116	0.0486	3.5768	0.268	778.109
E10L	PTH/PTH	0.1424	0.0566	4.0078	0.2347	806.922
E10R	PTH/PTH	0.1284	0.0483	3.8099	0.2518	800.452

Table G.13 Tibial metaphyseal cortical shell bone measures from 16-week-old wild type (WT) C57Bl/6J female mice pre-treated with PTH or VEH for 6 weeks prior to 2 weeks of tibial loading.

Animal Limb	Treatment Group	Ct.Ar (mm^2)	Ct.Th (mm)	I_{MAX} (mm^4)	I_{MIN} (mm^4)	ct.TMD (mg HA/cc)
C01L	VEH/VEH	1.06574	0.165	0.41943	0.31396	1007.7798
C01R	VEH/VEH	0.94794	0.16	0.35647	0.24615	1017.1864
C02L	VEH/VEH	1.00905	0.159	0.39331	0.26934	1017.3759
C02R	VEH/VEH	0.95968	0.153	0.32434	0.28067	1035.1791
C03L	VEH/VEH	1.05512	0.156	0.42831	0.30733	999.5726
C03R	VEH/VEH	0.98859	0.167	0.37481	0.24414	1034.6108
C04L	VEH/VEH	1.1697	0.162	0.51007	0.32554	1022.9314
C04R	VEH/VEH	0.90989	0.155	0.32119	0.23568	1032.3381
C05L	VEH/VEH	0.98056	0.155	0.36727	0.26506	1014.6611
C05R	VEH/VEH	0.87425	0.148	0.31997	0.22232	1022.0476
C06L	VEH/VEH	0.96749	0.154	0.35819	0.25858	986.3779
C06R	VEH/VEH	0.85258	0.153	0.26837	0.20371	1023.8784
C07L	VEH/VEH	0.9874	0.159	0.40269	0.2614	1005.412
C07R	VEH/VEH	0.91381	0.164	0.31098	0.21728	1035.6256
C08L	VEH/VEH	0.97094	0.167	0.32925	0.24154	1021.3525
C08R	VEH/VEH	0.80119	0.151	0.23908	0.18905	1026.2881
C09L	VEH/VEH	0.97931	0.171	0.35091	0.22846	1037.6932
C09R	VEH/VEH	0.84741	0.161	0.26198	0.18474	1039.5607
C10L	VEH/VEH	0.95211	0.156	0.37436	0.22756	997.6752
C10R	VEH/VEH	0.80422	0.147	0.27547	0.17619	1012.0149
D01L	VEH/PTH	1.07444	0.159	0.41843	0.26517	995.0902
D01R	VEH/PTH	0.89334	0.152	0.29597	0.2292	1010.0525
D02L	VEH/PTH	1.2919	0.163	0.55588	0.39654	990.9235
D02R	VEH/PTH	1.00953	0.168	0.39185	0.2552	1028.7396
D03L	VEH/PTH	1.11063	0.171	0.43177	0.27872	1020.7218
D03R	VEH/PTH	0.97719	0.162	0.37455	0.23883	1029.4341
D04L	VEH/PTH	1.13183	0.176	0.41139	0.31006	1009.5475
D04R	VEH/PTH	0.92852	0.162	0.33301	0.2107	1034.4215
D05L	VEH/PTH	1.01315	0.161	0.35653	0.26792	1010.4944
D05R	VEH/PTH	0.91712	0.162	0.3058	0.20768	1036.2523
D06L	VEH/PTH	0.986	0.159	0.3484	0.26191	978.1708
D06R	VEH/PTH	0.82894	0.147	0.27366	0.20079	967.5015
D07L	VEH/PTH	1.0994	0.183	0.40026	0.24798	998.2087
D07R	VEH/PTH	0.86892	0.164	0.26876	0.18878	1028.489
D08L	VEH/PTH	1.02186	0.176	0.36421	0.22047	1016.0835
D08R	VEH/PTH	0.91873	0.164	0.28059	0.22407	1034.6251
D09L	VEH/PTH	1.07366	0.178	0.41431	0.23601	1010.7477
D09R	VEH/PTH	0.86583	0.162	0.27355	0.17888	1032.0239
D10L	VEH/PTH	1.18883	0.198	0.45558	0.27556	1015.8167
D10R	VEH/PTH	0.92491	0.172	0.31314	0.19396	1052.8334
E01L	PTH/PTH	1.15406	0.181	0.44102	0.29598	1005.6964
E01R	PTH/PTH	1.07393	0.174	0.42996	0.25631	1010.4944
E02L	PTH/PTH	1.15103	0.174	0.43575	0.34197	1020.0273
E02R	PTH/PTH	1.02957	0.179	0.37226	0.23384	1045.9115

E03L	PTH/PTH	1.27284	0.193	0.51519	0.32508	1021.0375
E03R	PTH/PTH	1.08712	0.188	0.38748	0.2494	1023.1208
E-H12L	PTH/PTH	1.37382	0.201	0.51644	0.38322	1005.6333
E-H12R	PTH/PTH	1.00055	0.17	0.34334	0.25979	1030.6335
E05L	PTH/PTH	1.30938	0.19	0.52627	0.35253	1037.5781
E05R	PTH/PTH	1.09736	0.188	0.38694	0.27156	1037.2625
E06L	PTH/PTH	1.19689	0.191	0.45485	0.30352	1019.4592
E06R	PTH/PTH	0.9693	0.172	0.31195	0.2395	1047.9318
E07L	PTH/PTH	1.12346	0.193	0.39861	0.25118	1007.5463
E07R	PTH/PTH	0.89424	0.178	0.26641	0.17877	1025.4877
E08L	PTH/PTH	1.16085	0.191	0.46633	0.27548	1019.7517
E08R	PTH/PTH	1.03868	0.183	0.3818	0.24346	1017.3507
E09L	PTH/PTH	1.13501	0.191	0.4419	0.26415	1024.9541
E09R	PTH/PTH	0.99515	0.188	0.32974	0.20857	1025.3542
E10L	PTH/PTH	1.1715	0.192	0.40817	0.30111	1025.6211
E10R	PTH/PTH	0.92742	0.177	0.28416	0.19498	1041.5616

Table G.14 Tibial diaphyseal cortical bone measures from 16-week-old wild type (WT) C57Bl/6J female mice pre-treated with PTH or VEH for 6 weeks prior to 2 weeks of tibial loading.

Animal Limb	Treatment Group	Ct.Ar (mm^2)	Ma.Ar (mm^2)	Ct.Th (mm)	I_{MAX} (mm^4)	I_{MIN} (mm^4)	ct.TMD (mg HA/cc)
C01L	VEH/VEH	0.74246	0.41164	0.239	0.10851	0.0816	1072.6165
C01R	VEH/VEH	0.70899	0.45026	0.223	0.10183	0.08294	1075.2679
C02L	VEH/VEH	0.65084	0.39362	0.218	0.08634	0.0656	1083.2225
C02R	VEH/VEH	0.65448	0.37394	0.225	0.08577	0.06242	1081.5181
C03L	VEH/VEH	0.75466	0.48101	0.232	0.12538	0.08855	1077.5406
C03R	VEH/VEH	0.78221	0.44163	0.243	0.12222	0.08949	1071.922
C04L	VEH/VEH	0.74247	0.42446	0.237	0.1125	0.08063	1085.0535
C04R	VEH/VEH	0.66158	0.43545	0.216	0.09514	0.06869	1070.6593
C05L	VEH/VEH	0.63949	0.41985	0.215	0.0839	0.06609	1065.9875
C05R	VEH/VEH	0.66005	0.40745	0.219	0.09297	0.06566	1074.9523
C06L	VEH/VEH	0.65398	0.41529	0.217	0.08942	0.06987	1058.2854
C06R	VEH/VEH	0.63711	0.38097	0.219	0.08135	0.06161	1076.1517
C07L	VEH/VEH	0.65723	0.44574	0.209	0.09376	0.07318	1046.8973
C07R	VEH/VEH	0.68912	0.39421	0.226	0.10125	0.06804	1068.8406
C08L	VEH/VEH	0.64234	0.40343	0.214	0.08967	0.06342	1062.5044
C08R	VEH/VEH	0.66412	0.39405	0.219	0.09218	0.06776	1055.3011
C09L	VEH/VEH	0.7223	0.3902	0.236	0.10605	0.07339	1073.5094
C09R	VEH/VEH	0.68069	0.40671	0.223	0.0958	0.0705	1060.837
C10L	VEH/VEH	0.63293	0.40201	0.212	0.08003	0.06765	1059.1029
C10R	VEH/VEH	0.63352	0.43432	0.208	0.08882	0.06603	1054.8342
D01L	VEH/PTH	0.67486	0.41982	0.218	0.10185	0.06789	1061.2526
D01R	VEH/PTH	0.64884	0.4277	0.211	0.0924	0.06824	1042.9443
D02L	VEH/PTH	0.72668	0.43786	0.23	0.10913	0.08206	1070.028
D02R	VEH/PTH	0.70266	0.41364	0.227	0.09713	0.07631	1078.9927
D03L	VEH/PTH	0.673	0.39374	0.223	0.0903	0.06864	1065.1669
D03R	VEH/PTH	0.66987	0.43828	0.213	0.0996	0.07067	1043.1337
D04L	VEH/PTH	0.69819	0.40195	0.228	0.09814	0.07263	1053.4874
D04R	VEH/PTH	0.65648	0.40565	0.214	0.09092	0.06602	1052.6035
D05L	VEH/PTH	0.65756	0.38263	0.222	0.0923	0.06086	1068.0709
D05R	VEH/PTH	0.63399	0.36338	0.22	0.08503	0.05644	1068.7021
D06L	VEH/PTH	0.66114	0.38225	0.222	0.08508	0.0668	1053.2349
D06R	VEH/PTH	0.60373	0.37677	0.21	0.07399	0.05793	1052.1616
D07L	VEH/PTH	0.72164	0.41802	0.229	0.10264	0.08194	1051.7662
D07R	VEH/PTH	0.6721	0.41622	0.214	0.09486	0.07273	1033.7581
D08L	VEH/PTH	0.68239	0.41397	0.223	0.09833	0.07192	1054.3007
D08R	VEH/PTH	0.61678	0.38799	0.211	0.07593	0.06284	1046.964
D09L	VEH/PTH	0.66743	0.38794	0.224	0.08788	0.06885	1056.0348
D09R	VEH/PTH	0.63195	0.41417	0.211	0.08273	0.06747	1049.8987
D10L	VEH/PTH	0.80438	0.42524	0.253	0.1288	0.09118	1063.3715
D10R	VEH/PTH	0.73402	0.44895	0.228	0.11966	0.0814	1055.3011
E01L	PTH/PTH	0.72947	0.38236	0.243	0.09963	0.07746	1086.3792
E01R	PTH/PTH	0.74103	0.40276	0.238	0.11685	0.07367	1064.5986
E02L	PTH/PTH	0.74959	0.43535	0.236	0.11432	0.08624	1081.3917
E02R	PTH/PTH	0.71007	0.41719	0.233	0.10135	0.0759	1081.8969

E03L	PTH/PTH	0.76016	0.44204	0.239	0.11857	0.08445	1088.3994
E03R	PTH/PTH	0.77148	0.4441	0.237	0.1236	0.08558	1068.5759
E-H12L	PTH/PTH	0.82132	0.37411	0.263	0.12394	0.08596	1062.7047
E-H12R	PTH/PTH	0.72738	0.44799	0.226	0.11165	0.08248	1059.9269
E05L	PTH/PTH	0.85863	0.44564	0.26	0.15339	0.09846	1091.9348
E05R	PTH/PTH	0.7749	0.44929	0.24	0.12811	0.08431	1089.6621
E06L	PTH/PTH	0.73992	0.3344	0.251	0.10887	0.06525	1093.8287
E06R	PTH/PTH	0.65556	0.29728	0.24	0.07319	0.05768	1114.2205
E07L	PTH/PTH	0.73856	0.35654	0.249	0.09971	0.07534	1077.111
E07R	PTH/PTH	0.65056	0.37735	0.222	0.08237	0.06551	1062.5044
E08L	PTH/PTH	0.71432	0.43827	0.233	0.10733	0.08002	1061.3706
E08R	PTH/PTH	0.70724	0.42453	0.227	0.1007	0.07811	1067.1064
E09L	PTH/PTH	0.72742	0.4148	0.235	0.10353	0.07976	1072.8424
E09R	PTH/PTH	0.70128	0.45137	0.221	0.10401	0.08	1054.1674
E10L	PTH/PTH	0.7848	0.40422	0.25	0.12281	0.08475	1075.4436
E10R	PTH/PTH	0.7189	0.4352	0.224	0.1105	0.07945	1055.9681

Table G.15 Tibial metaphyseal cancellous bone measures from 16-week-old wild type (WT) C57Bl/6J female mice pre-treated with PTH or VEH for 6 weeks prior to 6 weeks of tibial loading.

Animal Limb	Treatment Group	BV/TV	Tb.Th (mm)	Tb.N (1/mm)	Tb.Sp (mm)	cn.TMD (mg HA/cc)
F01L	VEH/VEH	0.0969	0.0764	3.1463	0.3177	940.1022
F01R	VEH/VEH	0.0553	0.0461	3.0912	0.3236	956.137
F02L	VEH/VEH	0.1179	0.0664	3.6098	0.2754	945.1527
F02R	VEH/VEH	0.0703	0.0453	3.4121	0.2934	940.922
F03L	VEH/VEH	0.094	0.058	3.2793	0.3008	939.344
F03R	VEH/VEH	0.0822	0.0498	3.6069	0.2771	935.872
F04L	VEH/VEH	0.1061	0.072	3.2137	0.3146	941.3647
F04R	VEH/VEH	0.0836	0.0489	3.3732	0.2992	936.503
F05L	VEH/VEH	0.1049	0.067	3.0337	0.3254	970.4055
F05R	VEH/VEH	0.0727	0.0457	3.2351	0.3099	960.178
F06L	VEH/VEH	0.1028	0.0734	3.1278	0.3196	944.0164
F06R	VEH/VEH	0.0729	0.0513	3.1825	0.315	914.344
F07L	VEH/VEH	0.1011	0.0724	2.8361	0.3566	900.6447
F07R	VEH/VEH	0.0772	0.0517	3.0094	0.3326	953.865
F08L	VEH/VEH	0.1151	0.0684	3.4458	0.2895	905.4426
F08R	VEH/VEH	0.1026	0.0484	3.6815	0.2694	946.289
F09L	VEH/VEH	0.1069	0.0684	3.2639	0.2989	919.1423
F09R	VEH/VEH	0.0654	0.0446	3.2246	0.3162	942.248
F10L	VEH/VEH	0.1034	0.0674	2.9993	0.3299	899.1294
F10R	VEH/VEH	0.0673	0.0476	3.1233	0.3219	937.513
F11L	VEH/VEH	0.0859	0.0735	2.7838	0.3566	913.7761
F11R	VEH/VEH	0.0555	0.0475	2.8475	0.3531	945.91
G01L	VEH/PTH	0.1014	0.0617	3.2135	0.3086	912.8922
G01R	VEH/PTH	0.0926	0.0457	3.6222	0.2869	864.722
G02L	VEH/PTH	0.0872	0.0648	3.2383	0.3077	906.8947
G02R	VEH/PTH	0.075	0.0536	2.9177	0.3508	946.857
G03L	VEH/PTH	0.1124	0.0647	3.3401	0.2968	915.67
G03R	VEH/PTH	0.0798	0.0465	3.2657	0.3073	915.543
G04L	VEH/PTH	0.1047	0.069	3.175	0.3145	908.0942
G04R	VEH/PTH	0.0861	0.0458	3.4459	0.2898	902.412
G05L	VEH/PTH	0.1143	0.0761	3.2606	0.3032	929.4329
G05R	VEH/PTH	0.0944	0.0547	3.4694	0.2833	949.256
G06L	VEH/PTH	0.1024	0.062	2.9823	0.3398	914.9125
G06R	VEH/PTH	0.0871	0.053	3.1497	0.3198	943.637
G07L	VEH/PTH	0.0975	0.0644	3.5931	0.287	870.3412
G07R	VEH/PTH	0.0894	0.0495	3.4002	0.2986	893.132
G08L	VEH/PTH	0.0885	0.0734	2.868	0.3519	864.9119
G08R	VEH/PTH	0.084	0.0538	3.3594	0.3055	898.119
G09L	VEH/PTH	0.095	0.0656	3.2895	0.3074	891.2379
G09R	VEH/PTH	0.0836	0.0483	3.2078	0.3148	886.944
G10L	VEH/PTH	0.1277	0.0654	3.6342	0.2739	877.2227
G10R	VEH/PTH	0.1228	0.0522	3.9205	0.2573	906.894
G11L	VEH/PTH	0.0858	0.066	3.0263	0.3304	915.9857
G11R	VEH/PTH	0.0624	0.045	3.0767	0.3225	906.894

G12L	VEH/PTH	0.0921	0.0716	3.0133	0.3324	890.291
G12R	VEH/PTH	0.0782	0.047	2.9709	0.3408	921.099
H01L	PTH/PTH	0.1057	0.0781	2.8483	0.3494	886.0612
H01R	PTH/PTH	0.0777	0.0478	3.3688	0.2987	871.288
H02L	PTH/PTH	0.1024	0.0586	3.2785	0.3013	913.523
H02R	PTH/PTH	0.102	0.0531	3.3518	0.3002	910.808
H03L	PTH/PTH	0.1019	0.0755	3.3124	0.3031	914.0286
H03R	PTH/PTH	0.095	0.0522	3.7082	0.2656	939.533
H04L	PTH/PTH	0.1101	0.0905	2.8294	0.3551	943.1324
H04R	PTH/PTH	0.0663	0.0489	2.9202	0.3366	947.614
H05L	PTH/PTH	0.137	0.0821	3.0544	0.3228	886.6924
H05R	PTH/PTH	0.0692	0.0467	3.4643	0.2999	868.068
H06L	PTH/PTH	0.0974	0.071	3.1504	0.3212	871.2882
H06R	PTH/PTH	0.0838	0.0476	3.2937	0.303	931.2
H07L	PTH/PTH	0.1156	0.0694	3.3921	0.3014	923.2458
H07R	PTH/PTH	0.1012	0.053	3.5712	0.2826	893.132
H08L	PTH/PTH	0.1307	0.0779	3.2169	0.3074	888.3339
H08R	PTH/PTH	0.1095	0.0509	3.6038	0.27	921.225
H09L	PTH/PTH	0.1749	0.0694	3.553	0.2811	872.9297
H09R	PTH/PTH	0.1283	0.049	3.8614	0.261	883.472
H10L	PTH/PTH	0.1165	0.0772	3.3508	0.2927	903.6749
H10R	PTH/PTH	0.0911	0.0483	3.4157	0.2915	910.745
H11L	PTH/PTH	0.1226	0.0808	2.7251	0.3736	961.4408
H11R	PTH/PTH	0.0946	0.0521	2.8806	0.3445	944.205

Table G.16 Tibial metaphyseal cortical shell bone measures from 16-week-old wild type (WT) C57Bl/6J female mice pre-treated with PTH or VEH for 6 weeks prior to 6 weeks of tibial loading.

Animal Limb	Treatment Group	Ct.Ar (mm^2)	Ct.Th (mm)	I_{MAX} (mm^4)	I_{MIN} (mm^4)	ct.TMD (mg HA/cc)
F01L	VEH/VEH					
F01R	VEH/VEH	0.92059	0.164	0.3456	0.19644	1043.7019
F02L	VEH/VEH					
F02R	VEH/VEH	0.91028	0.155	0.32573	0.2221	1019.0172
F03L	VEH/VEH					
F03R	VEH/VEH	0.97998	0.163	0.35308	0.2658	1038.8407
F04L	VEH/VEH					
F04R	VEH/VEH	0.95521	0.153	0.38083	0.24249	1040.6084
F05L	VEH/VEH					
F05R	VEH/VEH	0.82769	0.145	0.28403	0.20122	1048.5
F06L	VEH/VEH					
F06R	VEH/VEH	0.92801	0.158	0.3184	0.26125	1021.795
F07L	VEH/VEH					
F07R	VEH/VEH	0.95169	0.161	0.32221	0.26316	1048.1211
F08L	VEH/VEH					
F08R	VEH/VEH	0.93866	0.157	0.34802	0.24644	1031.5175
F09L	VEH/VEH					
F09R	VEH/VEH	0.86011	0.153	0.28824	0.20437	1036.6942
F10L	VEH/VEH					
F10R	VEH/VEH	0.89983	0.155	0.30529	0.22629	1033.4745
F11L	VEH/VEH					
F11R	VEH/VEH	0.91854	0.157	0.31978	0.25122	1025.4568
G01L	VEH/PTH					
G01R	VEH/PTH					
G02L	VEH/PTH					
G02R	VEH/PTH	0.99822	0.168	0.35624	0.26874	1035.3684
G03L	VEH/PTH					
G03R	VEH/PTH	0.97476	0.164	0.34774	0.24555	1021.5426
G04L	VEH/PTH					
G04R	VEH/PTH	1.02619	0.166	0.36313	0.26895	1024.2572
G05L	VEH/PTH					
G05R	VEH/PTH	1.07569	0.176	0.40276	0.29512	1059.99
G06L	VEH/PTH					
G06R	VEH/PTH	1.03668	0.174	0.38817	0.26929	1042.0604
G07L	VEH/PTH					
G07R	VEH/PTH	0.99753	0.163	0.36663	0.26929	1015.4187
G08L	VEH/PTH					
G08R	VEH/PTH	0.97281	0.171	0.3219	0.23359	1034.2321
G09L	VEH/PTH					
G09R	VEH/PTH	0.89929	0.153	0.30071	0.23114	1003.9287
G10L	VEH/PTH					
G10R	VEH/PTH	1.0066	0.168	0.35156	0.267	1009.9894
G11L	VEH/PTH					
G11R	VEH/PTH	0.95685	0.167	0.31875	0.24199	1034.3584

G12L	VEH/PTH					
G12R	VEH/PTH	0.95374	0.161	0.3413	0.23404	1009.9263
H01L	PTH/PTH					
H01R	PTH/PTH	1.10036	0.189	0.38689	0.27556	1019.9642
H02L	PTH/PTH					
H02R	PTH/PTH	1.04879	0.178	0.35602	0.26182	1037.7043
H03L	PTH/PTH					
H03R	PTH/PTH	1.15686	0.194	0.43369	0.27801	1048.6893
H04L	PTH/PTH					
H04R	PTH/PTH	0.97642	0.169	0.34069	0.23327	1047.0479
H05L	PTH/PTH					
H05R	PTH/PTH	0.95647	0.167	0.28461	0.23854	958.9155
H06L	PTH/PTH					
H06R	PTH/PTH	1.02867	0.172	0.34723	0.2626	1027.4769
H07L	PTH/PTH					
H07R	PTH/PTH	1.06095	0.173	0.3546	0.29718	1014.5349
H08L	PTH/PTH					
H08R	PTH/PTH	1.13971	0.187	0.39399	0.30535	1043.7019
H09L	PTH/PTH					
H09R	PTH/PTH	0.94956	0.161	0.30886	0.23534	1001.8453
H10L	PTH/PTH					
H10R	PTH/PTH	1.00077	0.172	0.34351	0.23159	1012.7672
H11L	PTH/PTH					
H11R	PTH/PTH	0.93423	0.163	0.28571	0.24047	1043.8914

Table G.17 Tibial diaphyseal cortical bone measures from 16-week-old wild type (WT) C57Bl/6J female mice pre-treated with PTH or VEH for 6 weeks prior to 6 weeks of tibial loading.

Animal Limb	Treatment Group	Ct.Ar (mm^2)	Ma.Ar (mm^2)	Ct.Th (mm)	I_{MAX} (mm^4)	I_{MIN} (mm^4)	ct.TMD (mg HA/cc)
F01L	VEH/VEH	0.76791	0.45435	0.236	0.1278	0.08647	1088.5256
F01R	VEH/VEH	0.69964	0.44379	0.223	0.10066	0.08027	1084.1064
F02L	VEH/VEH	0.74091	0.41314	0.239	0.11028	0.07961	1095.849
F02R	VEH/VEH	0.62759	0.41024	0.211	0.08272	0.0639	1067.5027
F03L	VEH/VEH	0.78153	0.461	0.238	0.13527	0.08683	1080.3816
F03R	VEH/VEH	0.72852	0.43819	0.23	0.11153	0.08107	1067.1239
F04L	VEH/VEH	0.72879	0.38148	0.244	0.10524	0.07052	1096.8591
F04R	VEH/VEH	0.65714	0.40883	0.218	0.09128	0.0657	1065.8612
F05L	VEH/VEH	0.71302	0.39781	0.239	0.10432	0.06989	1100.142
F05R	VEH/VEH	0.66206	0.46215	0.21	0.09716	0.07311	1065.2931
F06L	VEH/VEH	0.77561	0.47568	0.232	0.13977	0.08776	1070.6593
F06R	VEH/VEH	0.63633	0.45104	0.207	0.08663	0.07151	1053.8662
F07L	VEH/VEH	0.72928	0.41904	0.233	0.11006	0.07806	1062.0103
F07R	VEH/VEH	0.67157	0.44598	0.214	0.09976	0.07157	1074.3209
F08L	VEH/VEH	0.73277	0.42804	0.235	0.11581	0.07484	1088.5256
F08R	VEH/VEH	0.73997	0.4468	0.232	0.11031	0.08633	1075.7729
F09L	VEH/VEH	0.72144	0.40434	0.233	0.11479	0.07079	1080.1292
F09R	VEH/VEH	0.64257	0.41088	0.215	0.08584	0.06728	1068.8285
F10L	VEH/VEH	0.71574	0.43811	0.225	0.11758	0.0732	1070.8488
F10R	VEH/VEH	0.65159	0.39961	0.218	0.08832	0.06584	1088.4625
F11L	VEH/VEH	0.72116	0.44272	0.226	0.11924	0.07523	1060.8738
F11R	VEH/VEH	0.68614	0.43534	0.214	0.10626	0.07154	1057.9697
G01L	VEH/PTH	0.76907	0.42348	0.244	0.11085	0.08969	1092.7555
G01R	VEH/PTH	0.7314	0.41771	0.231	0.10951	0.08087	1077.1619
G02L	VEH/PTH	0.74666	0.36381	0.245	0.1105	0.07161	1083.7908
G02R	VEH/PTH	0.67727	0.35684	0.233	0.08455	0.06668	1087.7681
G03L	VEH/PTH	0.75718	0.41305	0.243	0.11797	0.08049	1095.5333
G03R	VEH/PTH	0.66113	0.4385	0.212	0.09851	0.069	1065.1669
G04L	VEH/PTH	0.75921	0.41623	0.242	0.12338	0.07803	1084.4221
G04R	VEH/PTH	0.69455	0.42613	0.224	0.10034	0.07354	1096.6697
G05L	VEH/PTH	0.80189	0.41998	0.248	0.13918	0.08152	1094.9652
G05R	VEH/PTH	0.71502	0.40783	0.232	0.10534	0.07414	1089.7252
G06L	VEH/PTH	0.78347	0.4329	0.246	0.12874	0.08541	1079.8135
G06R	VEH/PTH	0.69395	0.37572	0.233	0.09427	0.06824	1086.7579
G07L	VEH/PTH	0.7939	0.41537	0.253	0.12265	0.08687	1069.1442
G07R	VEH/PTH	0.69352	0.38728	0.231	0.09531	0.07037	1077.5406
G08L	VEH/PTH	0.76585	0.40165	0.247	0.12026	0.07826	1057.3384
G08R	VEH/PTH	0.66172	0.34635	0.223	0.09568	0.05613	1076.7831
G09L	VEH/PTH	0.70946	0.39428	0.232	0.10464	0.07083	1086.316
G09R	VEH/PTH	0.61335	0.4023	0.209	0.07531	0.06374	1061.6315
G10L	VEH/PTH	0.72631	0.40479	0.236	0.10834	0.075	1060.3057
G10R	VEH/PTH	0.67507	0.40577	0.222	0.09217	0.07027	1065.9244
G11L	VEH/PTH	0.74326	0.37024	0.248	0.10371	0.07689	1094.8389
G11R	VEH/PTH	0.65467	0.39303	0.22	0.07661	0.07373	1086.3792

G12L	VEH/PTH	0.7494	0.38669	0.245	0.10548	0.07952	1078.2351
G12R	VEH/PTH	0.65606	0.32432	0.234	0.07584	0.0622	1083.9802
H01L	PTH/PTH	0.78595	0.40115	0.257	0.12577	0.08	1072.427
H01R	PTH/PTH	0.68146	0.39391	0.227	0.09385	0.06761	1078.5508
H02L	PTH/PTH	0.82178	0.46194	0.247	0.1509	0.09221	1091.9348
H02R	PTH/PTH	0.71516	0.43505	0.227	0.11183	0.0756	1082.0231
H03L	PTH/PTH	0.88493	0.42781	0.268	0.16052	0.09896	1087.7681
H03R	PTH/PTH	0.72549	0.3781	0.24	0.09476	0.0783	1104.498
H04L	PTH/PTH	0.73578	0.39273	0.241	0.10305	0.07676	1096.1647
H04R	PTH/PTH	0.62583	0.38392	0.21	0.07247	0.06663	1086.4423
H05L	PTH/PTH	0.76185	0.31339	0.258	0.10803	0.06474	1103.046
H05R	PTH/PTH	0.61925	0.33638	0.22	0.07836	0.0517	1091.0509
H06L	PTH/PTH	0.81662	0.41962	0.255	0.12857	0.09262	1077.4144
H06R	PTH/PTH	0.67943	0.38395	0.228	0.08672	0.07187	1085.811
H07L	PTH/PTH	0.7723	0.38091	0.254	0.12033	0.07486	1101.0259
H07R	PTH/PTH	0.70081	0.40258	0.228	0.10037	0.07364	1070.7855
H08L	PTH/PTH	0.82204	0.37838	0.266	0.12521	0.08621	1096.796
H08R	PTH/PTH	0.74175	0.4292	0.235	0.10599	0.08494	1095.9752
H09L	PTH/PTH	0.79972	0.46367	0.244	0.13693	0.0905	1060.8107
H09R	PTH/PTH	0.64209	0.43252	0.207	0.08734	0.06949	1052.6035
H10L	PTH/PTH	0.81272	0.41019	0.251	0.14492	0.08109	1075.7098
H10R	PTH/PTH	0.66551	0.38014	0.221	0.09457	0.06262	1069.3335
H11L	PTH/PTH	0.75659	0.34089	0.259	0.1047	0.07093	1108.0967
H11R	PTH/PTH	0.66573	0.35374	0.231	0.08391	0.0624	1095.0914

Appendix H

LOADING MODALITY ANALYSIS CODE

MATLAB code for analysis of the tensile, compressive, and neutral regions of the tibial mid-diaphysis for Ct.Ar and Ct.Th based on the principal axes of the 3D volume of interest. The functions freadVAXD, read_header, uint32le_to_VAXF, uint64le_to_VAXD, and uint64le_to_VAXG were obtained from Scanco Medical. The function read_aim was obtained from Scanco Medical and adjusted (read_aim_amr) to allow multiple files to be analyzed.

```
% Analyze Tensile, Compressive, & Neutral Quadrants of tibial mid-
diaphysis
% Imports AIM file of diaphyseal ROI from Scanco, outputs .csv file
with
% CtAr and CtTh values for entire diaphysis and tensile, compressive,
% and neutral regions

% Mandy Rooney
% edited 3/9/20

clear all; close all

% Name file to store data in
save_name = input('Input path/name of file to save to in ''string''
as .csv: \n');
threshold = input('Input threshold: \n'); %Threshold from Scanco in
HU
show_figs = input('Would you like to see the T/C/N regions? (Y-1/N-
0): \n'); %Threshold from Scanco in HU

%Prep the file you are saving to
sfile=fopen(save_name,'a');
    fprintf(sfile,'DATE,'); % today's date
    fprintf(sfile,'NAME,'); % Filename
    fprintf(sfile,'Threshold,'); % Threshold input by user
    fprintf(sfile,'Ct.Ar,'); % total Ct.Ar
    fprintf(sfile,'Ct.Ar-T,'); % tensile Ct.Ar
    fprintf(sfile,'Ct.Ar-C,'); % compressive Ct.Ar
    fprintf(sfile,'Ct.Ar-N,'); % neutral Ct.Ar
    fprintf(sfile,'Ct.Th,'); % total Ct.Th
    fprintf(sfile,'Ct.Th-T,'); % tensile Ct.Th
    fprintf(sfile,'Ct.Th-C,'); % compressive Ct.Th
    fprintf(sfile,'Ct.Th-N,'); % neutral Ct.Th
    fprintf(sfile,'\n'); % newline character
fclose(sfile);

mu_h20=0.57840; %mu of water from ISQ/AIM file header information
```

```
mu_scaling=4096; %scaling factor from ISQ/AIM file header info;4096
for most, 8192 for XtremeCT

    %Open all files you wish to select in the folder%
    [file,pathname]=uigetfile({'*.AIM', 'Select all files
backwards'},'Pick AIM files', 'Multiselect', 'on');

    %Account for one file input situation
    if strcmp(num2str(class(file)),'cell')
        filename = file;
    else
        filename{1} = file;
    end

    l=length(filename);

for sample=1:l
    clear vol BW tmask cmask nmask c centroids
    %read in file name, file path name, header info, and AIM file

[fn,pn,header_info,vol]=read_aim_amr(filename{sample},pathname(sample
));

    %get size of 3D image in pixels and resolution of pixels
    row=header_info(2);
    col=header_info(3);
    zmax=header_info(4);
    mid_slice=round(zmax/2);
    pix=header_info(8); %pixel size in mm

    %convert native units to HU
    HU_pix=-1000+vol.*(1000/(mu_h20*mu_scaling));

    %Set up variables
    CtAr=zeros(zmax,1);
    CtTh=zeros(zmax,1);
    CtArT=zeros(zmax,1);
    CtThT=zeros(zmax,1);
    CtArC=zeros(zmax,1);
    CtThC=zeros(zmax,1);
    CtArN=zeros(zmax,1);
    CtThN=zeros(zmax,1);

    %Make binary and inverse
    BW=double(HU_pix>=threshold);
    invBW=imcomplement(BW);

    %find centroid of 3D midshaft region
    s=regionprops3(BW,'centroid');
    centroids=cat(1,s.Centroid);
    c=centroids(1:2);

    %find principal axis of 3D midshaft
    a=regionprops3(BW,'EigenVectors');
    EigVec=cell2mat(a.EigenVectors);
```

```
    princ_axis=[EigVec(2,1),EigVec(1,1)];

    r=135; %radius of wedge for mask creation, needs to be large
enough to encompass full thickness

    %principal axis coordinates
    pa(1,:)=c+r*princ_axis;
    pa(2,:)=c-r*princ_axis;

    theta=atand((c(2)-pa(2,2))/(pa(2,1)-c(1)));

    if theta>=0
        xt=pa(1,1); %tensile end of principal axis
        yt=pa(1,2);
        xc=pa(2,1); %compressive end of principal axis
        yc=pa(2,2);

        %extend +/-45deg from princ axis
        %line from centroid to these points creates masks
        xtm=c(1)-r*cosd(theta+45);
        ytm=c(2)+r*sind(theta+45);
        xtm2=c(1)-r*cosd(theta-45);
        ytm2=c(2)+r*sind(theta-45);

        xcm=c(1)+r*cosd(theta+45);
        ycm=c(2)-r*sind(theta+45);
        xcm2=c(1)+r*cosd(theta-45);
        ycm2=c(2)-r*sind(theta-45);

        %neutral region points
        xnm=c(1)-r*cosd(theta+67.5);
        ynm=c(2)+r*sind(theta+67.5);
        xnm2=c(1)-r*cosd(theta-67.5);
        ynm2=c(2)+r*sind(theta-67.5);
        xnm3=c(1)+r*cosd(theta+67.5);
        ynm3=c(2)-r*sind(theta+67.5);
        xnm4=c(1)+r*cosd(theta-67.5);
        ynm4=c(2)-r*sind(theta-67.5);
    else
        xt=pa(2,1); %tensile end of principal axis
        yt=pa(2,2);
        xc=pa(1,1); %compressive end of principal axis
        yc=pa(1,2);

        %extend +/-45deg from princ axis
        %line from centroid to these points creates masks
        xtm=c(1)+r*cosd(theta+45);
        ytm=c(2)-r*sind(theta+45);
        xtm2=c(1)+r*cosd(theta-45);
        ytm2=c(2)-r*sind(theta-45);

        xcm=c(1)-r*cosd(theta+45);
        ycm=c(2)+r*sind(theta+45);
        xcm2=c(1)-r*cosd(theta-45);
        ycm2=c(2)+r*sind(theta-45);
```

```
        %neutral region points
        xnm=c(1)+r*cosd(theta+67.5);
        ynm=c(2)-r*sind(theta+67.5);
        xnm2=c(1)+r*cosd(theta-67.5);
        ynm2=c(2)-r*sind(theta-67.5);
        xnm3=c(1)-r*cosd(theta+67.5);
        ynm3=c(2)+r*sind(theta+67.5);
        xnm4=c(1)-r*cosd(theta-67.5);
        ynm4=c(2)+r*sind(theta-67.5);
    end

    %create masks
    xtmask=[c(1),xtm,xtm2,c(1)];
    ytmask=[c(2),ytm,ytm2,c(2)];
    tmask=poly2mask(xtmask,ytmask,row,col);

    xcmask=[c(1),xcm,xcm2,c(1)];
    ycmask=[c(2),ycm,ycm2,c(2)];
    cmask=poly2mask(xcmask,ycmask,row,col);

    xnmask=[xnm2,c(1),xnm,xnm4,c(1),xnm3,xnm2];
    ynmask=[ynm2,c(2),ynm,ynm4,c(2),ynm3,ynm2];
    nmask=poly2mask(xnmask,ynmask,row,col);

    for z=1:zmax
        tension=tmask.*BW(:,:,z);
        compression=cmask.*BW(:,:,z);
        neut=nmask.*BW(:,:,z);

        %Ct.Ar
        numpix=sum(sum(BW(:,:,z)));
        CtAr(z)=numpix*pix*pix;
        numpixt=sum(tension(:));
        CtArT(z)=numpixt*pix*pix;
        numpixc=sum(compression(:));
        CtArC(z)=numpixc*pix*pix;
        numpixn=sum(neut(:));
        CtArN(z)=numpixn*pix*pix;

        % CT.Th
        edtImage=bwdist(invBW(:,:,z)); %Euclidian distance transform
of inverted image calculates shortest distance to nearest white pixel
        skelImage=bwskel(logical(BW(:,:,z)),'MinBranchLength',10);
%skeletonize
        widthImage=pix*2*double(edtImage).*double(skelImage);
        Th=nonzeros(widthImage);
        CtTh(z)=sum(Th)/length(Th);

        widthImageT=tmask.*widthImage;
        ThT=nonzeros(widthImageT);
        CtThT(z)=sum(ThT)/length(ThT);

        widthImageC=cmask.*widthImage;
        ThC=nonzeros(widthImageC);
```

```
        CtThC(z)=sum(ThC)/length(ThC);

        widthImageN=nmask.*widthImage;
        ThN=nonzeros(widthImageN);
        CtThN(z)=sum(ThN)/length(ThN);

        if show_figs==1 && z==mid_slice
            hold on
            imshow(tension+0.75*compression+0.5*neut);
            title(sprintf('%s',filename{sample}))
            pause
            hold off
            clf
        end

    end

    CtArAvg=sum(CtAr)/length(CtAr);
    CtThAvg=sum(CtTh)/length(CtTh);

    CtArAvgT=sum(CtArT)/length(CtArT);
    CtThAvgT=sum(CtThT)/length(CtThT);

    CtArAvgC=sum(CtArC)/length(CtArC);
    CtThAvgC=sum(CtThC)/length(CtThC);

    CtArAvgN=sum(CtArN)/length(CtArN);
    CtThAvgN=sum(CtThN)/length(CtThN);

    sfile=fopen(save_name,'a');

        %General saved stuff
        fprintf(sfile,'%s,',date); % today's date
        fprintf(sfile,'%s,',filename{sample}); % Filename
        fprintf(sfile,'%f,',threshold); % Threshold input by user
        fprintf(sfile,'%.4f,',CtArAvg); % total Ct.Ar
        fprintf(sfile,'%.4f,',CtArAvgT); % tensile Ct.Ar
        fprintf(sfile,'%.4f,',CtArAvgC); % compressive Ct.Ar
        fprintf(sfile,'%.4f,',CtArAvgN); % neutral Ct.Ar
        fprintf(sfile,'%.4f,',CtThAvg); % total Ct.Th
        fprintf(sfile,'%.4f,',CtThAvgT); % tensile Ct.Th
        fprintf(sfile,'%.4f,',CtThAvgC); % compressive Ct.Th
        fprintf(sfile,'%.4f,',CtThAvgN); % neutral Ct.Th
        fprintf(sfile,'\n'); % newline character

    fclose(sfile);

end
```

```
%%%%%%%%%%%%%%%%%%%%%%%%%%%%%%
% Main routine read_aim.m
%%%%%%%%%%%%%%%%%%%%%%%%%%%%%%

function [fn, pn, header_info, vol] =read_aim_amr(fn, pn)
%This file returns the file name, the file path name, the
header_info, and the
%data from an Aim file. It also adds the file path to the MATLAB
search path.
%Written by Dan Mazzucco; last revised November 16, 2005

% Modified by Stephan Weiss; February 2010
%   read_aim_matlab_V4.txt
%   Matlab version R2008b and later does not support vaxd option in
fopen anymore
%   Replaced 'vaxd' by 'ieee-le'

% Modified by Stephan Weiss; March 2016
%   Supports AIM version 030
%   Output type vol change from double to data specific type (memory
%   considerations)
%   Bug in binary, compressed int8 data reading fixed
%   Changed dt-compressed reading (removed re-alloc)

% Modified by Stephan Weiss; Dezember 2016
%   Added fclose(fid)

% Modified by Stephan Weiss; June 2017
%   Bug in binary, compressed int8 data reading fixed

% prompt for input filename
% [fn, pn] = uigetfile('*.aim','Choose AIM file');
addpath(pn); %Add the directory of the selected file to the search
path

% read header and pre-header and proc_log
disp('Reading AIM...')
header_info=read_header(fn);

% finally open file to read image data
fid=fopen(fn,'r','ieee-le');
fseek(fid,header_info(1),-1);
%
disp('Input volume
dimensions:');disp(header_info(2));disp(header_info(3));disp(header_i
nfo(4));
disp('Input volume element
size:');disp(header_info(8));disp(header_info(9));disp(header_info(10
));

switch header_info(11)
    case 1*2^16+1 % 8_bit integer
        disp('Reading 8bit image data...');
        %read image data from file
        vol = fread(fid,header_info(12),'int8=>int8');
```

```
vol=reshape(vol,header_info(2),header_info(3),header_info(4));

    case 2*2^16+2 %16_bit_integer';
        disp('Reading 16bit image data...');
        %read image data from file
        temp=(fread(fid,header_info(12)/2,'short=>short'));

vol=reshape(temp,header_info(2),header_info(3),header_info(4));
        %Code not verified

    case 3*2^16+4 %32_bit_integer';
        disp('Reading 32bit image data...');
        %read image data from file
        warning off MATLAB:conversionToLogical;
        temp=(fread(fid,header_info(12)/4,'int=>int'));

vol=reshape(temp,header_info(2),header_info(3),header_info(4));
        %Code not verified

    case 8*2^16+2 %DT compresses';
        disp('Uncompressing image data...');
        %read image data from file
        comp=(fread(fid,header_info(12),'uint8=>uint8'));
        comp(end+1:end+2)=0; %%loop concstruction

        val = comp(1:2:end);
        len = comp(2:2:end);

        if (header_info(13)==2) %AimVer
            field_offs = 3;
        else %AimVer 3
            field_offs = 5;
        end

        cur_len = len(field_offs);
        cur_val = val(field_offs);


vol=zeros(header_info(2),header_info(3),header_info(4),'uint8');
        % Uncompression algorithm first data point is value, second
data point is number of repeats
        for k=1:header_info(4)
            for j=1:header_info(3)
                for i=1:header_info(2)
                    vol(i,j,k) = cur_val;
                    cur_len = cur_len - 1;
                    if (cur_len == 0)
                        field_offs = field_offs + 1;
                        cur_len = len(field_offs);
                        cur_val = val(field_offs);
                    end
                end
            end
        end
```

```
        vol2 = typecast(vol(:),'int8');
        vol = reshape(vol2,size(vol));

    case 26*2^16+4 %64_bit_float';
        disp('Data type not yet supported.');
    case 21*2^16+1 %8_bit_binary_compressed';
        disp('Uncompressing binary image data ...');

        %sw 20.06.2017 dat = fread(fid,header_info(12),'int8=>int8');
        dat = fread(fid,header_info(12),'uint8=>uint8');
        dat(end+1)=0; % add one element due to loop construction

        if (header_info(13)==2) %AimVer
            val1 = dat(5);
            val2 = dat(6);
            field_offs = 7;
        else %AimVer 3
            val1 = dat(9);
            val2 = dat(10);
            field_offs = 11;
        end

        cur_len = dat(field_offs);

        if (cur_len == 255)
            cur_len = 254;
            change_val = false;
        else
            change_val = true;
        end

        cur_val = val1;
        is_value_1 = true;


vol=zeros(header_info(2),header_info(3),header_info(4),'uint8');

        for k=1:header_info(4)
            for j=1:header_info(3)
                for i=1:header_info(2)
                    vol(i,j,k) = cur_val;
                    cur_len = cur_len - 1;
                    if (cur_len == 0)
                        if (change_val)
                            is_value_1 = ~is_value_1;
                            if (is_value_1)
                                cur_val = val1;
                            else
                                cur_val = val2;
                            end
                        end
                        field_offs = field_offs + 1;
                        cur_len = dat(field_offs);
                        if (cur_len==255)
```

```
                            cur_len=254;
                            change_val = false;
                        else
                            change_val = true;
                        end
                    end
                end
            end
        end

        vol2 = typecast(vol(:),'int8');
        vol = reshape(vol2,size(vol));

case 13*2^16+1 %8_bit';
    disp('Data type not yet supported.');
    otherwise
        disp('Data type unknown.');
end

fclose(fid);
```